Klaus-Henning Ahlert

Economics of Distributed Storage Systems

An economic analysis of arbitrage-maximizing storage systems at the end consumer level

KIT Scientific Publishing

Klaus-Henning Ahlert

Economics of Distributed Storage Systems

An economic analysis of arbitrage-maximizing storage systems at the end consumer level

Economics of Distributed Storage Systems

An economic analysis of arbitrage-maximizing storage systems at the end consumer level

by
Klaus-Henning Ahlert

KIT Scientific Publishing

Dissertation, Karlsruher Institut für Technologie
Fakultät für Wirtschaftswissenschaften,
Tag der mündlichen Prüfung: 23.02.2010
Referent: Prof. Dr. Christof Weinhardt
Korreferent: Prof. Dr. Wolf Fichtner

Impressum

Karlsruher Institut für Technologie (KIT)
KIT Scientific Publishing
Straße am Forum 2
D-76131 Karlsruhe
www.ksp.kit.edu

KIT – Universität des Landes Baden-Württemberg und nationales
Forschungszentrum in der Helmholtz-Gemeinschaft

KIT Scientific Publishing 2010
Print on Demand

ISBN 978-3-86644-561-1

Für Ingrid, Jürgen, Dieter und Carolina.

Danksagung

Für die Unterstützung während meiner Promotion in Karlsruhe möchte ich Kollegen, Freunden und meiner Familie herzlich danken. Meinem Doktorvater Prof. Dr. Christof Weinhardt danke ich für die stete Unterstützung, die inhaltlichen Anregungen und das Arbeitsumfeld, das diese Arbeit erst möglich gemacht hat. Dr. Clemens van Dinther danke ich für die fachliche Unterstützung bei der Planung und Veröffentlichung meiner Forschungsarbeiten. Meinem Zimmer-Kollegen Dr. Carsten Block danke ich für die Fachgespräche und Diskussionen, die während unserer täglichen Arbeitszeit eine stete Hilfe und Kalibrierung waren.

Ein besonderer Dank für die moralische Unterstützung und Geduld auch in arbeitsreichen Phasen geht an meine Familie: Ingrid, Jürgen, Dieter und Carolina.

Abstract

Increasing the shares of Renewable Energy Sources (RES) and Distributed Energy Resources (DER) is one of the most important levers in many countries to cope with the environmental, political, and economic challenges of future energy supply. The underlying question of this thesis is whether Distributed Storage Systems (DSSs) at the end consumer level can economically foster the integration of intermittent and non-dispatchable resources by providing demand-side flexibility.

The analyses reveal a substantial integration potential of such systems, if hourly flexible electricity prices are provided to end consumers and capacity costs for distributed storage devices decrease to 200-400 EUR/kWh. The combination of results from three different models shows the economics of DSSs under price and load forecast uncertainty as well as under the condition of load-variable market prices. The models investigate the influence of technical and economic parameters within and around DSSs.

The first model (Part I) analyzes the economics of a single storage system on the grid. In contrast to other papers dealing with the economic evaluation of storage systems and the solution of storage scheduling problems, the presented approach varies in three dimensions: (i) Instead of centralized (large) storage systems on the Generation or Transmission level, the focus is on DSSs. (ii) The objective function is a purely economic storage application aiming at arbitrage accommodation, whereas the existing literature mostly analyzed the economic impact of partly or primarily technical storage applications, like load leveling, peak shaving, or frequency control. (iii) The presented model accurately links technical characteristics of a storage device with economic parameters of the system and its environment, which most of the existing storage models in literature only rudimentary do.

Part II presents a simulation model that analyzes the performance of DSSs under uncertainty. The described simulation model contributes three new aspects to scientific literature in this area: (i) In comparison with all other papers analyzing the economic impact of forecast errors, the presented methodology provides a more generic and extensive functionality of forecast error simulation. (ii) Few of the existing storage models considered forecast uncertainties into their analyses, none does so for DSSs. (iii) The third major contribution to literature on storage models is a benchmark of optimal vs. heuristic scheduling algorithms.

The third model (Part III) takes a market-wide perspective and models the impact that the aggregated charge and discharge volumes of multiple DSSs have on the electricity price. This work complements the existing literature on Demand Response (DR) programs by evaluating such programs when based on DSSs at the end consumer level. It continues the thought of implementing automated communication and control devices on the consumer side. Such devices help to let demand automatically follow supply to better integrate intermittent and non-dispatchable resources and to reduce critical peak loads without requiring the interaction and the behavioral change of the consumer.

Contents

List of Figures **xiii**

List of Tables **xv**

Abbreviations **xvii**

1 Introduction **1**
1.1 Problem 1
1.2 Structure of the Thesis 2

I Sensitivity Analysis of the Economics of a Distributed Storage System at the End Consumer Level **5**

2 Storage Systems at the End Consumer Level **7**
2.1 Objective and Structure of Part I 8
2.2 Related Literature 9
2.2.1 Storage Applications 10
2.2.2 Existing Modeling Approaches 14

3 Design and Analysis of Storage Optimization Models **19**
3.1 Basic Estimation Model 19
3.1.1 Parameters and Data Sources 19
3.1.2 Model Definition 21
3.1.3 Results 22
3.2 Linear Optimization Model 24
3.2.1 Parameters 24
3.2.2 Model Definition 27
3.2.3 Data Sources and Analysis Scenarios 36
3.2.4 Analysis Results 36
3.3 Summary 48
3.3.1 Contribution to Scientific Literature 49
3.3.2 Practical Relevance of the Findings 49

II Economic Impact of Price and Load Forecast Errors on Distributed Storage Systems 51

4 Price and Load Forecasting in the Electricity Sector 53
4.1 Objective and Structure of Part II . . . 55
4.2 Related Literature . . . 55
4.2.1 Load Forecasting . . . 55
4.2.2 Small Unit Load Forecasting . . . 56
4.2.3 Price Forecasting . . . 56
4.2.4 Economic Impact of Forecast Errors . . . 57
4.2.5 Autocorrelation of Forecast Errors . . . 60
4.2.6 Forecast Uncertainties in Storage Models . . . 60

5 Forecast Error Simulation in Storage Models 63
5.1 Forecast Generation . . . 65
5.1.1 Derivation of the Standard Deviation σ_i . . . 67
5.1.2 Determining the Mean Absolute Percentage Error of Normally Distributed Variables . . . 67
5.2 Schedule Determination . . . 69
5.2.1 Scheduling Algorithm using Linear Optimization . . . 69
5.2.2 Heuristic Scheduling Algorithm . . . 70
5.3 Schedule Execution . . . 74
5.4 Simulation Scenarios . . . 74
5.4.1 Load Forecast Scenarios . . . 75
5.4.2 Price Forecast Scenarios . . . 75
5.4.3 Combined Price and Load Forecast Scenarios . . . 76
5.5 Simulation Results . . . 77
5.5.1 Load Forecast Scenarios . . . 77
5.5.2 Price Forecast Scenarios . . . 82
5.5.3 Combined Price and Load Forecast Scenarios . . . 85
5.6 Summary . . . 90
5.6.1 Contribution to Scientific Literature . . . 91
5.6.2 Practical Relevance of the Findings . . . 92

III Market-wide Potential of Distributed Storage Systems as Demand Response Agents 93

6 Demand Responsiveness on Electricity Markets 95
6.1 Objective and Structure of Part III . . . 97
6.2 Related Literature . . . 97
6.2.1 Definition of Elementary Terms . . . 98
6.2.2 Reviews of Demand Response Programs . . . 99
6.2.3 Economic Impact of Flexible Pricing and Price Elasticity . . . 100
6.2.4 Effects of Increasing Shares of Renewable Energy Sources . . . 102

7 Storage Models considering the Price Impact of Demand Response 105
7.1 Basic Analysis Variables . . . 105
7.1.1 Characteristics of the Load Curve . . . 107
7.1.2 Characteristics of the Price Curve . . . 109
7.2 Estimation Model . . . 112
7.2.1 Mathematical Formulation . . . 112
7.2.2 Results and Interpretation . . . 115
7.3 Market-wide Analysis Model . . . 116
7.3.1 Mathematical Formulation . . . 117
7.3.2 Generic Solution for the Minimization Problem . . . 118
7.3.3 Analysis Parameters and Assumptions . . . 121
7.4 Analysis Results . . . 123
7.4.1 Capacity Variation Analysis . . . 123
7.4.2 Constraint Analysis . . . 124
7.4.3 Storage Capacity Cost Analysis . . . 125
7.4.4 Sensitivity Analysis . . . 126
7.4.5 Spread Analysis . . . 128
7.5 Summary . . . 129
7.5.1 Contribution to Scientific Literature . . . 130
7.5.2 Practical Relevance of the Findings . . . 131

8 Conclusions & Outlook 133
8.1 Limitations of the Approach . . . 135
8.2 Further Research . . . 135

References 139

Appendix 151

A Derivation of Storage Depreciation Costs 151

B Overview of Model Variables 155

C Control Flows of the Heuristic Scheduling Algorithms 159

List of Figures

1.1 Structure of the thesis 4

2.1 Output power and duration - classification of existing storage sites . . . 10
2.2 Output power and duration - storage application requirements 11

3.1 Impact of varying the charging limit i 23
3.2 Impact of varying the discharging limit j 23
3.3 Overview of model parameters 25
3.4 Sample plots of different price granularities 25
3.5 Sample plots of different price curve shapes 26
3.6 Efficiency degrees of a storage system 27
3.7 Nominal cycles as function of DOD and temperature, example of NiMH batteries 28
3.8 Interrelation of depth of discharge and cost per nominal discharge cycle 31
3.9 Impact of capacity variations for different technology cases 37
3.10 Impact of storage capacity price variations on annual savings 38
3.11 Sensitivity analysis for technical and economic storage parameters . . . 39
3.12 Impact of market price level variations 40
3.13 Impact of price spread variations 41
3.14 Sample plots of price curve granularities 42
3.15 Impact of the price curve granularity on annual savings 42
3.16 Influence of the annual consumer demand on relative savings 43
3.17 Seasonal load distribution of the reference load profile 45
3.18 Weekday-specific load distribution of the reference load profile 45
3.19 Average intraday load distributions of the analyzed load profiles 45
3.20 Impact of the load profile distribution on relative savings 46
3.21 Correlation of annual savings with the load shape indicator χ^{shape} . . . 46

5.1 Control flow of the simulation model 64
5.2 Elements of the forecast period 66
5.3 Basic scenario frame 75
5.4 Simulation scenarios 76
5.5 Impact of load forecast horizon extensions 78
5.6 Impact of autocorrelation of load forecast errors 79
5.7 Impact of load forecast granularity 80
5.8 Impact of load forecast accuracy on economic result 81
5.9 Cumulative probability of deviations from the optimum (load forecast variations) 81
5.10 Impact of price forecast period length 83

5.11 Economic impact due to autocorrelation of price forecast errors 84
5.12 Impact of price forecast accuracy bounds 84
5.13 Cumulative probability of deviations from the optimum (price forecast) 85
5.14 Impact of forecast period length (combined price and load forecasts) . . 86
5.15 Impact of price forecast errors on the variants of the heuristic algorithm 87
5.16 Results of scheduling algorithms in combination with forecast error autocorrelation variations 89

6.1 Effect of price elasticity of the demand side (illustrative) 99
6.2 Merit-order effect of increasing supply volumes from RES (illustrative) 103

7.1 Interrelations of model parameters 106
7.2 Distribution of the aggregated and the standard household load curve . 108
7.3 Impact of spread level variations on the price function (illustrative) . . 111
7.4 Resulting aggregated load after load shifting between January 8 and January 14, 2007 116
7.5 Control flow of the iterative solution algorithm 121
7.6 Optimal power dimensioning in dependency from the installed capacity 122
7.7 Results of the capacity variation analysis 123
7.8 Results of the constraint analysis 125
7.9 Results of the storage capacity cost analysis 126
7.10 Optimal and maximal storage capacity sizes 126
7.11 Results of the sensitivity analysis 127
7.12 Results of the price spread analysis 129

C.1 Schedule generation algorithm 160
C.2 Price limit determination algorithm 161
C.3 Algorithm of the charge condition refinement procedure 162
C.4 Algorithm of the discharge condition refinement procedure 163

List of Tables

2.1 Detailed Review of Storage Models in Literature 16
2.2 Detailed Review of Storage Models in Literature 17

3.1 Parameter Values for Basic Estimation Model 21
3.2 Decision Parameters 24
3.3 Market and Consumer Parameters 26
3.4 Overview of Storage System Parameters 29
3.5 Technology Scenarios 36
3.6 Reference Parameter Values 37
3.7 Price Curve Variation Parameters 40
3.8 Load Curve Distribution Indicator Values 46

4.1 Load Forecasting Accuracies 56
4.2 Small Unit Load Forecasting Accuracies 57
4.3 Price Forecasting Accuracies 58
4.4 Economic Impact of Forecast Accuracy 59
4.5 Autocorrelation of Errors in Load Forecasting 61
4.6 Autocorrelation of Errors in Price Forecasting 62

5.1 Variants of the Heuristic Algorithm 73
5.2 Load Forecast Simulation Scenarios 76
5.3 Price Forecast Simulation Scenarios 76
5.4 MAPE at the End of the Forecast Horizon 78
5.5 MAPE at the End of the Forecast Horizon 82
5.6 Impact of the Price Margin Parameter 88
5.7 Impact of the Charge Index Buffer Parameter 88
5.8 Simulation Setups 89

6.1 Values for Price Elasticity of Demand in Literature 101

7.1 Additional Model Parameters on the Aggregated Level 106
7.2 Load Curve Characteristics 108
7.3 Adjusted R^2 Results 109
7.4 Definition of Regression Functions 109
7.5 Volatility of Price Curves 110
7.6 Results of the Estimation Model 115

B.1 Non-Technical Model Variables 155
B.2 Non-Technical Model Variables 156
B.3 Technical Model Variables 157

B.4 Technical Model Variables 158

Abbreviations

APX	Amsterdam Power Exchange
BDEW	German Energy and Water Association (Bundesverband der Energie- und Wasserwirtschaft)
CDS	Charge-Discharge-Schedule
DENA	Deutsche Energie-Agentur GmbH
DER	Distributed Energy Resources
DOD	Depth of Discharge
DR	Demand Response
DSM	Demand-Side Management
DSS	Distributed Storage System
DWT	Durbin-Watson Test
EEX	European Energy Exchange
ENTSOE	European Network of Transmission System Operators for Electricity
EUR	Euro (currency)
EV	Electric Vehicle
GW	Gigawatt
GWh	Gigawatt hour
kW	Kilowatt
kWh	Kilowatt hour
Li-ion	Lithium ion
MAPE	Mean Absolute Percentage Error
MW	Megawatt
MWh	Megawatt hour
NaS	Natrium Sulfur, *also:* Sodium Sulfur

NiCd	Nickel Cadmium
NiMH	Nickel Metal Hydride
PEV	Plug-in Electric Vehicle
PHEV	Plug-in Hybrid Electric Vehicle
PJM	Pennsylvania, New Jersey, Maryland
PV	Photovoltaic
RES	Renewable Energy Sources
RTP	Real-time pricing
SOC	State of Charge
TOU	Time-of-use [tariff]
TW	Terawatt
TWh	Terawatt hour
VDEW	German Electricity Association, today within BDEW (Verband der Elektrizitätswirtschaft)
VPP	Virtual Power Plant

Chapter 1

Introduction

Peaking oil prices and massive CO_2 emissions of fossil-fired power plant fuel an economically and environmentally motivated debate on how our future energy supply should look like. The evident scarcity of fossil resources as well as climate change require the energy sector to seek more sustainable alternative resources. The most recent debates on the European energy market show that the utilities industry as well as most energy consumers are facing significant changes in the future. Examples for the upcoming change are reflected in the frequent discussion of Smart Metering technologies in the daily press, the intended increase of energy generation from Renewable Energy Sources (RES) and Distributed Energy Resources (DER), the announced CO_2 reductions in the European Union until 2020, and a continuation of the ongoing liberalization and unbundling of the energy markets (European Union, 2008, German government, 2008).

The significant increase of power generation from DER and RES is a central target, which could positively contribute to an increase in energy autonomy and a reduction of CO_2 emissions. Depending on the ownership and market structure in the power generation sector, it could also contribute to further liberalization of the energy markets. Clearly, a shift from today's centralized market structure towards a decentralized model would cause problems in terms of keeping or improving quality and reliability of energy supply. It would require major investments and technological innovations in the electricity grid infrastructure and energy markets.

1.1 Problem

The underlying question of this research work is whether Distributed Storage Systems (DSSs) at the end consumer level can economically foster the integration of RES and DER by providing demand-side flexibility. Increasing the shares of RES and DER is one of the most important levers in many countries to cope with the environmental, political, and economic challenges of future energy supply. However, a number of issues have to be solved to successfully integrate such resources into the energy systems in place.

The main technical issue of integrating large shares of non-dispatchable and intermittent resources, which for example applies to wind and solar power (RES) and micro-CHP systems (combined head and power) (DER), is to maintain the stability of the grid. At each point in time, the volumes of demand and supply in the electricity system must be balanced. Traditionally, balancing these volumes has been achieved

entirely by adjusting the provided supply volume, since the short-term demand volume has been assumed inelastic. Responsiveness of directly controllable supply resources as well as additional reserve capacities ensured the flexibility of the supply volume. Unlike conventional generation resources, DER and especially RES often do not allow for such responsiveness in supply. The traditional paradigm to compensate for this flexibility decrease is to install additional reserve capacities, which leads to increasing costs and decreasing efficiency of the overall system due to a lower average utilization of the available resources. Instead, this work investigates a shift of this paradigm towards an increasingly flexible and responsive demand side through DSSs. In the focus of this investigation is the analysis of the economics of DSSs at the end consumer level that react to flexible market prices. The systems operate autonomously as automated agents that optimize the consumers' load profiles according to the market price. The systems only discharge for covering the consumers' demand, they do not sell electricity back to the market. The main advantage of such an automated Demand Response (DR) mechanism over conventional DR programs is that the flexibility potential is reliably and constantly available over time. It is not limited by the constraint of an actual behavioral change or action of the consumer and the related problem of preference elicitation. The analyses in this research work do not address related technical, political, and economic questions regarding a possible divestiture or decommission of utilities' existing assets, regulatory enforcements of integrating RES, or grid-related constraints.

1.2 Structure of the Thesis

Part I of the thesis analyzes the economics of DSSs at the end consumer level in detail. Sensitivity analyses are performed along the three main dimensions of market parameters, consumer parameters, and technical as well as economic storage system parameters. The analyses assume an hourly flexible price signal and model the DSS as a price taker, i.e., charge and discharge decisions of the analyzed system do not affect the market price. The market price itself is assumed to appropriately reflect the demand-supply-situation on the market and an increase in supply from RES and DER leads to a decreasing market price (Section 6.2.4). The numerical analyses build on standard household load profiles (VDEW, 2006), price data from the EEX (2007), and storage parameters from academic literature. The existing literature mainly investigates the economics of centralized storage models that operate on the wholesale market, operating DSS at the end consumer level is hardly investigated and understood. Therefore, the analyses in Part I address the following research questions:

Research Questions (Part I):

- *How does a Distributed Storage System influence the electricity costs of a standard household in case of hourly flexible electricity prices?*
- *How do market, consumer, and storage parameters impact the result and which are the most relevant parameters?*

Part II addresses the question whether the information required to operate such storage systems is actually available at the end consumer level. The autonomous agents

that operate the DSSs need to know the price and the load data of the upcoming days to derive an economically profitable Charge-Discharge-Schedule (CDS). The linear model in Part I optimized such CDS based on known data series. But since these data are not ex-ante available for real-world applications, the systems need to derive these schedules from price and load forecast data. Forecast errors will evidently lead to deviations from the economically optimal schedule. The numerical simulation model used to analyze the impact of forecast errors is an extension of the linear optimization model defined in Part I and builds on the same data sources. The analyses in Part II investigate the impact of forecast errors and assess the robustness of different forecast and scheduling approaches. Therefore, this part addresses the following research questions:

Research Questions (Part II):

- *To what extent do load and price forecast errors lead to a deviation from the optimal operational result of a Distributed Storage System?*
- *How much do the results deteriorate when price and load forecasts are derived through available standard forecast methods?*
- *What are the best scheduling algorithms and how robust are the achieved economic results with regard to increasing forecast errors?*

Part III finally analyzes the effect of operating multiple DSSs as DR agents on the system. Since the aggregated charge and discharge volumes of multiple DSSs will be substantially higher than in the one-consumer-case, which was analyzed in Part I, the DSSs are no longer modeled as price takers. Thus, the charge and discharge decisions of the storage systems influence the market price. Higher aggregated load volumes lead to higher prices and reverse. The analyses assume a perfect coordination of the systems and therefore treat the aggregated storage capacity as one large entity. The numerical analysis model is an extension of the analysis model defined in Part I, but it builds on partially different data. Instead of the load profile of a standard household, the aggregated load profile of Germany in 2007 is applied (ENTSOE, 2007). The analyses in Part III address the following research questions:

Research Questions (Part III):

- *What is the cost reduction potential of a perfectly responsive demand side in case of hourly flexible electricity prices?*
- *How do the costs for Distributed Storage Systems constrain this potential?*
- *What is the amount of economically operable distributed storage capacity in a market?*

Figure 1.1 illustrates the structure of the thesis. As described in the paragraphs above, the chapters of Part II and Part III build on the model and the results of Part I (in particular of Section 3.2).

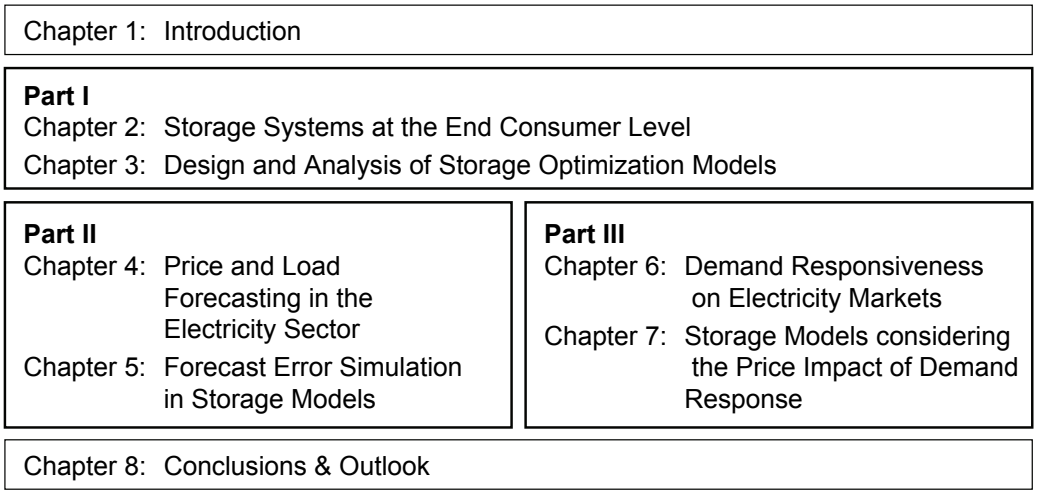

Figure 1.1: Structure of the thesis

Part I

Sensitivity Analysis of the Economics of a Distributed Storage System at the End Consumer Level

Chapter 2

Storage Systems at the End Consumer Level

The most recent developments and issues on the European energy market show that the utilities industry as well as most energy consumers are facing significant changes in the future. Examples for decisions and targets behind these changes are the intended increase of energy generation from Renewable Energy Sources (RES) and Distributed Energy Resources (DER), the announced CO_2 reductions in the European Union until 2020, and a continuation of the ongoing liberalization and unbundling movements in the market (European Union, 2008, German government, 2008).

The significant increase of power generation from DER and RES is a central target, which can positively contribute to an increase in energy autonomy and a reduction of CO_2 emissions. Depending on the ownership and market structure in the power generation sector, it could also contribute to further liberalization of the energy markets. Clearly, a shift from today's centralized market structure towards a decentralized model would cause problems in terms of keeping or improving quality and reliability of energy supply. It would require major investments and technological innovations in the electricity grid infrastructure and energy markets.

One of the key characteristics of electrical energy is that supply and demand must be in balance at each point in time to make the energy grid run stable. Therefore, Transmission System Operators are obliged to reserve a certain amount of capacity (Primary, Secondary, and Tertiary Control) in order to react appropriately to deviations from the demand forecast. An increasing amount of distributed energy production and intermittent sources like wind or solar energy complicates the process of balancing demand and supply. In comparison with coal or nuclear power plants, the output of these energy sources is more volatile and less predictable since it strongly depends on environmental (weather) conditions.

The traditional approach to balance supply and demand is supply-side-driven. The installation of additional control capacity ensures sufficient power supply at any time. Since control capacity is more expensive than regular capacity, this will lead to increasing market prices. Alternatively, market-based approaches for Demand-Side Management (DSM) are discussed, but only selectively realized. Up to now, energy suppliers and large industrial consumers have planned and adjusted their supply and demand volumes in order to balance the market. Commercial customers, public institutions and private households are not actively involved in matching demand and supply

of the electricity markets, although their share is about 50% of the total consumption[1]. The main reason is that commercial customers and private households do not have a direct economic incentive to change their load profiles, since energy tariffs are flat, i.e., do not depend on the current demand and supply levels. In Germany, this will change from beginning of 2011 onwards when load-dependent tariffs must be offered (Federal Law Gazette, 2008).The upcoming challenge is to provide consumers with market information (e.g., a price signal) so that consumers (humans and/or machines) can appropriately react to the market situation.

Smart Grid and *Smart Metering* are two terms that describe related technological innovations for the future grid. *Smart Grid* is a superordinate concept for the digitalization of the grid infrastructure containing *intelligent components*. Objectives of the concept are condition-based and remote maintenance, improved integration of DER and RES, increased reliability and flexibility through distributed decision making and control, and enabling DSM more effectively, e.g., through Real-time pricing (RTP), which requires *Smart Metering* technology. The objectives of *Smart Metering* are enabling DSM, installing a platform for value-added services, improving fraud protection, and increasing operational efficiency, e.g., through optimized business processes ("billing & collections") and remote meter reading, which is often an important functionality to achieve regulatory compliance. In its core, a smart metering device is a digital meter with a communication interface for sending and receiving data. The sending mode enables functionalities such as remote meter reading, while the receiving mode supports price updates for load- or time-dependent flexible pricing.

Assuming that the required market information and particularly flexible electricity tariffs are provided, consumers would have an economic incentive to reduce energy consumption in peak hours and shift it to off-peak hours. To avoid a reduction of this load shifting potential due to behavioral constraints of the consumer, storage applications could help to maximize demand-side flexibility, i.e., having the option to shift portions of demand to different times than those where they actually occur. This would allow maximizing the use of energy from renewable sources when it is available.

Instead of the difficulty to quantify behavioral constraints, the challenges of the storage-based approach contain the installation of an economically beneficial and technologically feasible storage system, the design of an appropriate (electronic) market that provides consumers with market information, and sufficiently accurate forecast mechanisms for load volumes and prices to determine operation schedules. Essentially, distributed storage devices must be able to follow or generate an economically beneficial Charge-Discharge-Schedule (CDS). An important assumption for the analyses is that flexible prices are provided to end consumers. The hypothesis is that storage applications can decrease the average costs for electricity through increasing demand-side flexibility. I.e., demand will follow a price incentive and could therefore also foster the integration of RES, if accordingly priced in the market[2].

2.1 Objective and Structure of Part I

To support the above hypotheses of decreasing average costs for electricity and fostering the integration of RES through Distributed Storage System (DSS), this part of

[1] Example of Germany, 2005 (BDEW, 2008).

[2] Part III of this work will deal with the last part of this hypothesis.

the research work defines and analyzes a detailed storage model that links technical, economic, market, and consumer parameters. The model calculates the maximal economic benefits of a distributed storage device at the end consumer level. Therefore, the model determines the optimal CDS of a storage system by solving a linear optimization problem. All parameters of the model are analyzed with respect to their impact on the resulting total cost.

The remainder of this part of the thesis gives an overview about existing research work on electricity storage (Section 2.2) and defines two storage models. The first storage model estimates the potential benefits from arbitrage accommodation and delivers first insights into the sensitivity of CDSs (Section 3.1). The second model combines detailed technical and economic parameters of a storage system into a linear optimization model. Systematic sensitivity analyses for all model parameters are run on this model (Section 3.2). Section 3.3 summarizes the findings and discusses their relevance.

2.2 Related Literature

Energy storage for power systems is a broadly discussed topic in academic literature since the 1980s. Related literature covers a wide range of storage applications and objectives of storage usage, e.g., for supporting the conventional power system, the operations of remote locations (*islands*), or the integration of DER or RES into the grid. Traditionally, large and centralized storage systems have been discussed and analyzed, whereas distributed storage is a more recent and less researched field.

Cook et al. (1991) present a historic overview of battery storage applications. A more recent overview by Divya and Østergaard (2009) references and structures many articles on battery storage systems and models. They point out that despite the numerous projects and research efforts in the area of storage technology very few examples of practical implementations exist. Divya and Østergaard (2009), Cook et al. (1991), and Kondoh et al. (2000) present overviews of existing sites of storage system implementations (without pumped hydro). According to Divya and Østergaard (2009), the variety and large amount of conventional generation resources as well as the interconnection between these resources made storage technology economically less attractive and technically not mandatory in the past. Additionally, a lack of practical experience and supporting tools hampered the realization of such projects. However, the increasing shares of non-conventional and non-dispatchable resources in today's and future power grid will change this trend in their opinion.

The potential of storage technology to foster a stronger decentralization of the power grid has also been discussed in early papers by Kirkham and Klein (1983), Harty et al. (1994), and Coles et al. (1995). Especially Harty et al. (1994) underline the large potential of existing and emerging storage technologies, but not limited to supporting stronger decentralization. Their article gives a qualitative overview of the benefits for generation and transmission companies as well as for end consumers from various storage technologies.

A recent overview of detailed technical and economic characteristics of 21 storage technologies is given in Chen et al. (2009). Schoenung and Hassenzahl (2003) present another detailed technology review of 16 technologies, which additionally links the technologies to potential applications. The (technical) characteristics of a storage technology must fulfill the (technical) requirements of an application, e.g., output power (power capacity), output duration (energy capacity), power density, energy density,

and the cycling period, as well as finally economic requirements. Kondoh et al. (2000), Ribeiro et al. (2001), and Barton and Infield (2004) match these technology characteristics with application requirements and graphically present their results. Figures 2.1 and 2.2 depict examples where the characteristics *output power* and *output duration* have been linked to requirements of storage applications.

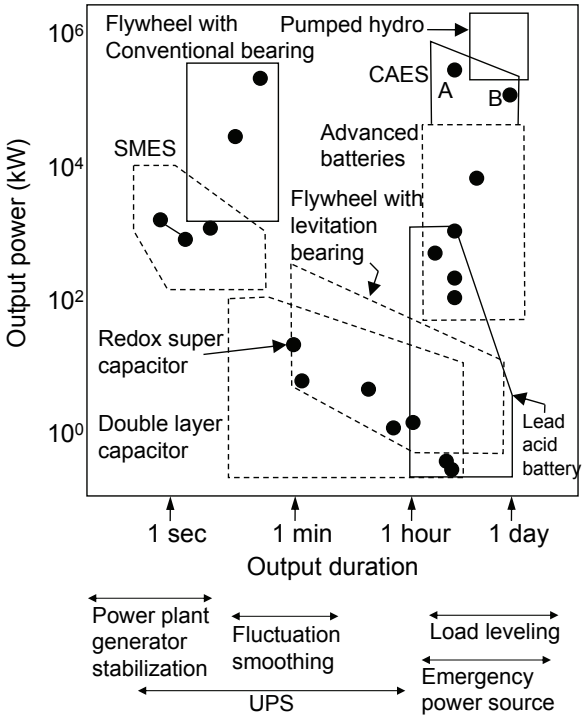

Figure 2.1: Output power and duration - classification of existing storage sites, in Kondoh et al. (2000)

2.2.1 Storage Applications

Storage applications describe the objectives that are pursued by storage usage. In the literature, many storage applications have been described and analyzed. E.g., Eyer et al. (2004), Baumann (1992) (slightly modified and extended in Jewell et al. (2004)), Cook et al. (1991), and Kottick and Blau (1993) give an overview of potential applications. However, often the terms used differ between these overviews and consistent terms do not always cover the exact same scope. This work will present a storage application overview that builds on the aforementioned references, but clearly goes beyond their combined scope and content.

The following paragraphs of this chapter will structure the identified storage applications. Each application is allocated in a two-dimensional matrix, where the first dimension indicates the location of the storage system and the second dimension describes the overall objective (generalized application domain) of the application. Table 2.1 depicts this matrix with 41 reviewed papers allocated to its cells. Many papers analyze multiple objectives with their models, but hardly any assign the storage system to multiple locations. Therefore, Sections 2.2.1 - 2.2.1 of this work present the literature review along the location dimension.

The locations of storage systems in the literature are situated

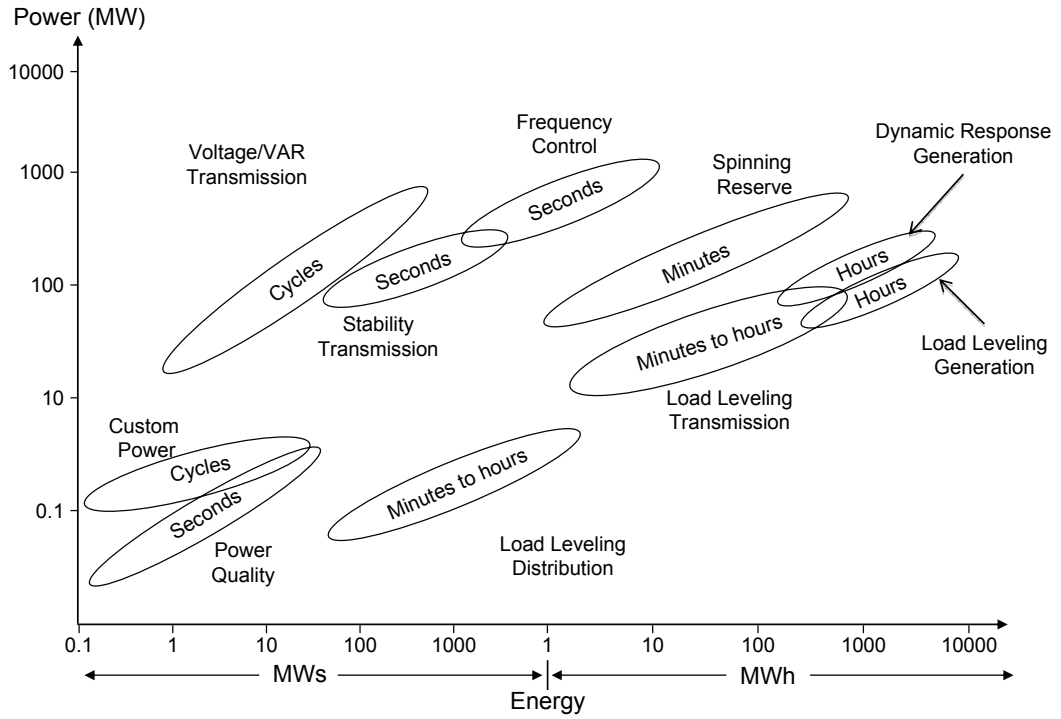

Figure 2.2: Output power and duration - storage application requirements, in Ribeiro et al. (2001)

- as co-locations to conventional generation units,
- as co-locations to substations and other components of the transmission and distribution (T&D) grid,
- as co-locations to renewable and distributed generation resources,
- at remote (island) locations,
- in proximity to end consumers,
- or within grid-integrated Electric Vehicle (EV).

This structure refines the grouping in Eyer et al. (2004), who suggest a distinction into *Grid System Applications*, *Consumer/End-use Applications*, and *Renewables*. In an earlier paper by Cook et al. (1991), only co-locations to generation and T&D sites are distinguished.

The overall objectives of storage applications are grouped into five main categories:

- Arbitrage,
- Investment Deferral,
- Power Quality,
- Reliability,
- and Load Curve Optimizations.

Applications aiming at **Arbitrage** accommodation always have a clearly economic objective. These applications either maximize the revenues of sellers or producers or minimize the costs of buyers or consumers. The basic principle of this storage application is to charge energy in low-price (off-peak) hours and to discharge energy in peak-price hours. Following this principle, arbitrage accommodation includes buying and selling on wholesale markets, time-shifted selling of produced and stored energy (bulk energy management) (cf. Exarchakos et al. (2009), Graves et al. (1999)), and cost minimization through load shifting in combination with Time-of-use (TOU) tariffs (also described as load shifting (Nieuwenhout et al., 2006), load redistribution (Maly and Kwan, 1995)).

The objective of **Investment Deferrals** applies mainly to storage at generation and T&D locations and follows an economic objective. If an increasing demand for electricity requires an expansion of the installed capacity, storage systems can be used to temporarily satisfy the additional demand and, thus, to delay the investment in conventional infrastructure components. Especially small additional capacity requirements that undergo the economic size of additional conventional installations can be economically served with storage applications (cf. Rau and Taylor (1998), Schoenung and Eyer (2005)).

The objective of maintaining and ensuring **Power Quality** includes voltage and frequency control, provision of reactive power control and a reduction of load shedding for under-frequency control (cf. Alt et al. (1997), Kottick and Blau (1993), Ribeiro et al. (2001), Schoenung and Burns (1996)). All these objectives are of primarily technical nature.

Achieving **Reliability** of the electricity supply can have both technical and economic objectives. Storage applications in this domain include providing power regulation (load following), spinning reserve, (emergency) backup supply, black start capability, as well as the integration of RES and DER, e.g., through ensuring contractual supply or reducing output fluctuations. (cf. Chacra et al. (2005), Clark and Isherwood (2004), Ferreira (1992), Jenkins et al. (2008), Ribeiro et al. (2001), Schoenung and Burns (1996), Sobieski and Bhavaraju (1985), Su and Huang (2001), Vosen and Keller (1999))

The objective of **Load Curve Optimizations** includes various storage applications that either actively shape the load curve (peak shaving, load leveling) (cf. Anderson and Lo (1999), Chowdhury and Rahman (1988), Jung et al. (1996), Sobieski and Bhavaraju (1985)) or optimize the operations of a grid component and, thus, alter the load curve indirectly. Such operational optimizations include the minimization of fuel or production costs (cf. Anderson and Lo (1999), Lee (1992), Lee and Chen (1993)), levelizing incremental costs (cf. Sullivan (1982)), and reducing losses. These objectives can either follow technical or economic objectives.

As the empty fields in the matrix of Table 2.1 show, not all combinations of storage locations and objectives are relevant. Although theoretically possible, e.g., arbitrage accommodation at remote locations or investment deferrals for other than generation or T&D components have not been investigated in literature. From a practical point of view, these combinations seem irrelevant. One exception are arbitrage applications for grid-integrated EVs. Up to now, authors have looked at regulation services in vehicle-to-grid (V2G) model. Although the primary purpose of an electric vehicle is clearly to ensure mobility, it seems possible and practically relevant to analyze arbitrage applications based on storage in grid-integrated electric vehicles, e.g., charging strategies

that build on TOU-based electricity prices and minimize the total operating costs of an EV.

Since the focus of this research work will be on arbitrage accommodation, the following sections will focus on arbitrage applications along the storage location dimension.

Arbitrage Accommodation on Wholesale Markets

Storage applications that are located on the grid system level focus on wholesale energy prices, if aiming at arbitrage accommodation. A comprehensive analysis of arbitrage value in Pennsylvania, New Jersey, Maryland (PJM) from 2002 to 2007 is presented in Sioshansi et al. (2009). When modeling their storage system as a price taker, i.e., charge and discharge decisions do not affect the market price, they reveal an arbitrage value range of 60-120 USD/kWh per year (variations due to different years).

Walawalkar et al. (2007) investigates the economics of energy storage systems in New York state's electricity market by modeling Natrium Sulfur (NaS) and flywheel storage systems. Their analysis indicates a strong economic case for storage system installations in New York City for arbitrage services using NaS-based systems, whereas they find significant opportunities for regulation services in New York state using flywheel-based systems.

A paper by Graves et al. (1999) analyzes revenues from arbitrage accommodation on electricity wholesale markets for different price granularities. They find out that hourly prices allow up to two times higher benefits from arbitrage services than blocked prices.

Nieuwenhout et al. (2006) analyze two settings for arbitrage accommodation using storage systems on the wholesale level. Based on data of the Amsterdam Power Exchange (APX) they analyze arbitrage on a day-ahead power market and on an imbalance market. Overall, the imbalance market reveals the highest revenues in their models with a theoretical maximum of 470 EUR/kWh per year.

A recent paper by Exarchakos et al. (2009) investigates the influence of DSM on electricity storage systems, under the condition that the only income is from arbitrage accommodation through optimized CDSs. They find that small amounts of load shifting due to DSM can significantly affect the profit of the storage application. Overall, they state a 10% revenue reduction for arbitrage services through DSM programs.

Maximizing Revenues of Renewable and Distributed Energy Resources

Especially small, non-conventional generation devices such as Photovoltaic (PV) panels, wind turbines, or microturbines can use storage systems to deliver energy to the grid preferably in peak price hours. Thus, time-shifting their delivery to the network will on the one hand maximize their revenues. On the other hand it also fosters the technical integration of such resources. Barton and Infield (2004) investigate such a case with intermittent RES for various storage technologies. Bathurst and Strbac (2003) describe a system that combines energy storage with two wind farms. They present an algorithm that calculates the optimal dispatch of the storage system. Depending on the forecast errors regarding the wind farm's energy production and the spreads on the imbalance market, their analysis reveals up to 25% higher profits.

Korpaas et al. (2003) also combine wind power plants with energy storage. They state that revenues of wind power plants can be increased through storage systems by time-shifting their delivery according to higher spot market prices. However, they state

that with current prices storage systems are likely to be a more expensive alternative than grid expansions.

A paper by Wu et al. (2002) investigates the combination of a PV system with battery storage. For a utility-financed model they confirm a profitable business case, whereas a consumer-financed model delivers negative economic results.

Arbitrage Accommodation through Load Shifting at the Consumer Level

The basic assumption on the consumer level is that storage devices are charged from the grid at low price hours and discharged in order to serve the consumer's demand at peak prices. I.e., discharging does not mean selling the energy back to the grid, but essentially shifting the effective load on the grid to an earlier point in time. This implies that flexible tariffs must be available to end consumers, in order to provide an economic incentive. Therefore, these storage applications are also described as (TOU) energy cost management applications.

Daryanian et al. (1991) describe a model based on electric thermal storage. Their paper investigates a consumer response algorithm that achieves 10% savings through load shifting. Their price signal is an experimental RTP rate.

Detailed analyses on the Taiwanese market are described in Lee and Chen (1994), Lee and Chen (1995), and Maly and Kwan (1995). The Taiwanese tariff consists of time-dependent price blocks during the day and a determination of the overall price level depending on the peak load during the consumption period. I.e., higher peak loads lead to higher blocked prices for the individual consumer. Therefore, these approaches also focus on peak shaving and a TOU optimization. Besides shifting load to cheaper time blocks, particularly a reduction of the peak load is economically beneficial under such conditions.

Nieuwenhout et al. (2006) analyze two setting for load shifting at the end consumer level. The first setting assesses arbitrage opportunities if a simple day-night-tariff is provided. The second setting analyzes the combination of a storage system with small generation units at the consumer's site that charge the storage instead of feeding the generated energy into the grid. Both settings do not reveal any relevant arbitrage value.

Additionally to papers that use storage applications, there is also a number of papers that present TOU optimization models without storage applications, e.g., Ashok and Banerjee (2001) and Soliman et al. (2007).

2.2.2 Existing Modeling Approaches

Besides the storage application, the reviewed papers differ regarding their modeling approaches. Generally, storage models can be distinguished into models with economic and/or technical objectives. Further distinctions can be made regarding the analyzed storage technology, the storage model's level of detail, and the algorithm applied to solve the modeled problem. Detailed storage models reflect both technical and economic parameters of the selected technology. Examples for such parameters in battery storage models are Depth of Discharge (DOD), separate efficiency degrees for storage and peripheral components, charging speeds (power capacity), storage and peripheral cost components and their depreciation over time. Divya and Østergaard (2009) criticize that many papers modeling battery storage models do not explicitly parameterize their calculations for a specific technology, e.g., lead-acid or li-ion. Furthermore, they

criticize that important technical details, such as the DOD, are often not included into the models. The results of a detailed paper review within this research work support this criticism (see Table 2.2). The table gives a detailed overview of 43 storage models described in related academic literature.

Regarding the algorithms applied to solve the modeled problem, most models use either a dynamic programming approach, linear optimization models, statistical methods, or simulations, which might involve the previous methods. An example that applies dynamic programming can be found in Ferreira (1992), where the focus is on the specific case of short-term scheduling of a pumped storage plant. Another example of a generation-side-focused model using dynamic programming is presented in Anderson and Lo (1999), where the objective of the storage application is on load leveling. Here, as well as in Alt et al. (1997), the modeling focus is rather on the grid parameters than on the storage modeling. Contrary, a technically more detailed storage model using dynamic programming is presented in Lee and Chen (1994) and Lee and Chen (1995). Most papers that use the approach of dynamic programming focus on load curve optimizations such as peak shaving or load leveling.

Contrary, nearly all papers investigating arbitrage values use linear optimization models. Bathurst and Strbac (2003) use a linear optimization model for increasing revenues of wind power plants. They use a generic storage model instead of parameterizing a particular storage technology. Exarchakos et al. (2009) also use a linear optimization model assessing the impact of DSM programs on the profitability of storage systems (see Section 2.2.1). They model various storage technologies, thereof also lead-acid batteries. Their model does not include a parameter that limits the DOD, which has a significant effect on the life time of the battery (leading to a longer battery life cycle in their model). Furthermore, they model fixed costs for storage usage, instead of a flexible, usage-dependent rate that approximates the actual depreciation costs based on the expected number of charge cycles. As a consequence, the capital costs in their model dominate the economic result. A very detailed model of a lead-acid batteries in storage systems is described in Wu et al. (2002).

A well-modeled, lead-acid-based storage system with a clearly technical focus is presented in Jenkins et al. (2008). They use a round-based simulation model on discrete time series to evaluate the value of storage in combination with microgeneration systems at the consumer site. This work presents a similar model in Section 3.2, but extended with economic parameters.

Table 2.1: Detailed Review of Storage Models in Literature

Location	Arbitrage	Investment Deferral	Power Quality	Reliability	Load Curve Optimization
Renewable and Distributed Generation Units	Barton and Infield (2004) Bathurst and Strbac (2003) Korpaas (2004) Wu et al. (2002)			Chowdhury and Rahman (1988) Jenkins et al. (2008) Rau and Short (1996) Su and Huang (2001) Vosen and Keller (1999) Wu et al. (2002)	Chowdhury and Rahman (1988) Vosen and Keller (1999)
Conventional Generation Plants (utility side)	Exarchakos et al. (2009) Graves et al. (1999) Nieuwenhout et al. (2006) Poonpun and Jewell (2008) Sioshansi et al. (2009) Walawalkar et al. (2007)	Kandil et al. (1990)	Schoenung and Burns (1996)	Ferreira (1992) Schoenung and Burns (1996) Sobieski and Bhavaraju (1985) Walawalkar et al. (2007)	Anderson and Lo (1999) Lee (1992) Lee and Chen (1993) Sobieski and Bhavaraju (1985) Sullivan (1982)
Transmission & Distribution	Chacra et al. (2005) Schoenung and Eyer (2005)	Chacra et al. (2005) Schoenung and Eyer (2005) Rau and Taylor (1998)	Chacra et al. (2005) Schoenung and Burns (1996) Ribeiro et al. (2001) Rehtanz (1999) Weissbach et al. (1999)	Chacra et al. (2005) Schoenung and Burns (1996) Ribeiro et al. (2001) Yau et al. (1981)	Chacra et al. (2005) Jung et al. (1996) Ribeiro et al. (2001) Tam and Kumar (1990) Yau et al. (1981)
Remote (Island) Locations			Alt et al. (1997) Kottick and Blau (1993) Kottick et al. (1993)	Alt et al. (1997) Clark and Isherwood (2004) Kottick and Blau (1993)	Alt et al. (1997) Clark and Isherwood (2004)
End Consumer	Daryanian et al. (1991) Lee and Chen (1995) Maly and Kwan (1995) Lee and Chen (1994) Nieuwenhout et al. (2006) Reckrodt et al. (1990)			Jenkins et al. (2008)	Lee and Chen (1995) Maly and Kwan (1995) Lee and Chen (1994) Reckrodt et al. (1990) Comnes et al. (1988)
Electric Vehicles				Kempton and Kubo (2000) Kempton and Tomic (2005) Kempton and Letendre (1997) Kempton et al. (2001)	Lund and Kempton (2008) Kempton and Letendre (1997) Pecas Lopes et al. (2009) Galus and Andersson (2009)

Table 2.2: Detailed Review of Storage Models in Literature

Reference	Algorithm	Objective	Modeled technology	Model details
Alt et al. (1997)	DP (using DYNASTORE)	econ.	battery	medium
Anderson and Lo (1999)	MPDP	econ.	battery	low
Barton and Infield (2004)	SIM, probabilistic methods	tech.	n/a	low
Bathurst and Strbac (2003)	LO	econ.	generic	medium
Baumann (1992)	n/a	env.	SMES	n/a
Chacra et al. (2005)	multi-objective optimization	econ.	PSB, VRB	medium
Chowdhury and Rahman (1988)	n/a	econ.	battery	medium
Clark and Isherwood (2004)	SUPERCODE optimization	econ.	zinc air, hydrogen	medium
Comnes et al. (1988)	n/a	econ.	thermal storage	low
Daryanian et al. (1991)	LO	econ.	thermal storage	low
Exarchakos et al. (2009)	LO	econ.	lead-acid, VRB, CAES, PHS (var)	medium
Ferreira (1992)	DP	econ.	PHS	high
Graves et al. (1999)	LO	econ.	generic	n/a
Jenkins et al. (2008)	round-based SIM	tech.	lead-acid	**high**[a]
Jung et al. (1996)	round-based SIM	tech.	battery	medium
Kandil et al. (1990)	LO	econ.	generic	low
Korpaas (2004)	DP	tech.	generic	n/a
Kottick et al. (1993)	n/a	tech.	battery	medium
Kottick and Blau (1993)	n/a	tech., econ.	battery	low
Lee (1992)	MPDP	tech., econ.	PHS, battery	medium
Lee and Chen (1993)	DP	econ.	battery	medium
Lee and Chen (1994)	adv. MPDP	tech., econ.	battery	medium
Lee and Chen (1995)	MPDP	econ.	battery	medium
Maly and Kwan (1995)	DP	econ.	battery	medium[b]
Nieuwenhout et al. (2006)	SA	econ.	lead-acid, Li-ion	medium
Poonpun and Jewell (2008)	SA	econ.	VRLA NaS, ZnBr, flywheel, VRB	high
Rau and Short (1996)	successive QOP	tech.	other hydro	low
Rau and Taylor (1998)	DP	econ.	battery	low
Reckrodt et al. (1990)	n/a	econ.	battery	high
Rehtanz (1999)	n/a	tech.	SMES	high
Ribeiro et al. (2001)	n/a	tech.	flywheel, battery	low
Schoenung and Burns (1996)	SA	econ.	SMES, flywheel, capacitors, CAES, CAS, PHS	low
Schoenung and Eyer (2005)	SA	econ.	VRLA, NiCd, VRB, ZnBr, Li-ion, flywheel (high speed), hydrogen	low
Sioshansi et al. (2009)	LO	econ.	generic	low
Sobieski and Bhavaraju (1985)	synthetic system D (EPRI)	econ.	battery	n/a[c]
Su and Huang (2001)	n/a	econ.	battery	n/a
Sullivan (1982)	QOP	econ.	battery	medium
Tam and Kumar (1990)	EMTP v2.0, EPRI	tech.	SMES	n/a
Vosen and Keller (1999)	HA, using NN	tech.	hydrogen, battery	medium
Walawalkar et al. (2007)	MC SIM, SA	econ.	NaS, flywheel	low
Weissbach et al. (1999)	n/a	tech.	flywheel	high
Wu et al. (2002)	LO	econ.	lead-acid	**high**[a]
Yau et al. (1981)	UMC hybrid SIM	tech.	battery	medium

DP=Dynamic Programming, HA=Heuristic Algorithm, LO=Linear Optimization, MDPD=Multi-Pass DP, QOP=Quadratic Optimization Problem, SA=Statistical Analysis, SIM=Simulation.
CAES=Compressed Air Energy Storage, CAS=Compressed Air in Vessels, NaS=Natrium Sulfur=Sodium Sulfur, PHS=Pumped Hydro Storage, PSB=Polysulfide-Bromine, SMES=Superconducting Magnetic Energy Storage, VRB=Vanadium Redox Battery, VRLA=Valve-Regulated Lead Acid, ZnBr=Zinc Bromide.

[a] Includes parameter for Depth of Discharge.
[b] Includes electro-technical details.
[c] Includes a detailed parameter specification.

Chapter 3

Design and Analysis of Storage Optimization Models

This chapter presents the analysis results and definition of an estimation model and a linear optimization model. The estimation model in Section 3.1 is used to derive a simple and transparent estimate of the saving potential through DSS at the end consumer level by performing a statistical analysis (published in Ahlert and van Dinther (2009a)). Section 3.2 defines a more complex model that accurately implements economic and technical characteristics of a storage system (published in Ahlert and van Dinther (2008)). In a second step, this models is transformed into a linear optimization model (published in Ahlert and van Dinther (2009b)). Section 3.3 gives a summary and a conclusion of the analysis results.

3.1 Basic Estimation Model

The main goal of the basic model is to estimate the economic benefits of a DSS at the end consumer level with a simple and transparent approach. The results of this model will give a first indication whether DSS at the end consumer level could result in a positive saving potential for the end consumers. The model uses a simple charge and discharge decision heuristic aiming at arbitrage accommodation. The basic approach is to charge the device at low prices and to discharge at peak prices. The decision heuristic indicates the system when to charge and discharge the storage device in order to maximize the average arbitrage accommodation per day in a given time period. The time period consists of T timeslots and D days. The index for timeslots is $t = 1 \dots T$, for days it is $d = 1 \dots D$. Each day has $T^D = T \cdot D^{-1}$ timeslots. The results of the model will allow to estimate the impact of the storage device on the total costs for the given time period.

In the following, Section 3.1.1 will define the basic parameters of the storage model and describe the data sources used. Section 3.1.2 defines a simple model that estimates the economic saving potential of DSS and Section 3.1.3 summarizes and critically evaluates the results of the estimation model.

3.1.1 Parameters and Data Sources

The parameters of the model describe the technical characteristics of the storage device, the energy demand for each timeslot (kWh), the market price per energy unit in

each timeslot (EUR/kWh) and the decision variables.

Storage parameters

- C is the maximal capacity of the storage device (kWh)
- η is the efficiency degree of the storage device (%), with $0 \leq \eta \leq 100$
- v is the number of timeslots needed to fully charge the storage device at the maximal charging speed (# of timeslots)
- ψ is the storage costs per nominal (full) charge cycle (EUR/nominal cycle), defined as the quotient $\psi = \alpha \cdot \gamma^{-1}$, where α is the total investment and operational costs over life time and γ the expected number of nominal (full) charge cycles over life time of the storage

Energy demand and market price parameters

- ℓ_t is the energy demand (load) in timeslot t (kWh)
- p_t is the market price per energy unit in timeslot t (EUR/kWh)

Auxiliary parameters

- $t_d := rank(p_t, d)$ indicates the rank of a market price p_t within a the day d from $t_d = 1$ for the lowest price of the day (timeslot with the lowest price) to $t_d = t^D$ for the highest price

Decision variables

- i is the limit for a ranked market price for off-peak timeslots in which the system charges the storage device, i.e., the system should charge the storage if the rank t_d of the current market price p_t is less than or equal to i, thus $t_d \leq i$ with $1 \leq i \leq T^D$
- j is the according limit for peak timeslots in which the storage is discharged, i.e., if the rank t_d of the current market price p_t is greater than or equal to j, thus $t_d \geq j$ with $1 < j \leq T^D$

Thus, the limits i and j define the lower bound of the peak timeslots for discharging respectively the upper bound of the off-peak timeslots for charging the storage device. Since the limit parameters i and j apply for the entire time period (365 days of the year 2007) with different weekdays and seasons, they are defined as index values instead of absolute prices, i.e., the i-lowest and the j-highest price for each day.

The data input was varied within four scenarios as presented in Table 3.1. The efficiency degrees and the storage costs are derived from battery storage technologies in a developmental stage (Sauer, 2007). Data for market prices accord to the price curve distribution of the published hourly prices in 2007 at the EEX (2007) and are normalized to a weighted average price of 0.20 EUR/kWh. The data for the energy demand (load) reflect the standard "H0 profile" (profile of a private household) published by the German Electricity Association[1](VDEW, 2006). The standard "H0 profile" is

[1]Today, the German Electricity Association (VDEW) is part of the German Energy and Water Association (BDEW).

normalized to an annual consumption of 1,000 kWh and multiplied with a random vector (± 15% for each value). The granularity of the load data corresponds to 15-minute-timeslots. The hourly market price data has therefore been transformed into 15-minute-timeslots as well. Thus, each day contains 96 timeslots for 365 days in 2007, resulting in 35,040 timeslots for the following analyses.

Table 3.1: Parameter Values for Basic Estimation Model

Scenario	**Capacity** C **(kWh)**	**Charging speed** v **(#timeslots)**	**Efficiency** η **(%)**	**Storage costs** ψ **(EUR/cycle)**
Scenario 1	0.5	2	80	0.10
Scenario 2	0.5	2	90	0.10
Scenario 3	1.0	4	80	0.10
Scenario 4	1.0	4	90	0.10

3.1.2 Model Definition

The model will determine the economic impact of varying the limits for off-peak timeslots and peak timeslots in which the system will charge respectively discharge the storage device in order to maximize the arbitrage accommodation. The model will therefore calculate the savings through storage usage for different charge and discharge limits. The savings are calculated against the costs baseline K (EUR) of a system without storage usage, based on the given vectors p_t for the market price and ℓ_t for the demand per timeslot:

$$K = \sum_{t=1}^{T} \ell_t \cdot p_t \tag{3.1}$$

For each day d, $\overline{\ell}_d^j$ determines the volume of the demand within the peak timeslots,

$$\overline{\ell}_d^j = \sum_{t \in \overline{t}_d^j} \ell_t \quad \text{where} \quad \overline{t}_d^j := \{t | t_d \geq j\} \tag{3.2}$$

The average costs per energy unit in the off-peak timeslots of day d is

$$\underline{k}_d^i = \frac{\sum\limits_{t \in \underline{t}_d^i} p_t}{i} \quad \text{where} \quad \underline{t}_d^i := \{t | t_d \leq i\} \tag{3.3}$$

The weighted average costs per energy unit in the peak timeslots is

$$\overline{k}_d^j = \frac{\sum\limits_{t \in \overline{t}_d^j} \ell_t \cdot p_t}{\overline{\ell}_d^j} \quad \text{where} \quad \overline{t}_d^j := \{t | t_d \geq j\} \tag{3.4}$$

The model determines the economic benefit of shifting load from peak timeslots (discharging) to off-peak timeslots (charging). The objective function of the model

calculates the savings against the baseline costs for each tuple and takes storage costs into account:

$$\max \rightarrow \frac{1}{K} \cdot \underbrace{\sum_{d=1}^{D} \overline{\ell}_d^j \cdot \left(\overline{k}_d^j - \frac{\underline{k}_d^i}{\eta} \right)}_{A} - \underbrace{\frac{\overline{\ell}_d^j \cdot \psi}{C}}_{B} \tag{3.5}$$

Term A determines the arbitrage benefit. In total, $\overline{\ell}_d^j$ energy units (kWh) will be shifted from peak timeslots to off-peak timeslots. The arbitrage benefit for each shifted energy unit corresponds to the difference between the weighted average costs per energy unit in the peak timeslots $\overline{k}_d^j$ and the average costs per energy unit in the off-peak timeslots $\underline{k}_d^i$. Due to the limited efficiency degree of the storage device, the amount of energy charged into the storage device (respectively the price paid) must be higher than the amount that is actually discharged, therefore $\underline{k}_d^i \cdot \eta^{-1}$. The arbitrage benefits from Term A must be reduced by the costs for storage usage in Term B. Given the amount of load shifted $\overline{\ell}_d^j$ and the maximal capacity of the storage device C, $\overline{\ell}_d^j \cdot C^{-1}$ charge cycles are required with costs of ψ per nominal charge cycle.

To obtain a valid solution, the input parameters for the objective function must comply with two constraints. The tuple (i, j) must not lead to overlapping off-peak and peak timeslots:

$$i < j \tag{3.6}$$

The second constraint reflects the maximal charging speed of the storage device. Since the required number of timeslots to fully charge the storage device is v and $\overline{\ell}_d^j \cdot C^{-1}$ energy units need to be shifted, the charging limit i must fulfill

$$i \geq v \cdot \frac{\underline{\ell}_d^i}{C} \qquad \forall d \tag{3.7}$$

3.1.3 Results

Figure 3.1 shows the result for variations of the charging limit i. In this case, the optimal (i.e., resulting in maximal reduction of total costs) value for the discharging limit j has been chosen automatically. Accordingly, Figure 3.2 shows the result for variations of the discharging limit j with optimal values for the charging limit i. The maximal reduction of total costs with the basic model is estimated at $\sim 9\%$.

The results reveal that the underlying costs per capacity unit (which links the parameters capacity and storage costs) is the most important factor to reduce the total costs. Scenario 3 and 4 with a storage capacity of 1,000 Wh and storage costs of 0.10 EUR per nominal charge cycle result in a maximal reduction of total costs of $\sim$ 9%, whereas Scenarios 1 and 2 with a 500Wh-capacity-storage device and the same storage costs (i.e., relatively twice as high as in Scenarios 3 and 4) achieve $\sim$ 3% total costs reduction only. Clearly, these results must be interpreted in the context of the given load profile with a normalized annual load of 1,000 kWh, which is below the consumption volume of an average household in Europe or the US.

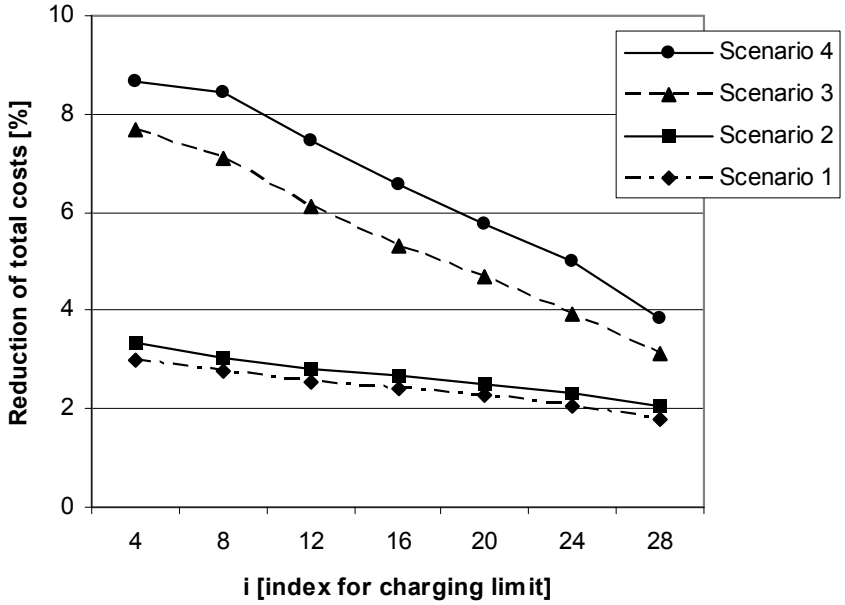

Figure 3.1: Impact of varying the charging limit i

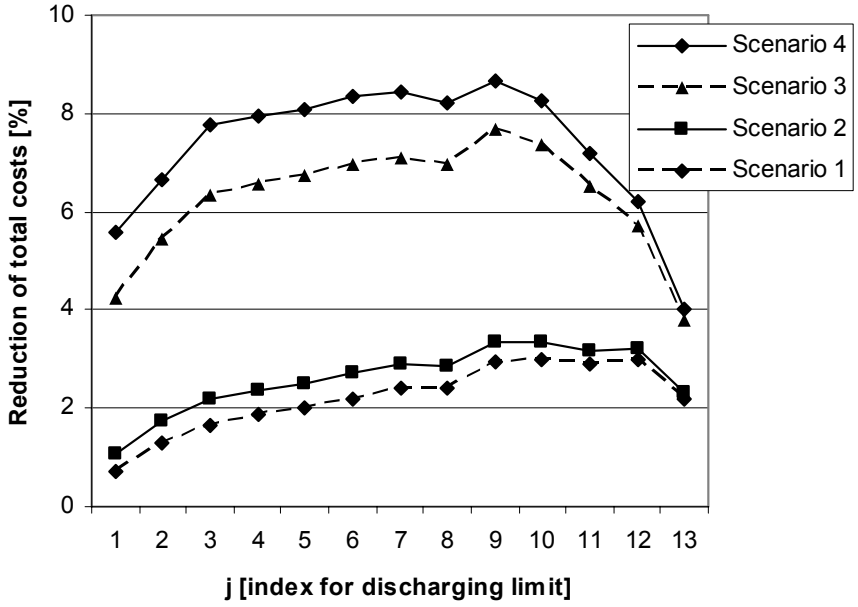

Figure 3.2: Impact of varying the discharging limit j

Regarding the definition of the limit values, the results reveal that setting the charging limit has a significant impact on the overall results. A too largely defined period of off-peak timeslots will result in significantly lower reduction of total costs. In contrast, the limit for defining the peak timeslots has little influence on the reduction, if the limit is in the range of $j = 56$ to $j = 80$. In case of the charging limit, the realized reduction of total costs decreased significantly for limit values of $i > 8$. For a heuristic decision algorithm without (precise) ex-ante knowledge of the price curve's distribution this implies a greater risk when setting the absolute charging limit for a day (depending on the expected price distribution for the day): if the limit is set too high, the realized arbitrage accommodation will be significantly lower than the best

(with this algorithm) achievable value. If set too low, no arbitrage accommodation will be realized on that day. In case of setting the discharging limit, this risk is lower due to the larger range of discharge limits that lead to a solution close to the best achievable result with this algorithm.

For a heuristic decision algorithm including a forecast function, this implies that the quality of price forecasting for off-peak timeslots (i.e., lowest market prices for a day) has greater importance than price forecasting for peak timeslots (i.e., highest market prices of a day).

As described, the presented model estimates the total costs reduction achieved by a simple heuristic decision algorithm; it does not calculate the maximal reduction of total costs for the described scenarios. In order to benchmark the results of this model and to evaluate the improvement potential of the presented model, Section 3.2 presents a linear optimization model that outlines the theoretically maximal reduction of total costs.

3.2 Linear Optimization Model

The objective of the linear optimization model is to determine the minimal total costs for a given time period. For each timeslot t in the given period, the model can determine the amount of energy to charge into the storage device respectively to discharge from it. The time period consists of T time-slots t with $t = 1 \dots T$. The decision variables are $\varphi_t \in [0; 1]$ for charging and $\lambda_t \in [0; 1]$ for discharging the storage device (see Table 3.2). The decision variables indicate the percentage of time at which the storage is charged respectively discharged in timeslot t.

Hence, the possible modes for the storage device are charging ($\varphi_t > 0$), waiting/idle ($\varphi_t = 0 \wedge \lambda_t = 0$) and discharging ($\lambda_t > 0$).

Table 3.2: Decision Parameters

Parameter Description	Symbol	Unit	Value
Charge parameter for timeslot t	φ_t	(%)	$0 \leq \varphi_t \leq 100$
Discharge parameter for timeslot t	λ_t	(%)	$0 \leq \lambda_t \leq 100$

3.2.1 Parameters

Analyzing and assessing the economic benefits of a storage system at the end consumer level requires a detailed description of the storage system's technical specification and of the external parameters of the environment where the storage system is located. The storage system consists of the storage device and peripherals, e.g., power converters. The external parameters contain information about the context of the consumer and the energy market where the consumer obtains its energy from. Figure 3.3 depicts an overview of the basic parameters and their interdependencies.

Market Parameters

The relevant parameters from the energy market are the price curve with its specific granularity and distribution. The extremes of the price curve's granularity are flat

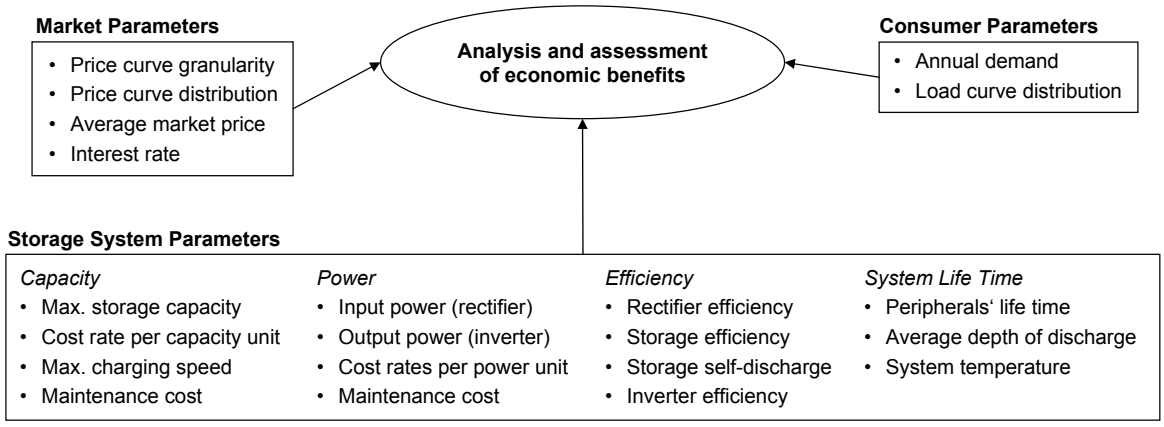

Figure 3.3: Overview of model parameters (build on Kowal and Sauer (2007))

tariffs, i.e., the same price per energy unit for the entire time period, and RTP, i.e., potentially varying prices for each point in time. Between these two extremes, one can distinguish several tariff variants, e.g., day-vs.-night tariffs, blocked tariffs, and hourly tariffs. Figure 3.4 illustratively depicts price curves with different time-block tariffs. In the case of hourly or RTP the shape of the price curves can differ depending on how supply and demand match on the market, as shown in Figure 3.5. All given price curve examples have the same average prices. The parameter p_t models the price curve by indicating the energy price (EUR/kWh) per timeslot t and, thus, combines the price curve's granularity and distribution.

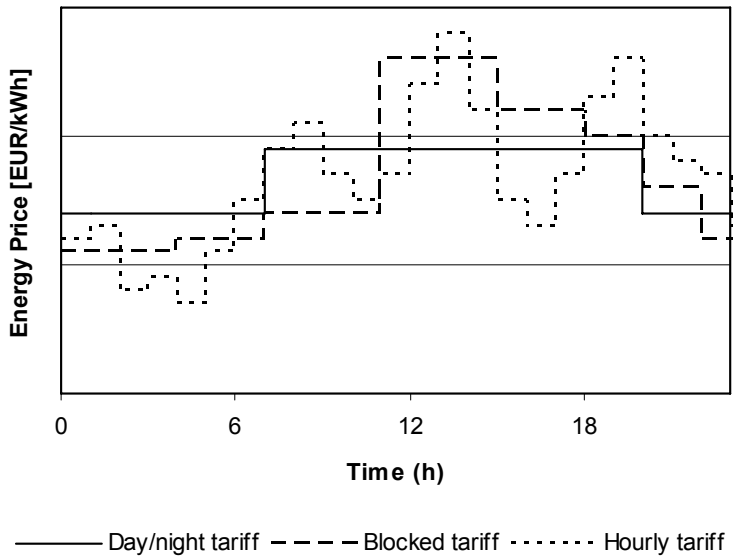

Figure 3.4: Sample plots of different price granularities

Another market parameter, which is not directly related to the energy market, is the interest rate i (%). The interest rate is the key parameter for determining the capital cost of the storage system's investment costs. Table 3.3 contains the market and consumer parameters.

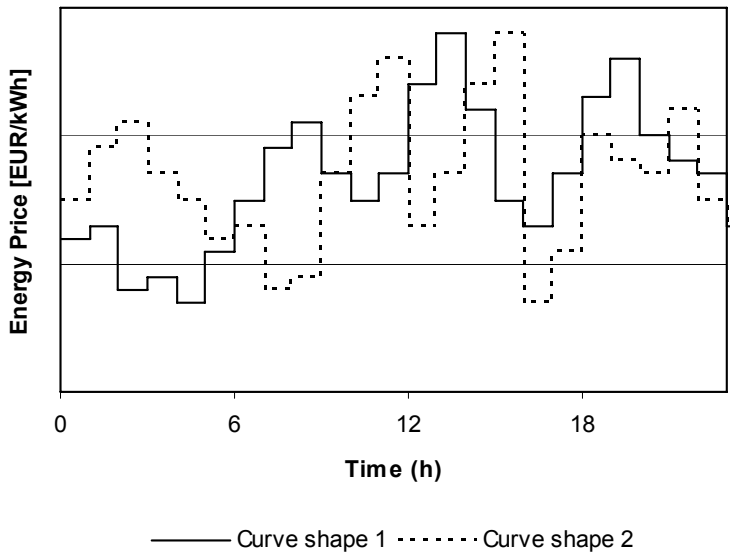

Figure 3.5: Sample plots of different price curve shapes

Consumers Parameters

The relevant parameters for the consumer side describe the load curve (synonymously for consumption or demand) with its shape and the annual load. The shape and the aggregated height (annual load) of the load curve can differ depending on the end user living situation, habits, and electrical devices used.

According to the market price curve in Paragraph 3.2.1, the parameter l_t models the load curve by indicating the load (kWh) per timeslot t. To use load data in a model, the availability of load data and its granularity respectively are the determining factors.

Table 3.3: Market and Consumer Parameters

Parameter Description	Symbol	Unit	Value
Price per energy unit in timeslot t	p_t	(EUR/kWh)	Flexible end consumer prices
Interest rate	i	(%)	7
Load (demand) in timeslot t	ℓ_t	(kWh)	Standard household profiles

Storage System Parameters

The key parameters of a storage system are its dimensions *capacity, power, efficiency*, and *estimated system life time*, as well as their corresponding cost components. The capacity dimension contains the maximal storage capacity C (kWh) of the storage device, the cost per storage capacity unit κ (EUR/kWh), and the charging speed of the chosen storage technology v^{store} (h), which indicates the time required for a nominal charge cycle.

The power dimension can be split into input and output. The power of the rectifier (ac to dc) determines the input power P^{in} (kW) and the power of the inverter (dc to ac) determines the output power P^{out} (kW) of the storage system. The costs per

power unit are π^{in} (EUR/kW) respectively π^{out} (EUR/kW). Additionally to the costs for capacity and power, the storage system has annual maintenance cost. The annual maintenance share m (%) is a percentage of the system's initial investment cost.

The efficiency of the storage system is determined by the efficiency of the power input component (rectifier) η^{in} (%), the charging efficiency of the storage device η^{store} (%), and the power output component (inverter) η^{out} (%) (Bodach, 2006). Additionally, the self-discharge rate per hour of the storage technology η^{selfdch} (% per hour) determines the overall efficiency of the system. Figure 3.6 gives an overview of the efficiencies.

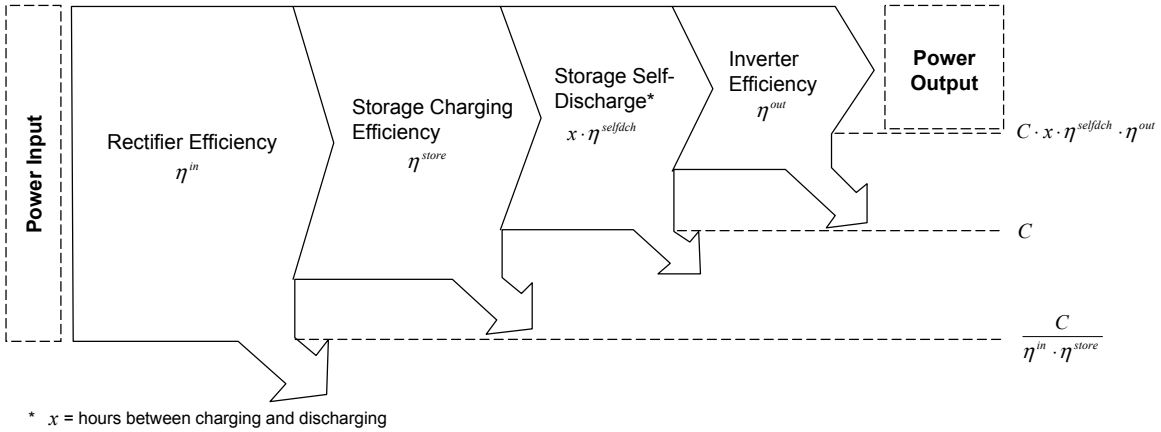

Figure 3.6: Efficiency degrees of a storage system[2]

The estimated life time of the system can be distinguished into the expected life time of the peripherals τ (years) and the number of expected nominal (full) charge cycles of the storage device γ (#), according to a defined limit for the maximal DOD $\bar{\delta}$ (%). It is assumed that the life time of the peripherals τ (years) is independent from the usage intensity, given regular maintenance. Contrary, the number of expected nominal (full) charge cycles γ (#) highly depends on the usage intensity, namely the average DOD δ (%) and the temperature of the storage system θ ($^{\circ}C$). Figure 3.7 shows the interdependencies of these parameters and Table 3.4 contains an overview of all storage system parameters.

3.2.2 Model Definition

The total costs of installing and operating the storage system consist of a fixed and a variable component:

$$K^{total} = K^{fixed} + \sum_{t=1}^{T} K_t^{variable} \tag{3.8}$$

Sections 3.2.2 and 3.2.2 describe the fixed and variable cost component in more detail. Section 3.2.2 contains the mathematical model formulation and Section 3.2.2 presents the simplified model implementation.

[2]Based on Ter-Gazarian (1994).

[3]Left side taken from Kowal and Sauer (2007), cited after Varta and Johnson Control (2007) (unknown source).

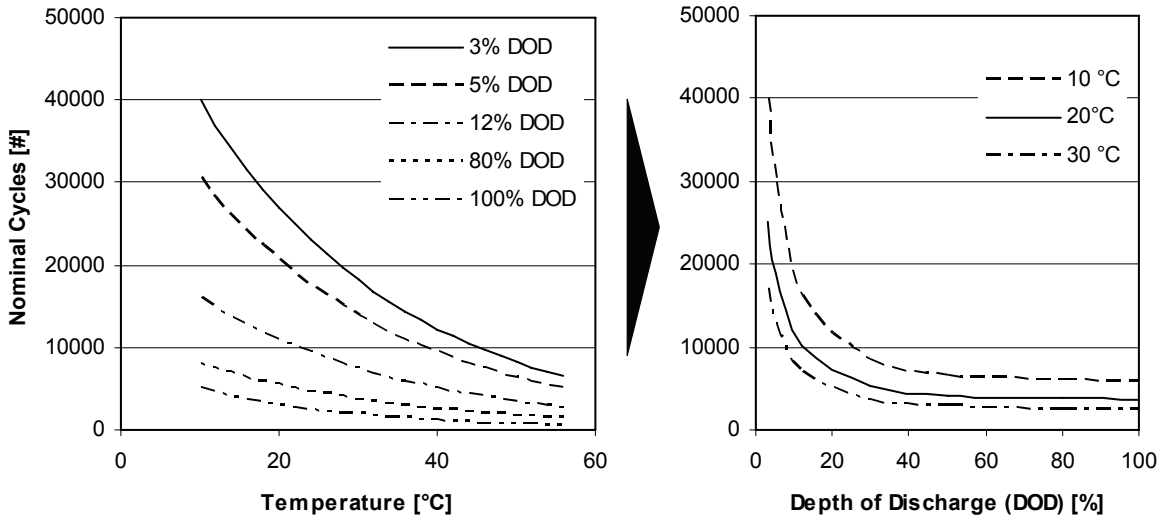

Figure 3.7: Nominal cycles as function of DOD and temperature, example of NiMH batteries[3]

Fixed Cost Components

The fixed costs are independent from the charge and discharge cycles of the storage system. They contain the annual depreciation rate for the peripheral components, the capital cost of the initial investment into the storage system, and the annual maintenance cost for the storage system, i.e., the storage device and the peripheral components.

$$K^{fixed} = K^{peripherals\_depreciation} + K^{capital\_cost} + K^{maintenace} \tag{3.9}$$

It is assumed that the life time of the peripherals τ (years) is independent from the usage intensity, given regular maintenance. Components for power input and output represent the storage system's peripherals in this model.

$$K^{depreciation\_peripherals} = \frac{P^{in} \cdot \pi^{in} + P^{out} \cdot \pi^{out}}{\tau} \tag{3.10}$$

Both capital cost and maintenance cost are defined as percentages of the initial investment in the storage device (capacity) and the system peripherals (power):

$$K^{capital\_cost} = i \cdot (P^{in} \cdot \pi^{in} + P^{out} \cdot \pi^{out} + C \cdot \kappa) \tag{3.11}$$

$$K^{maintenance} = m \cdot (P^{in} \cdot \pi^{in} + P^{out} \cdot \pi^{out} + C \cdot \kappa) \tag{3.12}$$

Variable Cost Components

The variable costs are dependent on the scheduling and the volume of the charge and discharge cycles. They contain the energy cost components for (external) market supply, the savings due to supply from the (internal) storage system, and the costs for

Table 3.4: Overview of Storage System Parameters

Parameter Description	**Symbol**	**Unit**
Maximal capacity of the storage device	C	(kWh)
Cost per storage capacity unit	κ	(EUR/kWh)
Maximal charging speed of the device (hours required for a full charge cycle)	v^{store}	(h)
Power-in of the storage system (rectifier)	P^{in}	(kW)
Power-out of the storage system (inverter)	P^{out}	(kW)
Cost per power unit (in)	π^{in}	(EUR/kW)
Cost per power unit (out)	π^{out}	(EUR/kW)
Annual maintenance cost as percentage of the initial investment	m	(%)
Rectifier efficiency (in)	η^{in}	(%)
Storage efficiency	η^{store}	(%)
Inverter efficiency (out)	η^{out}	(%)
Self-discharge rate of the storage device	η^{selfdch}	(%)
Estimated life time of system peripherals	τ	(years)
Expected nominal cycles of the storage device	γ	(#)
Maximal DOD allowed	$\bar{\delta}$	(%)
Average DOD until timeslot t	δ_t	(%)
Temperature of the storage system	θ	($^\circ C$)

charging the storage device. All these components are independent from the system's (charging) state. Additionally, the variable costs contain the storage depreciation costs, which are a state-dependent cost component.

$$K_t^{variable} = K_t^{market\_supply} - K_t^{storage\_supply} + K_t^{storage\_charging} + K_t^{storage\_depreciation} \tag{3.13}$$

State-independent cost components The costs for (external) market supply correspond to the costs the consumer would have without using a storage system, i.e., the price per energy unit in timeslot multiplied with the load (demand) volume in the same timeslot:

$$K_t^{market\_supply} = p_t \cdot \ell_t \tag{3.14}$$

The savings due to supply from the (internal) storage system in timeslot t indicate the cost reduction respectively reduction of demand on the external market due to storage discharge ($\lambda > 1$), i.e., the demand is partly or fully served from the storage device.

$$K_t^{storage\_supply} = p_t \cdot \lambda_t \cdot q_t^{out} \tag{3.15}$$

The potential discharge volume q_t^{out} in timeslot t is limited by the power output P^{out} and the maximal capacity C of the storage system (T^h is a model parameter that indicates the number of timeslots per hour):

$$q_t^{out} = \min\left(\lambda_t; \min\left(C; \frac{P^{out}}{T_h}\right)\right) \tag{3.16}$$

The costs for charging the storage device in timeslot t ($\varphi_t > 0$) base on the price per energy unit in the current timeslot p_t and the potential charge volume q^{in} .

$$K_t^{storage\_charging} = p_t \cdot \varphi_t \cdot q^{in} \tag{3.17}$$

The storable volume per timeslot is limited by the maximal charging speed v to $C \cdot v^{-1}$. The necessary charge volume q^{in} exceeds the stored volume due to limited efficiency degrees of the power input component and the storage device itself.

$$q^{in} = \frac{C}{\eta^{in} \cdot \eta^{store} \cdot v} \tag{3.18}$$

The maximal charging speed of the storage system v (#) indicates the required timeslots for a nominal charge cycle. It depends on the slowest component (system's peripherals power limitation vs. charging speed of the storage device v^{store}):

$$v = T^h \cdot \max\left(\frac{C}{P^{in}}; v^{store}\right) \tag{3.19}$$

State-dependent cost components As explained in Paragraph 3.2.1, the number of expected nominal (full) charge cycles γ (#) of a storage device highly depends on the usage intensity, namely the average DOD δ (%) and the temperature of the storage system θ ($^\circ C$). In the following, the temperature θ is assumed constant.

A higher average DOD leads to a reduction of nominal charge cycles γ , which again has a direct influence on the depreciation of the storage device. One can formulate the costs for a full charge cycle ψ (EUR) as follows:

$$\psi = \frac{C \cdot \kappa}{\gamma} \tag{3.20}$$

The deeper the storage device is discharged, the higher the marginal cost per nominal charge cycle (see Figure 3.8). Since a discharge cycle can last for several timeslots, the discharge action in timeslot t must also cover the increasing marginal costs for the previous discharge action. A discharge action is defined as a reduction of the system's storage level due to intended discharge or self-discharge of the storage device. Thus, the storage depreciation cost in timeslot t must cover the marginal depreciation cost for the discharge action in timeslot t and the difference between the marginal depreciation cost in t and $t-1$ for the previous discharge:

$$K_t^{storage\_depreciation} = sg \cdot (1 - \varphi_t) \cdot [(\xi_t - \xi_{t-1}) \cdot \psi_t + \widehat{q}_{t-1} \cdot (\psi_t - \psi_{t-1})] \tag{3.21}$$

The auxiliary function $sg(x)$ is defined as follows:

$$sg(x) = \begin{cases} 1 & x > 0 \\ 0 & else \end{cases} \tag{3.22}$$

An alternative formulation of the storage depreciation cost is more compact[4]:

$$K^{storage\_depreciation} = C \cdot \kappa \left(\frac{\widehat{q}_t}{\gamma_t} - \frac{\widehat{q}_{t-1}}{\gamma_{t-1}} \right) \tag{3.23}$$

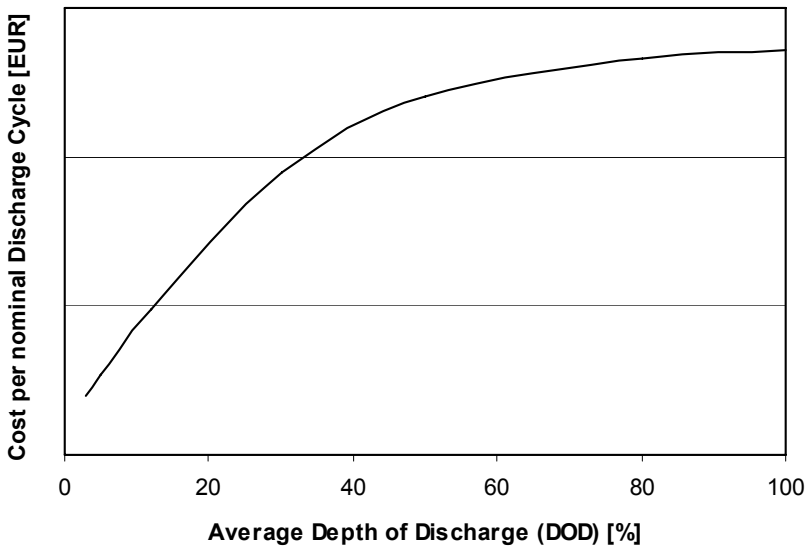

Figure 3.8: Interrelation of depth of discharge and cost per nominal discharge cycle

The previous discharge actions (sum of discharge volumes until $t-1$) $\widehat{q}_{t-1}$ is defined as:

$$\widehat{q}_t = \sum_{t'=1}^{t} \xi_{t'} - \xi_{t'-1} = \widehat{q}_{t-1} + (\xi_t - \xi_{t-1}) \tag{3.24}$$

where ξ_t indicates the system's state (storage level) in timeslot t . ξ_t takes the intended charge and discharge actions as well as self-discharge of the system during idle phases ($\varphi_t = 0 \wedge \lambda_t = 0$) into account:

$$\xi_t = \begin{cases} \sum_{t'=1}^{t} \frac{C}{v} \cdot \varphi_{t'} - \frac{q_{t'}^{out}}{\eta^{out}} \cdot \lambda_{t'} - \frac{\eta^{\text{selfdch}}}{T^h} \cdot (1 - \varphi_{t'} - \lambda_{t'} \xi_{t'-1}) & t > 0 \\ 0 & else \end{cases} \tag{3.25}$$

The marginal depreciation costs for a nominal cycle ψ_t in timeslot t are defined as:

$$\psi_t = \frac{C \cdot \kappa}{\gamma_t} \tag{3.26}$$

γ_t is the expected nominal cycles of the storage device, which is a technology-specific function. The function requires the system temperature θ and the average DOD δ_t until timeslot t as input factors (see Figure 3.7):

$$\gamma_t = f(\theta, \delta_t) \tag{3.27}$$

[4]Appendix A contains a derivation of equation (3.23) as well as a mathematical prove of the identity of equations (3.21) and (3.23).

$$\delta_t = 1 - \frac{\widetilde{\xi}_t}{C} \tag{3.28}$$

$\widetilde{\xi}_t$ is the average of load states (storage levels) after completed discharge cycles until timeslot t:

$$\widetilde{\xi}_t = \begin{cases} \frac{sg(1-\varphi_t)\cdot\xi_t + \sum_{t'=1}^{t}\max(0,\xi_{t'})}{sg(1-\varphi_t)+(t-1)+\sum_{t'=1}^{t}\min(0,\xi_{t'})} & t > 1 \wedge \sum_{t'=1}^{t} sg(\xi_{t'} - \xi_{t'-1}) > 0 \\ C & else \end{cases} \tag{3.29}$$

The auxiliary function $\overline{sg}(x)$ is defined as follows:

$$\overline{sg}(x) = \begin{cases} 1 & x < 0 \\ 0 & else \end{cases} \tag{3.30}$$

ξ_t indicates a local minimum in the sequence of load states with a value of $\xi_t \geq 0$. All other values are invalid values, i.e., no local minima.

$$\xi_t = \begin{cases} \xi_t & \xi_{t-1} \geq \xi_t \wedge \xi_t < \xi_{t+1} \wedge t > 0 \\ -1 & else \end{cases} \tag{3.31}$$

Mathematical Formulation

Based on the definitions and equations of the preceding paragraphs, one can now formulate the optimization problem. The objectives of the optimization model are to determine the optimal timeslots for charging and discharging the storage device in order to minimize the total cost for the given time period ($t = 1 \ldots T$). For each timeslot t, the model must determine the amount of energy to charge into the storage device respectively to discharge from it. The costs resulting by using an optimally dispatched storage system are calculated against the annual baseline cost $K^{baseline}$ (EUR) for an identical consumer scenario without a storage system.

$$K^{baseline} = \sum_{t=1}^{T} p_t \cdot \ell_t \tag{3.32}$$

Hence, the objective function of the linear optimization model is

$$\max \rightarrow 1 - \frac{1}{K^{baseline}} \cdot \left(K^{fixed} + \sum_{t=1}^{T} K_t^{variable} \right) \tag{3.33}$$

The constraints for the optimization problem are as follows: A solution is valid only if the decision variables φ_t and λ_t are kept within their range (3.34). Charging and discharging within the same timeslot t is allowed, but must not overlap (3.35). At each point in time, the system's state (storage level) must be positive, but not exceeding the maximal capacity of the storage device (3.36). After a start-up phase until $t^{startup}$ (initial charging), the State of Charge (SOC) ξ_t must not fall below the maximal DOD

$\bar{\delta}$ (%) (3.37). The SOC ξ_t in timeslot t must take the intended charge and discharge actions into account (3.25):

$$0 \leq \varphi_t, \lambda_t \leq 1 \quad \forall t \tag{3.34}$$

$$\varphi_t + \lambda_t \leq 1 \quad \forall t \tag{3.35}$$

$$0 \leq \xi_t \leq C \quad \forall t \tag{3.36}$$

$$(1 - \bar{\delta}) \cdot C \leq \xi_t \qquad \forall t > t^{startup} \tag{3.37}$$

The start-up phase until $t^{startup}$ can be set arbitrary, but must be in the following range to ensure a sufficiently long initial charging phase with respect to the system's charging speed v.

$$\left\lceil \left(1 - \bar{\delta}\right) \cdot v \right\rceil \leq t^{startup} \leq T \tag{3.38}$$

As formula 3.33 expresses, the usage of a storage system with the objective of arbitrage accommodation is beneficial, if the avoided cost for external supply in the moment of discharge are higher than the previously required cost for charging and using (depreciating) the storage device. If the cost for using (depreciating) the storage device are greater zero (standard case), this implies that the cost per unit for charging the device must be less than the cost for external supply (per unit) in the moment of discharge, i.e., flexible electricity tariffs are required.

Model Implementation

Modeling the fixed cost components and the variable, state-independent costs, i.e., independent from the system's state (storage level), can be realized in a linear optimization model with a standard format (scalar a is a constant, vectors A are constants and x are decision variables):

$$\min \rightarrow a + \sum A_{1.t} \cdot x_{1.t} + \ldots + A_{n.t} \cdot x_{n.t} \tag{3.39}$$

Also the SOC parameter ξ_t with its recursive definition as well as the accumulated discharge volume q_t , which bases on the SOC parameter, can be resolved and transformed into the format above. However, the variable, state-dependent costs, namely the storage depreciation costs, cannot be transformed into the format above, since the calculation of the costs for a nominal discharge cycle ψ_t cannot be linearized.

The implementation of the linear optimization model will transform the previously defined model into a standard form of a mixed-integer problem (3.39). Therefore, in contrast to the above defined mathematical model, its implementation assumes the number of expected nominal charge cycles as constant. This simplification implies

that the costs per discharge cycle are fixed, as well as the according average DOD δ. Thus, the costs of discharging the storage device are not state-dependent but state-independent, like the other cost components. The costs of a nominal charge cycle ψ (EUR) are therefore defined as

$$\psi = \frac{C \cdot \kappa}{\gamma} \tag{3.40}$$

The storage depreciation costs $K_t^{storage\_depreciation}$ in timeslot t are the product of the discharged volume relative to the storage system's capacity ($\lambda_t \cdot q_t^{out} \cdot C^{-1}$) and the costs for a nominal discharge cycle ψ (EUR):

$$K_t^{storage\_depreciation} = \frac{\lambda_t \cdot q_t^{out}}{C} \cdot \frac{C \cdot \kappa}{\gamma} = \lambda_t \cdot q_t^{out} \frac{\kappa}{\gamma} \tag{3.41}$$

Thus, the variable costs are defined as follows:

$$K_t^{variable} = p_t \cdot \ell_t - p_t \cdot q_t^{out} \cdot \lambda_t + p_t \cdot q^{in} \cdot \varphi_t + \frac{\kappa}{\gamma} \cdot q_t^{out} \cdot \lambda_t \tag{3.42}$$

For the formulation of the linear optimization model, $K^{variable}$ can be transformed into (3.43) with A_x as ex-ante given vectors.

$$K_t^{variable} = \lambda_t \underbrace{\left(q_t^{out} \left(\frac{\kappa}{\gamma} - p_t \right) \right)}_{A_1} + \varphi_t \underbrace{\left(q^{in} \cdot p_t \right)}_{A_2} + \underbrace{p_t \cdot \ell_t}_{A_3} \tag{3.43}$$

Analogously, (3.9) can be transformed into an ex-ante given scalar a_0, since all contained variables are constant and previously known. Also $K^{baseline}$ can be transformed into an ex-ante known scalar a_3, since p_t and ℓ_t are given. This implies that (3.43) can be further simplified to

$$K_t^{variable} = \lambda_t \cdot A_{1.t} + \varphi_t \cdot A_{2.t} \tag{3.44}$$

when transforming the objective function of the linear optimization model (3.33) to

$$\max \rightarrow 1 - \frac{1}{a_3} \cdot \left(a_0 + a_3 \cdot \sum_{t=1}^{T} \lambda_t \cdot A_{1.t} + \varphi_t \cdot A_{2.t} \right) \tag{3.45}$$

$$\Leftrightarrow \qquad \max \rightarrow a + \sum_{t=1}^{T} \lambda_t \cdot A_{1.t} + \varphi_t \cdot A_{2.t} \tag{3.46}$$

with

$$a = 1 - \frac{a_0}{a_3} \tag{3.47}$$

Thus, the objective function now corresponds to the standard format for linear optimization problems. The constraints of the model remain unchanged for the implementation:

$$0 \leq \varphi_t, \lambda_t \leq 1 \quad \forall t \tag{3.48}$$

$$\varphi_t + \lambda_t \leq 1 \quad \forall t \tag{3.49}$$

$$0 \leq \xi_t \leq C \quad \forall t \tag{3.50}$$

$$(1 - \bar{\delta}) \cdot C \leq \xi_t \qquad \forall t > t^{startup} \tag{3.51}$$

The start-up phase until $t^{startup}$ can be set arbitrary, but must be in the following range to ensure a sufficiently long initial charging phase with respect to the system's charging speed v.

$$\left\lceil 1 - \bar{\delta} \right\rceil \cdot v \leq t^{startup} \leq T \tag{3.52}$$

However, the SOC ξ_t need to be simplified. The current definition of ξ_t leads to a complex, recursive implementation due to the integration of self-discharge effects. For the implemented model it is assumed that the effects of self-discharge of the system are negligible within a period T^{selfdch} (# of timeslots).[5] The SOC ξ_t of the implemented model therefore disregards self-discharge and is reduced to

$$\xi_t = \sum_{t'=1}^{t} \frac{C}{v} \cdot \varphi_{t'} - \frac{q_{t'}^{out}}{\eta^{out}} \cdot \lambda_{t'} \tag{3.53}$$

An additional constraint of the linear optimization models avoids exceeding the technology-specific self-discharge tolerant time period T^{selfdch}. The distance between the charge volume and the discharge volume must be smaller than T^{selfdch}.

$$\varphi_t - \sum_{t'=t}^{t+T^{\text{selfdch}}} \lambda_{t'} \leq 0 \qquad \forall \;\; 1 \leq t \leq T - T^{\text{selfdch}} \tag{3.54}$$

[5]For battery storage technologies within the analyzed system, this assumption of $T^{\text{selfdch}} = 168$ (1 week) is made, since batteries have a very low self-discharge rate of 0.1-0.3% on a daily basis, i.e., around 0.7-2.1% per week. Since the average storage duration of a kilowatt hour in the analysis model turned out to be 0.7 days, the self-discharge effects under the given assumption are negligible. In other technology simulation, e.g., flywheel storage or capacitors, self-discharge over a time period of several hours is significant and will therefore deteriorate the results significantly. (cf. Chen et al. (2009))

3.2.3 Data Sources and Analysis Scenarios

The input values for the technical storage parameters reflect an average and a best case of a developmental stage of known technologies (see Table 3.5), published in Kowal and Sauer (2007). The best case of the lead-acid technology scenario is the reference case for all simulation results. Table 3.6 depicts the reference values for the remaining storage and market parameters. Data for market prices accord to the price distribution of the published hourly prices in 2007 on the EEX (2007) and are normalized to a weighted average price of 0.20 EUR/kWh. The data for the load curve (electricity demand) reflect the standard "H0 profile" (profile of a private household) published by the VDEW (2006). This reference load profile is normalized to an annual consumption of 2,000 kWh and multiplied with a random vector (±15% for each timeslot).

The granularity of the load data corresponds to 15-minute-timeslots. The hourly market prices have therefore been transformed into 15-minute-timeslots as well. Thus, each day contains 96 timeslots (timeslots per hour $T^h = 4$) for 365 days, resulting in 35,040 timeslots for the following analyses.

Table 3.5: Technology Scenarios[a]

	Technology	γ[b]	κ	π^{in}, π^{out}	η^{store}
Best Case	Lead-acid *(ref. scenario)*[c]	3000	100	120	85
	Nickel Cadmium	10000	400	120	70
	Li-ion	10000	300	130	95
Average case	Lead-acid	2100	175	175	82
	Nickel Cadmium	7500	550	177	65
	Li-ion	7000	650	315	92

[a] Published in Kowal and Sauer (2007)
[b] Maximum DOD: 80%.
[c] The best case of the lead-acid technology is the reference scenario for all later simulation results, unless differently stated.

3.2.4 Analysis Results

The linear optimization model calculated the optimal annual savings that a consumer could realize when using a storage system in comparison to the baseline scenario without a storage system.

The following paragraphs present the results of varying the input parameters of the reference case, namely the impact of sizing the storage system's capacity, performing sensitivity analyses to all technical and economic parameters, and modifying the characteristics of price and load curves.

Capacity Variation

The larger the storage system capacity, the more load can be shifted from peak to off-peak hours. Such load shifting is beneficial, if the spread between off-peak and peak tariffs is greater than the costs for using the storage device. The costs for using the device are determined by the technology used, namely its costs per storage capacity

Table 3.6: Reference Parameter Values

Symbol	Unit	Reference Value
p_t	(EUR/kWh)	Flexible end consumer prices[a]
ℓ_t	(kWh)	VDEW load profile[b]
i	(%)	7
m	(%)	2
τ	(years)	10
C	(kWh)	5.0[c]
P^{in}	(kW)	1.0[c]
P^{out}	(kW)	0.5[c]
η^{in}	(%)	95
η^{out}	(%)	98
η^{selfdch}	(%/h)	0[d]
T^{selfdch}	(#)	168
v^{store}	(h)	5.0
$\bar{\delta}$	(%)	80
T^h	(#/h)	4[e]

[a] Flexible end consumer price, weighted average 0.20 EUR/kWh, same distribution as spot market prices at the European Energy Exchange (EEX) in 2007.
[b] Standard household load profile in VDEW (2006).
[c] The optimal values for C, P^{in}, and P^{out} are adjusted depending on the simulated technology, consumer load curve, and market price curve. The reference values are the optimal values for the reference scenario.
[d] Self-discharge is neglected for the selected technology scenarios within the time period of T^{selfdch} timeslots.
[e] Model parameter (no storage system parameter).

unit and the expected number of nominal (dis-)charge cycles (see equations (3.16) and (3.18)). Disadvantageously, extending the capacity leads to higher fixed costs due to higher capital costs of the system (see equation (3.42)). Figure 3.9 shows the impact of capacity extensions for the technology cases presented in Table 3.5.

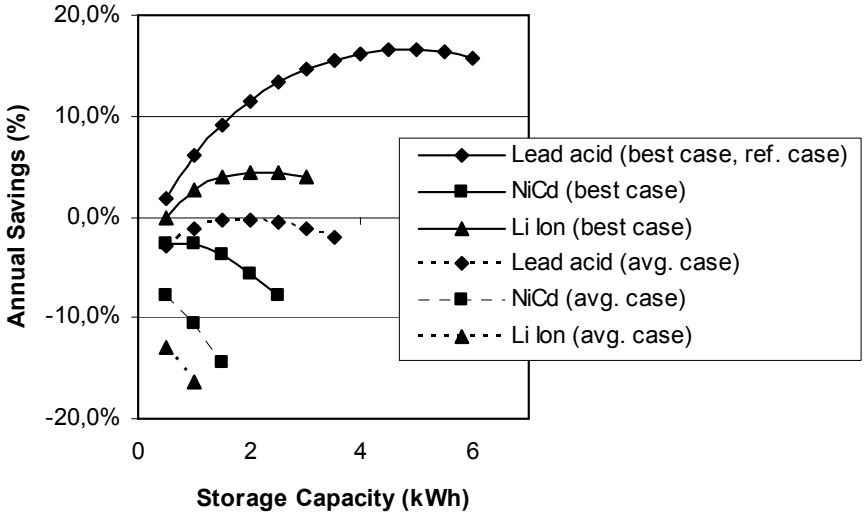

Figure 3.9: Impact of capacity variations for different technology cases

The results of the capacity variation reveal that the parameter "cost per storage capacity unit" κ (EUR/kWh) has the largest impact on the overall result. Although the li-ion technology (best case) has a by factor 3.3 higher number of expected life cycles and a higher storage efficiency than the lead-acid technology (best case), the lead-acid technology with its by factor 3.3 lower costs per capacity unit leads to significantly better results of ∼17% vs. ∼5% annual savings.

For the reference scenario, the system based on lead-acid technology has an optimal storage capacity of 5 kWh, while this is 2.5 kWh for the li-ion-based system. For larger capacity values, both cases result in lower percentage of annual savings, i.e., capital costs of the investment into additional storage capacity exceed its benefits through arbitrage accommodation.

For all other technologies, the analysis reveals negative annual savings. Thus, in these cases the use of a storage system is not beneficial for the given scenario.

For the following simulation results, the lead-acid technology scenario (best case) is the reference, unless a different scenario is explicitly named.

Variation of the Storage Price

The capacity variation analysis for the six different technology cases revealed that the lead-acid-based storage system had superior result to the li-ion-based system. The key differentiating parameter between these technology cases are the costs per storage capacity unit κ (EUR/kWh). Figure 3.10 shows the annual savings in dependency from κ for the lead-acid and the li-ion technology. The li-ion based case scenario achieves the same annual savings as the lead-acid-based case for storage capacity costs of approximately 175 (EUR/kWh). The analysis reveals that lead-acid system return positive savings in the given scenario, if the price per storage capacity unit falls below ∼200 EUR/kWh respectively ∼375 EUR/kWh for the li-ion technology.

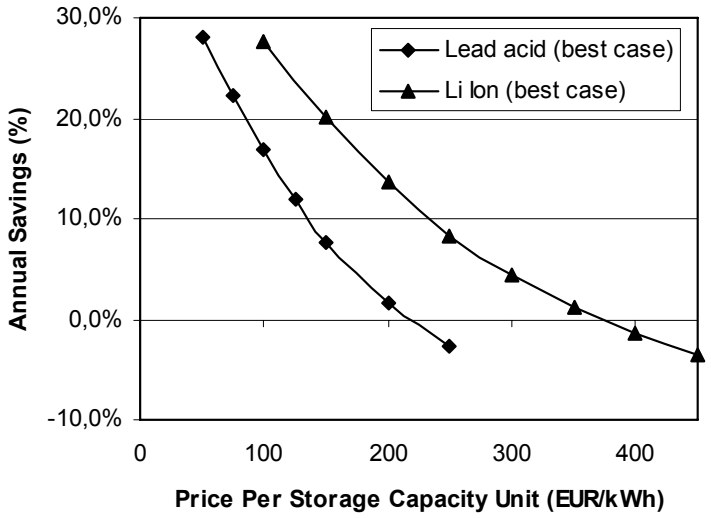

Figure 3.10: Impact of storage capacity price variations on annual savings

Sensitivity Analysis of System Parameters

Besides the storage system's capacity, technical and economic parameters of the storage system determine the annual savings. In order to assess their impact on the savings,

each parameter is varied separately in 4 levels (±1%, ±10%) from the reference value in Table 3.5 respectively 3.6 (all parameters are varied separately from each other). The results in Figure 3.11 reveal that variations of the efficiency parameters[6] and the costs per storage unit show the highest sensitivity on the annual savings. These results are in line with the findings of a sensitivity analysis in Sobieski and Bhavaraju (1985).

Although the variation of the cost per storage capacity unit shows a lower sensitivity than the efficiency degrees, it still has the highest absolute impact on the savings (see previous paragraph) due to the larger absolute differences between the parameter values (100 EUR/kWh (lead-acid) vs. 300 EUR/kWh (li-ion)). Variations of the remaining parameters have a minor influence on the savings.

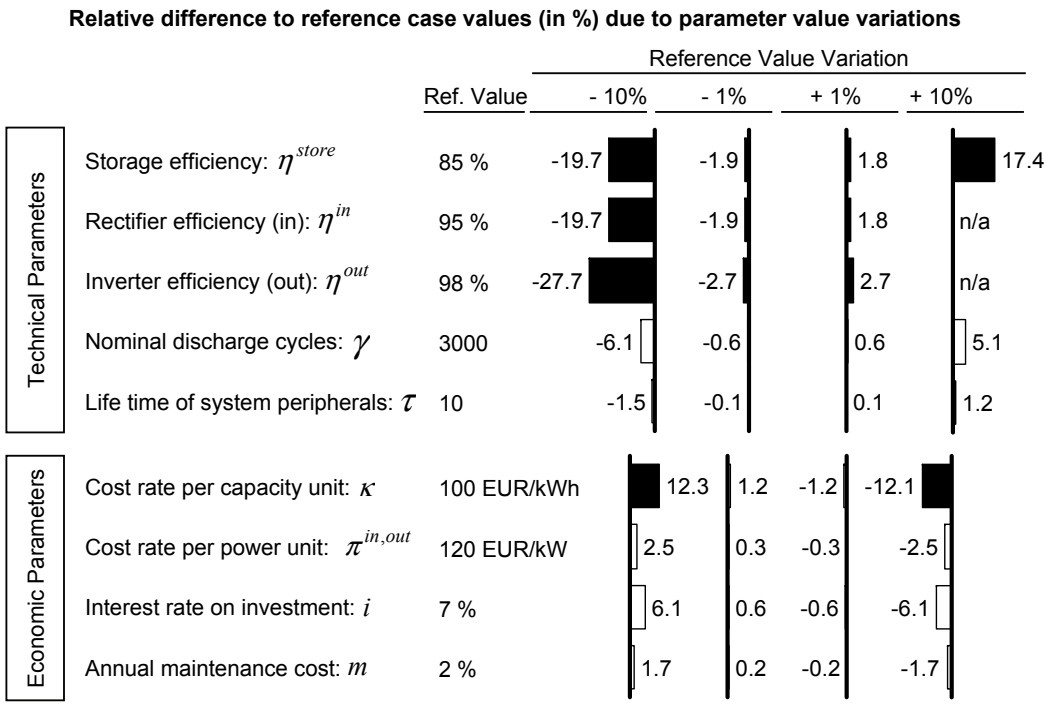

Figure 3.11: Sensitivity analysis for technical and economic storage parameters

Price Curve Variation

The fluctuations of the market price determine the off-peak and peak periods when the storage system can be charged respectively discharged. Additionally, the price level and the spread between peak and off-peak prices determine the charge and discharge volumes.

The following paragraphs analyze the relative impact of the average price spread, the average price level, and the price curve granularity on the annual savings. The point in time of peak and off-peak periods does not shift.[7] Table 3.7 contains the variables that were used to model the price curve variations.

[6]Storage efficiency and rectifier efficiency have the same impact due to the model formulation, see equation (3.18). An increase of the rectifier and inverter efficiency by 10% from the reference value is not applicable, since this would lead to efficiency values >100%.

[7]The effect of shifting peak and off-peak hours is indirectly analyzed in Paragraph 3.2.4, where the load curve distribution is varied.

Variation of the Average Market Price The market price vector contains a price p_t for each timeslot t. For the market price variation analysis, each price is increased respectively decreased with the same constant value. Price vectors with average market prices of 90%, 99%, 101%, and 110% of the reference vector's average price are compared in the analysis. For each price vector, Figure 3.12 depicts the relative savings in the context of the reference scenario.

Table 3.7: Price Curve Variation Parameters

Parameter Description	Symbol	Unit
Price per energy unit in timeslot t	p_t	(EUR/kWh)
Price vector $(p_1, \ldots, p_T)$ (reference)	P	
Average market price (reference)	$avg(P)$	(EUR/kWh)
Modified price in timeslot t	p_t^*	(EUR/kWh)
Variation factor	α	

The new market prices p_t^* (EUR/kWh) are calculated as

$$p_t^* = p_t + (avg(P) \cdot (\alpha - 1)) \tag{3.55}$$

Figure 3.12 compares the annual savings for each factor. It shows that the relative savings decrease in case of an increasing market price. Since all market prices for the analyzed time period are varied by the same constant factor, the realizable spreads remain the same. Thus, the absolute savings also remain equal. Since a decrease in market prices also leads to lower baseline cost (compare equation (3.32)), the relative savings decrease. Additionally, limited efficiency degrees even decrease the absolute savings in case of higher average market prices (see equations (3.42) and (3.18)).

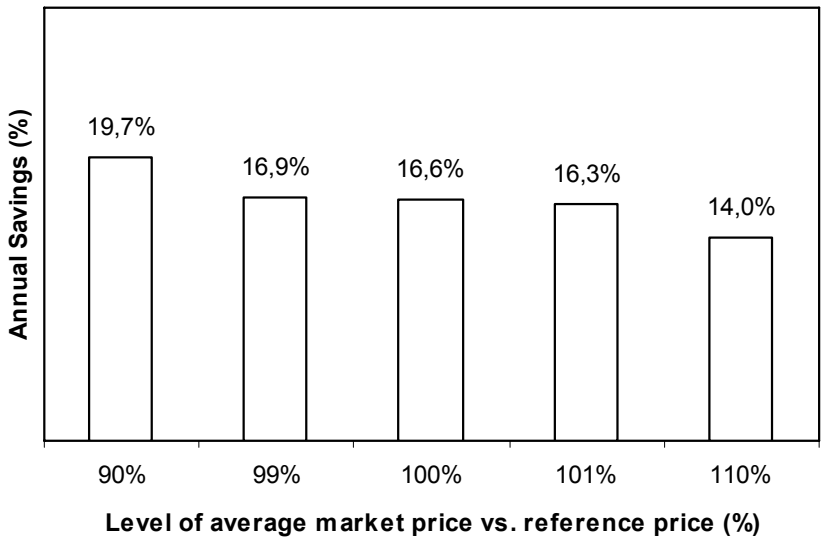

Figure 3.12: Impact of market price level variations

Variation of Price Spreads The variation of the average price spread analyzes an increase respectively decrease of the average spread, i.e., the average price difference between peak and off-peak timeslots. The average (annual) market price is constant in all compared cases in Figure 3.13. The factor α indicates the percentage change of the average price spread and the new market prices p_t^* (EUR/kWh) are calculated as

$$p_t^* = \alpha \cdot (p_t - avg(P)) + p_t \tag{3.56}$$

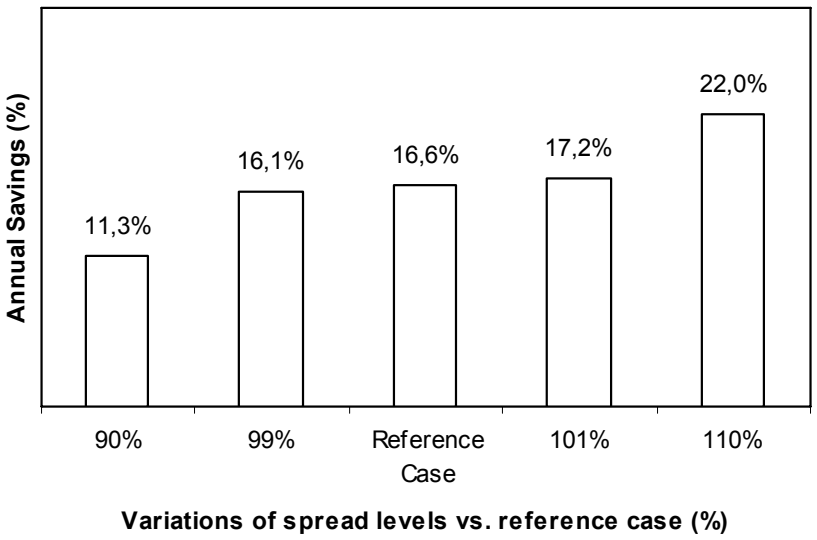

Figure 3.13: Impact of price spread variations

For the reference scenario, an increase of the average price spread by 1% leads to 0.6% point higher annual savings. An increase by 10% raises the annual benefits through the storage system to 22.0% (+5.4% points). In the context of increasing shares of intermittent energy sources that are likely to cause more volatility on future electricity prices, the significant influence of the spread supports the benefits of the storage model.

Variation of the Price Curve Granularity The price curve granularity determines the number of (potentially) different price blocks per day. The assumption is that all price blocks are of equal size, i.e., account for the same number of timeslots. The market price within a price block is constant. Figure 3.14 shows a sample plot of three price curve granularities.

All market price variations base on the reference price vector, which has 24 different price blocks per day. Figure 3.15 depicts the relative savings in dependency from the price curves granularity.

The block tariff vector p_t^* (EUR/kWh) with the block size β (# of timeslots per block) ($\beta \in \{1, 2, 3, \ldots\}$) is calculated on the basis of the reference price vector P:

$$p_t^* = \beta^{-1} \cdot \sum_{x=0}^{\beta-1} p_{t'+x} \tag{3.57}$$

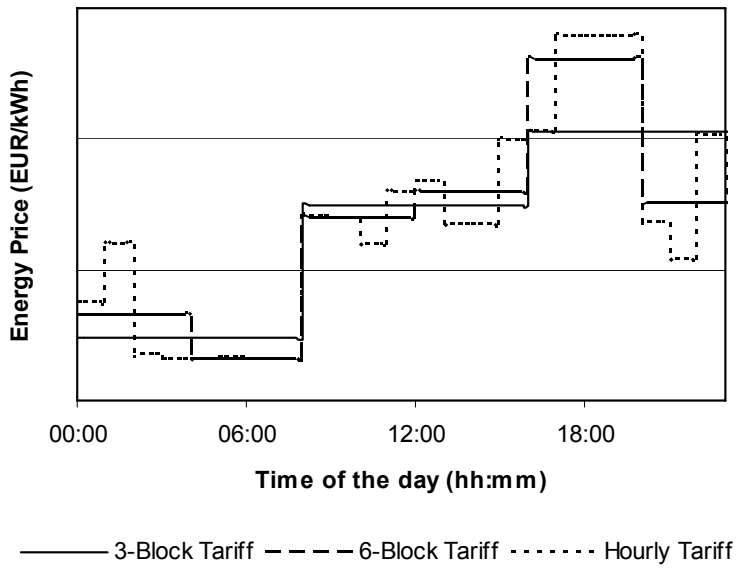

Figure 3.14: Sample plots of price curve granularities

where

$$t' = ((t-1) \bmod \beta) \tag{3.58}$$

The analysis shows that an increasing number of market price blocks per day increases the benefits from a storage system. A larger number of price blocks allow the storage system to charge in particularly low-price timeslots and to avoid external market supply in timeslots with extremely high prices. A decreasing number of price blocks flattens the extreme values of a price curve and impedes the arbitrage accommodation strategy of the storage system.

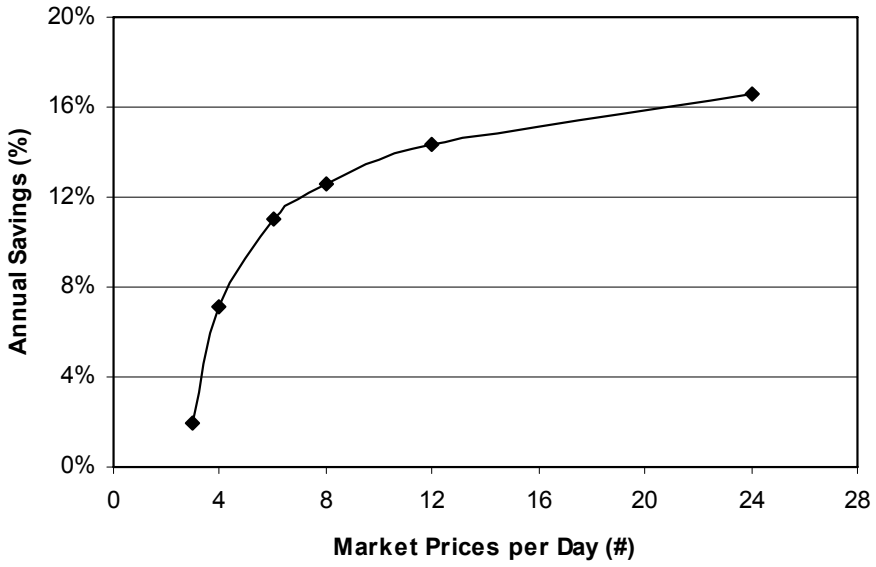

Figure 3.15: Impact of the price curve granularity on annual savings

Hence, this market parameter is an important decision and steering (incentive) variable for consumers, providers, and regulators.[8]

Load Curve Variation

The load curve represents the electricity demand of the analyzed consumer case for each timeslot. It is assumed that the load data are ex-ante given. The determining characteristics of the load curve are its distribution and the overall annual load (electricity demand) of the consumer. The following paragraphs analyze the influence of these components on the relative savings.

Annual Load Variation The variation of the annual load is a linear modification of the consumer's annual consumption. Each load value l_t of the load curve vector is multiplied with a constant variation factor. The analysis compares annual loads from 1000 kWh to 8000 kWh for a lead-acid-based storage system and a li-ion-based storage system.

Due to the higher annual load, the load shift volumes also increase. Therefore, each data point in Figure 3.16 is based on the optimally sized storage system for the corresponding situation.[9]

The simulation results in Figure 3.16 reveal that higher annual loads do not necessarily lead to higher relative savings. Besides the optimization of the storage system capacity, an optimization of the power converter dimensions is required. Nevertheless, size variations for the power and storage capacity can not always achieve positive annual savings. Both, the charging speed limit and the increasing power converter costs are bottlenecks in case of larger annual loads (compare equations (3.9) and (3.42)).

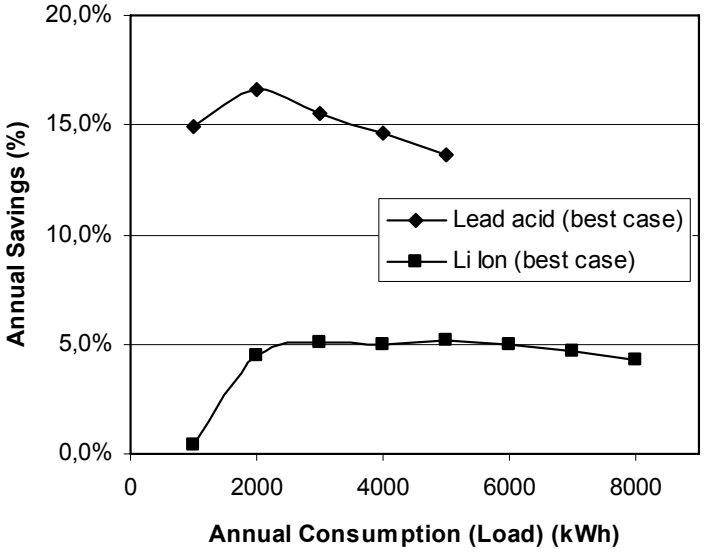

Figure 3.16: Influence of the annual consumer demand on relative savings

[8] E.g., the offering of flexible tariffs is legally required in Germany from beginning of 2011 onwards (Federal Law Gazette, 2008), but the detailed granularities of future tariffs remain to be seen.

[9] The optimal storage capacity has been determined separately for each annual load variation and technology scenario.

Variation of the Load Curve Distribution Load distribution variations, i.e., shifting the time of electricity demand and level of load peaks, change the characteristic of the load curve. As a consequence, the optimal CDS differs for each load distribution (assuming the same price curve). The saving potential of a storage system depends on the distribution of the load curve in comparison with the price curve's distribution. Load distribution variations do not change the annual load.

Besides the reference load curve, two additional load curves were generated: a load curve l_t^* with an approximately equably distribution as the price curve and a generated load curve of a single working household.

A load profile ℓ_t^* with a similar distribution to the price curve p_t is generated in two steps: (1) Derivation of a load profile $\widetilde{\ell}_t$ with a price curve-equivalent distribution and an annual load equal to that of ℓ_t, (2) variation of $\widetilde{\ell}_t$ with a factor α:

$$\widetilde{\ell}_t = p_t \cdot \left(\sum_{t'=1}^{T} \ell_{t'}\right) \cdot \left(\sum_{t'=1}^{T} p_{t'}\right)^{-1} \tag{3.59}$$

$$\Rightarrow \qquad \sum_{t=1}^{T} \ell_t = \sum_{t=1}^{T} \widetilde{\ell}_t \tag{3.60}$$

$$\ell_t^* = \begin{cases} \widetilde{\ell}_t - \alpha & p_t < \text{median}(P) \\ \widetilde{\ell}_t + \alpha & else \end{cases} \tag{3.61}$$

In order to avoid negative values for ℓ_t^*, α must not be greater than the minimal value of $\widetilde{\ell}_t$:

$$\alpha = t_{min}\left(\widetilde{\ell}_t\right) \tag{3.62}$$

If $\alpha > 0$, the resulting load curve ℓ_t^* will be pro-cyclic in comparison with the price curve p_t, i.e., the load peaks will be relatively higher than the price peaks and off-peak values relatively lower. In case of $\alpha < 0$, the effect inverts.

The reference load profile and the generated load profile of the single working household differ only in their intra-day load distribution. The seasonal and weekday-specific load distributions are equal and correspond to the distributions given in Figures 3.17-3.19.

As Figure 3.20 shows, the variation of the load curve's distribution has a significant impact on the relative savings that can be achieved by operating a storage system.

The more the load curve distribution differs from the given price curve distribution, the more the relative savings decrease. The indicator χ^{shape} measures the similarity of the load curve distribution to the price curve distribution.

$$\chi^{shape} = \frac{1}{T} \cdot \sum_{t=1}^{T} \text{abs}\left(\frac{\ell_t}{\widetilde{\ell}_t} - 1\right) \tag{3.63}$$

A series of simulations with 60 randomly generated load profiles of 1- and 2-person households (30 households each, includes 67% of households with inhabitants that

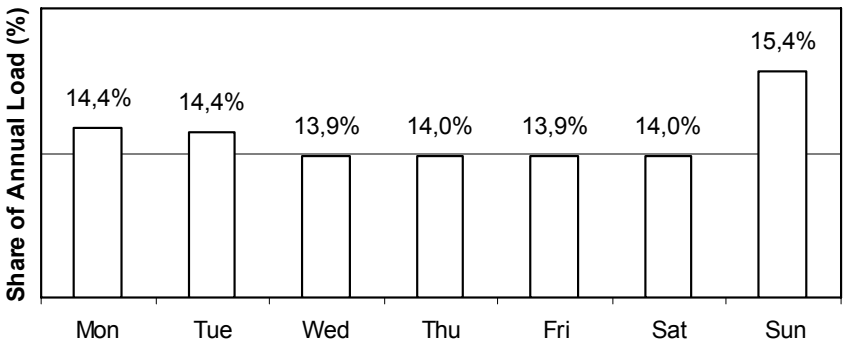

Figure 3.17: Seasonal load distribution of the reference load profile

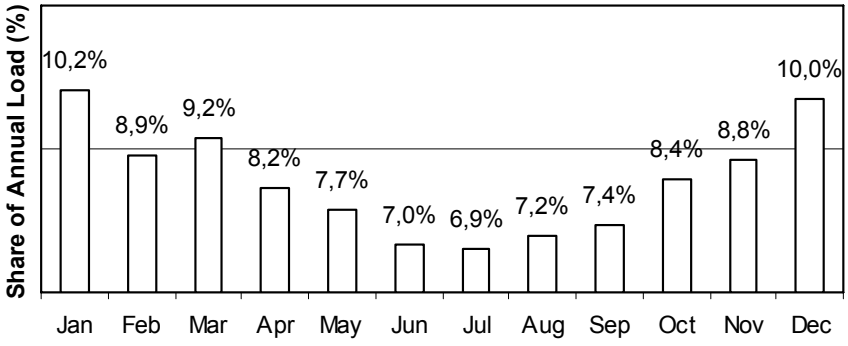

Figure 3.18: Weekday-specific load distribution of the reference load profile

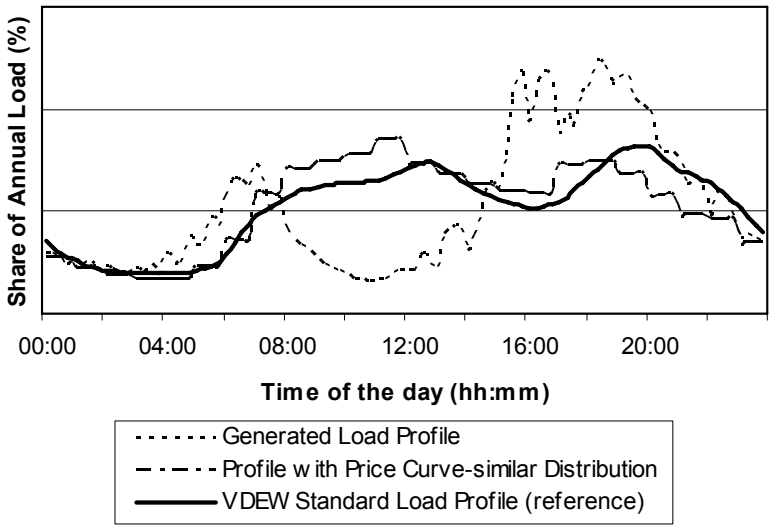

Figure 3.19: Average intraday load distributions of the analyzed load profiles

frequently leave to work and 33% of households of retired inhabitants) confirms the correlation of χ^{shape} and the relative annual savings (see Figure 3.21), which is not intuitive regarding the number of possible load distributions and their effects on the savings through the storage system. Thus, the indicator χ^{shape} can be seen as an

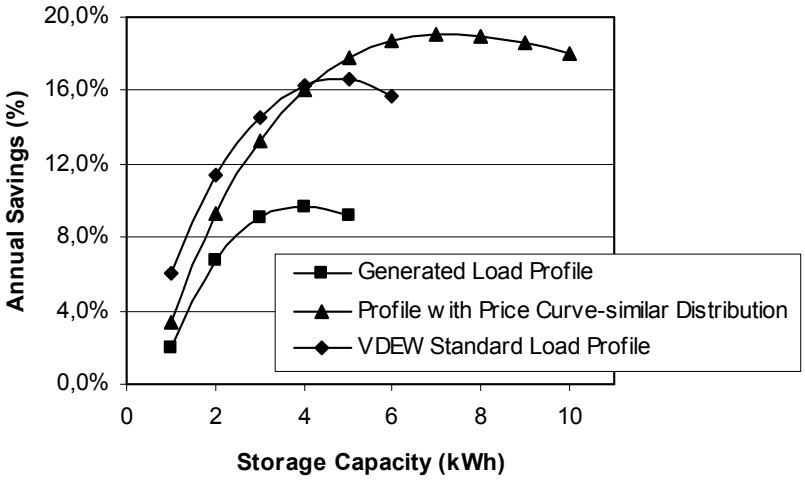

Figure 3.20: Impact of the load profile distribution on relative savings

Table 3.8: Load Curve Distribution Indicator Values

Load Curve	χ^{shape}	**Annual Savings (%)**
VDEW Standard Load Curve Profile (reference)	0.51	16.6
Profile with Price Curve-similar Distribution	0.29	19.1
Generated Load Profile of a single working household	1.57	9.6

indicator for investment decisions that allows an ex-ante estimation of potential benefits from a storage system for a given consumer profile.

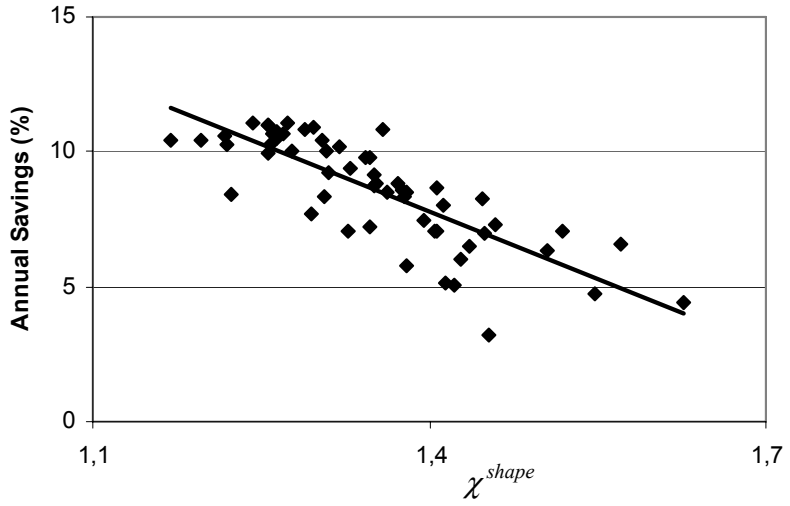

Figure 3.21: Correlation of annual savings with the load shape indicator χ^{shape}

Furthermore, the optimal system capacity varies depending on the load curve distribution. If the consumer's load is high in low-price timeslots and low in peak price

timeslots, the baseline cost and the saving potential are low due to low load shifting volumes, which again results in a lower optimal storage capacity value. If the load curve distribution is pro-cyclic with the price curve (highest electricity demand occurs in price peak timeslots), the annual savings potential, the load shifting volumes and the corresponding optimal storage capacity value are high.

Technology Comparison

The input parameters for the simulations represent three different technologies for the storage devices: lead-acid, li-ion, and NiCd storage technology. For each technology, input parameter values for the dimensions number of expected nominal charge cycles (ENCC), storage costs (SC), peripheral costs (PC), and storage efficiency (SE) have been defined (Table 3.5).

The best values regarding ENCC relate to li-ion and NiCd-based storage technologies. The best value regarding SC related to lead-acid-based technology. PC do not differ much between technologies and are therefore not expected to make a difference. The ranks of SE values relate in descending order to li-ion, lead-acid, and NiCd-based technology. The open question before running the analysis was which of the technologies would offer the best package of characteristics for the defined context and how big the influence of single parameters would be.

As a hypothesis, li-ion and lead-acid-based storage systems were expected to deliver best results. Due to a 3 times worse value in ENCC, but a 3 times better value in SC, the lead-acid technology was expected to have a slight advantage over the li-ion technology. Although the costs per nominal charge cycle (quotient of SC and ENCC) are alike, the capital costs for the lead-acid technology are lower. The NiCd technology was expected to deliver the lowest savings, since it represented worse parameter values for the dimensions SC and SE than the other technologies.

The simulation results reveal that the lead-acid-based storage systems performed significantly better in the given setting than li-ion and NiCd-based systems (up to 17% lead-acid vs. 5% li-ion). This implies for the given parameter values that the dimension SC has a much stronger impact on the results than SE and ENCC. As expected, the NiCd technology delivered lowest savings. Overall, only the best case scenarios of the lead-acid and the li-ion technology lead to a financially positive business case.

The results show that selecting the best storage technology depends significantly on the given context. In the given setting of stationary storage systems at the end consumer level, aspects like size, weight (mobility), capacity density and power density are of little or no relevance. In contrast, storage applications in mobile phones, laptops, or electric vehicles particularly require these dimensions. Therefore, the main disadvantages of the lead-acid technology do not negatively impact the results in the simulated context, and the li-ion technology could not benefit from its greatest strengths. A detailed sensitivity analysis of the lead-acid-based storage system (best case) examined how a variation of the input parameters affects the saving results. Based on the results of the technology analysis that simulated the individual parameters as a package, it is expected that the most important dimension is the SC, followed by ENCC and SE.

The simulations revealed a different picture from these expectations. The most economically sensitive parameter is the SE, followed by SC and ENCC. The results make clear that the influence of ENCC had been overestimated. In fact, it is only half the influence of SC. However, the most influential parameter is SE (factor 1.5 more influential than SE in the given setting). Comparing again li-ion and lead-acid based

technology, one could expect a clearer advantage respectively less disadvantage for the li-ion-based system. Taking a detailed look at the compared technology packages shows that the relative difference of the input values regarding this parameter is only 1.1 between li-ion and lead-acid technology (95% vs. 85%), whereas it is about a factor 3.3 for SC (disadvantageously for li-ion). Therefore, it is clear that SC is the most important parameter within this setting in absolute terms, while storage efficiency variations have the highest relative impact on the results. Additionally, the sensitivity analysis shows that the variations of technical parameters do not have a linear impact on the results, whereas this is the case for economic parameters.

3.3 Summary

This part of the research work addressed the question whether it is economically beneficial to install small, distributed storage devices on the electricity grid. Therefore, two models were presented, which measure the economic impact of DSSs at the end consumer level aiming at arbitrage accommodation (Basic Estimation Model in Section 3.1, Linear Optimization Model in Section 3.2). Both models address the decision problem when to charge and discharge the storage devices in order to maximize arbitrage accommodation. The first model estimates the benefits that could be achieved using heuristic decision algorithms that base on a lower limit for charging and an upper limit for discharging the storage system. The second model is a more complex linear optimization model that determines the optimal charge-discharge-strategy for a given time period and a given set of input parameters. It takes various cost components into account, such as capital and maintenance costs (fixed costs), time-dependent electricity supply costs (variable costs), and storage depreciations (variable and storage state-dependent costs). The technical parameters of the storage system model the dimensions *capacity, power, efficiency, and estimated system life time*, as well as their corresponding cost components.

For technical parameters of storage devices that are currently in a developmental stage, the linear optimization model resulted in a 17% reduction of total costs, while the basic model estimated a 9% reduction using a simple heuristic algorithm.

The main reason for the lower cost reduction of the heuristic algorithm in comparison with the optimal solution is the rough granularity of the charge and discharge limits. The basic estimation model sets only one, even though relative, value for the discharge and charge limits within the given time period. Thus, it calculates the limits that result in the highest average cost reduction per day, but not the highest absolute cost reduction for each day. In contrast, the linear optimization model determines the optimal CDS and therefore indicates the theoretically maximal savings. Moreover, the basic estimation model calculates the costs of charging the storage device on the average market price within the off-peak timeslots, whereas the linear optimization model calculates on the actual price per timeslot. Although the heuristic decision algorithm is obviously simple and offers a lot of room for improvement, it results in a saving potential on total cost of 9% (vs. 17% optimal solution). Thus, it is to assume that more sophisticated heuristic algorithms in realistic settings are likely to achieve more than 10% savings on total costs.

3.3.1 Contribution to Scientific Literature

In contrast to other papers dealing with the economic evaluation of storage systems and solutions for storage scheduling problems, this work varies in three dimensions: (i) Instead of centralized (large) storage systems on the Generation or Transmission level, the focus is on DSSs at the end consumer level. (ii) The objective function is a purely economic storage application aiming at arbitrage accommodation, whereas the existing literature mostly analyzed the economic impact of primarily technical storage applications (see Section 2.2), like load leveling, peak shaving, or frequency control. (iii) The simulation is based on a linear optimization model instead of a dynamic programming algorithm. Unlike the primarily technically-focused models, the presented mathematical model accurately links the technical characteristics of a storage device with the economic parameters of the system and its environment by variable pricing of system usage. The pricing depends on the effects that the intended usage has on the technical characteristics and the state of the system. E.g., charge-discharge decisions of the storage model reflect the relation between the average DOD and the expected nominal charge cycles of a storage device, which again impacts the costs per nominal charge cycle (depreciation costs).

3.3.2 Practical Relevance of the Findings

The linear optimization model reveals a cost reduction potential of up to 17% on total annual costs with a lead-acid-based storage system, whereas a li-ion-based system achieves only 5% savings. The results indicate that - in dependence on the system environment - lead-acid technology may be superior to li-ion technology. The sensitivity analyses underline the outstanding impact of the costs per storage unit (EUR/kWh) and the high sensitivity of the efficiency degrees on the achievable benefits. Other parameters such as the expected system life time, power converter costs, and capital costs show a significantly lower economic impact in the analyses.

The analysis of the market price curve revealed two major findings. Firstly, the analysis shows that the level of peak prices vs. off-peak prices is a strong driver for the achievable savings. In contrast, a purely constant price increase, which does not lead to higher spreads, has a negative influence on the results. I.e., the system's benefits increase with the volatility of the market price. The analyzed influence of the price curve variations on the overall savings reveals that a 1% increase of the average spread leads to 0.6% points higher overall savings. A 10% increase will raise the savings by 5.4% points to 22% annual savings. In the context of increasing shares of distributed and renewable (and intermittent) energy sources, the volatility of the electricity market is likely to increase. Given the predicted shortage of supply (cf. DENA (2008)), especially peak prices are expected to increase due to greater demand for expensive control capacity. All this would lead to more price volatility and, thus, a significant increase in potential benefits from storage applications that aim at arbitrage accommodation.

The second finding of the market price analysis concerns the electricity tariffs available. Increasing the granularity of the available electricity tariff from 3 to 6 market prices per day (e.g., a time-dependent tariff for morning, day, and night hours) will increase the savings by a factor 5 ($\sim$2% vs. $\sim$10%). Providing hourly tariffs to the consumer raises the savings to $\sim$17%. Decreasing the market price granularity will significantly limit potential arbitrage accommodation and thus, limit the incentives for

DSM and for consumers to adapt their behavior. Therefore, the market price granularity is an important decision and steering variable for consumer, providers, and regulators. E.g., the offering of flexible electricity tariffs is legally required in Germany from beginning of 2011 onwards, but the existing law does not prescribe the market price granularity in detail (compare §40 (3) in Federal Law Gazette (2008)).

Regarding the consumer parameters, the simulation results reveal a strong correlation between the annual savings and the similarity of the load and price curve distributions. Due to the large number of possible variation, this result is not intuitive, but could be confirmed through Monte-Carlo simulations. Each simulation run based on a different load profile that reflected a realistic, bottom-up generated consumer curve. The profiles were randomly created on the basis of realistic base parameter values and normalized to the same annual load.

The measured correlation implies that the introduced indicator χ^{shape} for measuring the similarity between load and price curve distribution can be seen as an indicator for investment decisions. The indicator allows an ex-ante estimation of potential benefits from storage systems for a given consumer profile in combination with a given price profile.

Part II

Economic Impact of Price and Load Forecast Errors on Distributed Storage Systems

Chapter 4

Price and Load Forecasting in the Electricity Sector

The integration of an increasing share of non-conventional energy resources will pose great challenges in the upcoming modernization and restructuring of the power grids. Non-conventional resources include distributed and renewable generation capacities as well as Demand-Side Management (DSM) applications of increasingly informed and responsive end consumers.

On the supply side, increasing the shares of Renewable Energy Sources (RES) and Distributed Energy Resources (DER) is a clear goal in most industrialized countries. The European Union targets a share of 20% overall energy production from renewable resources until the year 2020 (European Union, 2008). In Germany, the grid regulation authority expects DER to contribute 30% of the overall power production by 2020 (DENA, 2005). On the demand side, smart metering technologies, DSM applications, and electric vehilces begin to change the known consumption patterns of end consumers. In Germany, smart metering technology is set to be introduced into new buildings starting by the end of 2010 (with one year grace period for existing houses). E.g., smart metering allows for immediate energy flow visualizations, which is known to change consumption patterns significantly (Darby, 2006). Additionally, the anticipated increase of Plug-in Electric Vehicle (PEV) and Plug-in Hybrid Electric Vehicle (PHEV) requires smart charging strategies to integrate these new loads into the energy grid (about 1 million units targeted in Germany by 2020 (German government, 2008)).

Hence, ensuring the grid's stability by balancing demand and supply at each point in time becomes more challenging due to new supply and consumption patterns. In the traditional grid, the supply side provides the required flexibility through control capacity. While the supply side has always been flexible and responsive, a higher share of RES and DER, i.e., intermittent and non-dispatchable resources will reduce the supply side's degree of flexibility. To compensate the higher volatility induced through RES and DER, either the supply side, or the demand side, or both sides have to provide additional flexibility. Providing supply-side flexibility is typically based on comparatively expensive gas power plants that produce CO_2 emissions and increase the dependency on natural gas. An alternative concept on the supply side are Virtual Power Plant (VPP), an innovative concept that has been investigated in the last years. VPP combine several energy resources to a virtual unit with a predictable output, where resources are predominantly RES and DER. It is often supported with storage solutions. (Setiawan, 2007)

When changing the traditional paradigm of a purely supply-side-focused flexibility provision, storage systems and DSM programs can provide flexibility on the demand side by realizing or creating load shifting potentials. More flexibility on the demand side shifts demand to timeslots where supply is available from RES or DER. Storage systems will hide load shifting towards the end consumer.

All options on both, the supply and the demand side, need price and load forecast data in order to economically optimize the schedules of the underlying measures. Forecasts are essential for an effective coordination of the energy market. But maintaining or even improving the quality level of traditional short-term load forecasts becomes more difficult if shares of RES and DER increase. The output of these resources is much harder to predict than for conventional power plants (Konjic et al., 2005). Assuming an increasing amount of economically scheduled distributed generation and consumption units implies that coordinating demand and distributed supply volumes will require forecasts for smaller units, i.e., on a less aggregated level than the traditional grid (Konjic et al., 2005). Due to the lack of averaging effects, this causes additional difficulties (Pahasa and Theera-Umpon, 2008). Moreover, an increasingly flexible and reactive demand side will lead to new demand patterns that might not be fully compatible with the traditional forecasting tools.[1] The same accounts for price forecasts. Flexible prices - especially on a Real-time pricing (RTP) basis - will increase the complexity of load forecasting since prices and loads are correlated (Bunn, 2000) (even though the degree of price elasticity and, thus, the precise relation between load and price is hard to determine (Yun et al., 2008)).

A prerequisite for a shift from passive energy consumption to an active, distributed, and load-responsive DSM are flexible electricity prices that provide an economic incentive for load shifting. It is assumed that flexible prices appropriately reflect the demand-supply-situation on the market. Traditionally, flexible prices only apply to producers and large industrial consumers. This is about to change by aiming at *smarter*, i.e., more responsive households and consumers in the future. In Germany, according legal changes are already passed. End consumers will have access to load- and time-dependent electricity tariffs from 2011 onwards (Federal Law Gazette, 2008).

With new time- and load-dependent tariffs in place, customers will have an incentive to shift their consumption towards off-peak hours while during peak hours their PEV, PHEV, or stationary battery storage devices might (temporarily) feed energy back into the grid given an appropriate monetary compensation. Thus, DSM applications will need to calculate price forecasts in order to effectively schedule their energy consuming devices.

On the load forecasting side, upcoming technologies like Smart Metering in combination with modern information and communication technologies will provide precise consumption data on the low-voltage level. Potentially, this can be a major enabler for load forecasting on a less aggregated level.

Future grids will contain a larger share of RES and DER as well as a more flexible and reactive demand side triggered by price-sensitive consumers. To cope with the increasing volatility on both the supply and the demand side, storage will become more important. Accurate price and load predictions are necessary to optimize the operation schedules of such storage devices. In the case of Distributed Storage System (DSS), load forecasts on a distributed, less aggregated level are required.

[1] E.g., if the forecast methods use historic data for their input, but DSM programs significantly change these data.

4.1 Objective and Structure of Part II

Within a context of uncertain price and load forecasts, this part of the thesis will analyze the impact of price and load forecast errors on the economics of a DSS at the end consumer level. The analyses build on the basic model in Ahlert and van Dinther (2009b) (Part I), which aims at arbitrage accommodation using a battery storage. But the analysis within this part relax the assumption of ex-ante known price and load data, since these data would not be available for real-world application. The presented battery storage management algorithm in Section 3.2 achieves approximately 17% savings on the annual electricity costs of a prototypical 2-person household. The algorithm computes an optimal Charge-Discharge-Schedule (CDS) for the storage system given ex-ante known load and price data. The research questions of this part of the thesis investigate to what extent load and price forecasts deteriorate the economics of the derived CDS in comparison to the previously calculated optimal CDS. Furthermore, the economic robustness of different scheduling and forecast algorithms are calculated.

After a review of related literature on price and load forecasting (Section 4.2), this part of the thesis simulates various scenarios of load and price forecasts. Chapter 5 defines the simulation model (Sections 5.1-5.3) and simulation scenarios (Section 5.4). Section 5.5 analyses the results of the price and load forecast scenarios and the robustness of economic results in dependence on the scheduling algorithms in a DSS. The effects of load and price forecast characteristics like forecast accuracy, autocorrelation of forecast errors, and the scope of the forecast horizon, as well as the influence of scheduling algorithms are benchmarked against the optimal result calculated in the first part of this work. Section 5.6 summarizes the findings and discusses their relevance.

4.2 Related Literature

The number of scientific articles on forecasting in the energy sector is extremely large. The majority of articles deals with load forecasting, since price forecasting is a comparably new research area. Sections 4.2.1 and 4.2.2 will give a short, clearly not exhaustive overview of load forecasting, including a discussion of load forecasting for low-volume consumption entities (*Small Unit Load Forecasting*). Section 4.2.3 will present an according overview of price forecasting. The sections will reflect which forecast methodologies and approaches are available and what level of forecast accuracy they can achieve. Section 4.2.4 presents a review of existing economic analyses on forecast accuracy impact, Section 4.2.5 discusses the issue of autocorrelation in forecast errors, and Section 4.2.6 describes how storage models in the literature have integrated forecast uncertainties into their analyses.

4.2.1 Load Forecasting

Load forecasting and particularly short-term load forecasting have been subject to research since the 1960s. The reviews in IEEE Committee Report (1980) and Mahmoud et al. (1981) give an overview of numerous articles on the topic until 1981. Until that time, the predominantly used approaches were statistical methods that modeled time series (for a detailed explanation of the most important statistical forecasting methods see Moghram and Rahman (1989)). Starting in the 1980s until today, various

models using methods from artificial intelligence (AI) are presented in literature (for a comparative overview see Metaxiotis (2003)).

AI-based models are not generally superior to statistical models, but they have shown an ability to better performance in dealing with non-linearity and other difficulties in modeling time series. Statistical models are often unable to adapt to unusual weather conditions and varied holidays. Among the various models using neural networks, it is hard to predict when and under which conditions certain models will deliver best results. (Metaxiotis, 2003)

In order to give an idea of available forecast methods and their accuracies, Table 4.1 depicts a review of 7 papers using different modeling approaches (not exhaustive).

Table 4.1: Load Forecasting Accuracies

Lead Time	**Error**	**Error Measure**	**Test Period[a]**	**Method**	**Reference**
1 HA	1.4%	DMAPE	5×6	ANN	Park et al. (1991)
1 HA	<1%	RSME	1	FL, NN	Liu et al. (1996)
1 DA	1.8%	MAPE	180	ANN+BP	Lee et al. (1992)
1 DA	1-5%	DMAPE	1	ST	Moghram and Rahman (1989)
1 DA	1.7%	DMAPE	n/a	RBF NN+ANFIS	Yun et al. (2008)
1 DA	1.5%	DMAPE	1	NN+BP	Chang and Yi (1998)
1 DA	1.7%	DMAPE	5×6	ANN	Park et al. (1991)
1 DA	2.0-2.4	DMAPE	1	WAV, PSO NN	Bashir and El-Hawary (2009)

[a] Period length in days.
NN=Neural Networks, ANN=Artificial NN, FL=Fuzzy Logic, BP=Back Propagation, ST=Statistical Techniques (Multiple Linear Regression, Stochastic Time Series, General Exponential Smoothing, State Space Method), RBF=Radial Basis Function, ANFIS=Adaptive Neural Fuzzy Inference System, WAV=Wavelets, PSO=Particle Swarm Optimization.
MAPE=Mean Absolute Percentage Error, DMAPE=daily MAPE, RSME=Root Square Mean Error
HA=hour ahead, DA=day ahead

4.2.2 Small Unit Load Forecasting

All approaches presented in Table 4.1 perform load forecasting on a high aggregation level, i.e., for large volumes that contain the demand of numerous small units. Forecasting load volumes on a less aggregated level, e.g., on a substation level, leads to less accurate forecasts. It exhibits a weaker statistical pattern due to a lack of averaging effects and incomplete historical load and weather data (Pahasa and Theera-Umpon, 2008, Sargunaraj and Gupta, 1997, Worawit and Wanchai, 2002). As distributed generation has made forecasts on the aggregated level more complex (see Chapter 4), this accounts in particular for the substation level (Konjic et al., 2005). For compensating this statistical issue, expert systems with human input are sometimes used (Pahasa and Theera-Umpon, 2008).

To give an overview of the available results of load forecasting techniques for low-volume consumption units, Table 4.2 depicts a comparative overview of 7 approaches and their observed accuracies. Table 4.1 and 4.2 shall give an orientation for scenarios defined in Section 5.4 and the interpretation of results in Section 5.5.

4.2.3 Price Forecasting

In comparison to load forecasting, energy price forecasting is a less researched topic. Most literature available is dated after the year 2000, when the deregulation of the

Table 4.2: Small Unit Load Forecasting Accuracies

Lead Time	Error	Error Measure	Test Period[a]	Method	Reference
1 HA	1.4%	MAPE	>365	PAR	Espinoza et al. (2005)
1 HA	6.6%	MAPE	7	KF	Sargunaraj and Gupta (1997)
1 DA	5.5-6.7	MAPE	365	ANN+SVM	Pahasa and Theera-Umpon (2008)
1 DA	3.0-8.7%[b]	MAPE	n/a	FR	Nazarko and Zalewski (1999)
1 DA	1.7/90%	BWE/CI	14	FIS	Konjic et al. (2005)
1 DA	7.3%	MAPE	n/a	NN+GA	Worawit and Wanchai (2002)
1 DA	6.0%	MAPE	365	DWT+SVM	Pahasa and Theera-Umpon (2007)
1 DA	4.3%	MAPE	>365	PAR	Espinoza et al. (2005)
1 WA	11.5%	MAPE	7	KF	Sargunaraj and Gupta (1997)

[a] Period length in days.
[b] Peak load forecast
PAR=Periodic Autoregression, KF=Kalman Filtering, NN=Neural Networks, ANN=Artificial NN, SVM=Support Vector Machine, FR=Fuzzy Regression, FIS=Fuzzy Inference System, GA=Genetic Algorithm, DWT=Discrete Wavelet Transformation.
MAPE=Mean Absolute Percentage Error, BWE/CI=Bandwidth Error at a Confidence Interval
HA=hour ahead, DA=day ahead, WA=week ahead

energy markets in the US, UK, and other European countries started (Bunn, 2000). Price forecasts are more complex and therefore less accurate than load forecasts, since price curves are much more volatile than load curves (Benini et al., 2002) and price volatility usually increases when prices increase. This phenomenon can be particularly observed for peak prices (Bunn, 2000). Reasons for volatility are the characteristics of electricity and of electricity markets: limited storability, required demand and supply balance at any given point in time, short-term inelasticity of the demand, and typically an oligopoly structure on the supply side (Aggarwal et al., 2009). In addition to the last aspect, strategic behavior of market participants may impact the prices significantly. Overall, price forecasting is a less mature research field than load forecasting (Aggarwal et al., 2009, Benini et al., 2002, Bunn, 2000).

To give an overview of the price forecasting techniques available and their accuracies, Table 4.3 presents a selection of the forecasting methods reviewed and compared in Aggarwal et al. (2009). *"In conclusion, there is no systematic evidence of out-performance of one model over the other models on a consistent basis"* (Aggarwal et al., 2009).

4.2.4 Economic Impact of Forecast Errors

An early paper evaluating the effect of load uncertainty on unit commitment risk is Zhai et al. (1994). The authors use a Gauss-Markov model to evaluate the probability of having insufficient committed capacity for the compensation of unexpected load variations, but they do not quantify the effect in economic terms. Ranaweera et al. (1997) determine the economic impact of load forecast accuracy improvements by simulating independent, normally distributed forecast errors. Hobbs (1998) and Hobbs et al. (1999) vary a given relative error vector with a constant scalar to simulate variations of the forecast accuracy. They additionally rely on real-world examples, which underline the potentially significant economic impact of load forecast accuracy. A mixed-integer optimization approach to determine the value of forecasting is presented in Delarue and Dhaeseleer (2008). They use a constant absolute error term and, in a second analysis, a linearly growing absolute error term to simulate forecast errors. Teisberg

Table 4.3: Price Forecasting Accuracies

Lead Time	Error	Error Measure	Test Period[a]	Method	Reference
1 HA	6.04%	DMAPE	30	NN(MLP)+BP	Lee et al. (2005)
1 DA	3%	WMAE	45	AR,ARMA	Cuaresma et al. (2004)
1 DA	2.5-11.11%	DMAPE	7	2OWAVT	Kim et al. (2002)
1 DA	3-11.11%	WMAPE	28	ARMA, ARX ARMAX, AR	Weron and Misiorek (2005)
1 DA	3-5%	DMAPE	7-14	DR,TF	Nogales et al. (2002)
1 DA	3.5-5.16%	DMAPE	7	NN(MLP)+ AFSA	Li and Wang (2006)
1 DA	15.5%	WMAPE	7	NN(MLP)+ BP	Hu et al. (2008)
1 DA	7.5%	MAPE	7×4 seasons	NN(MLP)+ GDR	Amjady (2006)
1 WA	7%	WMAE	45	AR, ARMA	Cuaresma et al. (2004)

[a] Period length in days.
NN=Neural Networks, MLP=Multilayer Perceptron, BP=Back Propagation, AR=Autoregressive Model, ARMA=AR Moving Average, 2OWAVT=2nd order polynomial wavelet transformation, ARX=AR with exogenous variable, DR=Dynamic Regression, TF=Transfer Function, AFSA=Artificial Fish Swarm Algorithm, GDR=Generalized Delta Rule.
MAPE=Mean Absolute Percentage Error, DMAPE=Daily MAPE, WMAPE=Weekly MAPE, WMAE=Weekly Mean Absolute Error.
HA=hour ahead, DA=day ahead, WA=week ahead.

et al. (2005) analyze the economic impact of load forecasts that have been improved by weather forecast information on the optimal dispatch of spinning reserves. Their analysis builds on the model in Hobbs et al. (1999). Ortega-Vazquez and Kirschen (2006) assess the economic impact of forecast errors measured in terms of costs for generation interruptions, i.e., generation outages. In their paper, a variable degree of forecast error autocorrelation is modeled and analyzed, which none of the other papers before did explicitly. E.g., Hobbs et al. (1999) explicitly used real forecast data with strongly autocorrelated forecast errors while load forecast errors in Ranaweera et al. (1997) are completely uncorrelated random numbers.

The aforementioned papers reveal a positive economic value of forecasting accuracy (between 0.08 and 0.3% of operating costs per 1% point accuracy improvement), but these results are very hard to compare due to different settings and assumptions.

A fairly simple, but effective approach to simulate imperfect price forecasts is investigated in Sioshansi et al. (2009). They apply the optimal schedule of the previous period to the current period. This method achieves 85% of the optimal result. In Conejo et al. (2005), this approach is described as '*a naïve, but challenging test*' for more sophisticated forecast methods. Still, this approach does not allow for assessing the economic impact of stepwise forecast accuracy improvements. Table 4.4 summarizes the approaches and findings of the related articles.

All aforementioned articles perform the economic analysis from the perspective of a (centralized) large utility company and focus purely on load forecast accuracy (except for Sioshansi et al. (2009)). In contrast, this research work focuses on a (distributed) consumer perspective and analyzes the impact of price and load forecast accuracies on a locally optimized dispatch of storage capacity aiming at arbitrage accommodation.

Table 4.4: Economic Impact of Forecast Accuracy

Reference	**Forecast Error Simulation**	**Relative Economic Result**
Zhai et al. (1994)	Gauss-Markov random sequence model	n/a
Ranaweera et al. (1997)	Independent normally distributed variables	1% point improvement of forecast error leads to 0.08% improvement of operating costs
Hobbs et al. (1999)	Variation of a given relative error vector with a constant scalar	1% point improvement of the forecast error (MAPE) leads to 0.12-0.3% change of operating costs
Ortega-Vazquez and Kirschen (2006)	Random Walk-like method	1% point improvement of forecast error leads to 0.09% improvement of operating costs
Delarue and Dhaeseleer (2008)	(1) Constant absolute error term, (2) linearly growing absolute error term	5% error lead to up to 1% deterioration of the optimal result
Sioshansi et al. (2009)	*Naive* forecast, optimal schedule for the previous period is applied to the current period	Achieves 85% of the optimal result

The model in this work combines the strengths of the aforementioned articles, i.e., an adjustable degree of forecast error autocorrelation and an adjustable level of forecast errors.

As in most literature on forecasting, the measure for the assessment of forecast errors is the Mean Absolute Percentage Error (MAPE). In the context of electricity loads, data values are typically non-zero and positive. MAPE is therefore a suitable, standardized and commonly applied measure (see Hyndman and Koehler (2006), Misiorek et al. (2006) for a more detailed discussion and comparison with other measures).

4.2.5 Autocorrelation of Forecast Errors

Relative forecast errors of load and price forecasts tend to be autocorrelated (Hobbs et al., 1999). I.e., succeeding timeslots tend to have similar (relative) forecast errors, which reflects a systematic over- or underestimation within a certain period of time. A method to determine the degree of autocorrelation of a time series is the Durbin-Watson Test (DWT) (Durbin and Watson, 1950):

$$DWT = \frac{\sum_{t=2}^{T} (X_t - X_{t-1})^2}{\sum_{t=1}^{T} (X_t)^2} \tag{4.1}$$

where a DWT value of 0 indicates a perfect positive autocorrelation, 4 indicates a perfect negative autocorrelation, and 2 indicates no autocorrelation.

Among the referenced papers in Tables 4.1, 4.2, and 4.3, 4 papers presented the relative error data of their forecasts. The analysis of these papers reveals that the forecast errors in these papers are autocorrelated for all applied methods, although there are notable differences depending on the method used, the season, and the time period analyzed. In average, the DWT autocorrelation value equals 0.69 for load forecasts and 0.47 for price forecasts. Tables 4.5 and 4.6 summarize the results.

4.2.6 Forecast Uncertainties in Storage Models

Storage optimization models aiming at arbitrage accommodation[2] can be distinguished into four groups with respect to their solution approaches and applied algorithms. The difference that shall be emphasized in this work is that the first three groups do not take forecast uncertainties into account when optimizing storage schedules, while the last group does so.

The first group contains models using a (static) statistical analysis to assess the economics of DSSs. E.g., Nieuwenhout et al. (2006) analyze two settings for load shifting at the end consumer level. The second group is models building on (multi-pass) dynamic programming methods to determine the optimal CDS for the storage system. Examples are Lee and Chen (1994), Lee and Chen (1995) as well as Maly and Kwan (1995) that present analyses with a particular focus on the Taiwanese tariff system, which provides combined incentives for TOU optimization and peak load reduction. The third group contains papers that present linear optimization models determining the optimal CDS. E.g., Wu et al. (2002) and Bathurst and Strbac (2003) analyze how storage systems can foster the integration of renewable (intermittent) sources from an economic perspective. Exarchakos et al. (2009), Graves et al. (1999), Sioshansi

[2]This includes storage models that optimize their schedules according to Time-of-use (TOU) tariffs.

Table 4.5: Autocorrelation of Errors in Load Forecasting

Reference	Test Period Length	Method	Autocorrelation[a]	Comment
Yun et al. (2008)	48 (1/2 h)	RBFNN+ HD	1.51	
	48 (1/2 h)	RBFNN HD+PC	1.28	
	48 (1/2 h)	ANFIS HD+PC	0.71	
	48 (1/2 h)	RFBNN+ ANFIS	1.51	
Moghram and Rahman (1989)	24 (h)	MLR	0.85	Summer
	24 (h)	MLR	1.31	Winter
	24 (h)	ARIMA	0.61	Summer
	24 (h)	ARIMA	0.12	Winter
	24 (h)	TF	1.63	Summer
	24 (h)	TF	0.12	Winter
	24 (h)	GES	0.14	Summer
	24 (h)	GES	0.14	Winter
	24 (h)	SS	0.34	Summer
	24 (h)	SS	0.28	Winter
	24 (h)	KBES	0.24	Summer
	24 (h)	KBES	0.25	Winter

[a] Durbin-Watson Test (DWT) value
RBFNN=Radial Basis Function Neural Network, HD=Historic Data, PC=Price Change, ANFIS=Adaptive Neural Fuzzy Inference System, MLR=Multiple Linear Repression, ARIMA=Autoregressive Integrated Moving Average, TF=Transfer Function, GES=General Exponential Smoothing, SS=Static Space Approach, KBES=Knowledge-based Expert System

et al. (2009) analyze arbitrage opportunities on wholesale markets, and Ahlert and van Dinther (2009b) analyze arbitrage accommodation based on TOU at the end consumer level.

All of the aforementioned models assess the economics of DSSs on ex-ante given data and do not incorporate the uncertainty induced through forecast errors. The forth group builds on simulations that incorporate data streams underlying probabilistic distributions. Barton and Infield (2004) investigate how time-shifting the supply from wind farms can be used to maximize revenues. The uncertainty in their model stems from the distribution of wind speeds, which are an essential input factor for the wind farm's electricity production. Walawalkar et al. (2007) analyze the economics of energy storage systems in New York. They use probabilistic input data streams for revenues and charging costs in order to analyze the net present value of two defined storage systems.

In the following, this part of the thesis will present a simulation model that incorporates uncertainty through imperfect price and load forecasts into the economic evaluation of a DSS model.

Table 4.6: Autocorrelation of Errors in Price Forecasting

Reference	Test Period Length	Method	Autocorrelation[a]	Comment
Conejo et al. (2005)	3x24 (h)	TF	0.64	Spring
	3x24 (h)	TF	0.62	Summer
	3x24 (h)	TF	0.54	Fall
	3x24 (h)	TF	1.20	Winter
	3x24 (h)	ARIMA	0.25	Spring
	3x24 (h)	ARIMA	0.20	Summer
	3x24 (h)	ARIMA	0.18	Fall
	3x24 (h)	ARIMA	0.54	Winter
	3x24 (h)	WL	0.42	Spring
	3x24 (h)	WL	0.19	Summer
	3x24 (h)	WL	0.44	Fall
	3x24 (h)	WL	0.60	Winter
	3x24 (h)	DR	0.67	Spring
	3x24 (h)	DR	0.63	Summer
	3x24 (h)	DR	0.60	Fall
	3x24 (h)	DR	1.13	Winter
	3x24 (h)	NN	0.25	Spring
	3x24 (h)	NN	0.19	Summer
	3x24 (h)	NN	0.14	Fall
	3x24 (h)	NN	0.58	Winter
	3x24 (h)	NAIVE	0.36	Spring
	3x24 (h)	NAIVE	0.26	Summer
	3x24 (h)	NAIVE	0.20	Fall
	3x24 (h)	NAIVE	0.25	Winter
Misiorek et al. (2006)	35 (weeks)	AR	0.52	
	35 (weeks)	ARX	0.54	
	35 (weeks)	AR-G	0.53	
	35 (weeks)	ARX-G	0.50	
	35 (weeks)	TAR	0.53	
	35 (weeks)	TARX	0.50	
	35 (weeks)	RS	0.51	
	35 (weeks)	NAIVE	0.37	

[a] Durbin-Watson Test (DWT) value
TF=Transfer Function, ARIMA=Autoregressive Integrated Moving Average, WL=Wavelets, DR=Dynamic Regression, NN=Neural Networks, AR=Autoregression, ARX=AR with exogenous variable, G=GARCH (Generalized autoregressive conditional heteroscendasticity), TAR=Threshold + AR, RS=Regime Switching

Chapter 5

Forecast Error Simulation in Storage Models

In order to study the economic impact of price and load forecast errors on the operations of a DSS, this research work simulates forecast data streams with defined characteristics and uses them as input data for deriving operation schedules for a DSS. The results in Section 5.5 reflect the three main simulation settings that have been analyzed: (i) simulations with load forecast errors, (ii) simulations with price forecast errors (published in Ahlert and Block (2010)), and (iii) simulations of combined price and load forecast errors (published in Ahlert (2009a) and Ahlert (2009b)). Additionally, an economic robustness analysis of different scheduling algorithms is performed for the last setting (published in Ahlert and Dinther (2010)).

The forecast simulation model implements three characteristics of a forecast, namely the relative forecast errors, the autocorrelation of forecast errors, and the length of the forecast horizon. The simulation model consists of three main steps for each day of the simulation period: (1) Generating a forecast, (2) determining an arbitrage-maximizing CDS, and (3) executing the CDS. Figure 5.1 depicts the overall control flow of the simulation model.

Step 1 generates a forecast of the hourly load volumes and electricity prices for the next forecast period. The forecasts are derived from the actual data with a procedure presented in Section 5.1. This procedure ensures a forecast with predefined characteristics like specific forecast accuracy levels within the forecast period and a specified degree of autocorrelation of forecast errors.

Step 2 determines an arbitrage-maximizing CDS for the forecast period based on the forecast generated in Step 1. For most simulation scenarios within this part of the thesis (except simulations in Sections 5.2.2, 5.5.3), a linear optimization model derives a 'pseudo optimal' schedule, i.e., optimal according to the load and price forecasts, instead of a 'truly' optimal schedule based on the (ex-ante unknown) actual price and load data. It calculates the CDS by solving a unit commitment problem for the DSS, which is conceptually similar to a unit commitment problem for pumped-hydro plants, but simulated at the end consumer level with a 5-kWh-storage device. The DSS does not sell electricity back to the wholesale market, but avoids peak prices for the end consumer. I.e., it performs a TOU optimization with respect to the load (profile) of a given consumer and the technical constraints of the DSS.

Some scenarios use an alternative scheduling approach that is based on a heuristic algorithm (Sections 5.2.2, 5.5.3). The scheduling problem is subject to various papers,

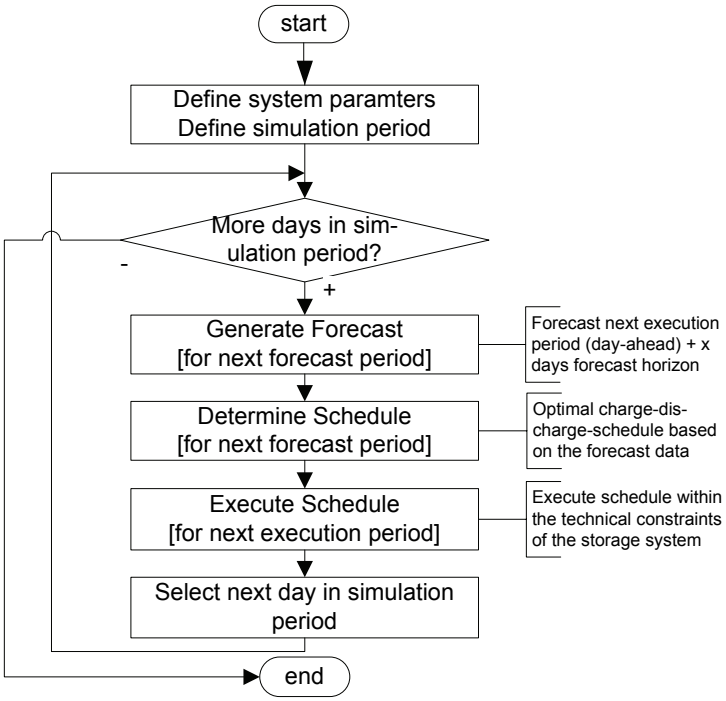

Figure 5.1: Control flow of the simulation model

e.g., Ahlert and van Dinther (2009b), Exarchakos et al. (2009), Sioshansi et al. (2009) using linear optimization models, or Lee and Chen (1995), Maly and Kwan (1995) using dynamic programming methods. The aforementioned models assume ex-ante known load data to determine the optimal CDS. This work relaxes that assumption and uses artificially generated forecasts instead (Step 1).

In Step 3, the simulation model tries to operate the battery storage within the execution period based on this schedule whenever technically possible, i.e., the schedule is kept as long as it does not violate any technical constraints of the given storage system, e.g., maximum or minimum State of Charge (SOC). The more a forecast deviates from the actual data, the more often the proposed schedule will violate the constraints and, thus, has to be adapted to accommodate the real load situation in the affected timeslots.

The total costs of the simulated period are calculated based on the same model as in Part I of this thesis, which minimizes the total costs of electricity supply, DSS installation and operation:

$$min \rightarrow K^{fixed} + \sum_{t=1}^{T} K_t^{variable} \tag{5.1}$$

with K^{fixed} being a constant representing the capital and maintenance costs as well as annual depreciations and $K_t^{variable}$ being the variable operation costs that result from the executed CDS (see Section 5.3) including costs for charging and using (depreciating) the storage device. The simulation model within this part of the research work builds on the same assumptions, specifications, and input datasets as the basic model.[1] Appendix

[1]The distribution of the electricity prices reflects the price distribution of market prices from the EEX (2007). The load data distribution corresponds to the VDEW standard household profiles

B contains a description of all parameters, including their symbols and reference values (further details on the definition of the cost components in Section 5.2.1).

The forecast generation module (Step 1) within this Monte Carlo simulation involves random numbers. Thus, the result of a single simulation run is subject to statistical fluctuations. To obtain a stable simulation result not exceeding a predefined error E, the method presented in Hahn and Shapiro (1968, p. 245) is used to calculate the number of required simulation runs n:

$$n = \left[\frac{z_{1-\alpha/2} \cdot \sigma'}{E} \right]^2 \tag{5.2}$$

where

- E: maximum allowable error for average MAPE deviation
- $1-\alpha$: desired probability that true average MAPE deviation does not differ from the estimated deviation by more than $\pm E$
- σ': (estimate of the) standard deviation of the average MAPE deviation
- $z_{1-\alpha/2}$: $(1-\alpha/2) \cdot 100$ percent point of the standard normal distribution

For all simulation results presented in this research work, up to 500 simulation runs have been performed to ensure a precision of $\pm E < 1$ in a 95% confidence interval ($\alpha = 5\%$). The following sections describe the detailed computational steps within the simulation model (Sections 5.1 - 5.3) and the simulation scenarios (Section 5.4).

5.1 Forecast Generation

The forecast generation module derives an artificial forecast F_t ($1 \leq t \leq T^{FP}$) for a forecast period of length T^{FP} from the actual data. The artificial forecast F_t deviates from the given actual data A_t by a percentage error X_t:

$$F_t = (1 + X_t) \cdot A_t \qquad \forall t \tag{5.3}$$

The MAPE $\bar{x}_t$ of forecast data points F_t^n (forecast value in simulation n) to an actual data point A_t is calculated over all simulation runs n ($1 \leq n \leq N$).

$$\bar{x}_t = \frac{1}{N} \sum_{n=1}^{N} \frac{|F_t^n - A_t|}{A_t} \tag{5.4}$$

The stochastic process for generating the percentage error X_t is a modified Random Walk with a normally distributed error variable ε_i ($1 \leq i \leq t$)

$$X_t = \varepsilon_t + \alpha \sum_{i=1}^{t-1} \varepsilon_i \quad \text{with} \quad \varepsilon_i \sim \mathcal{N}(0, \sigma_i) \tag{5.5}$$

where the factor α allows for a variation of the autocorrelation of the error stream. A value of $\alpha = 1$ leads to highly autocorrelated relative forecast errors X_t, i.e., a DWT

(VDEW, 2006) and an annual load of 2000 kWh (approximately the consumption of an average German two-person household). For the technical parameter specification of the lead-acid-based battery storage system see Section 3.2.

value of 0, whereas $\alpha = 0$ leads to completely uncorrelated forecast errors, i.e., a DWT value of 2. To match a specified DWT value of a scenario, α is manually adjusted for each simulation scenario.

The standard deviation σ_i (derivation of y_i in Section 5.1.1) is defined as

$$\sigma_i = \tilde{\sigma} \cdot y_i \tag{5.6}$$

with

$$\tilde{\sigma} = \underline{a} \cdot \frac{\sqrt{2\pi}}{2} \tag{5.7}$$

since a MAPE of normally distributed values is $\sqrt{2\pi} \cdot 2^{-1}$ times smaller than its standard deviation (see Section 5.1.2).

The MAPE at the first timeslot of a forecast period is specified with $\underline{a}$ and analogously $\bar{a}$ for the last timeslot, which reflects that forecast errors increase over time. This work assumes a linear increase of the MAPE $\bar{x}_t$ (at timeslot t) during the forecast period (see Figure 5.2). This simplifying assumption can be relaxed if more accurate data from empirical observations or simulation models are available.

$$\bar{x}_t = \tilde{\sigma} \cdot \left(1 + \frac{(t-1)\,(\bar{a} \cdot \underline{a}^{-1} - 1)}{T^{FP} - 1}\right) \tag{5.8}$$

The defined standard deviation σ_i ensures that the expected value of F_t deviates by $\bar{x}_t$ for each timeslot t and that it has a specified degree of autocorrelation.

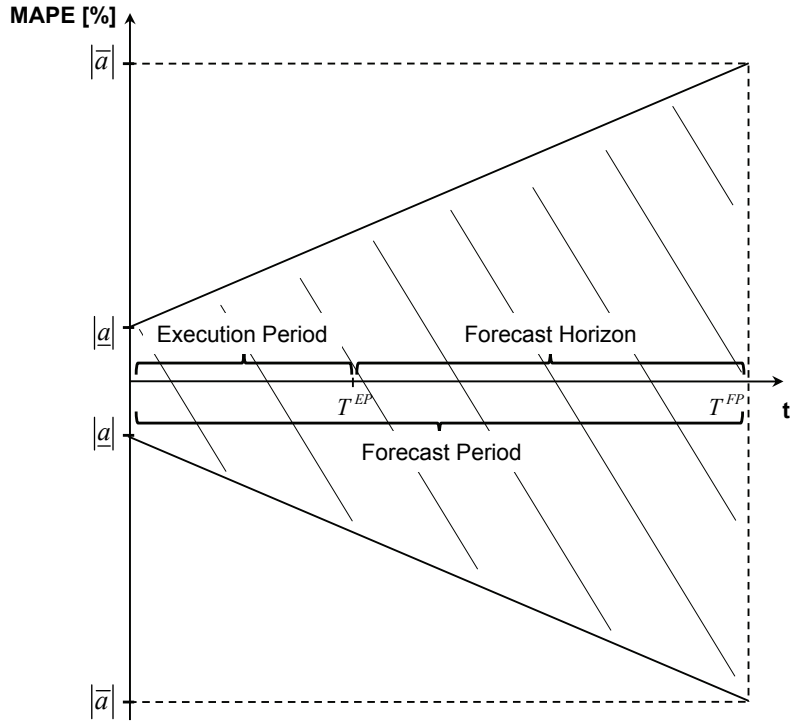

Figure 5.2: Elements of the forecast period

5.1.1 Derivation of the Standard Deviation σ_i

The modified Random Walk process shall meet the MAPE $\bar{x}_t$ for each timeslot t (equation (5.8)). Thus, the process shall have the following property:

$$Var(X_t) = \tilde{\sigma}^2 \left(1 + \frac{(t-1)(\bar{a} \cdot \underline{a}^{-1} - 1)}{T^{FP} - 1}\right)^2 \tag{5.9}$$

$Var(X_t)$ is continuously growing from $Var(X_1) = \tilde{\sigma}^2$ to $Var(X_{T^{FP}}) = (\bar{a} \cdot \underline{a}^{-1})^2 \cdot \tilde{\sigma}^2$. To achieve the desired characteristics of the process, $\tilde{\sigma}$ is defined as in equation (5.7) and y_i must be determined. The variance of the modified Random Walk is

$$Var(X_t) = Var\left(\varepsilon_t + \alpha \sum_{i=1}^{t-1} \varepsilon_i\right) \tag{5.10}$$

Since all ε_i $(1 \leq i \leq t)$ are independent and normally distributed random variables and α is a constant factor, one can transform the equation to

$$Var(X_t) = Var(\varepsilon_t) + \alpha^2 \sum_{i=1}^{t-1} Var(\varepsilon_i) \tag{5.11}$$

Replacing $Var(\varepsilon_i)$ $(1 \leq i \leq t)$ with $\tilde{\sigma}^2 \cdot y_i^2$ and factoring out $\tilde{\sigma}^2$ results in

$$Var(X_t) = \tilde{\sigma}^2 \cdot (y_t^2 + \alpha^2 \sum_{i=1}^{t-1} y_i^2) \tag{5.12}$$

To determine y_i, equations (5.9) and (5.12) are matched

$$\tilde{\sigma}^2 \left(1 + \frac{(t-1)(\bar{a} \cdot \underline{a}^{-1} - 1)}{T^{FP} - 1}\right)^2 = \tilde{\sigma}^2 \left(y_t^2 + \alpha^2 \sum_{i=1}^{t-1} y_i^2\right) \tag{5.13}$$

and solved for y_i:

$$y_i = \frac{T^{FP} + i \cdot \bar{a} \cdot \underline{a}^{-1} - i - \bar{a} \cdot \underline{a}^{-1}}{\sqrt{1 + \alpha^2 \cdot i - \alpha^2} \cdot (T^{FP} - 1)} \tag{5.14}$$

The combination of equations (5.14) and (5.6) results in the standard equation σ_i:

$$\sigma_i = \tilde{\sigma} \cdot \frac{T^{FP} + i \cdot \bar{a} \cdot \underline{a}^{-1} - i - \bar{a} \cdot \underline{a}^{-1}}{\sqrt{1 + \alpha^2 i - \alpha^2} \cdot (T^{FP} - 1)} \tag{5.15}$$

5.1.2 Determining the Mean Absolute Percentage Error of Normally Distributed Variables

A random number generator $\mathcal{N}$ with a normal probability distribution produces a Series of N random variables $X_i (1 \leq i \leq N)$ with

$$X_i \sim \mathcal{N}(\mu, \sigma), \mu > 0 \tag{5.16}$$

The MAPE $\bar{x}$ of $\vec{X}$ $(1 \times N)$ is defined as

$$\bar{x} = \frac{1}{N} \cdot \sum_{i=1}^{N} \frac{|X_i - \mu|}{\mu} \tag{5.17}$$

The question is how to determine the standard deviation σ in order to match $\bar{x}$. Since $\bar{x}$ is by definition relative to the expected value μ, σ is defined as

$$\sigma = \alpha \cdot \bar{x} \tag{5.18}$$

The probability density function of $\mathcal{N}$ is defined as

$$f(x) := \frac{1}{\sigma \cdot \sqrt{2\pi}} \cdot e^{-\frac{1}{2}\left(\frac{x-\mu}{\sigma}\right)^2} \tag{5.19}$$

One now combines $g(x)$ as the relative deviation of a value x from its expected value μ with its probability:

$$g(x) := \frac{x-\mu}{\mu} \cdot f(x) \tag{5.20}$$

Since the relative deviation of x is supposed to equal $\bar{x} \cdot \mu$ and the probability density function $f(x)$ is symmetric, one can define the following equation to calculate α:

$$\int_{\mu}^{\infty} g(x)dx = \frac{1}{2} \cdot \bar{x} \cdot \mu \tag{5.21}$$

Solving the integral function leads to

$$\lim_{x\to\infty} \left(\frac{\bar{x} \cdot \alpha \cdot e^{-\frac{1}{2}\left(\frac{x-\mu}{\sigma}\right)^2} - 1}{(-1) \cdot \sqrt{2\pi}} \right) = \frac{\bar{x} \cdot \mu}{2} \tag{5.22}$$

This equation converges against

$$\frac{\bar{x} \cdot \alpha}{\sqrt{2\pi}} = \frac{\bar{x} \cdot \mu}{2} \tag{5.23}$$

so that

$$\alpha = \frac{\sqrt{2\pi} \cdot \mu}{2} \tag{5.24}$$

If $\mu = 0$, equation (5.17) for calculating $\bar{x}$ is replaced by the Mean Absolute Error (MAE), which is defined as

$$mae = \frac{1}{N} \sum_{i=1}^{N} |x_i| \tag{5.25}$$

and $g(x)$ is defined as

$$g(x) := x \cdot f(x) \tag{5.26}$$

since x itself is the deviation from the expected volume in this case. The relative deviation of x is supposed to equal mae:

$$\int_{0}^{\infty} g(x)\, dx = \frac{1}{2} \cdot mae \tag{5.27}$$

This equation can be analogously solved for α, resulting in

$$\alpha = \frac{\sqrt{2\pi}}{2} \tag{5.28}$$

5.2 Schedule Determination

Determining an arbitrage-maximizing CDS is subject to various papers (see beginning of Chapter 5). As an alternative to linear optimization algorithms and dynamic programming approaches, this work additionally defines and analyzes a heuristic scheduling algorithm. Results from the implementation of the linear optimization model, which was presented in Part I of this work, and the heuristic algorithm are benchmarked in Section 5.5.3. The main idea of the heuristic algorithm is to quickly generate a robust schedule, i.e., being less vulnerable to fluctuations of the forecast accuracy and the degree of forecast error autocorrelation.

5.2.1 Scheduling Algorithm using Linear Optimization

The schedule for the storage system determines when to charge and discharge the storage device. Formally, the vector φ $(1 \times T^{FP})$ defines the charge schedule and λ $(1 \times T^{FP})$ the discharge schedule $(0 \leq \varphi_t, \lambda_t \leq 1)$. For each timeslot of the current forecast period, the linear optimization model minimizes the variable costs $K_t^{variable}$:

$$K_t^{variable} = p_t \ell_t - p_t q_t^{out} \lambda_t + p_t q^{in} \varphi_t + \frac{\kappa}{\gamma} q_t^{out} \lambda_t \tag{5.29}$$

where ℓ is the load (forecast), p the price (forecast), $\kappa \cdot \gamma^{-1}$ the storage costs per discharge cycle for using (depreciating) the storage system, φ and λ the charge and discharge decision parameters, q_t^{out} the maximal discharge volume in timeslot t

$$q_t^{out} = min\left(\ell_t; min\left(C; \frac{P^{out}}{T^h}\right)\right) \tag{5.30}$$

and q^{in} the maximal charge volume.

$$q^{in} = \frac{C}{\eta_{in} \cdot \eta_{store} \cdot \nu} \tag{5.31}$$

The constraints of the linear optimization model are

$$0 \leq \varphi_t, \lambda_t \leq 1 \qquad \forall t \tag{5.32}$$

$$\varphi_t + \lambda_t \leq 1 \qquad \forall t \tag{5.33}$$

$$0 \leq \xi_t \leq C \qquad \forall t \tag{5.34}$$

with

$$\xi_t = \sum_{t'=1}^{t} \frac{C}{\nu} \cdot \varphi_{t'} - \frac{q_{t'}^{out}}{\eta^{out}} \cdot \lambda_{t'} \tag{5.35}$$

φ and λ are the decision variables of the linear optimization model. Thus, solving the linear optimization problem reveals the values for φ and λ (further details on the linear optimization model in Section 3.2).

To determine the optimal CDS, the model is fed with the load forecast, the electricity price forecast, and the technical system specification. If the data for load and

prices are actual values, i.e., forecasts with no error, a linear optimization algorithm as presented in Section 3.2 determines the optimal CDS. In case of forecast errors, the CDS is 'pseudo optimal' since the applied load and price values deviate from the actual ones in the next step (schedule execution). The higher the MAPE of a forecast, the more a CDS deviates from the economically optimal CDS that builds on the actual data.

The procedure determines the CDS for the entire forecast period, while - in the next step - the schedule will be applied only to the execution period. Producing CDS for a forecast period larger than the next execution period avoids myopic schedule optimizations by anticipating inter-day load shifting, which might be economically beneficial.

5.2.2 Heuristic Scheduling Algorithm

As the linear optimization model in the previous section, the heuristic algorithm presented in this section will also determine a CDS. In contrast to the linear optimization algorithm, the heuristic algorithm will not determine an optimal schedule, but it intents to derive a more robust schedule against forecast fluctuations. The heuristic algorithm works in the two phases. The first phase determines the price limits. The second phase then derives the schedule using these price limits. Both phases are described in detail in the following paragraphs.

Price Limit Determination

In the first phase, the algorithm determines price limits for charging and discharging. I.e., the storage system considers charging as soon as the forecast price falls below the charge limit price, analogously it considers discharging when the forecast price exceeds the discharge limit price. The parameters used for the price limit determination function are:

- $L_t(price.fo, load.fo)$: List of Price-Load-Tuples (forecasts) for each timeslot t in the forecast period $1 \leq t \leq T$. Accessing the price is defined as $L_{t'}^{price.fo}$ (load analogously).
- $\vec{L}_{t'}(price.fo, load.fo)$: Sorted list (by ascending forecast prices), i.e., $\vec{L}_{t'}^{price.fo} \leq \vec{L}_{t''}^{price.fo} \quad \forall \ t' < t'' \ \ (1 \leq t', t'' \leq T^{FP})$.
- κ: Price per storage capacity unit (EUR/kWh).
- γ: Number of expected nominal (full) charge cycles over the lifetime of the storage device (#).
- cm : Contribution margin on top of the variable costs of storage usage, $cm \geq 0$ (%) enforces higher charge-discharge price spreads in the CDS.
- $\Delta = \kappa \cdot \gamma^{-1} \cdot (1 + cm)$: Required price difference between charge and discharge timeslots (EUR/kWh).
- $p^{charge} = \vec{L}_i^{price.fo}$: Charge price limit (EUR/kWh), i is the charge index for list $\vec{L}$.

- $p^{discharge} = \vec{L}_j^{price.fo}$: Discharge price limit (EUR/kWh), j is the discharge index for list $\vec{L}$.
- b^{charge}: Buffer on the charge index (#) ($b^{charge} < T$), sets the lower bound for the charge index i.
- η^{out}: is the output efficiency of the storage system (%).

Determining the price limits follows two rules:

- **Rule 1**: The difference between the highest charging price and the lowest discharging price must always be greater or equal than the required price difference Δ. This ensures that each charge-discharge-cycle covers the variable costs of storage usage, regardless of the order in which the prices occur.
- **Rule 2**: The expected charge volume and the aggregated volume of the expected discharge timeslots are always balanced. I.e., the aggregated volume of the expected discharge timeslots never exceeds the expected charge volume and the expected charge volume never exceeds the expected discharge volume by more than the volume of one nominal charge timeslots.

Formally, the price limit determination function is defined as

$$\min \rightarrow j - i \tag{5.36}$$

aiming at a maximization of the economically beneficial charge and discharge volumes. The constraints are Rule 1 (equation (5.37)) and Rule 2 (equation (5.38)). Equation 5.39 ensures that values of i and j do not cross and remain in valid ranges.

$$\vec{L}_j^{price.fo} - \vec{L}_i^{price.fo} \geq \Delta \tag{5.37}$$

$$i \cdot \frac{C}{v} - \frac{1}{\eta^{out}} \sum_{t'=j}^{T^{FP}} \vec{L}_{t'}^{load.fo} < \frac{C}{v} \tag{5.38}$$

$$1 + b^{charge} \leq i \leq T^{FP} - 1, \quad 2 \leq j \leq T^{FP}, \quad i < j \tag{5.39}$$

Schedule Derivation

In the second phase, the algorithm determines the CDS. Additionally to the simplest variant *Heuristic 1*, variants *Heuristic 2*, *Heuristic 3*, and *Heuristic 4* base the decision whether to actually charge or discharge the DSS not only on the previously determined price limits, but also on the expected alternatives in the succeeding timeslots (based on the forecast). In both cases, the rationale behind the additional conditions is to find local minima for charging and discharging in the forecast data (refinement of Rule 1). Appendix C contains the flow chart diagrams of the heuristic algorithm, including incremental refinements of its variants. Additionally to the parameters defined for the previous phase, Phase 2 uses the following parameters:

- p_t^{fo}: Price forecast for timeslot t (EUR/kWh).

- ℓ_t^{fo}: Load forecast for timeslot t (EUR/kWh).
- $q_t^{out.fo}$: Maximal discharge volume in timeslot t according to the load forecast (kWh).
- ξ_t : State of Charge (SOC), stored electricity in timeslot t (kWh).
- $\bar{\delta}$: Maximal Depth of Discharge (DOD) (%).
- C : Maximal storage capacity (kWh).
- v : Maximal charging speed, i.e. required timeslots for a nominal charge cycle (#).

The variant *Heuristic 1* marks timeslots for charging as soon as the expected price falls below the charge price limit (discharging analogously).

$$\textbf{Condition C1}: \quad p_t^{fo} \leq p^{charge} \quad \forall t \tag{5.40}$$

$$\textbf{Condition C2}: \quad p_t^{fo} \geq p^{discharge} \quad \forall t \tag{5.41}$$

The variant *Heuristic 2* additionally performs a refinement of the charge condition. A timeslot is only marked for charging, if the volume that could be charged in later timeslots with relatively lower prices (until the next discharge cycle) does not exceed the expected discharge volume of the next discharge cycle.

$$\textbf{Condition C3}: \quad \frac{C}{v} \cdot |T'_1| < C - \xi_t \tag{5.42}$$

with

$$T'_1 = \left\{ t' | p_{t'}^{fo} < p_t^{fo} : t' > t \ \wedge \ \nexists t'' \leq t' : p_{t''}^{fo} \geq p_t^{discharge} \right\}$$

Heuristic 3 extends *Heuristic 2* by an additional discharge condition. A timeslot is only marked for discharging, if the expected discharge volume of later timeslots with relatively higher prices does not exceed the available volume in the DSS until the next charge cycle.

$$\textbf{Condition C4}: \quad \frac{1}{\eta^{out}} \cdot \sum_{t' \in T'_2} q_{t'}^{out.fo} < \xi_t - (1 - \bar{\delta}) \cdot C \tag{5.43}$$

with

$$T'_2 = \left\{ t' | p_{t'}^{fo} > p_t^{fo} : t' > t \ \wedge \ \nexists t'' \leq t' : p_{t''}^{fo} \leq p_t^{charge} \right\} \tag{5.44}$$

Heuristic 4 extends *Heuristic 3* by an additional charge and an additional discharge condition. These refinements allow the algorithm to assume a temporary charge cycle within a discharge period (respectively a temporary discharge cycle within a charge period). Table 5.1 summarizes all variants of the heuristic algorithm and their charge and discharge conditions.

$$\textbf{Condition C5}: \quad \frac{C}{v} \cdot |T'_3| < C - \xi_t + \frac{1}{\eta^{out}} \cdot \sum_{t'' \in T''} \ell_{t''}^{fo} \tag{5.45}$$

with

$$T'_3 = \left\{ t' | p^{fo}_{t'} < p^{fo}_t : t' > t \ \wedge \ \frac{C}{v} \cdot \left| \widetilde{T'_3} \right| - \sum_{t'' \in T''_3} q^{out.fo}_{t''} > (1 - \xi_t) \cdot C \right\} \tag{5.46}$$

and

$$\widetilde{T'_3} = \left\{ \widetilde{t'} | \widetilde{t'} > t \ \wedge \ \widetilde{t'} \leq t' \wedge p^{fo}_{\widetilde{t'}} < p^{fo}_t \right\} \tag{5.47}$$

and

$$T''_3 = \left\{ t'' | t'' < t' \ \wedge \ p^{fo}_{t''} \geq p^{discharge}_t \right\} \tag{5.48}$$

$$\textbf{Condition C6}: \quad \frac{1}{\eta^{out}} \cdot \sum_{t' \in T'_4} q^{out.fo}_{t'} < \xi_t - (1 - \bar{\delta}) \cdot C + \frac{C}{v} \cdot |T''_4| \tag{5.49}$$

with

$$T'_4 = \left\{ t' | p^{fo}_{t'} > p^{fo}_t : t' > t \wedge \Gamma \right\} \tag{5.50}$$

where

$$\Gamma := \left(\frac{1}{\eta^{out}} \cdot \sum_{\widetilde{t'} \in \widetilde{T'}} q^{out.fo}_{\widetilde{t'}} - \frac{C}{v} \cdot |T''_4| < \xi_t - (1 - \bar{\delta}) \cdot C \right) \tag{5.51}$$

containing

$$\widetilde{T'} = \left\{ \widetilde{t'} | \widetilde{t'} \leq t' \wedge \widetilde{t'} > t \wedge p^{fo}_{\widetilde{t'}} > p^{fo}_t \right\} \tag{5.52}$$

and

$$T''_4 = \left\{ t'' | t'' > t \wedge t'' \leq t' \wedge p^{fo}_{t''} \leq CLP \right\} \tag{5.53}$$

Table 5.1: Variants of the Heuristic Algorithm

Algorithm	**Charge condition for timeslot t**	**Discharge condition for timeslot t**
Heuristic 1	C1	C2
Heuristic 2	C1 $\wedge$ C3	C2
Heuristic 3	C1 $\wedge$ C3	C2 $\wedge$ C4
Heuristic 4	C1 $\wedge$ C3 $\wedge$ C5	C2 $\wedge$ C4 $\wedge$ C6

5.3 Schedule Execution

The previous step of the simulation model determined a charge schedule φ_t ($1 \leq t \leq T^{FP}$) and a discharge schedule λ_t based on the price and load forecasts. Due to deviations between the forecast and the actual data, this schedule might violate the (technical) constraints of the storage device. In particular, the constraints are the lower and upper bound of the SOC, i.e., the realized DOD and the maximal storage capacity C. The schedule execution algorithm applies the actual price and load data p_t and ℓ_t instead of the forecast data and tries to execute the CDS as complete as possible within these constraints. If necessary, $\varphi_{t'}$ and $\lambda_{t'}$ are updated according to the technical constraints within the execution period $1 \leq t' \leq T^{EP}$.

Charging must not exceed the maximal capacity of the storage device. Thus, $\varphi_{t'}$ might have to be less than 1 (partial charging in t'):

$$\varphi_{t'} = min\left(\varphi_{t'}\ ,\ \frac{(C - \xi_{t'-1}) \cdot v}{C}\right) \quad \forall t' \tag{5.54}$$

Discharging must not exceed the available electricity stored, i.e., the difference between the current SOC ξ_t (including the charged capacity in t') and the maximal DOD (i.e., minimal SOC) allowed:

$$\lambda_{t'} = min\left(\lambda_{t'}\ ,\ \ \xi_{t'-1} + \varphi_{t'} \cdot \frac{C}{v} - \frac{(1 - \bar{\delta}) \cdot C \cdot \eta^{out}}{q^{out}_{t'}}\right) \quad \forall t' \tag{5.55}$$

where $q^{out}_{t'}$ is the maximal discharge volume in timeslot t'. Accordingly, theSOC of the executed timeslot t' is

$$\xi_{t'} = \xi_{t'-1} + \varphi_{t'} \cdot \frac{C}{v} - \lambda_{t'} \cdot \frac{q^{out}_{t'}}{\eta^{out}} \quad \forall t' \tag{5.56}$$

The variable costs $K^{variable}_{t'}$ of timeslot t' within equation (5.1) that result from the updated (executed) CDS equal to

$$K^{variable}_{t'} = \varphi_{t'} \cdot p_{t'} \cdot q^{in} + \lambda_{t'}\left(q^{out}_{t'}\left(\frac{\kappa}{\gamma} - p_{t'}\right)\right) \quad \forall t' \tag{5.57}$$

5.4 Simulation Scenarios

The scenarios define the reference frame for the simulated price and load forecasts. Generally, four basic settings are possible (Figure 5.3):

- Simulations with actual data only
- Price Forecast Simulations
- Load Forecast Simulations
- Combined Price and Load Forecast Scenarios

Simulations with actual data only deliver optimal results, if the schedule is determined with an optimization algorithm. These simulations (respectively analyses) have

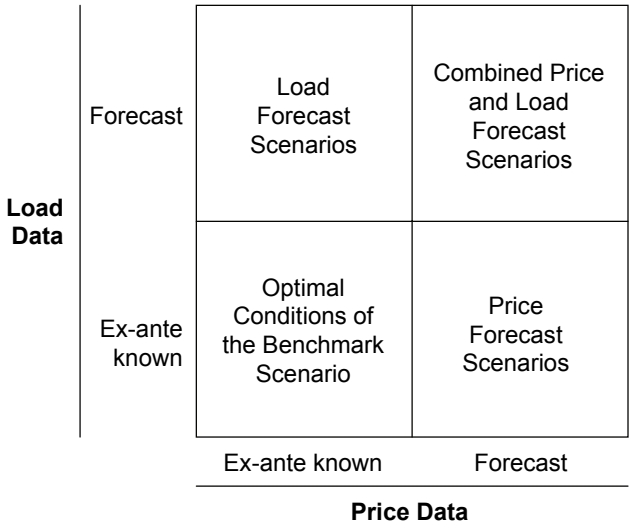

Figure 5.3: Basic scenario frame

been performed in the first part of this research work and form the benchmark case for all further simulations in this chapter.

All simulations in the following chapter build on the same data and specifications of the DSS as the basic model in Section 3.2, as already pointed out at the beginning of Chapter 5. This accounts for the technical system parameter values, the actual data on electricity prices and on consumer load profiles. The distribution of the electricity prices reflects the price distribution of market prices from the EEX (2007). The load data distribution corresponds to the VDEW standard household profiles (VDEW, 2006) and an annual load of 2000 kWh. Appendix B contains an overview of these parameters.

For the other cases (load forecast scenarios, price forecast scenarios, combined price and load forecast scenarios), Sections 5.4.1 - 5.4.3 will describe the simulation scenarios. Besides the MAPE of a forecast (see Section 5.1) these scenarios also simulate a specific level of autocorrelation of the forecast errors, which is measured as a DWT value (Section 4.2.5).

5.4.1 Load Forecast Scenarios

The load forecast scenarios assume load forecasts with specified forecast errors and given price data. These scenarios reflect situations where an hourly price signal is ex-ante to the planning period provided to a consumer, e.g., because the hourly price curve is part of a predefined tariff. Scenario 1 reflects the accuracies that have been reported in Table 4.2. Scenario 2 and 3 deteriorate the accuracy levels of Scenario 1 by a factor 2 respectively 3. Thus, these scenarios are very conservative. The reference value of the forecast errors' autocorrelation is 0.75 (DWT value), which is the average (rounded) value within the reviewed papers in Section 4.2.5. Table 5.2 summarizes the load forecast simulation scenarios.

5.4.2 Price Forecast Scenarios

The price forecast scenarios assume price forecasts with specified forecast errors and given load data. Scenario 4 reflects the accuracies that have been reported in Table 4.3. Scenario 5 and 6 deteriorate the accuracy levels of Scenario 4 by a factor 2 respectively

Table 5.2: Load Forecast Simulation Scenarios

	MAPE at the beginning of day 1 (%)	**MAPE at the end of day 7 (%)**	**Autocorrelation (DWT)[a]**
Scenario 1	7.5	15	0.75
Scenario 2	15	30	0.75
Scenario 3	22.5	45	0.75

[a] Durbin-Watson Test (DWT) value

3 (see Table 5.3). Thus, these scenarios are rather conservative. The reference value of the forecast errors' autocorrelation is 0.5 (DWT value), which is the average (rounded) autocorrelation value within the reviewed papers in Section 4.2.5.

Table 5.3: Price Forecast Simulation Scenarios

	MAPE at the beginning of day 1 (%)	**MAPE at the end of day 7 (%)**	**Autocorrelation (DWT)[a]**
Scenario 4	5	15	0.5
Scenario 5	10	30	0.5
Scenario 6	15	45	0.5

[a] Durbin-Watson Test (DWT) value

5.4.3 Combined Price and Load Forecast Scenarios

The set of price and load forecast scenarios combines three basic scenarios of price forecast scenarios (Section 5.4.2) and load forecasts scenarios (Section 5.4.1) to 9 scenarios in total (Figure 5.4). As the previously defined Scenarios 1 to 6, each scenario has three parameters: (1) MAPE at the beginning of the first day of the forecast period (lower accuracy bound), (2) MAPE at the end of the last day of the forecast period (upper accuracy bound), and (3) a specific degree of autocorrelation of relative forecast errors (indicated with the DWT value). All of these parameter values are set as defined in Scenarios 1 to 6, just that each of the Scenarios 7 to 15 contains both a load forecast setting (Scenarios 1 to 3) and a price forecast setting (Scenarios 4 to 6).

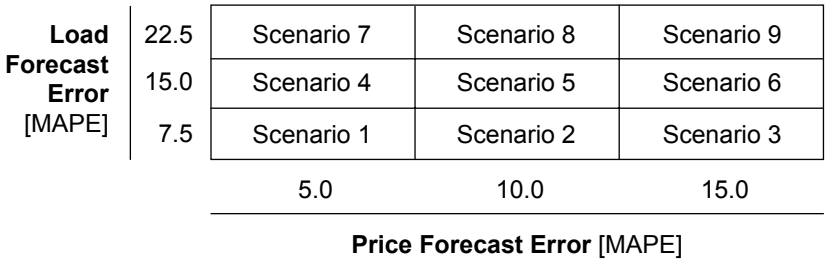

Figure 5.4: Simulation scenarios

Scenarios 7, 8, 10, and 11 reflect realistic, but conservative assumptions (compare Sections 4.2.1 - 4.2.3), whereas Scenarios 9, 12, 13, 14, and 15 reflect very conservative assumptions with regard to the achievable load and price forecast accuracies.

5.5 Simulation Results

The simulation model calculated the annual savings that a DSS could realize using price and load forecast data. All results are indicated relative to the optimal result. The optimal result is determined through a linear optimization algorithm that derives an optimal CDS from the actual price and load data. Each scenario simulates forecasts with a specified MAPE of the lower and the upper accuracy bound, as well as a specified degree of autocorrelation of forecast errors (see Section 5.1). Since the forecast generation procedure uses random number streams, each Monte Carlo simulation is run up to 500 times to average out statistical effects (see beginning of Chapter 5).

The following paragraphs present the economic analysis of load forecast scenarios, price forecast scenarios, and combined load and price forecast scenarios, as defined in Section 5.4. Results in Sections 5.5.1 and 5.5.2 use a linear optimization algorithm to determine the CDS. In Section 5.5.3, the linear optimization algorithm and a heuristic scheduling algorithm are compared.

5.5.1 Load Forecast Scenarios

The following paragraphs present the economic analysis of load forecast impacts on the annual savings of the DSS. The analyzed forecast characteristics are forecast accuracy, the degree of autocorrelation in forecast errors, the granularity of forecast data, and the variation of the forecast horizon length.

Forecast Horizon

Extending the forecast horizon allows for more effective intertemporal optimizations of the scheduling algorithm. The forecast horizon is defined as that part of the forecast period, which exceeds the execution period (see Figure 5.2). A short forecast horizon leads to myopic charge and discharge actions and does not take advantage of the opportunity to shift portions of load over one or more days. Clearly, a larger forecast horizon also increases the MAPE at the end of the forecast period. Table 5.4 depicts the assumed (linear) relation between forecast errors and the length of the forecast period.

Figure 5.5 shows the economic impact of extending the forecast horizon. While a myopic schedule that only considers the immediately next execution period, i.e., the next day in our simulations, shows high deviations of more than 8% from the optimum for all scenarios, already a forecast horizon of one day leads to much lower deviations. For a 6 days forecast horizon, one can observe a result of 2.0-7.5% (Scenario 1-3) from the optimal result. Forecast horizons of 6 to 20 days remain on the approximately same level for Scenarios 1 and 2; marginal result improvements (about 1% point) can be observed. Only Scenario 3 with the highest forecast errors shows a more substantial improvement of 2% points for longer forecast periods than 7 days, although the MAPE at the end of the forecast period increases significantly. Thus, the results indicate that

Table 5.4: MAPE at the End of the Forecast Horizon

Forecast Horizon (days)	**Scenario 1 (%)**	**Scenario 2 (%)**	**Scenario 3 (%)**
0	8.6	17.1	25.7
1	9.6	19.3	28.9
2	10.7	21.4	32.1
6 (ref.)	**15.0**	**30.0**	**45.0**
13	22.5	45.0	67.5
20	30.0	60.0	90.0

the lower accuracy bound at the beginning of the forecast period has a much higher impact on the overall result than the upper bound at the end.

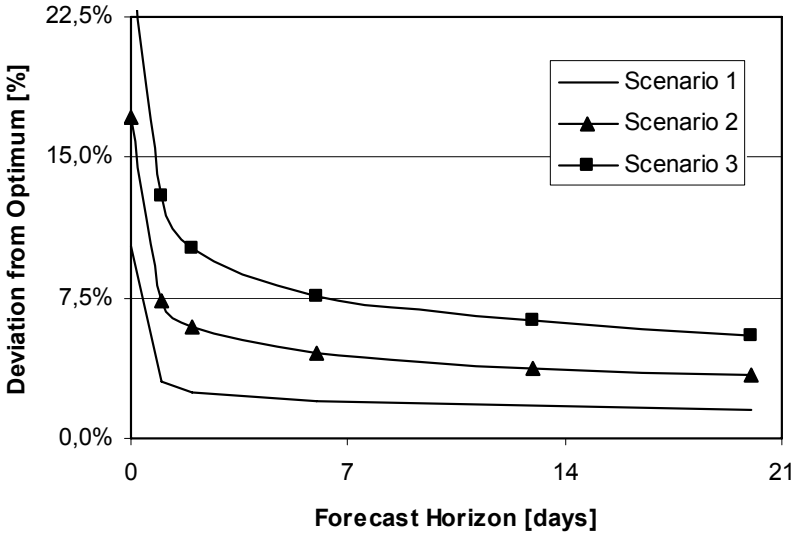

Figure 5.5: Impact of load forecast horizon extensions

In conclusion, the forecast horizon is an important parameter for the model. In our simulations, load shifts over more than 7 days obviously occurred very rarely so that the effect of optimizing beyond this horizon economically did not have a substantial impact. Therefore, all following simulations for Scenarios 1-3 have been performed with a forecast horizon of 6 days.

Autocorrelation of Forecast Errors

As pointed out by Hobbs et al. (1999), load forecast errors tend to be autocorrelated. Our analysis of the published forecast data streams in the reviewed papers confirms this (Section 4.2.5). I.e., succeeding timeslots tend to have similar (relative) forecast errors, which reflects a systematic over- or underestimation within a certain period of time. For all simulated scenarios, the standard value for the autocorrelation is 0.75 (DWT value).

The results in Figure 5.6 show that autocorrelated forecast errors negatively impact the deviation from the optimal result. Forecasts without autocorrelated errors achieve

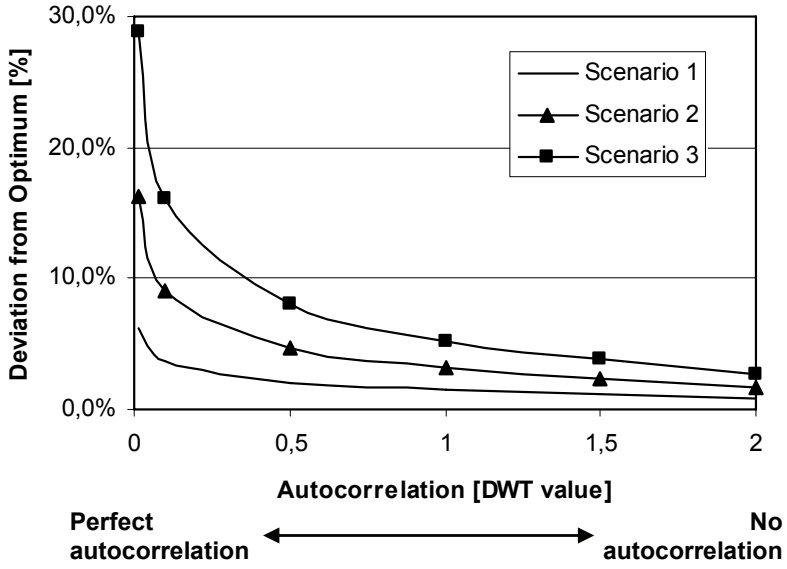

Figure 5.6: Impact of autocorrelation of load forecast errors

the best results. While a DWT value of 1-2 leads to a marginal deterioration of the result (1-5% deviation from the optimum for Secnarios 1-3), DWT values smaller than 1 significantly deteriorate the result. The explanation behind this obeservation is that highly autocorrelated forecast errors of load forecasts lead to a systematic over- or underestimation of a period. Thus, the CDS will systematically violate the technical constraints of the system, which preludes an economically optimal operation. Forecasts with low autocorrelation of relative errors average out the errors and, thus, do not systematically operate the storage at its limits.

Thus, the chosen load forecast method within a scheduling algorithm for a DSS must be tested towards the autocorrelation of its forecast errors. Methods delivering highly autocorrelated forecast errors might even be inferior to less accurate forecast techniques with lower error autocorrelation.

Load Forecast Granularity

Especially load forecast for (very) small consumer units, e.g., entities below the substation level, faces significant difficulties to achieve accurate load forecasts. Since statistical deviations in the load profile are not averaged out as on more aggregated levels (aggregation of multiple units), aggregating timeslots is a possible alternative for small units. The reference case are hourly load forecast streams. Instead, the following analysis simulated load forecasts of blocks of 2-8 hours length. Thus, these blocks are more aggregated and therefore allow for higher forecast accuracy within these timeblocks. In a second step, these forecasts are transformed into streams of hourly forecasts by simply dividing the load forecast into equally large pieces for the hourly data stream. E.g., if a forecast of a 3-hour-timeslot from 8 am to 11 am indicates a load volume of 750 Watt hours (Wh), it is transformed into 250 Wh load within each hourly timeslots from 8 am to 11 am. Figure 5.7 shows the results of this analysis.

The results show that aggregating timeslots can even have a positive impact on the result. The straight lines indicate the results of the scenarios using the (standard) autocorrelation value of forecast errors of 0.75 (see Table 5.2). The dotted lines refer to Scenarios 1-3, but without autocorrelation of forecast errors. For all standard scenarios

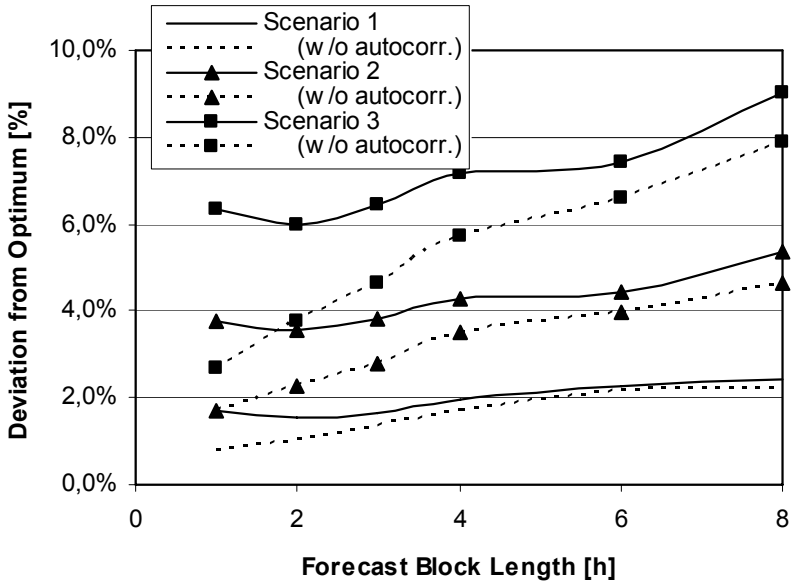

Figure 5.7: Impact of load forecast granularity

(straight lines), one can observe that the result slightly improves when extending the forecast block size from 1 to 2 hours. For forecast blocks of more than 2 hours the results deteriorate steadily. In contrast, the scenarios without autocorrelated forecast errors (dotted lines) show a steady increase in the deviation from the optimal result for all forecast block size enlargements. Thus, the described approach of first aggregating and then equally dividing timeslots helps to average out the negative effects of autocorrelation in load forecast errors (see Section 5.5.1) when extending the forecast block size from 1 to 2 hours.

Increasing the forecast block length from 1 to 8 hours increases the deviation from the optimal result by 1-3% points (Scenarios 1-3). This result seems to be a very important lever for small unit load forecasting. Potentially, an aggregation of several timeslots allows for averaging out forecast errors, while causing only a minor deterioration of the result due to the aggregation. Forecasting methods for small unit load forecasting will have to investigate what benefits on the accuracy side can be obtained from forecasting larger timeslots. E.g., if the forecast accuracy can be improved from 15% MAPE to 7.5% MAPE by increasing the forecast block size from 1 to 4 hours, the deviation from the optimum could be reduced from 3.8% (Scenario 2, 1-hour forecast blocks) to 2.0% (Scenario 1, 4-hour forecast blocks). In this case, aggregating timeslots would have an overall positive effect on the result.

Load Forecast Accuracy

The more accurate a load forecast is, the better the (day-ahead) derived CDS realizes its objective of arbitrage accommodation. I.e., charging the storage system with precisely the right volume in the cheapest timeslots and discharging the optimal volume in the most expensive ones.

Figure 5.8 depicts the deviations from the optimal result depending on the upper accuracy bound at the end of the forecast period (14 days). The lower accuracy bound is kept constant within each scenario.

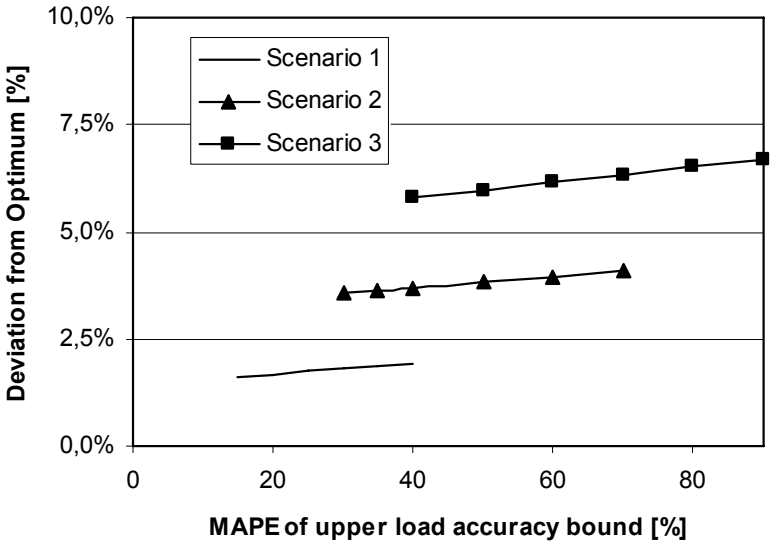

Figure 5.8: Impact of load forecast accuracy on economic result

One can see that the results of each scenario remain on distinct levels - independent of the variation of the upper accuracy bound (Scenario 1 at 2%, Scenario 2 at 4%, Scenario 3 at 6%). Hence, the lower accuracy bound determines the overall level of realizable savings. The upper bound has only a marginal effect. The results in Section 5.5.1 already indicated this observation.

Figure 5.9 shows the cumulative probability of up to 500 simulation runs of Scenarios 1-3. It reveals that each scenario delivers already distinct results. Decreasing the MAPE at the beginning of the forecast period by 1% point leads to an average reduction of the deviation from the optimal result of 0.25% points (from 6% for Scenario 3 with 22.5% MAPE to 2% for Scenario 1 with 7.5% MAPE).

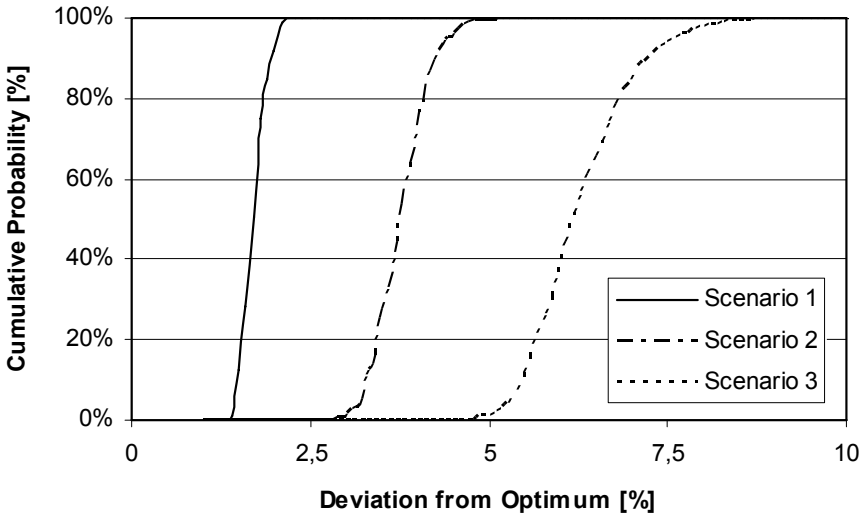

Figure 5.9: Cumulative probability of deviations from the optimum (load forecast variations)

Furthermore, these results indicate a high robustness of the mechanism towards load forecast accuracy deviations. In comparison with the possible forecast accuracies reported in literature (see Tables 4.1 and 4.2), the required forecast quality is relatively low. The context of the analysis in this research work reflects forecasting of (very)

small units (end consumer level). Table 4.2 presents upper-case reference points for substation levels and delivers the values for Scenario 1 (average accuracy in literature) in Table 5.2. Since for an end consumer level the volumes are even lower and forecasts therefore less accurate than on the substation level, the more conservative Scenarios 2 and 3 reflect this deterioration. In conclusion, the required load forecast accuracy for economically operating a DSS is considerably low and within a feasible scope for existing forecast methods.

5.5.2 Price Forecast Scenarios

The following paragraphs present the economic analysis of price forecast impacts on the annual savings of the DSS. The analyzed forecast characteristics are forecast accuracy, the degree of autocorrelation in forecast errors, and the variation of the forecast horizon length.

Forecast Horizon

As explained in Section 5.5.1, extending the forecast horizon allows for more effective intertemporal optimizations of the scheduling algorithm. A short forecast horizon leads to myopic charge and discharge actions and does not take advantage of the opportunity to shift portions of load over one or more days. As for load forecasts, a larger forecast horizon also decreases the achievable price forecast accuracy level at its end. This work assumes a linear decrease of the achievable price forecast accuracy level from the beginning to the end of the forecast period (see Table 5.5).

Table 5.5: MAPE at the End of the Forecast Horizon

Forecast Horizon (days)	**Scenario 4 (%)**	**Scenario 5 (%)**	**Scenario 6 (%)**
0	6.4	12.9	19.3
1	7.9	15.7	23.6
2	9.3	18.6	27.9
6 (ref.)	**15.0**	**30**	**45**
13	25.0	50.0	75.0

Figure 5.10 shows the economic impact of extending the forecast horizon. An extremely myopic optimization that only optimizes the immediately next execution period and does not consider any *additional* forecast horizon results in substantial deviations from the optimal result: 8.2% for Scenario 4, 12.9% for Scenario 5, and 21.2% for Scenario 6. For all scenarios, a forecast period including one additional day in its forecast horizon delivers the best results: 1.8% for Scenario 4, 7.2% for Scenario 5, and 16.6% for Scenario 6. For forecast horizons of more than one day, economic results decrease again. This implies that the benefits from intraday optimizations beyond a scope of one day undergo the costs of deteriorating forecast accuracies for such longer forecast horizons. Thus, the analyzed storage application mainly realizes arbitrage from load shifting between two consecutive days. This is a relevant piece of information for selecting the right storage technology with regard to self-discharge rates of different storage technologies. In comparison to the results of the load forecast

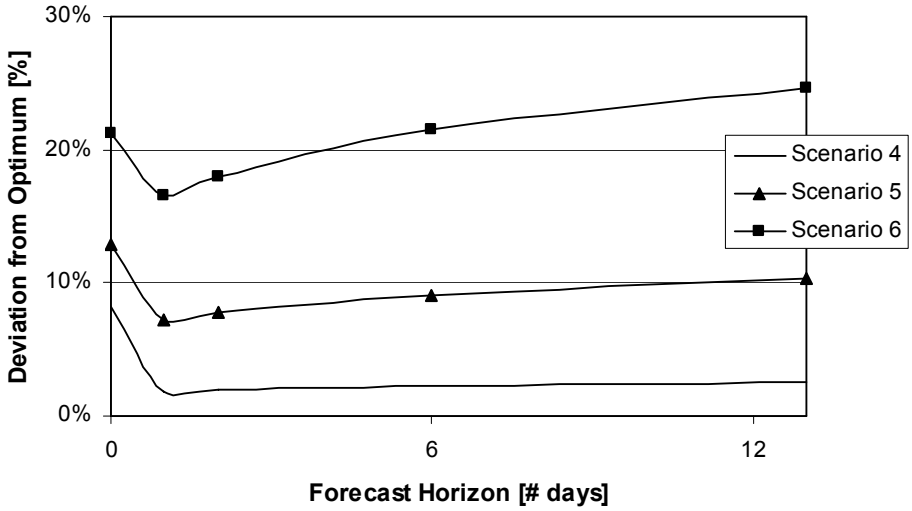

Figure 5.10: Impact of price forecast period length

horizon analysis, the results of this analysis are much more dependent on the MAPE at the end of the forecast horizon. A deterioration of this parameter has a much stronger negative impact on the achievable results. All following analyses for Scenarios 4-6 will be performed with the optimal forecast horizon dimension of one day.

Autocorrelation of Forecast Errors

Empirical examples in Hobbs et al. (1999) indicate that relative forecast errors tend to be autocorrelated. I.e., succeeding timeslots tend to have similar (relative) forecast errors, which reflects a systematic over- or underestimation within a certain period of time. The analysis of the referenced forecast methodologies in Section 4.2.5 also confirms this observation in scientific literature. The results in Figure 5.11 show that stronger autocorrelation of price forecast errors leads to better results for the analyzed storage system.

For devices that derive a schedule for arbitrage accommodation through optimization algorithms, this can be explained as follows: A systematic over- or underestimation of a price within a given period, i.e., strong autocorrelation of relative forecast errors, fosters the correct selection of the relatively lowest (for charging) and highest prices (for discharging) respectively. Thus, the CDS gets closer to the truly optimal CDS with regard to the actual data.[2] With or without intending the effect of autocorrelated errors, available forecast implementations tend to have this characteristic which improves the economic result of the analyzed storage system.

Price Forecast Accuracy

The more accurate a price forecast, the better the (day-ahead) derived CDS realizes its objective of arbitrage accommodation. I.e., charging the system precisely at the cheapest timeslots respectively discharging it at the most expensive ones.

Figure 5.12 depicts deviations from the optimal result depending on the MAPE at the end of the forecast period. Thus, this analysis varies the parameter “MAPE at day

[2]The opposite is the case for load forecasts. The more the CDS contains a systematic over- or underestimation of charge and discharge volumes, the less it matches the truly optimal CDS.

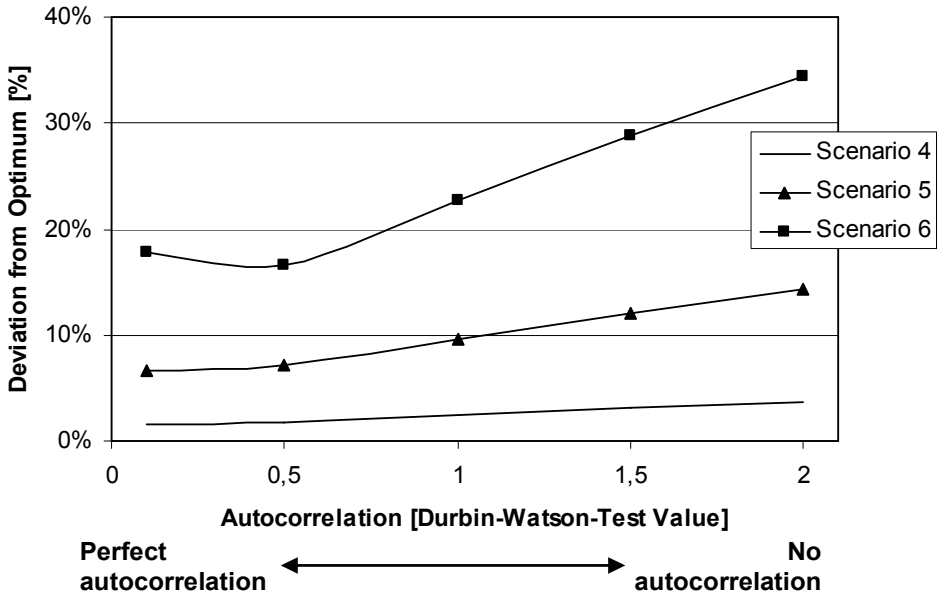

Figure 5.11: Economic impact due to autocorrelation of price forecast errors

the end of day 7" for each scenario, the lower accuracy bound at the beginning of the forecast period is kept constant.

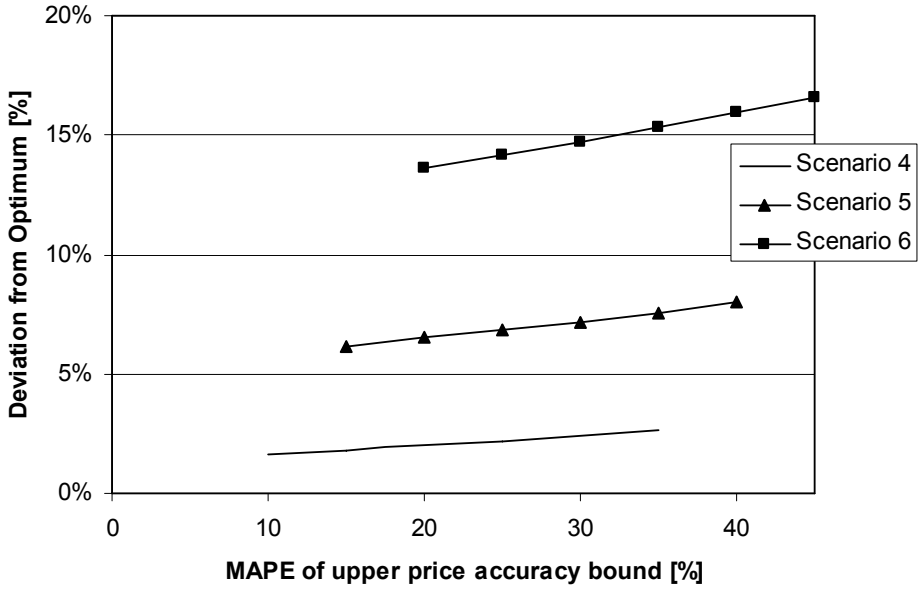

Figure 5.12: Impact of price forecast accuracy bounds

As Figure 5.12 shows, even large deviations of this upper accuracy bound have comparably limited impact on the economic result: ±0.5% point for Scenario 4 up to ±1.5% points for Scenario 6. Significantly greater importance can be assigend to the lower accuracy bound ("MAPE at the beginning of day 1"). Regardless of the upper accuracy bound variations, the result for Scenario 4 to 6 are clearly distinct.[3] This can also be observed from Figure 5.13, which shows the cumulative probability of the

[3]The remaining parameters *forecast period* and *autocorrelation of forecast errors* are equal for all scenarios.

deviations from the optimal result. The higher the price forecast accuracy, the smaller the variance of the achieved economic result.

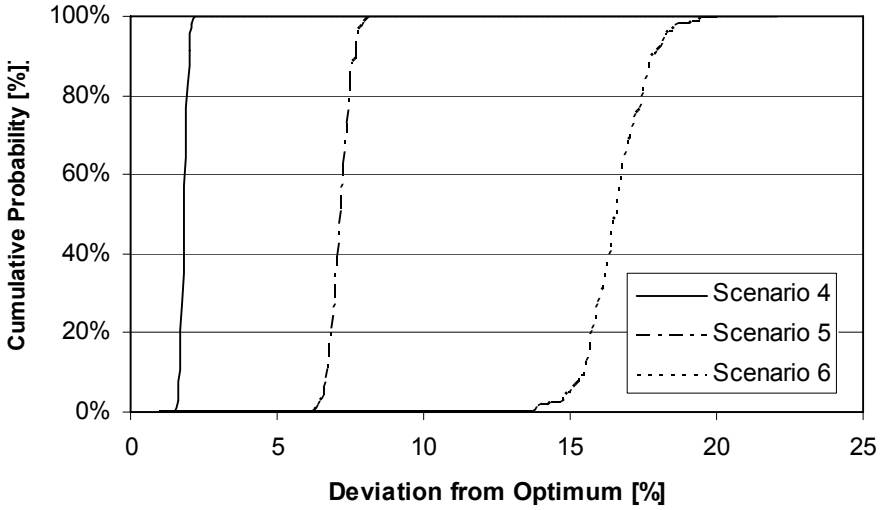

Figure 5.13: Cumulative probability of deviations from the optimum (price forecast)

Decreasing the MAPE at the beginning of the forecast period by 1% point leads to a reduction of the deviation from the optimal result of 1.4% points in average (from 19.2% for Scenario 3 with 15% MAPE to 4.9% for Scenario 1 with 5% MAPE). Comparing all scenarios, the deviation from the optimum increases over-proportionally to the increase of the forecast error (MAPE) at the beginning of the forecast period.

Both analyses (Figure 5.12 and 5.13) reveal that the most important parameter for choosing a specific forecast method is the method's MAPE for day-ahead forecasts, i.e., the daily MAPE (DMAPE). Even if a forecast method deteriorates hugely over time, e.g., delivering a high weekly MAPE (WMAPE), a low DMAPE is still the key parameter. Moreover, the available price forecast accuracies (see Table 4.3), which were used to derive Scenario 4, produce schedules that deviate of no more than 2% from the optimal result.

5.5.3 Combined Price and Load Forecast Scenarios

Price and load forecast scenarios will be analyzed with respect to the combined influence of price and load forecast characteristics. Additionally, the impact of different scheduling algorithms on the overall result will be investigated. The first paragraph of this section will analyze the impact of the forecast horizon length, the second paragraph will present an evaluation of different heuristic scheduling algorithms, and the third paragraph will benchmark the results of the heuristic scheduling algorithm against the results of the linear optimization scheduling algorithm. The last paragraph will also include an analysis of the impact of forecast error autocorrelation.

Forecast Horizon

As already discussed in Sections 5.5.1 and 5.5.2, a longer forecast horizon allows for a more effective intertemporal optimization of the CDS. The results reveal that a short, myopic forecast period that only takes the immediately next execution period into account leads to substantially lower savings of the DSS. However, the optimal length

of the forecast horizon differs. A forecast horizon length of one day was the optimal value for price forecasts, whereas load forecast scenarios continuously improved with the length of the load forecast horizon, although only marginally beyond a forecast horizon of more than 6 days.

Figure 5.14 presents the analysis of a forecast horizon length variation for Scenarios 7-9, i.e., scenarios with low load forecast errors and increasing price forecast errors. Figure 5.14 shows the same pattern as Figure 5.10. Thus, the decreasing price forecast accuracy, which is the limiting factor for the optimal price forecast horizon length in Section 5.5.2, has a greater weight than the increasing savings for longer load forecast horizons in Section 5.5.1. In other words, the optimal length of the forecast horizon in the price forecast scenarios determines the optimal length of the forecast horizon in the combined Scenarios 7-15.

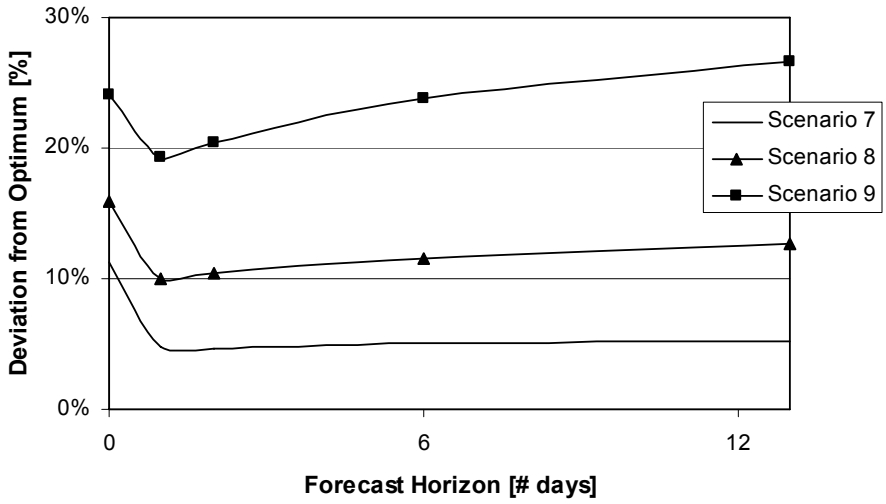

Figure 5.14: Impact of forecast period length (combined price and load forecasts)

The results for Scenarios 7-9 show that the lowest deviations from the optimal result are reached for forecast horizons of one day (4-19%). For Scenario 7, longer forecast horizons marginally increase the deviation. Deviations in Scenario 8 increase by 3% points for forecast horizons of 13 days length. Scenario 9 shows the most substantial increase for a forecast horizon length of 13 days with 27% (+8% points).

Comparison of Heuristic Scheduling Algorithms

As explained in Section 5.2.2, *Heuristic 1* defines the simplest and most myopic algorithm, whereas *Heuristic 2* includes a refinement of the charge condition and *Heuristic 3* includes an additional refinement of the discharge condition. *Heuristic 4* as the most complex variant includes another refinement of both the charge and the discharge condition. The question is to what extent these refinements impact the robustness of the heuristic algorithm towards variations of the forecast accuracy.

The variation of the lower price forecast accuracy bound reveals that variants *Heuristic 1-3* lead to approximately equal deviations from the optimum for a MAPE above 35%, whereas the results of *Heuristic 4* become considerably worse for a MAPE above 20%. Variants *Heuristic 1-3* result in a deviation of more than 60% from the optimal benchmark value. The results are different for lower price forecast errors.

Schedules determined with *Heuristic 1* lead to much higher deviations from the optimum (40-60%) than *Heuristic 2-4* (15-60%). When comparing the second and the third variant, there is hardly any difference visible in Figure 5.15 (the numeric results reveal that *Heuristic 3* is marginally superior up to a MAPE of 15%). The numeric results also show that *Heuristic 4* delivers the best results for a MAPE below 15%. I.e., the additional refinements of the charge and discharge algorithm are marginally beneficial in case of low price forecast MAPE, but they lead to a significant deterioration of results for higher MAPE values, which becomes particularly obvious for *Heuristic 4* with its detailed refinement steps.

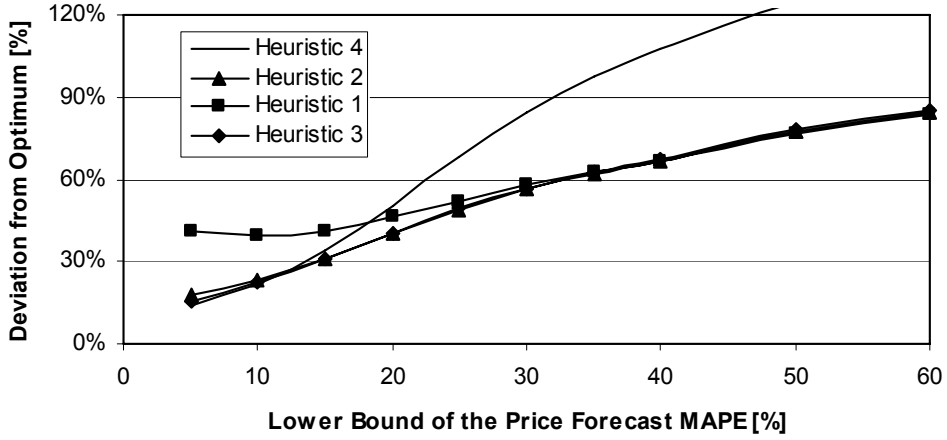

Figure 5.15: Impact of price forecast errors on the variants of the heuristic algorithm

The implication of these results is that the refinement of the charge schedule determination leads to a result improvement for forecasts with errors below 40% MAPE, whereas the refined discharge schedule determination only has a marginal effect for forecasts with up to 15% MAPE. Hence, determining the charge price limit correctly is more important than determining the discharge price limit, as already stated in Section 3.1 (different analysis approach used). For real-world applications, only *Heuristic 2* and *Heuristic 3* are relevant variants, since forecasts with a MAPE of more than 40% lead to unacceptable high deviations from the optimum anyway. *Heuristic 4* is actually not relevant in any setting, since for forecast with very low MAPE other scheduling algorithms will deliver much better results (Section 5.5.3).

Price Margin Parameter The price margin parameter describes a relative (percentage) increment of the required price difference Δ (Section 5.2.2). I.e., an increase of the price margin parameter value leads to CDS where the charge and discharge prices are lower or/and the discharge prices are higher. Table 5.6 shows the results of price margin variations.

The results show that the price margin parameter is fairly independent from the overall forecast accuracy level (below $\pm 0.5\%$ for all simulated combinations of scenarios and algorithms). It shows some dependency on the chosen variant of the heuristic algorithm. The more complex the heuristic variant, i.e., the more its charge and discharge conditions are refined, the lower the optimal value of the price margin parameter. The simples variant *Heuristic 1*, which does not perform any refinements of the charge and discharge conditions, delivers best results for a price margin value of 0.6-0.7. *Heuristic 2* delivers best results at price margins values of 0.3, *Heuristic 3* delivers best results

Table 5.6: Impact of the Price Margin Parameter

Algorithm	Scenario	0.0	0.1	0.2	0.3	0.4	0.5	0.6	0.7	0.8
Heuristic 1	**Scenario 7**				36.0%	35.5%	35.1%	34.8%	34.7%*	34.8%
	Scenario 11				39.4%	39.0%	38.8%	38.6%*	38.8%	39.0%
	Scenario 15				49.1%	48.8%	48.6%	48.6%*	48.8%	49.2%
Heuristic 2	**Scenario 7**	15.1%	14.8%	14.7%	14.7%*	14.8%	15.0%			
	Scenario 11	22.3%	21.9%	21.7%	21.6%*	21.6%	21.9%			
	Scenario 15	33.0%	32.5%	32.2%	32.1%*	32.1%	32.4%			
Heuristic 3	**Scenario 7**	12.8%	12.6%	12.6%*	12.7%	13.0%	13.4%			
	Scenario 11	22.0%	21.7%	21.6%*	21.7%	21.8%	22.1%			
	Scenario 15	33.8%	33.3%	33.1%	33.0%*	33.2%	33.5%			
Heuristic 4	**Scenario 7**	10.8%	10.7%*	10.8%	11.0%	11.3%	11.7%			
	Scenario 11	20.6%*	20.6%	20.7%	21.0%	21.3%	21.8%			
	Scenario 15	36.4%*	36.5%	36.7%	37.0%	37.5%	38.0%			

Note: Results of simulations for scenarios without price forecast error autocorrelation. The head row of the table contains the simulated price margin parameter values.
* Best value within a scenario simulation (row).

at price margins values of 0.2-0.3, and *Heuristic 1* delivers best results at price margins values of up to 0.1. Overall, the influence of the price margin parameter on the results is very limited.

Charge Buffer Parameter The charge index buffer parameter forces the scheduling algorithm to assume a higher charge price limit p^{charge} than it would be determined by matching the charge and discharge volumes. The mechanism is supposed to compensate for forecast inaccuracies. Table 5.7 depicts the results of the analysis using the scheduling algorithm variant *Heuristic 3* (the other variants reveal the same implications). The results show that the charge index buffer parameter has a clear impact on the deviation from the optimal result and that it correlates with the lower price forecast accuracy bound. Scenarios 7, 10, and 13 (MAPE of the price forecast error 7.5%) deliver best results for a charge index buffer value of 3 to 4. Scenarios 8, 11, and 14 require a charge index buffer value of 5 to 6, and Scenarios 9, 12, and 15 perform best at charge index buffer values of 7 to 8. Thus, there is a clear correlation between the level of the charge index buffer value and the overall accuracy of the simulated forecast scenario. This qualitative implication account for all variant of the heuristic algorithm, but the optimal parameter values for *Heuristic 1* are slightly higher.

Table 5.7: Impact of the Charge Index Buffer Parameter

	0	1	2	3	4	5	6	7	8	9
Scenario 7	14.6%	13.4%	12.8%*	12.8%	13.2%	14.2%	15.4%	16.9%	18.8%	21.0%
Scenario 10	18.6%	17%	16.0%*	15.7%	15.8%	16.5%	17.6%	19%	20.8%	22.9%
Scenario 13	25.1%	22.9%	21.5%	20.6%*	20.3%	20.5%	21.1%	22.3%	24%	25.9%
Scenario 8	27.6%	24.2%	21.7%	20.2%	19.4%	19.3%*	19.7%	20.7%	22%	23.8%
Scenario 11	32.0%	28.3%	25.6%	23.6%	22.5%	22.0%*	22.2%	23%	24.1%	25.9%
Scenario 14	39%	34.9%	31.8%	29.2%	27.7%	26.8%	26.5%*	26.8%	27.6%	29.2%
Scenario 9	50.1%	43.1%	37.3%	32.7%	29.6%	27.4%	26.2%	25.9%*	26.5%	27.8%
Scenario 12	54.2%	47.7%	41.7%	37%	33.3%	30.8%	29.4%	29.0%*	29.2%	30.3%
Scenario 15	60.4%	54%	48.4%	43.8%	39.8%	36.9%	34.9%	33.9%	33.8%*	34.4%

Note: Results of simulations using the scheduling algorithm variant *Heuristic 3* and scenarios without price forecast error autocorrelation. The head row of the table contains the simulated charge index buffer parameter values.
* Best value within a scenario simulation (row).

Heuristic vs. Linear Optimization Scheduling Algorithm

To compare the performance of the heuristic and the linear optimization algorithm, 4 simulation setups have been defined and run for each of the 9 scenarios. The first two simulation setups use the linear optimization algorithm for determining the CDS. Setup 3 and 4 use the heuristic algorithm. Moreover, Setup 1 and 3 use price forecasts with autocorrelated forecast errors, whereas the scheduling algorithms in Setup 2 and 4 operate on forecast without autocorrelated forecast errors. Table 5.8 summarizes the simulation setups.

Table 5.8: Simulation Setups

	Scheduling Algorithm	Autocorrelation of Price Forecast Error
Setup 1	Linear Optimization	yes[a]
Setup 2	Linear Optimization	no
Setup 3	Heuristic	yes[a]
Setup 4	Heuristic	no

[a] Durbin-Watson Test (DWT) value 0.5

As already stated in Section 5.5.2, autocorrelation of price forecast errors improves the results when using a linear optimization algorithm for determining the CDS. If forecast errors are not autocorrelated, results deteriorate substantially. The results in Figure 5.16 confirm this observation, when comparing the results of Setup 1 and Setup 2 for each scenario. The reason behind this observation is the systematic over- or underestimation of prices in consecutive timeslots. The structural condition supports the linear optimization algorithm, which selects the timeslots with the relatively highest (lowest) prices for discharging (charging).

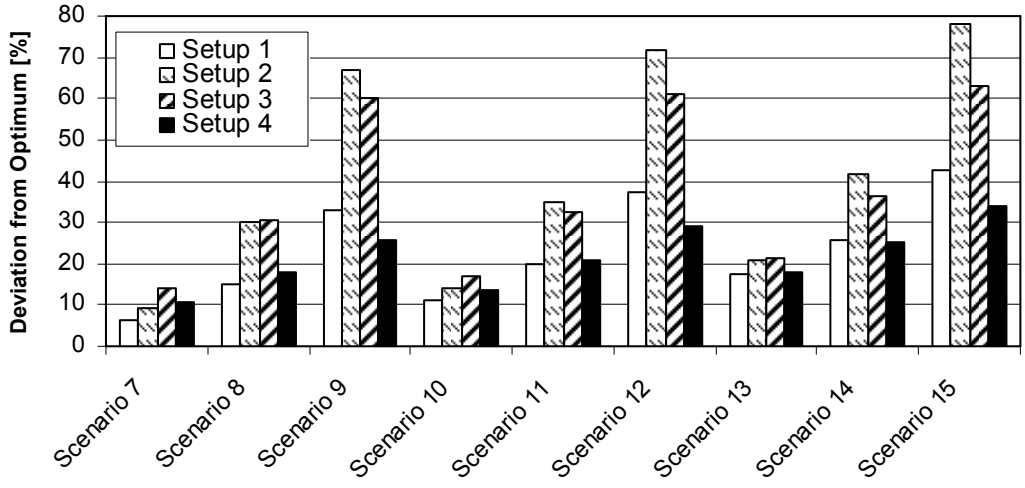

Figure 5.16: Results of scheduling algorithms in combination with forecast error autocorrelation variations

The aim of the heuristic algorithm is to deliver a robust alternative scheduling procedure for both setups (3 and 4) and all scenarios. The results in Figure 5.16 reveal that the algorithm achieves its objective only for Setup 4, but not for Setup 3. In

comparison to the linear optimization algorithm, the heuristic algorithm cannot deal with autocorrelated forecast errors. A comparison of the results for Setup 3 and 4 reveals that the heuristic scheduling algorithm deals much better with uncorrelated than with autocorrelated price forecast errors in each of the 9 scenarios. When comparing the results of Setup 2 and 4 (no autocorrelation of price forecast errors), the heuristic algorithm clearly delivers better results. For Setups 1 and 3 the contrary is the case.

A key finding of the analysis among the 9 scenarios is that the heuristic algorithm delivers better, i.e., more robust results than the linear optimization algorithm for increasing price forecast errors (lower increase of the deviation from the optimum when increasing the price forecast error and/or the load forecast error - comparison of Setups 1 and 4).

The result overview for all scenarios also reveals that primarily the price forecast error sets the level for the achievable savings. For all setups, the average results of Scenarios 7, 10, 13 (price forecast with 5% MAPE, results deviate in a range of 7-18% from the optimum) are distinct from the average results of Scenarios 8, 11, 14 (10% MAPE, 15-28% deviation from the optimum) and Scenarios 9, 12, 15 (15% MAPE, 26-42% deviation from the optimum). Extreme load forecast errors have a much lower impact than price forecast errors.

In conclusion, the choice of the schedule determination algorithm depends on the available price forecast data. If the price forecast errors are autocorrelated, a linear optimization algorithm will deliver best results. Otherwise the heuristic algorithm delivers superior results.

5.6 Summary

This part of the research work analyzed the economic impact of price and load forecast errors on the optimal operations of a DSS. It presented a method to derive artificial forecast streams from actual data that systematically simulate forecast data characteristics like accuracy levels, forecast period lengths, autocorrelation of forecast errors, and forecast granularities. The results are based on Monte Carlo simulations.

In conclusion, the system tolerates significant forecast errors while still operating close to the economic optimum. Price forecast errors have a stronger negative impact on the economics of the DSS than load forecast errors. The key parameter of both price and load forecasts is the day-ahead MAPE of the forecast. This parameter defines the overall level of achievable savings. Price forecasts with a MAPE of 5% (10%, 15%) lead to deviations from the optimal result of 1.8% (7.2%, 16.6%). Load forecasts with a MAPE of 7.5% (15%, 22.5%) lead to deviations of 1.7% (3.8%, 6.3%). Scenarios combining price and load forecasts deviate much stronger from the optimal results than the sum of price and load deviations. Still, for (conservative) average scenarios with 10% MAPE for price forecasts and 15% MAPE for load forecasts, the results deviate less than 20% from the optimum.

Another important parameter of the forecast data is the autocorrelation of forecast errors. This parameter has a significant impact on the achievable results. While the autocorrelation of price forecast errors has a positive influence on the results, the opposite is the case for load forecast errors. Therefore, observing the autocorrelation of forecast errors and selecting appropriate forecast methods is an important aspect for the realization of a DSS, which might even trade-off forecast accuracy to a certain extent.

Also the analysis of the optimal forecast horizon length reveal opposed results for price and load forecasts. Longer forecast horizons allow for more effective intertemporal optimizations of the scheduling algorithm, but they also decrease the achievable forecast accuracy level at the end of the forecast horizon. The optimal forecast horizon length for price forecasts is one additional day to the next execution period, whereas load forecast scenarios continuously improved their results for longer forecast horizons - although marginally. For scenarios that simulate both price and load forecasts, the optimal forecast horizon length of price forecasts is decisive. The benefits from longer forecast horizons in load forecast scenarios cannot offset the deterioration of results in case of longer price forecast horizons.

The optimal scheduling algorithm depends on the autocorrelation of price forecast errors. In case of a strong autocorrelation, optimization algorithms deliver the best operation schedules for the DSS. In case of uncorrelated price forecast errors, the presented heuristic algorithm delivers the best schedules. The best case results of both algorithms are very similar. The linear optimization algorithm shows slightly better performance for forecasts with low MAPE, whereas the heuristic algorithms show a higher robustness in case of increasing forecast errors.

In conclusion, price and load forecast accuracies of available forecast methods are sufficient to ensure economically beneficial operations of DSSs.

5.6.1 Contribution to Scientific Literature

The presented simulation model defines a DSS aiming at arbitrage accommodation at the end consumer level. The DSS operations are scheduled based on price and load forecasts. The forecast generation module allows a detailed specification of the forecast stream characteristics for the simulation.

The described simulation model contributes three new aspects to scientific literature in this area: (i) The forecast generation module allows a detailed economic assessment of the impact of forecast accuracy on the operations of the DSS. Additionally to forecast accuracy, the generation module allows to specify the degree of autocorrelation of forecast error, which has a significant influence on the economics of the DSS. In comparison with all other papers analyzing the economic impact of forecast errors (Section 4.2.4), the presented methodology provides a more generic and extensive functionality. (ii) Additionally, few of the existing storage models in literature considered forecast uncertainties into their analyses, and actually none of them considered load and price forecast uncertainties (Section 4.2.6). This work provides a comprehensive analysis on how forecasts impact the economics of DSS, depending on, e.g., forecast accuracies and forecast error autocorrelations. (iii) The third major contribution to literature on storage models is the benchmark of different scheduling algorithm classes. Most papers on storage models use optimization algorithms to determine the optimal schedules for charging and discharging the storage system. The algorithms typically base on either linear optimization models or dynamic programming. Additionally to the class of optimization algorithms, this work presents differently complex variants of a heuristic scheduling algorithm and benchmarks their results against a linear optimization algorithm. The results show that these algorithms are complementary to each other: Optimization algorithms perform best in combination with highly autocorrelated price forecast errors, whereas their results dramatically deteriorate for uncorrelated price

forecast errors. The heuristic scheduling algorithms show exactly the opposite characteristic.

5.6.2 Practical Relevance of the Findings

Available forecast methods deliver sufficiently accurate forecasts to economically operate DSS, most likely even for small unit load forecasting. Even conservative scenarios, i.e., 2-3 times higher forecast errors (MAPE) than reported in literature, lead to less than 20% deviation from the theoretical optimum. The results of this research work deliver a quantitative basis for assessing the economic benefits that can be achieved by further forecast enhancements.

Especially in the context of end consumer environments, ensuring high levels of forecast accuracy is difficult due to small volumes and a lack of averaging effects. The analyses within this work revealed that decreasing the load forecast granularity, i.e., forecasting the load for blocks of several hours instead of hourly blocks, hardly deteriorates the economic result, although it potentially increases the achievable forecast accuracy significantly.

The results of this research work are applicable to all kind of DSM programs and appliances that perform load shifting in order to benefit from TOU or flexible tariffs respectively. Upcoming technologies like Smart Metering that enable concepts of Smart Homes will increasingly use such decentrally coordinated DSM programs. The simulation results along the characteristics of forecast data streams will therefore be valuable to future DSM programs.

Smart Metering and further information and communication technology integration in the electricity grid fuel a number of recent research initiative that investigate how to make the grid *smarter*. Clearly, Smart Meters with a bidirectional communication interface will provide a data set on the low-voltage level of the grid that has not been available so far. Therefore, research projects investigate how to decentrally use this information for DSM programs, e.g., aiming at controlled load shifting. Load forecasting on the end consumer level plays an important role for local (decentral) decisions in this context. The results of this part of the work give a first impression on the required accuracy of load forecasts on the end consumer level.

Part III

Market-wide Potential of Distributed Storage Systems as Demand Response Agents

Chapter 6

Demand Responsiveness on Electricity Markets

In many countries, the structure and the organization of the electricity markets has changed substantially over the last decades. The major trends were a move from monopolistic or oligopolistic, regulated markets to deregulated markets with increasing competition. Generally, this involved restructuring the sector by unbundling vertically integrated utilities and reducing their horizontal concentration. The aim of vertical unbundling is to separate potentially competitive generation and supply from the natural monopoly activities of transmission and distribution networks. The aim of horizontal separation is to create enough effective competition in generation and retailing where economies of scale favor competition. (Jamasb and Pollitt, 2005, Joskow, 2000)

The regulated objective of the erstwhile vertically integrated utilities was to maximize social welfare with distributional equity, i.e., meeting the load at all time. The prevailing paradigm of the market was to guarantee stable, secure, and reliable market operations by investing into generating capacity. Consequently, generating units that were to cover peak load had very low load factors. The costs for installing and maintaining this system were charged to the consumer. The deregulation of electricity markets aimed at increasing competition and fostering profit-maximizing strategies. Thus, utilities had to decrease the number of generating units with extremely low load factors. I.e., the pursued paradigm is maximizing social welfare with efficiency (description of the paradigm shift in Ng'uni and Tuan (2006)).

As a consequence, ensuring the reliability and the stability of the grid is not the task of generating companies, but it is the task of the deregulated market itself. The market's incentives for generators to provide additional capacity when required are high prices. The particular problem of electricity markets arose from its low level of demand elasticity. *"This is due not only to the peculiar characteristics of [electricity], such as non-storability, lack of good substitutes and the relatively small portions of the typical customers' budget but also to the relation between wholesale and retail electricity markets"* (Bompard et al., 2007). Deregulated markets typically offer no opportunity and no incentive to the majority of consumers to actively participate in the market, which leads to a mostly unresponsive demand, although consumers would certainly not be completely unresponsive (Faruqui and George, 2002, Ilic et al., 2002, Spees and Lave, 2008). Assuming an inelastic demand is a serious weakness of deregulated electricity markets, which led to severe systemic issues (extreme peak prices) in several electricity

markets, e.g., in California (Borenstein, 2002). Even if suppliers do not conspire, they can raise market prices in such situations (Spees and Lave, 2008).

Regulators have taken several measures to cope with this problem, e.g., by fostering bilateral contracts between suppliers and large consumers, setting price caps, and forcing divestiture in cases of extremely large market shares. All of these measures address the supply side and ignore the potential of a price-responsive demand side. (Bompard et al., 2007)

As this work will present in further detail in Section 6.2, many research projects have shown that a more responsive demand can mitigate the effect of extreme price peaks effectively. Most of the related work on Demand Response (DR) programs has its focus on avoiding load peaks and the thereof resulting price peaks. Thus, literature on DR programs describes a shift from the classical philosophy where supply follows demand to a new philosophy where efficient market systems minimize demand fluctuations to avoid load and price peaks (Albadi and El Saadany, 2007).

When relating a load- and price-responsive demand side to the effective integration of Renewable Energy Sources (RES), avoiding load peaks is not the right objective anymore. It will rather become important to coordinate availability of demand resources (Spees and Lave, 2008), i.e., a demand shift towards time periods where supply from intermittent resources like wind and Photovoltaic (PV) is available. Only if demand profiles better match supply profiles from RES, excessive fossil-based control capacity with low load factors can be decommissioned. This would have a positive impact on both electricity prices and environmental pollution.

Due to the uncertainty of production forecasts and the irregular pattern of the production profiles of intermittent energy resources, the required demand-side flexibility to match demand and supply profiles is high. Most likely, these flexibility requirements would exceed the demand elasticity of private households and commercial and industrial consumers, if assuming price levels in the same order of magnitude as today (more on the issue of determining the price elasticity of the demand side in Section 6.2.3). I.e., achieving the required demand flexibility through behavioral changes seems unrealistic. Spees and Lave (2007a) suggest that end consumers could purchase electricity on an hourly basis by using automated devices. The installation of automated demand-side control equipment could achieve a significantly higher and more reliable degree of demand elasticity, as experiments with bi-directional communication control devices have proven (Braithwait, 2000). Certainly, the disadvantage of automated devices is the required investment into additional components on the consumer side.

The typical devices at the end consumer level that are considered for a fully or semi-automated, price-responsive load control are air condition units, thermostats, fridges, freezers, washing machines, and tumble dryers. These devices can provide automated or semi-automated load shifting potential, if equipped with additional control components. Nevertheless, it is also obvious that all of these devices have operational constraints that significantly limit the flexibility and the reliable availability of the potential load shifting volume[1]. Distributed Storage Systems (DSSs) at the end consumer level would not have such constraints. In contrast, storage systems decouple the

[1]Examples of such constraints are the presence of humans, temperature and other weather conditions, limitations in rental contracts or insurance contracts that do not allow operations of electrical devices without supervision, noise disturbance that bother neighbors or children during night hours, sequential dependencies between different devices (washing machine and tumble dryer), and, of course, people's habits.

actual load profile of a consumer from the load profile visible towards the grid, without requiring the actual load profile to change. The extent of the system's load shifting potential depends on its economic parameters and technical constraints, such as storage capacity, power converter capacity, and efficiency degrees. I.e., within their technical and economic constraints, DSSs can provide reliably available demand flexibility, given an economic incentive to shift load.

6.1 Objective and Structure of Part III

This part of the thesis will analyze the saving potential and the volume of an optimal load shifting schedule. All analyzes are calculated on historic data of the German electricity market from 2007 (see Section 7.1). The analyses consider the market price as an endogenous, load-dependent variable. I.e., incremental load shifts from peak to off-peak periods decrease the load volume and the market price in the peak period, whereas they increase them in the off-peak period. Hence, it is modeled that the Charge-Discharge-Schedule (CDS) of multiple DSS mutually influence their economics, even in case of optimal coordination. The overall amount of electricity consumed is not changed (excluding the losses of storage units due to imperfect efficiency degrees, which increase the overall load volume). I.e., there are no pure load reductions, but only load shifts.

The first research question investigates the general potential of an optimally responsive demand side in case of hourly flexible electricity tariffs. In a second step, this potential is analyzed given the constraints and costs of DSSs. I.e., the second step addressed the question what saving potential could be realized through DSSs. The objective of the third research question and the final analyses is to determine the optimal and the maximal amount of storage capacity that can be economically operated in the market in dependency on the storage prices, the given load curve, and the determined price functions. If the optimal amount of storage capacity is installed, savings through load shifting can reach a theoretical maximum in case of optimal coordination and average electricity prices are reduced. If the maximal amount of storage capacity is installed, total savings are marginally positive.

Section 6.2 will give an overview of related work. Section 7.1 explains the basic variables of the analyses and their interrelations. In Section 7.2, an estimation model determining the economic potential of perfect load shifting in the German electricity market is presented. Section 7.3 describes the detailed analysis model and the according algorithmic solution to it and Section 7.4 presents the results of the analyses. Section 7.5 gives a summary of the key findings and discusses their practical and academic relevance.

6.2 Related Literature

The following sections will give an overview of related academic literature on the impact and effect of Demand Response programs (Sections 6.2.2 and 6.2.3) and on the market price impact of integrating RES (Section 6.2.4). Beforehand, Section 6.2.1 defines some elementary terms in this domain.

6.2.1 Definition of Elementary Terms

The most general term that describes the active efforts of utilities to influence the level or timing of customers' usage patterns is Demand-Side Management (DSM). It can either refer to programs that promote energy efficiency[2], i.e., a reduction of the total demand volume, or to programs that promote specific load-shape objectives, like peak load reductions, load shifting, or off-peak building (Eto, 1996). The focus of the following sections is on those programs that aim at shaping the demand profile to achieve more efficient market outcomes. These programs are also called *Demand Response Programs*.

Demand Response is achieved through direct or indirect payments designed to induce lower electricity consumption at times of high wholesale market prices or when system reliability is at risk (USDE, 2006). Generally, three actions can lead to the intended lower electricity consumption: (i) reducing consumption during critical peak periods without increasing load in other periods, (ii) shifting parts of the peak demand volume to off-peak periods, and (iii) avoiding system load during peak periods through on-site generation. These actions are achieved through either price-based programs or incentive-based programs. Price-based programs build on variable electricity tariffs that charge higher prices at peak periods. Examples are Time-of-use (TOU) tariffs, critical peak pricing, extreme day pricing, dynamic pricing, and Real-time pricing (RTP). Incentive-based programs are either utility-controlled or market-based. Utility-controlled programs directly control devices on the consumer side that can be shut down. The consumer is offered lower electricity rates if the utility is allowed to curtail load. In market-based programs, the consumers either bid on the electricity market for demand reserves (potential load reduction volumes) or they receive prenegotiated payments if they reduce load in critical peak hours. In contrast to the utility-controlled incentive programs, consumers have the final decision whether or not to actually curtail load in critical peak periods. (Albadi and El Saadany, 2007, USDE, 2006)

All DR programs base on the change of the consumers' demand profile. The effectiveness of a program is measured with the price elasticity of the consumers' demand. The price elasticity indicates to what extent a change in the electricity price leads to a change in the demand volume. *"It is a unit-less coefficient, obtained by dividing the percentage change in quantity demanded by the percentage change in price"* (Faruqui and George, 2002). In Kirschen et al. (2000), price elasticity is decomposed into *self-elasticity* (or *own-price elasticity*) and *cross-price elasticity*. A related concept to cross-price elasticity is the *elasticity of substitution* (Faruqui and George, 2002). In the case of electricity, own-price elasticity measures the percentage demand variation divided by the percentage price variation within the same time interval. Cross-price elasticity measures the effect of price variations in a certain time period on demand variations in another time period. Elasticity of substitution describes the ratio of the percentage change in the ratio of the demand between two period (e.g., peak and off-peak period) to the percentage change in the corresponding price ratio (Braithwait, 2000, Faruqui and George, 2002). Each type of elasticity effects a variation of the demand for electricity depending on its price. High prices will reduce the demand and,

[2]Programs providing information to raise the consumers' general awareness of energy consumption, distributing technical information for improvements in energy usage, granting subsidies or loans for the installation of energy-efficient technologies, and incentives for performance contracting (Eto, 1996).

thus, reduce load peak, whereas low prices can increase the demand, as Figure 6.1 illustrates.

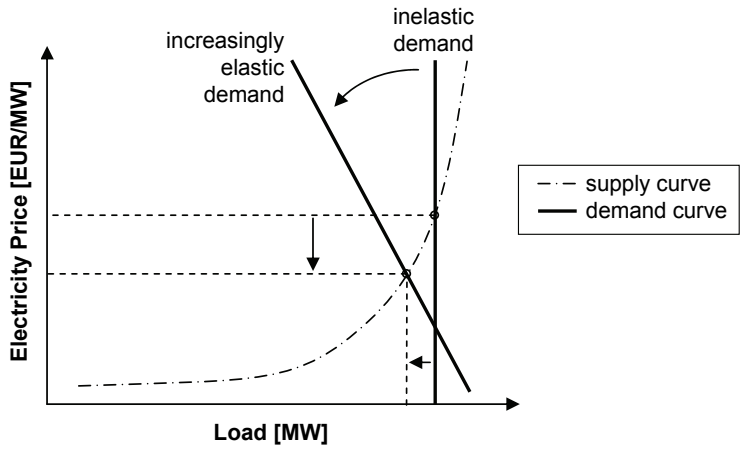

Figure 6.1: Effect of price elasticity of the demand side (illustrative)

6.2.2 Reviews of Demand Response Programs

There is a number of reports (e.g., USDE (2006), FERC (2006)) and reviews that give an overview of existing DR programs and their performance, especially for the North American market (e.g., Faruqui and George (2002), Spees and Lave (2007a)). A further review by Ng'uni and Tuan (2006) also includes DR programs from Sweden and Finland in their review. They point out that DR programs must be designed specifically to the consumers' perceptions, which may differ significantly between markets. Heffner (2002) analyzes 45 studies on DR and concludes that utility-controlled programs (*contingency programs*) show better performance than market-based programs with respect to the demand actually curtailed when needed in critical peak hours. Hence, programs with automated control actually curtail or shift a larger share of the potentially available volume than price-based programs.

The paper of Hwang (2001) reports on the successful implementation of an interruptible load program in Taiwan. The core of the program are radio-controlled air condition appliances that can be switched off in a coordinated manner in critical peak hours. The program effectively reduces critical peak loads while maintaining a high level of comfort on the consumer side. King and Chatterjee (2003) reviewed numerous studies on end consumer responsiveness. They summarize that the effectiveness of DR programs, i.e., the price elasticity of the demand side, hugely depends on different factors. These hardly quantifiable factors are for example the availability of large electrical appliances in a household, the income of the household, the weather, the time of the day, and the geographical area. Patrick and Wolak (2001) report similar results for industrial and commercial consumers in England and Wales. Price elasticity varies substantially across industries and for different times of the day. Spees and Lave (2008) conclude that consumer responsiveness is not known with confidence. Additional factors that affect elasticity values besides the aforementioned ones are the unavailability

of substitutes for electricity and the dependence on the timing perspective[3]. Table 6.1 presents an overview of selected studies on DR programs and their measured price elasticity of the demand side.

6.2.3 Economic Impact of Flexible Pricing and Price Elasticity

Borenstein (2005) investigates the long-run efficiency of RTP and states that the magnitude of efficiency gains from RTP is likely to be significant, even if demand shows very little elasticity. If all consumers are on RTP rates and own-price elasticity equals -0.5, consumers could save up to 12% on their annual bills. If the own-price elasticity value is reduced to -0.1, the annual savings are reduced to 5.9%. Borenstein (2005) also compares RTP tariffs with TOU tariffs. He concludes that TOU tariffs are a poor substitute for RTP, since such tariffs only capture about 20% of the possible welfare effects. The results in Spees and Lave (2008) are lower, but overall comparable. Their simulations on Pennsylvania, New Jersey, Maryland (PJM) market data reveal that elasticity values of -0.1 result in 0.7% consumer surplus in case of TOU rates and 3.2% in case of RTP. I.e., the ratio of the resulting savings between the TOU and the RTP scenario is also around 20% (as in Borenstein (2005)), but the absolute consumer surplus is only about 50% of the previously described results. The main reason for the difference is that Spees and Lave model a rather short-run scenario, whereas Borenstein models a long-run scenario.

Holland and Mansur (2006) present quite different findings when analyzing the short-run effects of RTP. They only report up to 2.5% welfare increase in case of RTP. According to their analyses, flat electricity tariffs that are adjusted on a monthly basis would have many of the same effects as RTP adoption. They argue that such monthly rates capture more of the deadweight loss than TOU tariffs, without requiring new metering equipment. Therefore, such rates shall be favored in short-run scenarios. Faruqui and George (2002) conclude this point differently. According to them, TOU tariffs are certainly a first necessary step to go in the right direction. Still, TOU rates do not recognize the inherent uncertainty in supply costs, since these tariffs are designed to reflect prices under expected long-term conditions. Thus, TOU rates do not allow for mitigating the price risk on the consumer side of the meter, as real-time or dynamic pricing would do.

But mitigating this risk is most likely beneficial for consumers. Different market models analyze the effect of a more elastic demand side and conclude that even small elasticity degrees (-0.15 or greater) increase the market efficiency significantly. E.g., Bompard et al. (2007) show the increasing value of elasticity in case of decreasing levels of market competition. Wang et al. (2003) model a market including demand-side bidding for load and load reserves. Their market reveals a positive effect on the consumers' surplus and limits the market power of producers. Similarly, Strbac et al. (1996) model a competitive electricity market incorporating demand-side bidding. They also report on the positive effects of even limited demand-side elasticity, since small production cost reductions (due to peak load reductions) may lead to significant benefit redistributions between producers and consumers due to large differences between marginal

[3]Long-run vs. short-run elasticity. In short-run scenarios, consumers have few options to change their load profiles. In long-run scenarios, consumers have more possibilities to react and to adapt, e.g., through technological and contractual changes.

Table 6.1: Values for Price Elasticity of Demand in Literature

Reference	Price Elasticity of Demand	Comment
Faruqui and Malko (1983)	0 to -0.45	short-run own-price elasticity from 12 pricing experiments involving 7,000 customers
Caves (1984)	-0.07 vs. -0.21	elasticity of substitution in household without vs. with major electrical appliances, average results from EPRI studies in the 1980s
Aubin et al. (1995)	-0.79 vs. -0.18	on-peak vs. off-peak elasticity in a French study
Filippini (1995)	-0.6 vs. 0.79	on-peak vs. off-peak elasticity in a Swiss study
Braithwait (2000)	-0.31 to -0.4	elasticity of substitution in households with bi-directional communication equipment to automate load control, GPU experiment
Patrick and Wolak (2001)	0 to -0.05	average own-price elasticity of large industrial and commercial consumers in England and Wales
King and Chatterjee (2003)[a]	-0.2 vs. -0.9	average value of short-run vs. long-run own-price elasticity from 34 studies (min -0.12 vs. -0.6; max -0.35 vs. -1.2)
King and Chatterjee (2003)	-0.21 to -0.47	average value of short-run own-price elasticity degrees of 56 studies in dependence on geography
USDE (2006)	0.02 to 0.27	elasticity of substitution under TOU rates from several studies
Boisvert et al. (2007)	-0.11	average demand elasticity of substitution after 5 years of experience with large customers (>2MW) on RTP
NIEIR (2007)[b]	-0.25; -0.35; -0.38	long-term own-price elasticity of residential, commercial, and industrial consumers

[a] Cited reference 'Aucton and Park (1984)' unavailable and not further specified.
[b] Original source not available. Cited according to Bompard et al. (2007).

prices (large savings for consumers) and marginal benefits from load reductions (small profit loss for the producer since the most expensive generation units typically run on small margins). Equally, Spees and Lave (2008) assert that producers will not see large reductions in profits.

From the consumers' perspective, hourly flexible tariffs will actually not lead to higher costs, since consumers already pay the weighted average of all high- and low-price hours. In any case, each degree of increase in responsiveness will reduce the electricity bill and even lower the costs of unresponsive consumers due to generally decreasing peak prices (Spees and Lave, 2007a).

Sioshansi and Short (2009) evaluate the impact of RTP on the usage of wind generation, which is a similar thought as pursued in the work at hand. They simulate how much additional supply from wind generation can be integrated (increase of wind power usage) depending on the degree of demand-side elasticity. Their simulation data are historical system, market, and wind availability data from 2005 in the Electricity Reliability Council of Texas (ERCOT). They show that RTP can increase the usage of potential wind generation up to 7%. Nevertheless, due to the fairly low wind generation share of 10% in the analyzed region, it remains unclear how RTP in combination with average elasticity values of -0.1 would integrate larger shares of wind power supply. Examples from Spain and Denmark have shown that integration of wind energy becomes critical, as soon as its share exceeds 30% of the market share. If for example wind power supply peaks during the night, providing a reliably available load shifting potential could be a task of automated load control agents and storage systems, as discussed in this research work.

6.2.4 Effects of Increasing Shares of Renewable Energy Sources

On the positive side, the key characteristic of RES like wind or PV generation units are a reduction of the emissions from energy production. On the negative side, their characteristics are non-dispatchability and variable and uncertain real-time availability of the resources.[4] The negative aspects are the most severe impediments to a large-scale implementation of such RES into the power grid, since additional reserve capacity might be required and supply might be curtailed to ensure the grid's reliability. (Sioshansi and Short, 2009)

Klobasa and Ragwitz (2006) quote an additional need for ancillary service capacity of 10-20% of the additionally installed renewable generation capacities. Neubarth et al. (2006) state that for the volume of 26.9 TWh from wind power plants about 17 TWh balancing capacity were required.[5] The issue of integrating RES grows disproportionally strong with increasing their shares of capacity installed (Sioshansi and Short, 2009). In order to reliably integrate RES into the grid, the only alternative to supply curtailments and additional reserve capacity is to achieve a more responsive demand that follows the fluctuating supply patterns of RES.

Achieving the required flexibility on the demand side is not only ecologically desirable, but also economically beneficial. A number of studies have calculated the

[4] Although the cited references in this section mostly refer to energy from wind power plants, the following analysis within literature can also apply to PV generation units, if their operational costs further decrease. Those units have the same characteristics like wind units with respect to the performed analyses: very low marginal costs and a stochastic, hard to predict supply pattern.

[5] September 1, 2004 to August 31, 2005 on the German market

merit-order effect of power supply from RES on the spot market price, which describes a price decrease on the spot market in case of an increasing offer from RES due to their low marginal costs. *"The price in the wholesale electricity market is the result of the intersection of the electricity demand curve and the supply curve"* (Sáenz de Miera et al., 2008). The supply unit with the highest marginal costs that still has to be selected to satisfy demand sets the wholesale price. An increase of RES with very low marginal costs like for wind and PV would consequently reduce the price of the most expensive supply unit selected, i.e., reduce the market price. Graphically, the increase of the supply from RES shifts the supply curve to the right and leads to a lower intersection point of the demand and the supply curve (Figure 6.2). A more detailed description of the effect is given in Sensfuss et al. (2008) and Sáenz de Miera et al. (2008).

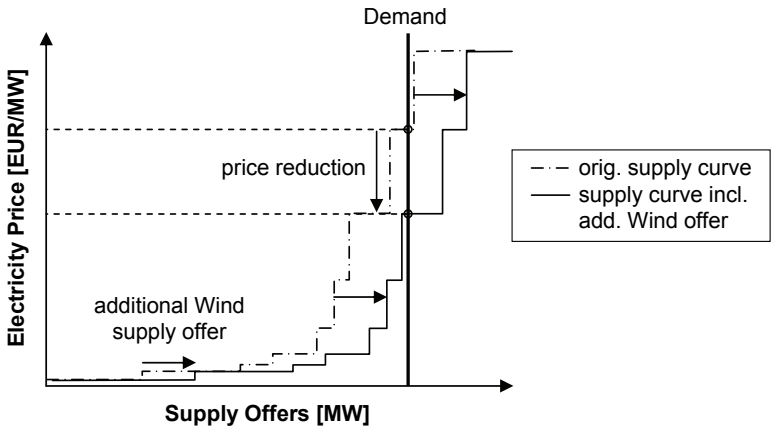

Figure 6.2: Merit-order effect of increasing supply volumes from RES (illustrative)

The first article (indirectly) describing this effect focused on emission trading schemes (Jensen and Skytte, 2003). They used an analytical approach and showed that if marginal costs of RES were lower than those of conventional resources, supply from RES would reduce the market price. Their original intention was to show that if such offset occurs, renewable energy resource promotion schemes could be combined with emission trading schemes to achieve RES deployment, cost-effective emission reduction, and lower energy prices at the same time.

Neubarth et al. (2006) perform a statistical time series analysis, which reveals that the power supply from wind power plants has reduced the spot market price on the European Energy Exchange (EEX) in the period from September 1st, 2004 until August 31st, 2005 by 5% per 1,000 MW of wind power supply (translating into an absolute price effect of 6.08 EUR/MWh). They show that the effect is robust and statistically significant. Sensfuss et al. (2008) use a multi-agent simulation model and reveal a price effect of 2.50 EUR/MWh in 2004, 4.25 EUR/MWh in 2005, and 7.83 EUR/MWh in 2006 for the German market. They emphasize that the simulation results heavily depend on the assumptions regarding gas prices, emission certificate prices, and other fuel prices. Sáenz de Miera et al. (2008) use an empirical analysis of data from the Spanish market. Their analysis reveals a price effect of 7.08 EUR/MWh in 2005, 4.75 EUR/MWh in 2006, and 12.44 EUR/MWh in 2007[6]. They additionally calculate the net costs for the end consumer by subtracting the subsidies and supports granted to

[6]January 1st, 2007 to May 31st, 2007

RES. For each period (2005-2007), they find net savings for the end consumers. Martin (2004) presents a *thought experiment* on how supply from PV units would impact the regional power market price in New England. An additional volume of 1 GW installed PV capacity would have reduced market prices in New England by 2-5% in 2002.

Sioshansi and Short (2009) remarks that such merit-order effects increase disproportionally, if the original peak prices were cleared on a previously less competitive market. The merit-order effect, as presented in the above mentioned analyses, theoretically shifts the surplus from generators to consumers. If the surplus is actually passed on depends on the competitiveness on the retail market (Sensfuss et al., 2008).

In conclusion, a higher expected supply volume of RES leads to a lower spot market price. Since RES like PV and wind are intermittent resources, their impact on the spot market price will automatically cause higher price volatility. Additionally, low demand elasticity in combination with the integration of RES also leads to higher spot market volatility. *"[...] the more one insists on a particular market quantity in the face of uncertainty regarding supply and demand, the more variability one will expect in prices. The expected volatility in prices will be higher the less elastic is supply and demand."* (Chupka, 2003)[7]. Hence, it is essential to increase demand elasticity in order to more effectively integrate RES, to efficiently capture the merit-order effect on the spot market, and to ensure passing on the surplus to the end consumers through more competitive markets[8].

The following chapters will therefore present models that first estimate the value of optimal demand responsiveness, and then calculate the realizable value when DR is implemented based on DSS.

[7]Chupka cites the 'price vs. quantities' trade-off under uncertainty analyzed by Weitzman (1974) and Laffont (1977).

[8]Demand elasticity increases market competition and efficiency, as explained in the previous section of this chapter.

Chapter 7

Storage Models considering the Price Impact of Demand Response

One of the most important constraints to the models in Part I and II of this thesis is the limitation to a price taker model, i.e., a storage model that considers the market price as an exogenous variable. This chapter will present two models that relax this assumption and treat the price as an endogenous variable. These models will determine the optimal and the maximal amount of storage capacity that can be economically operated within a specified market. To develop a model that determines these values under consideration of the price impact of demand response through DSSs, a number of parameters and their interdependencies need to be defined. Section 7.1 will give an overview of the key parameters to be determined and their relation to each other. Besides the technology parameters of the storage systems, load and price distribution functions determine the analysis (see Figure 3.3 in Section 3.2.1). Section 7.2 will then define a simplified estimation model and Section 7.3 will present a more detailed market-wide analysis model based on linear programming.

7.1 Basic Analysis Variables

Generally, storage model parameters of the market-wide analysis model are the same as for the *one household* analysis model as given in Table 3.4 (Section 3.2.1). Additionally, the capacity dimensioning model uses the aggregated capacity $\hat{C}$ (sum of capacities over all DSSs in the market). The maximal and the optimal values for the installed capacity that can be operated economically on the system are indicated with $\hat{C}_{\kappa}^{max}$ and $\hat{C}_{\kappa}^{opt}$, where κ specifies the level of storage capacity costs per unit (EUR/kWh). Analogously to the total costs K in the one-household-model and the cost baseline $K^{baseline}$ for a scenario without storage capacity, this model uses $\hat{K}$ for the aggregated total costs on the system level and $\hat{K}^{baseline}$ for the total costs baseline on the aggregated level. Table 7.1 contains the additional model parameters on the aggregated level.

The optimal and the maximal amount of storage capacity that can be operated economically in a given market as well as the total costs are closely linked to the costs per storage capacity unit κ (EUR/kWh). Figure 7.1 gives a schematic overview of the interrelations between the costs per storage capacity unit, the amount of storage capacity installed on the system, and the savings that can be achieved.

Since the costs per storage capacity unit revealed to be the key determining parameter of a technology scenario (see Section 3.3), it will also be the key parameter for the

Table 7.1: Additional Model Parameters on the Aggregated Level

Parameter Description	Symbol	Unit
Total costs on the aggregated (market-wide) level	$\hat{K}$	(EUR)
Total costs baseline on the aggregated (system-wide) level (costs without a storage system)	$\hat{K}^{baseline}$	(EUR)
Maximal storage capacity on the aggregated level that can be economically operated	$\hat{C}_{\kappa}^{max}$	(kWh)
Optimal storage capacity on the aggregated level that leads to maximal savings	$\hat{C}_{\kappa}^{opt}$	(kWh)

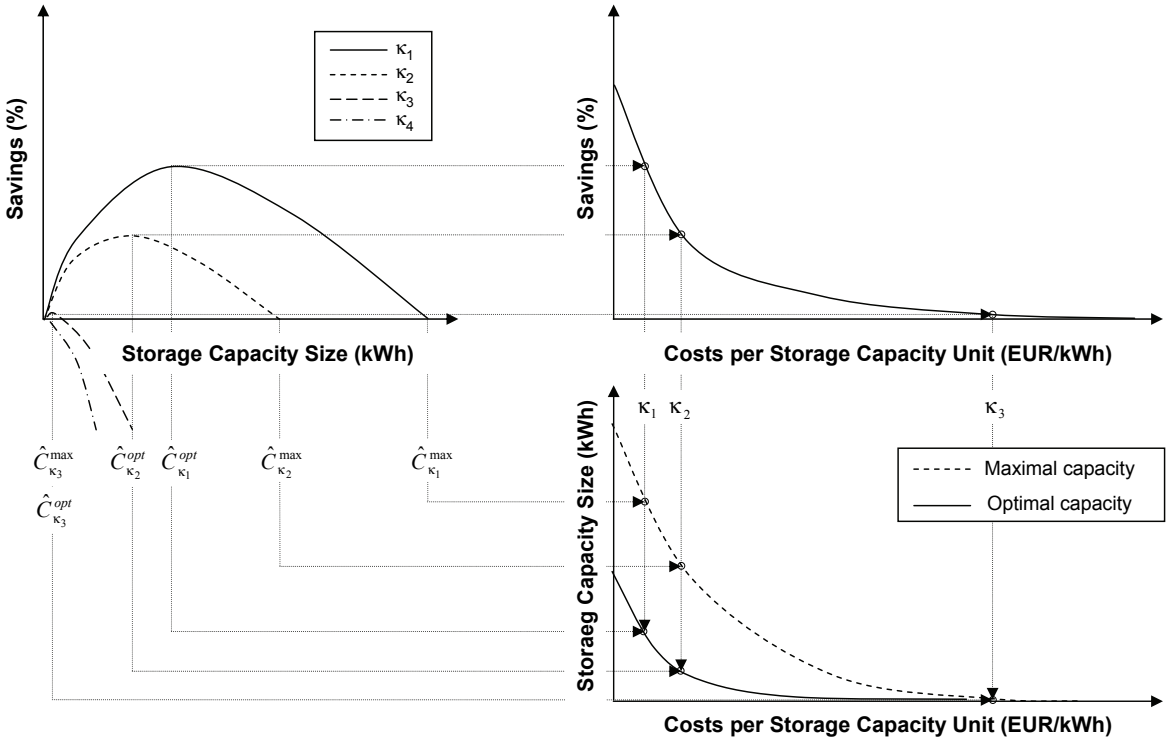

Figure 7.1: Interrelations of model parameters

storage capacity dimensioning problem. As Figure 7.1 shows in the upper left chart, one can determine the level of savings in combination with a value $\hat{C}$ for the capacity installed for each storage cost level κ_x. For each storage cost level, it exists an economically maximal and an economically optimal amount of installed storage capacity $\hat{C}_{\kappa_x}^{max}$ respectively $\hat{C}_{\kappa_x}^{opt}$.

If the optimal capacity level $\hat{C}_{\kappa_x}^{opt}$ leads to marginally positive savings, the maximal capacity level $\hat{C}_{\kappa_x}^{max}$ is only marginally greater than the optimal capacity. The curve of κ_3 in Figure 7.1 represents this cost level. All cost levels below κ_3 will lead to higher positive values for the optimal capacity $\hat{C}_{\kappa_x}^{opt}$ and the maximal capacity $\hat{C}_{\kappa_x}^{max}$. The optimal capacity $\hat{C}_{\kappa_x}^{opt}$ is always less than the maximal capacity $\hat{C}_{\kappa_x}^{max}$ in these cases.

$$\hat{C}_{\kappa'}^{max} > \hat{C}_{\kappa''}^{max} > 0 \quad \wedge \quad \hat{C}_{\kappa'}^{opt} > \hat{C}_{\kappa''}^{opt} > 0 \quad \forall \ \kappa', \kappa'' : 0 < \kappa' < \kappa'' \leq \kappa_3 \tag{7.1}$$

$$\hat{C}^{max}_{\kappa'} > \hat{C}^{opt}_{\kappa'} > 0 \quad \forall \;\; 0 < \kappa' < \kappa_3 \tag{7.2}$$

Capacity values below the maximal capacity $\hat{C}^{max}_{\kappa_x}$ lead to positive savings, if $\kappa_x \geq \kappa_3$. Capacity values above the maximal capacity lead to negative savings. Economically, the benefits from load shifting exceed the costs for installing and operating the storage capacity up to a capacity level of $\hat{C}^{max}$.

$$savings\left(\hat{C}_{\kappa'}\right) > 0 \quad \forall \;\; \hat{C}_{\kappa'} < \hat{C}^{max}_{\kappa'} : \kappa' < \kappa_3 \tag{7.3}$$

$$savings\left(\hat{C}_{\kappa'}\right) \leq 0 \quad \forall \;\; \hat{C}_{\kappa'} > \hat{C}^{max}_{\kappa'} : \kappa' < \kappa_3 \tag{7.4}$$

If the maximal capacity level $\hat{C}^{max}_{\kappa_x}$ equals zero, the optimal capacity level $\hat{C}^{opt}_{\kappa_x}$ must also equal zero. In such a case, the costs for using the storage system (variable costs) exceed the benefits from load shifting. In Figure 7.1, κ_4 indicates such a cost level. For all storage cost levels κ_x between κ_3 and κ_4, the values for $\hat{C}^{max}_{\kappa_x}$ and $\hat{C}^{opt}_{\kappa_x}$ equal zero, as well as for all cost levels above κ_4.

$$\hat{C}^{max}_{\kappa'} = \hat{C}^{opt}_{\kappa'} = 0 \quad \forall \;\; \kappa' \geq \kappa_3 \tag{7.5}$$

The chart in the upper right corner of Figure 7.1 presents the relation between the costs per storage capacity unit κ and the maximal savings that can be achieved by installing the optimal amount of storage capacity $\hat{C}^{opt}_{\kappa}$. This chart can be derived from the previously discussed chart, as graphically illustrated. The chart in the lower right corner of Figure 7.1 depicts the optimal and the maximal level of installed storage capacity in dependency from the level of costs per storage capacity unit. This chart can be derived from the two previous charts.

7.1.1 Characteristics of the Load Curve

The basic data of the load curve represent the market-wide load in Germany in 2007. The data were provided by ENTSOE (2007) and have a granularity of one price per hour, rounded on megawatts. Thus, the load data differ from the load data used in Section 3.2 for the one-household-model, where a standard household profile was used.

Since the market-wide analysis model in this part of the work intends to determine the maximal and the optimal storage capacity dimension that can be economically operated in a market, the market-wide load data fit the analysis better than a scaled standard household profile. It better matches the price data from the EEX, which is also a market-wide variable. This is very important for the analysis in the following chapters, since the model will build on load-variable prices that are derived from historic spot market prices.

The key characteristic of the load curve is its distribution. The absolute peaks and the annual load volume itself can be neglected for the interpretation of the results, since the result figures will be indicated in relative terms to the absolute load volume. More precisely, they will be indicated as the percentage of the average weekly load

volume. One of the key result figures is the installed capacity $\hat{C}$ (and its derivatives $\hat{C}^{opt}$ and $\hat{C}^{max}$), which depends primarily on the distribution of the load curve and scales with the volume of the load curve. Thus, all results in Section 7.4 can be applied to any market with the same (or a fairly similar) price and load curve distribution to the German market in 2007, independently from the absolute market size. Table 7.2 gives the absolute values of the reference load curve that is used in the analysis model.

Table 7.2: Load Curve Characteristics

Characteristic	**Value**
Annual load volume	496,632,963 MWh
Average weekly load volume	9,524,468 MWh
Maximum hourly load (peak)	78,377 MWh
Minimum hourly load	33,651 MWh

When comparing the distribution of the market-wide annual load volume with the annual load volume of a standard household, the main differences can be seen in the diurnal load pattern. The average weekday and weekend patterns as well as the average seasonal patterns differ only marginally. Figure 7.2 graphically illustrates these differences.

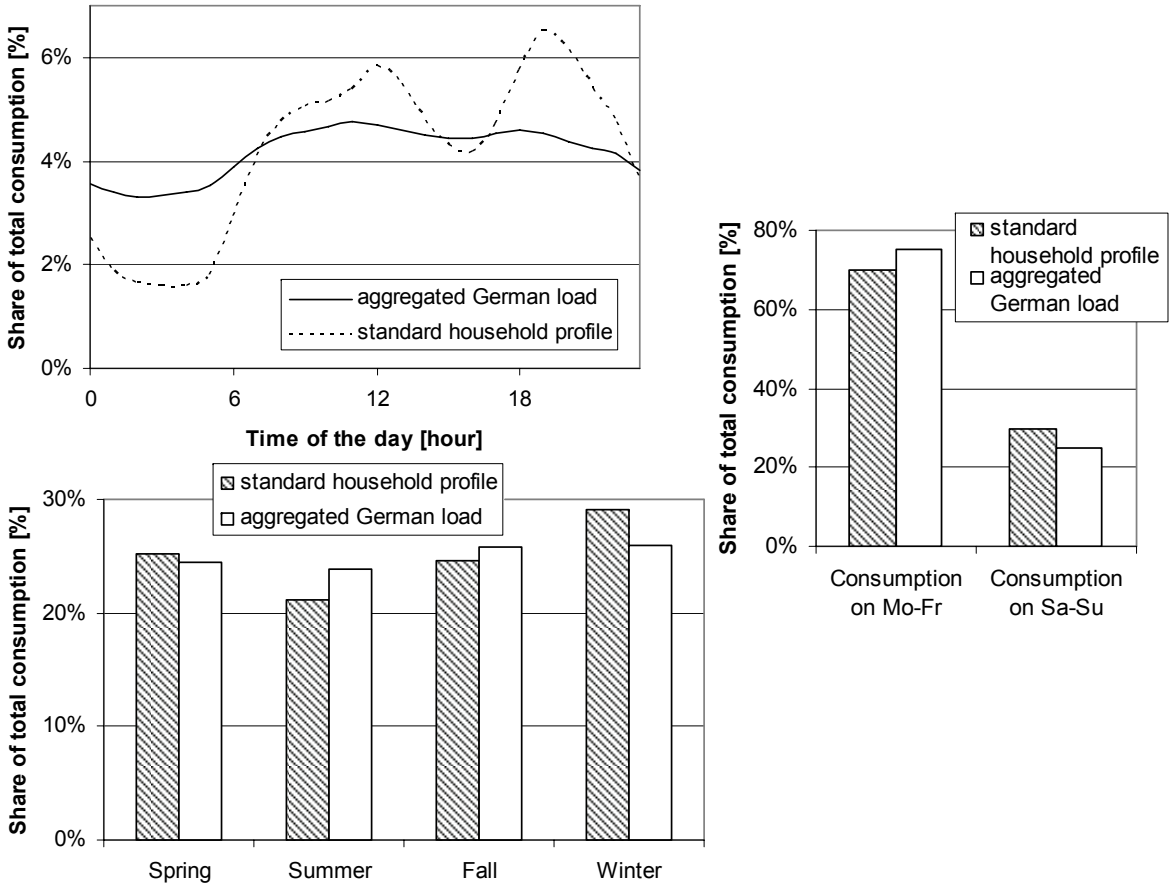

Figure 7.2: Distribution of the aggregated and the standard household load curve

7.1.2 Characteristics of the Price Curve

The basic data of the price curve are the same as for the single household analysis model in Section 3.2, but the market-wide analysis model treats the price as an endogenous variable. The price is now modeled as a load-variable parameter, i.e., it changes in timeslot t if the aggregated load changes in this timeslot.

The methodology for modeling an appropriate price function and determining its parameters builds on the approach presented in Spees and Lave (2007b). The work at hand uses linear and non-linear regression functions to approximate the observed prices on the market. The input variable for the price function is the aggregated load. The load data are sliced in various ways, e.g., by day, by weekend, or by month in order to determine the most appropriate price functions and parameters. The comparison of the different variants bases on the goodness of fit (adjusted R^2) of the obtained curves. Table 7.3 presents the results of the regression analyses and gives an overview of the functions and temporal resolution patterns analyzed. The definitions of the regression functions are given in Table 7.4.

Table 7.3: Adjusted R^2 Results

Temporal Resolution Pattern	**Linear Function**	**Exponential Function**	**Polynomial Function**	**Power Function**
Year	0.3935	0.4426	0.4381	0.3869
Day of Year	0.7523	0.8048	0.8025	0.7491
Month of Year	0.5864	0.6068	0.6034	0.5822
Week of Year	0.6846	0.7150	0.7091	0.6808
Hour of Day	0.2782	0.3056	0.3053	0.2746
Day of Week	0.3551	0.3948	0.3923	0.3502
Week or Weekend	0.6643	0.6968	0.6945	0.6609

Table 7.4: Definition of Regression Functions

Type	**Function**
Linear function	$f^{lin}(x) = a_0 + a_1 \cdot x$
Exponential function	$f^{exp}(x) = a_0 + a_1 \cdot e^{a_2 + a_3 \cdot x}$
Polynomial function	$f^{pol}(x) = a_0 + a_1 \cdot x + a_2 \cdot x^2 + a_3 \cdot x^3$
Power function	$f^{pow}(x) = a_0 + x^{a_1}$

The regression analysis qualitatively reveals the same results as in Spees and Lave (2007b), although their analyses delivered overall better fits for the price data. The best fit for the price function could be achieved by resolving the historic data with the temporal *Day of Year* pattern, i.e., determining daily price functions. This accounts for all regression functions analyzed. Among the regression functions, the exponential function $f^{exp}()$ delivered the best goodness of fit.

The main reason for the quantitative differences between the results in this work and the results in Spees and Lave derives from the different data sets used. Spees and Lave used load and price data from the PJM region, where nearly all electricity is traded over the day-ahead market price. They used market-wide average PJM market clearing prices and loads in the day-ahead market and real-time market over 2006

(Spees and Lave, 2008, p. 6). The basic price data in this work is obtained from the EEX (2007) and the load data is obtained from the European Network of Transmission System Operators for Electricity (ENTSOE) for Germany in 2007 (ENTSOE, 2007). In Germany, the spot market price only applies to 16.5% of the electricity delivered, since a large share is handled in bilateral contracts outside the market (Sensfuss et al., 2008). Thus, the market price data do not reflect the current load situation as well as in the PJM region, but with an adjusted R^2 of 0.8 still on a useful level. A similarity is that both regions have day-ahead markets that determine hourly prices. I.e., the day-ahead demand-supply-situation and the according commitments shape the daily market price curves, as the results in Table 7.3 reflect. The analyses clearly reflect the character of day-ahead markets. Bids and prices for a specified load depend on the daily situations that differ in availability of generation resources, weather conditions, or fuel prices (which certainly also have a mid- and long-term effect on the price curve).

As already stated in Spees and Lave (2008), *"temporal resolution always improves the explanatory power of [a] model, but the meaning of this observation is clouded by the fact that higher temporal resolution models use more complex parameters"*. Therefore, they try to limit the number of parameters as much as possible while maintaining a high level of goodness of fit. I.e., they remove those parameters that have very little explanatory power. The purpose of the price function derived in the work at hand is to model the historic price-load-relationship in the German market in 2007 as precise as possible. It is not intended to identify explaining parameters of historic or future prices functions. Therefore, the following analyses within this work will build on the price function $f^{exp}()$ with the best goodness of fit without attempting to further reduce the number of parameters.

As in Spees and Lave, this work builds the analyses on daily price curves. This extreme resolution fits best to model the supply-side relationship between price and load. The opposite extreme of this resolution is a price function that fits the entire year, which has one among the lowest values of explanatory power in the analysis of this work and the work of Spees and Lave (see Table 7.3).

Besides the reference price data that correspond to the price distribution at the EEX in 2007, the analyses in Section 7.4.5 will use modified price data with lower and higher spreads. I.e., these price data also reflect different volatility levels of the market price, as Table 7.5 shows. The methodology of deriving the modified price curves is explained in Section 3.2.4. Applying the regression functions on the modified price data reveals the same goodness of fit values as on the reference price data ($\pm 1\%$).

Table 7.5: Volatility of Price Curves

Price Data[a]	**Historic Volatility**	**Realized Volatility**
Reduced spread, $\alpha = 0.9$	0.2018	0.0437
Reduced spread, $\alpha = 0.99$	0.2346	0.0601
Reference data, $\alpha = 1$	0.2388	0.0625
Increased spread, $\alpha = 1.01$	0.2432	0.0651
Increased spread, $\alpha = 1.1$	0.2995	0.1139

[a] The value for α refers to equation (3.56) in Section 3.2.4 that defines how the price data were transformed.

The daily historic volatility HV_d is calculated as the daily standard deviation of (hourly) returns (Brooks, 2008). The overall historic volatility HV is the average of the daily historic volatilities HV_d.

$$HV_d = std_{h \in d}\left(r_h\right) \tag{7.6}$$

$$HV = \frac{1}{365} \cdot \sum_{d=1}^{365} HV_d \tag{7.7}$$

The daily realized volatility RV_d is calculated as the average of (hourly) squared returns. The overall realized volatility RV is the average of the daily realized volatilities.

$$RV_d = \frac{1}{24} \cdot \sum_{h=1}^{24} r_h^2 \tag{7.8}$$

$$RV = \frac{1}{365} \cdot \sum_{d=1}^{365} RV_d \tag{7.9}$$

As the volatility definitions, also the definition of the return has been taken from financial literature. The return r is defined as the continuously compounded return (Campbell et al., 1997), which is the natural logarithm of the quotient of the current price and the price of the previous period.

$$r = ln\left(\frac{p_t}{p_{t-1}}\right) \tag{7.10}$$

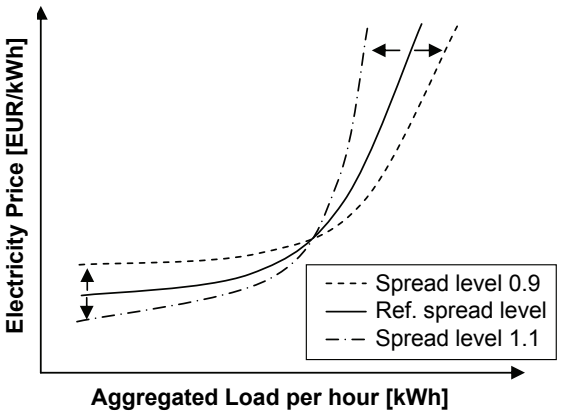

Figure 7.3: Impact of spread level variations on the price function (illustrative)

As Figure 7.3 shows, variations of the spread level influence the resulting price function. Higher spreads lead to a steeper price curve, whereas lower spreads flatten the price curve.

7.2 Estimation Model

The purpose of the estimation model is to get rough estimates for the results of the capacity dimensioning problem. In particular, the model will estimate the market-wide savings potential, the amount of storage capacity required, and the impact of the most important constraints.

The estimation model will only reflect the basic functioning of storage systems aiming at arbitrage accommodation. It will not describe detailed technical parameters of any storage technology. Furthermore, the estimation model uses the simplest price function available for the purpose of the analysis, which is a single price function for the entire analysis period. As presented in Table 7.3, such a price function has a much lower goodness of fit than for example the daily price functions. But for the purpose of defining a highly transparent, simple, and robust model, a single price function seems appropriate. The estimation model is less complex and therefore less error-prone to complex interdependencies of the technical and the economic parameters and constraints.

7.2.1 Mathematical Formulation

The objective of the estimation model is to minimize the total costs by shifting parts of the aggregated (market-wide) load volume $\hat{\ell}$ from timeslots with peak prices to timeslots with low prices. The analysis period consists of T timeslots t, $t = 1...T$. The aggregated load volume in timeslot t is indicated with $\hat{\ell}_t$ (kWh), which is always greater or equal zero. The shifted load in timeslot t is indicated with s_t (kWh). Its value can be positive for additional load in timeslot t, negative for a load reduction in timeslot t, or zero if no load shifting takes place. The total load volume $\hat{L}$ (kWh) during the entire analysis period is not altered through load shifting, i.e., the sum of all load shifted volumes is zero.

$$\hat{L} = \sum_{t=1}^{T} \hat{\ell}_t = \sum_{t=1}^{T} \left(\hat{\ell}_t + s_t \right) \tag{7.11}$$

$$\sum_{t=1}^{T} s_t = 0 \tag{7.12}$$

An important condition is that load shifting must not lead to a negative aggregated load, i.e., the maximal possible load shift in timeslot t is set by the given aggregated load volume $\hat{\ell}_t$.

$$(-1) \cdot s_t \leq \hat{\ell}_t \quad \forall t \tag{7.13}$$

The price p_t (EUR/kWh) in timeslot t is defined through a price function $f()$ that receives the aggregated load as an input parameter. Load shifting alters the price p_t: higher load leads to a price increase and reverse.

$$p_t = f\left(\hat{\ell}_t + s_t \right) \quad \forall t \tag{7.14}$$

The estimation model assumes a single price function $f()$ for the entire analysis period, i.e., the price function represents the market price for a requested volume of electricity in any timeslot of the analysis period. The market price in a competitive market increases monotonically, since cheaper supply (generation units) is allocated first and more expensive supply is only added, if all cheaper units cannot supply the requested volume (see also the explanation of the merit-order curve in Section 6.2.4). The marginal market price sets the uniform market price, i.e., the price of the most expensive supply unit applies for all selected units in that timeslot.[1]

The total costs $\hat{K}$ (EUR) of the analysis period are defined as the sum of total costs over all timeslots. The total costs of a timeslot are the product of the price and the actual system load:

$$\hat{K} = \sum_{t=1}^{T} p_t \cdot \left(\hat{\ell}_t + s_t\right) = \sum_{t=1}^{T} f\left(\hat{\ell}_t + s_t\right) \cdot \left(\hat{\ell}_t + s_t\right) \tag{7.15}$$

The baseline of the total costs $\hat{K}^{baseline}$ are the costs for electricity supply without load shifting:

$$\hat{K}^{baseline} = \sum_{t=1}^{T} f\left(\hat{\ell}_t\right) \cdot \hat{\ell}_t \tag{7.16}$$

The objective of the estimation model is to minimize $\hat{K}$ by deciding on the load shift volumes s_t.

$$min \rightarrow \hat{K} = \sum_{t=1}^{T} f\left(\hat{\ell}_t + s_t\right) \cdot \left(\hat{\ell}_t + s_t\right) \tag{7.17}$$

Since the price function $f()$ increases monotonically, minimizing the value of the term $(\hat{\ell}_t + s_t)$ for every timeslot t minimizes the entire equation. Due to the constraint that the total aggregated load volume $\hat{L}$ must not be altered, the average load per timeslot $\tilde{\ell}^{avg}$ is the optimal load for each timeslot to minimize the total costs.

$$\tilde{\ell}^{avg} = \frac{1}{T} \cdot \hat{L} \tag{7.18}$$

The average load volume $\tilde{\ell}^{avg}$ can be achieved for every timeslot by defining the load shift volume as the difference of the average load volume per timeslot and the given load $\hat{\ell}_t$:

$$\tilde{\ell}^{avg} = \hat{\ell}_t + s_t \qquad \forall t \tag{7.19}$$

$$\Leftrightarrow \qquad s_t = \tilde{\ell}^{avg} - \hat{\ell}_t \qquad \forall t \tag{7.20}$$

[1] The alternative settlement rule to uniform pricing is pay-as-bid pricing (Shahidehpour et al., 2002, p. 336). All models and analyses in this work refer to markets applying uniform pricing.

Since the average load volume $\tilde{\ell}^{avg}$ must be positive by definition of $\hat{L}$ respectively $\hat{\ell}_t$, the non-negativity constraint for the system load (equation (7.13)) is fulfilled:

$$s_t - \tilde{\ell}^{avg} = -\hat{\ell}_t \ \wedge \ \tilde{\ell}^{avg} > 0 \quad \forall t \tag{7.21}$$

$$\Rightarrow s_t \geq -\hat{\ell}_t \quad \forall t \tag{7.22}$$

Furthermore, the sum of all load shifting volumes s_t is zero (constraint in equation (7.12)):

$$\sum_{t=1}^{T} s_t = \sum_{t=1}^{T} \left(\tilde{\ell}^{avg} - \hat{\ell}_t \right) = T \cdot \tilde{\ell}^{avg} - \sum_{t=1}^{T} \hat{\ell}_t = 0 \tag{7.23}$$

Thus, applying the average load $\tilde{\ell}^{avg}$ fulfills all constraints of the minimization problem. By comparing the baseline costs $\hat{K}^{baseline}$ with the achieved total costs $\hat{K}$ in a load shifting scenario, the realized savings can be determined. The savings are the first result.

$$savings = \frac{\left(\hat{K}^{baseline} - K \right)}{\hat{K}^{baseline}} \tag{7.24}$$

The second result is the load shifting capacity required to realize the load shift volumes s_t. The required capacity is the maximum State of Charge (SOC) of a storage device that performs the load shifts. The SOC S_t in timeslot t is the cumulative sum of load shift volumes s_t until t.

$$S_t = \sum_{t'=1}^{t} s_{t'} \quad \forall t \tag{7.25}$$

If any SOC S_t has a negative value, the storage device would be in a technically invalid state. Thus, the initially calculated load shift volumes s_t are not actionable and therefore have to be modified. Any modification that leads to a technically valid series of load shift volumes will decrease the savings. The up to now calculated savings result underestimate the required capacity and overestimate the realizable savings. For the estimation model, these savings mark the upper bound of the savings potential.

To transform the calculated load shift volumes s_t into a valid form, the estimation model defines a simple correction loop that is executed until no SOC value S_t violates the non-negativity condition anymore. The *corrective step* distributes the highest negative SOC S_t^{min} in timeslot t^{min} equally to all preceding timeslots:

$$s_t = s_t - \frac{1}{t^{min} - 1} \cdot S_t^{min} \quad \forall t < t^{min} \tag{7.26}$$

Clearly, this measure unbalances the load shift volumes and leads to a higher total aggregated load $\hat{L}$, which obviously deteriorates the result. In an optimal solution,

the determination of the charge and discharge volumes considers the minimization objective and the constraints at the same time. Such a solution will certainly lead to higher savings that the proposed corrective loop in the estimation model. Therefore, the savings and the required total costs resulting from the corrected load shift volumes mark the lower bound of the savings potential. The result of the estimation model averages the results of the lower and the upper bound at equal weights.

7.2.2 Results and Interpretation

Based on the data of the German market from 2007, the estimation model reveals an average saving potential of 19.8% at a required storage capacity size of 10.6 GWh. The results of the lower and the upper result bound are 16.9% and 22.7% savings on the total costs baseline. The required storage capacity to realize these savings varies between 6.4 GWh and 14.8 GWh (see Table 7.6). The upper result bound does not fulfill the non-negativity condition for the SOC. I.e., it would overcharge the storage capacity (trying to discharge more than has been charged before). Consequently, this result overestimates the saving potential due to partially underestimating the required charge volumes, which would lead to additional costs. Alternatively, this result overestimates the savings potential due to partially overestimating the possible discharge volumes, which leads to savings that can actually not be realized.

Table 7.6: Results of the Estimation Model

	Lower Result Bound	**Upper Result Bound**	**Average Result**
Savings	16.9%	22.7%	19.8%
Required capacity	14.8 GWh	6.4 GWh	10.6 GWh

The lower result bound does fulfill the non-negativity condition for the SOC. Due to additional charge volumes (in comparison with the previous case), a storage device would always be sufficiently charged. The additional charge volumes disregard any economic constraints or justifications. They are equally distributed to timeslots at the beginning of the analysis period, i.e., they do not consider low or high charging prices. Furthermore, the estimation model does not economically compare the alternatives of not discharging (reducing the discharge volumes) instead of increasing the charge volumes (as applied). Thus, the lower result bound underestimates the potential savings and overestimates the required storage capacity. Figure 7.4 depicts the results of a sample week graphically. Both resulting load curves (before and after the corrective loop) flatten the aggregated load curve. Due to the additional charge volumes, the corrected load shift volumes lead to an overall higher load at the beginning of the period.

The results were obtained by applying the ENTSOE (2007) load data as described in Section 7.1.1 as well as the price function $f^{exp}()$ at the temporal resolution level of one function for the entire analysis period (one function per year). The price function fits the real prices *on average* fairly precise despite its lower goodness of fit value. The total costs baseline based on the static price curve varies from the total costs baseline based on the functional price curve by 0.04%. I.e., deviations in the functional price curve from the given price curve average out over the analysis period. The estimation

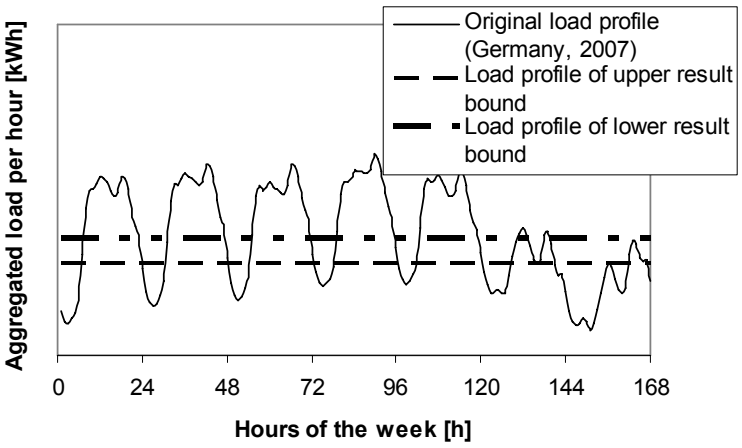

Figure 7.4: Resulting aggregated load after load shifting between January 8 and January 14, 2007

model disregards any technical or economic constraints of the storage system. I.e., the model assumes costs per storage capacity unit of zero, unlimited charging speed, a Depth of Discharge (DOD) of 100%, and perfect efficiency degrees of 100%. Moreover, the model did not limit the market-wide load. Not including these storage system parameters clearly overestimates the realistic potential of load shifting through storage systems. But it gives a good indication for the potential of DR through load shifting in general, for which the installation of storage systems is only one realization option. E.g., load shifting through behavioral changes of the consumer or the installation of automated and semi-automated devices that autonomously shift their load would also tap the potential. The general cost reduction potential through load shifting is actually even higher, if daily price functions are applied instead of a single function for the entire period. Daily price functions will fit the real prices better and will therefore more precisely identify the economic load shifting volumes, and, thus, lead to a greater saving potential, as the results of the precise analysis model in Section 7.3 and Section 7.4 will show.

7.3 Market-wide Analysis Model

The objective of the market-wide analysis model is to determine the minimal total costs for a given analysis period when performing price-responsive load shifting (arbitrage accommodation) with DSS. Regarding its structure and its parameters, the market-wide analysis model is similar to the linear optimization model in Section 3.2. Both models build on the same technical and economic storage parameters and constraints. The major difference between the models is the determination of the price. While the linear optimization model in Chapter 3.2 uses a fixed price curve that is independent from load variations (exogenous variable), the market-wide analysis model in this chapter uses a specific load-variable price function for each day of the analysis period (price is an endogenous variable)[2]. A second small difference is the underlying

[2]The model in Section 3.2 models a *one-household-case*. Such a small unit can be regarded as a price taker on the market, which has no impact on the market price.

load profile. Instead of a standard household profile as in Section 3.2, this model uses the aggregated, market-wide load for Germany in 2007 (ENTSOE, 2007).

7.3.1 Mathematical Formulation

As in the linear optimization model, the total costs $\hat{K}$ are composed of the fixed costs $\hat{K}^{fixed}$ and the variable costs $\hat{K}^{variable}$. Fixed costs are capital costs, maintenance costs, and depreciations of the peripheral components. Variable costs are the costs for electricity supply from the grid reduced by the share that is served through stored capacity, costs for charging the storage system, and costs for depreciating (using) the storage system. The decision parameters of the analysis model are the charge volume c_t in timeslot t and the discharge volume d_t. The quotient of the costs per storage capacity unit κ (EUR/kWh) and the expected number of nominal discharge cycles γ (#) determines the depreciation (usage) costs for a kilowatt hour of discharge. The price function $f_t(\hat{\ell}_t)$ determines the market price p_t for a specific amount of load $\hat{\ell}_t$ in timeslot t.

$$min \rightarrow \hat{K} = \hat{K}^{fixed} + \sum_{t=1}^{T} \hat{K}_t^{variable} \tag{7.27}$$

$$\hat{K}^{fixed} = \frac{\hat{P}^{in}\pi^{in} + \hat{P}^{out}\pi^{out}}{\tau} + (m+i) \cdot (\hat{P}^{in}\pi^{in} + \hat{P}^{out}\pi^{out} + C \cdot \kappa) \tag{7.28}$$

$$\hat{K}_t^{variable} = p_t \cdot \left(\hat{\ell}_t + \frac{c_t}{\eta^{in} \cdot \eta^{store}} - d_t \right) + d_t \cdot \frac{\kappa}{\gamma} \tag{7.29}$$

where

$$p_t = f_t \left(\hat{\ell}_t + \frac{c_t}{\eta^{in} \cdot \eta^{store}} - d_t \right) \tag{7.30}$$

The charge volumes c_t and the discharge volumes d_t are the decision variables of the minimization problem. The constraints of the problem reflect the maximal capacity of the power components and the maximal charging speed (equations (7.31) (7.33)), as well as the constraints of the SOC (equations (7.34), (7.35), (7.36)).

$$d_t \leq \frac{\hat{P}^{out}}{T^h} \quad \forall t \tag{7.31}$$

$$c_t \leq \frac{C}{v} \quad \forall t \tag{7.32}$$

with

$$v = T^h \cdot max \left(\frac{C}{\hat{P}^{in}}; v^{store} \right) \tag{7.33}$$

$$d_t \leq \hat{\ell}_t + c_t \quad \forall t \tag{7.34}$$

$$0 \leq \xi_t \leq C \quad \forall t \tag{7.35}$$

with

$$\xi_t = \sum_{t'=1}^{t} c_t - \frac{d_t}{\eta^{out}} \quad \forall t \tag{7.36}$$

The SOC ξ_t must not fall below the maximal DOD $\bar{\delta}$ after an initial start-up phase. The start-up phase is defined as in Section 3.2.2:

$$\left\lceil \left(1 - \bar{\delta}\right) \cdot v \right\rceil \leq t^{startup} \leq T \tag{7.37}$$

$$(1 - \bar{\delta}) \cdot C \leq \xi_t \qquad \forall t > t^{startup} \tag{7.38}$$

7.3.2 Generic Solution for the Minimization Problem

The generic formulation of the price function $f_t()$ inhibits solving the minimization problem without further specification. Only if the price function was a constant function $f_t^{const}()$, the problem would turn into a linear optimization problem with c_t and d_t as decision variables (similar to the linear optimization model in Section 3.2):

$$\begin{aligned} min \rightarrow \hat{K} = \hat{K}^{fixed} + \\ \sum_{t=1}^{T} \underbrace{f_t^{const}\left(\hat{\ell}_t + \frac{c_t}{\eta^{in} \cdot \eta^{store}} - d_t\right)}_{a} \cdot \left(\hat{\ell}_t + \frac{c_t}{\eta^{in} \cdot \eta^{store}} - d_t\right) + d_t \frac{\kappa}{\gamma} \end{aligned} \tag{7.39}$$

$$\Leftrightarrow \quad min \rightarrow \hat{K} = \hat{K}^{fixed} + a \cdot \sum_{t=1}^{T} \hat{\ell}_t + \frac{c_t}{\eta^{in} \cdot \eta^{store}} - d_t + \frac{d_t}{a} \cdot \frac{\kappa}{\gamma} \tag{7.40}$$

In the context of electricity spot market prices, it is highly unlikely that a constant function models the market prices properly. If the price function was a linear function f_t^{lin}, which is also highly unlikely in this context, the problem would turn into a quadratic optimization problem.

$$f_t^{lin}(x_t) = a_t \cdot x_t + b_t \tag{7.41}$$

$$x_t := \hat{\ell}_t + \frac{c_t}{\eta^{in} \cdot \eta^{store}} - d_t \tag{7.42}$$

By resolving $f_t()$ with f_t^{lin}, equation (7.27) could be transformed into

$$min \rightarrow \hat{K} = \hat{K}^{fixed} + \sum_{t=1}^{T} (a_t \cdot x_t + b_t) \cdot x_t + d_t \cdot \frac{\kappa}{\gamma} \tag{7.43}$$

$$\Leftrightarrow \quad min \rightarrow \hat{K} = \hat{K}^{fixed} + \sum_{t=1}^{T} a_t \cdot x_t^2 + b_t \cdot x_t + d_t \cdot \frac{\kappa}{\gamma} \tag{7.44}$$

To provide a generic solution for the minimization problem that works for all function types, the following paragraphs present a decomposition of the problem into linearized problems that can be solved iteratively, regardless of the price function applied. The only requirement to the price function is that it increases monotonically (see Section 7.2.1).

The solution algorithm increases the shifted load, i.e., the charge and the discharge volumes, iteratively until further load shifting does not lead to an economic improvement of the result anymore. In each iteration step j, the constant charge volume increment $\tilde{c}$ and the constant discharge volume increment $\tilde{d}$ are assigned to those timeslots that have the highest economic impact (highest reduction of supply costs through discharging (b_t^j) and lowest increase of charging costs (a_t^j)) by setting the decision variable vectors φ for charging and λ for discharging. The resulting costs in iteration step j are indicated with $\hat{K}^j$.

$$\begin{aligned} min \rightarrow \hat{K}^j = \sum_{t=1}^{T} & \underbrace{\left[f_t\left(\hat{\ell}_t^{j-1} + \tilde{c}\right) \cdot \left(\hat{\ell}_t^{j-1} + \tilde{c}\right) - f_t\left(\hat{\ell}_t^{j-1}\right) \cdot \ \hat{\ell}_t^{j-1}\right]}_{a_t^j} \cdot \varphi_t^j + \\ & \underbrace{\left[f_t\left(\hat{\ell}_t^{j-1} - \tilde{d}\right) \cdot \left(\hat{\ell}_t^{j-1} - \tilde{d}\right) - f_t\left(\hat{\ell}_t^{j-1}\right) \cdot \hat{\ell}_t^{j-1} + \tilde{d} \cdot \frac{\kappa}{\gamma}\right]}_{b_t^j} \cdot \lambda_t^j \end{aligned} \tag{7.45}$$

The charge and the discharge increments $\tilde{c}$ and $\tilde{d}$ adjust the constant increment value ϵ for efficiency losses.

$$\tilde{c} = \frac{\epsilon}{\eta^{in} \cdot \eta^{store}} \tag{7.46}$$

$$\tilde{d} = \epsilon \cdot \eta^{out} \tag{7.47}$$

The discharge volume $\tilde{d}$ must be assigned to a later timeslot than the charge volume $\tilde{c}$ to avoid a negative SOC in any timeslot t. During the time period between charging and discharging, the maximal storage capacity must not be exceeded.

$$0 \leq \sum_{t'=1}^{t} \varphi_{t'}^j - \lambda_{t'}^j \leq \frac{C}{\epsilon} \quad \forall t, j \tag{7.48}$$

$$0 \leq \varphi_t^j, \lambda_t^j \leq 1 \quad \forall t, j \tag{7.49}$$

$$\sum_{t=1}^{T} \varphi_t^j = 1 \quad \forall j \tag{7.50}$$

The distance between the charge volume and the discharge volume must be smaller than a given technology-specific self-discharge tolerant time period T^{selfdch}.

$$\sum_{t'=t}^{t+T^{\text{selfdch}}} \varphi_{t'} - \lambda_{t'} \leq 0 \;\; \forall t \tag{7.51}$$

At the end of each iteration step j, the additional charge and discharge volumes are included into the current aggregated load $\hat{\ell}_t^j$.

$$\hat{\ell}_t^j = \hat{\ell}_t^{j-1} + \varphi_t^j \cdot \tilde{c} - \lambda_t^j \cdot \tilde{d} \quad \forall t, j \tag{7.52}$$

$$\hat{\ell}_t^0 = \hat{\ell}_t \quad \forall t \tag{7.53}$$

Additional charge and discharge volumes to the load curve of the previous iteration step must not violate the power capacity constraints $\hat{P}^{in}$ and $\hat{P}^{out}$ in any iteration j.

$$\textbf{Constraint C1}: \quad \hat{\ell}_t^{j-1} + \varphi_t^j \cdot \tilde{c} - \hat{\ell}_t \leq \hat{P}^{in} \cdot T^h \;\; \forall t, j \tag{7.54}$$

$$\textbf{Constraint C2}: \quad \hat{\ell}_t + \lambda_t^j \cdot \tilde{d} - \hat{\ell}_t^{j-1} \leq \hat{P}^{out} \cdot T^h \;\; \forall t, j \tag{7.55}$$

Additionally, the charge volume must not violate the global load maximum $\bar{\ell}$.

$$\textbf{Constraint C3}: \quad \hat{\ell}_t^{j-1} + \varphi_t^j \cdot \tilde{c} \leq \bar{\ell} \;\; \forall t, j \tag{7.56}$$

Discharging during the initial start-up phase is prohibited.

$$\textbf{Constraint C4}: \quad \lambda_t^j = 0 \;\; \forall t < t^{startup}, j \tag{7.57}$$

The constraints C1-C4 can be incorporated into the static vectors a and b $[1 \times T]$ that simplify equation (7.45):

$$a_t^j = \begin{cases} \infty & C1 = \text{false} \vee C3 = \text{false} \\ f_t\left(\hat{\ell}_t^{j-1} + \tilde{c}\right) \cdot \left(\hat{\ell}_t^{j-1} + \tilde{c}\right) - f_t\left(\hat{\ell}_t^{j-1}\right) \cdot \; \hat{\ell}_t^{j-1} & else \end{cases} \tag{7.58}$$

$$b_t^j = \begin{cases} \infty & C2 = \text{false} \vee C4 = \text{false} \\ f_t\left(\hat{\ell}_t^{j-1} - \tilde{d}\right) \cdot \left(\hat{\ell}_t^{j-1} - \tilde{d}\right) - & \\ \qquad f_t\left(\hat{\ell}_t^{j-1}\right) \cdot \hat{\ell}_t^{j-1} + \epsilon \cdot \eta^{out} \cdot \frac{\kappa}{\gamma} & else \end{cases} \tag{7.59}$$

Thus, equation (7.45) with its constraints (7.49)-(7.51) forms a linear optimization problem. The complexity of the price function $f_t()$ is hidden in the static vectors a_t and b_t, which have to be calculated in each iteration step j. The run time of the solution algorithm is primarily determined by the load increment constant ϵ. The higher the constant, the less precise the result (optimal solution is underestimated[3]),

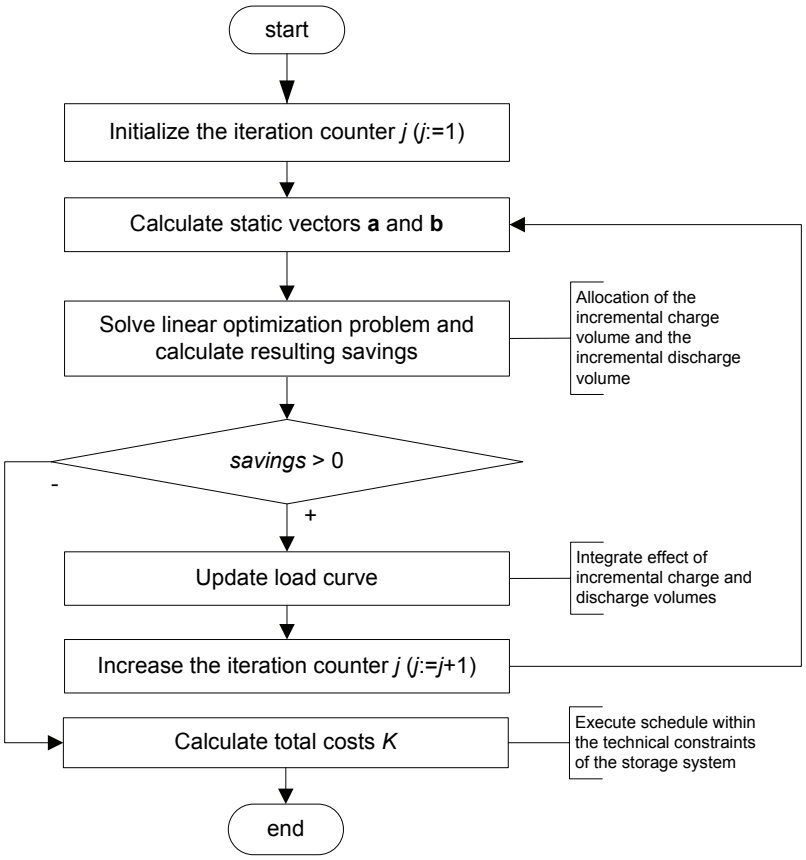

Figure 7.5: Control flow of the iterative solution algorithm

but the faster the runtime of the algorithm. Figure 7.5 summarizes the control flow of the iterative solution algorithm.

The total costs $\hat{K}$ are calculated at the end of the iterative algorithm. The total costs are the sum of fixed costs, costs for the resulting load curve $\hat{\ell}^J$ (J indicates the last iteration step that led to an improvement of the result), and the costs for storage depreciations. The savings are calculated relative to the baseline costs $\hat{K}^{baseline}$.

$$\hat{K} = \hat{K}^{fixed} + \sum_{t=1}^{T} f\left(\hat{\ell}_t^J\right) \cdot \hat{\ell}_t^J + \epsilon \cdot J \cdot \frac{\kappa}{\gamma} \tag{7.60}$$

$$savings = \frac{\left(\hat{K}^{baseline} - \hat{K}\right)}{\hat{K}^{baseline}} \tag{7.61}$$

7.3.3 Analysis Parameters and Assumptions

The analysis parameters of the market-wide analysis model build on the parameter values for the optimization model in Section 3.2. Each calculation of the model determines the savings in comparison to a baseline case without storage capacity for a

[3]Due to the characteristic of the merit-order price curve, additional load in low-price periods lead to a lower price increase than the same amount of load reductions causes as savings during peak-price periods.

specified scenario. For each scenario, there is a fixed parameter setting. To calculate the optimal and the maximal storage capacity that can be economically operated on the market, these settings are run repeatedly for a series of capacity sizes.

A parameter setting specifies the basic value parameters as in Table 3.6. The value for the capacity size is set separately, since the impact of its variation is to be analyzed. Directly linked to the capacity size is the optimal sizing of the power capacity parameters $\hat{P}^{in}$ and $\hat{P}^{out}$. The optimal values for these parameters are determined separately. Figure 7.6 shows that the values follow a logarithmic function in dependency from the capacity size and the costs per storage capacity unit κ.

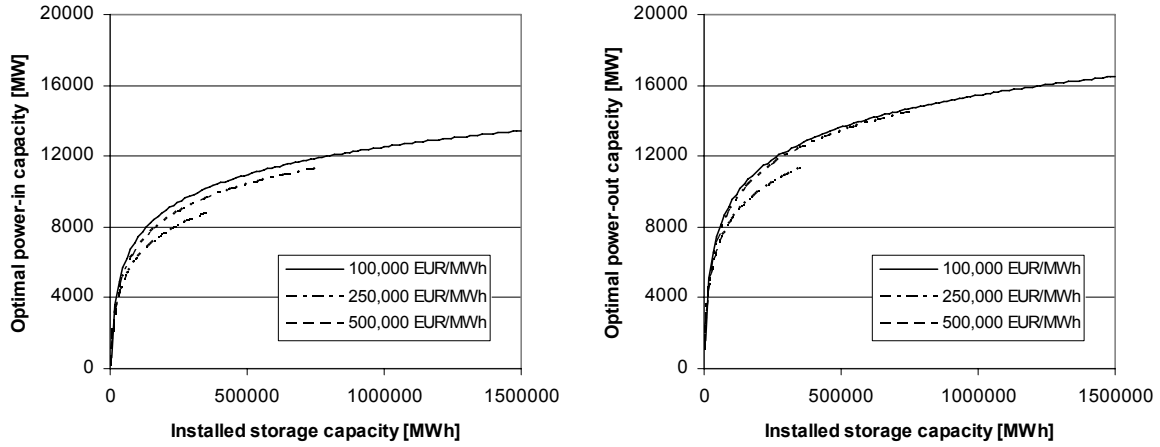

Figure 7.6: Optimal dimensions of $\hat{P}^{in}$ (left) and $\hat{P}^{out}$ (right) in dependency from the installed capacity $\hat{C}$

Additional parameters in comparison to the *one-household-model* of Section 3.2 are the maximal system load $\bar{\ell}$ and the (dis-)charge increment parameter ϵ. The maximal system load limits the load that additional charge volumes create. It is assumed that the maximal system load $\bar{\ell}$ equals the maximal peak load of the original aggregated load curve $\hat{\ell}$. I.e., the proposed load shifts will not require higher transmission and distribution capacities in the grid.

The increment parameter ϵ influences the accuracy and the performance of the analysis model, as described in the previous section. The value is set to 2,000 (MWh) for the following analysis. The analysis results, which are presented in the following section, underestimate the truly optimal value by approximately 1.5% points (presented results are *not* adjusted for this error).

The prices are modeled through daily price functions that depend on the aggregated load on the system. I.e., there is no static price vector as in the linear optimization model in Section 3.2. The price function used in the following analyses is the exponential function $f_t^{exp}(x_t) = a_0 + a_1 \cdot exp(a_2 + a_3 \cdot x_t)$ (see Table 7.4) with daily-specific parameters a_x. I.e., every day of the analysis period has its own set of values for each parameter a_0 to a_3. As for the static price vector in Chapter 3.2, the weighted average price of the basic price curve is 0.20 EUR/kWh.

The load curve represents the aggregated load for Germany in 2007 (ENTSOE, 2007). This profile contains all consumer groups (large industrial companies, small and medium enterprises, public sector, and private households). Table 7.2 presents some absolute data points of the load curve.

7.4 Analysis Results

The market-wide analysis model calculated the market-wide annual savings that Demand Response Agents could realize when using DSSs in comparison to the baseline case of a scenario without storage systems. The electricity price is a load-dependent, endogenous variable in these analyses.

The following paragraphs present the results of varying the input parameters of the reference case, namely the impact of the overall installed capacity on the storage system, the technical storage system constraints, and the storage capacity costs. These analyses are followed by a sensitivity analyses to all technical and economic parameters and an analysis of the price spread's impact.

7.4.1 Capacity Variation Analysis

Depending on the costs of storage capacity and the amount of capacity installed on the system, storage systems can achieve different levels of annual savings. Lower storage capacity costs lead to higher savings due to lower capital costs and lower depreciation on the storage devices themselves. For each technology profile, i.e., each level of storage capacity costs, there is an optimal and a maximal value of installed storage capacity that can be operated economically. Economically means that the total annual savings in the system are at least marginally positive. The savings are maximal for the optimal value of installed storage capacity and they are marginally positive for the maximal value of installed capacity.

Figure 7.7 shows the annual savings in dependency on the amount of storage capacity installed in the system for different storage capacity cost levels. Each curve represents a distinct level of costs per storage capacity unit. The results show that increasing storage costs decreases the achievable savings substantially. While storage capacity costs of 100,000 EUR/MWh (100 EUR/kWh) lead to maximal savings of 9%, costs of 750,000 EUR/MWh reduce the achievable savings to maximally 1.5%. The optimal dimensions of the storage capacity installed on the system vary between 3.7% and 0.3% of the average weekly load.

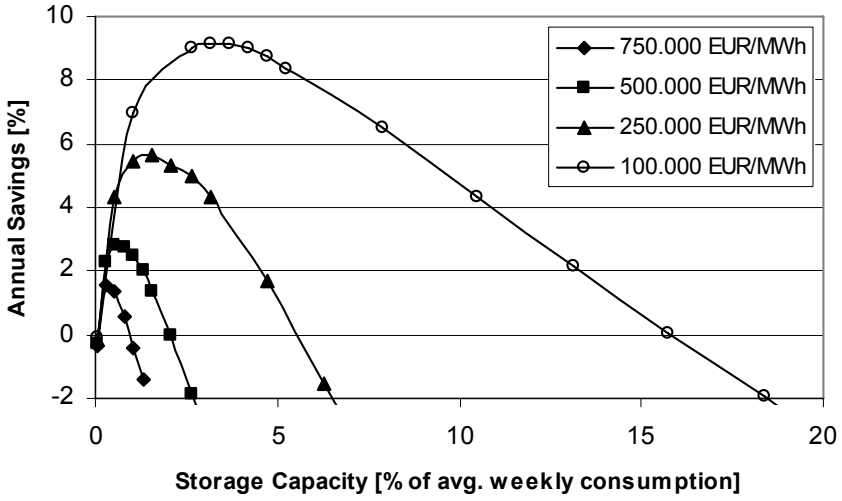

Figure 7.7: Results of the capacity variation analysis

More remarkable are the different results for cases where the installed capacity exceeds the optimal size. The higher the capacity costs, the steeper the annual savings decline with each additional storage capacity unit installed beyond the optimal size. The reference case with storage costs of 100,000 EUR/MWh reveals negative savings, if the amount of installed capacity exceeds 16% of the average weekly load. In case of 750,000 EUR/MWh, results turn negative if the installed capacity exceeds 1% of the average weekly load.

7.4.2 Constraint Analysis

The analysis model in Section 7.3 contains several technical constraints that influence and shape the economic result. To investigate the limiting effects of purely technical constraints, the following analyses assume that the costs per storage capacity unit κ (EUR/kWh) and the costs per power capacity unit π^{in} and π^{out} (EUR/kW) are zero. The two goals of this analysis are to understand the impact of the purely technical constraints in the model and to compare the results of such an unconstraint model with the results of the estimation model, which did not consider technical and economic constraints either. Since the estimation model used a different analysis approach, the comparison of the results will be a plausibility check for the overall model results. Due to the price assumptions of this analysis, some technical parameters lose their limiting character to the economic result, namely the maximal DOD $\bar{\delta}$ (%), the expected number of nominal charge cycles over lifetime γ (#), the expected system lifetime τ (years), the power capacity constraints P^{in} and P^{out}, as well as the capacity constraint C (kWh). Moreover, the interest rate i (%) and the maintenance rate m (%) (economic parameters) do not impact the economic result anymore.

The only remaining parameters that still impact the economic result are the efficiency degrees η^{in}, η^{out}, and η^{store} (%), as well as the constraint of the maximal system load $\bar{\ell}$ (kW). Figure 7.8 shows the results of three cases that relaxed these parameters step by step. The first case reveals 15.8% annual savings. This case holds the efficiency degrees as given in Table 3.6 for the reference case, as well as the maximal system load, which is limited to the maximum of the original load curve. Parameters like the overall capacity C and the installed power capacities P^{in} and P^{out} are unlimited, since they do not impact the economic result anymore (according costs parameter values are assumed zero).

The second case releases the efficiency degree constraints, i.e., all efficiency degrees equal 100%. The annual savings are 24.1%, which is 8.3% points (52%) higher than for the first case. The third case additionally releases the maximal load constraints $\bar{\ell}$ and reveals 24.8% annual savings, which is 0.7% points (3%) higher than for the second case.

The analysis reveals the outstanding impact of the efficiency degrees in case of low costs per storage capacity unit. Furthermore, the results validate the analysis model. The estimation model revealed an annual saving potential of 19.8% in the average case. Since the estimation model uses a less accurate price function (one price function for the entire analysis period) than the analysis model (one price function for each day of the analysis period), the result of the estimation model is lower.

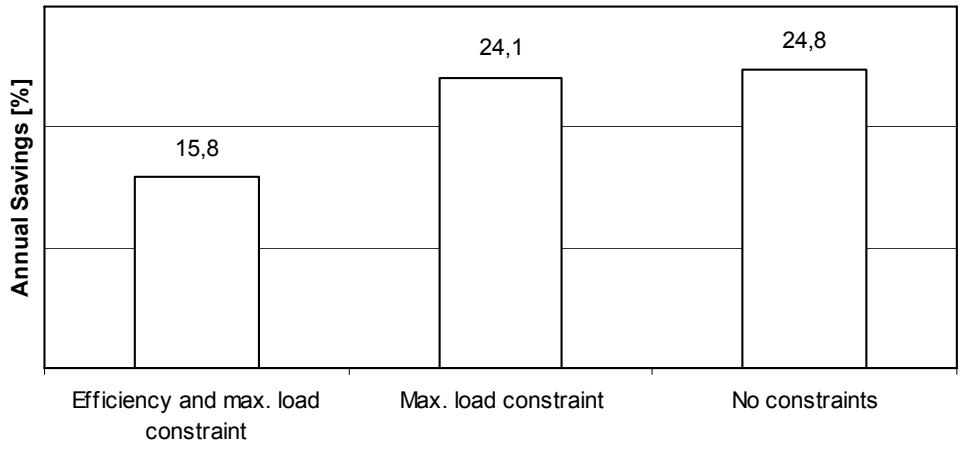

Figure 7.8: Results of the constraint analysis

7.4.3 Storage Capacity Cost Analysis

Capacity costs are one of the key parameters of the analysis model. Cost levels differ significantly between storage technologies and between different developmental stages of the technology. The capacity cost per storage unit impact the economic result in two ways: Firstly, capacity costs are directly linked to the initial investment into the storage system and therefore determine a large share of the capital costs. Secondly, the quotient of the capacity price and the number of expected nominal discharge cycles (costs per nominal discharge cycle) determines the depreciation costs for using the storage system. Higher depreciations costs require higher spreads to economically operate the system, i.e., reduce the number of arbitrage opportunities for a given price curve. Figure 7.9 depicts the achievable annual savings in dependency on the storage capacity costs. The analysis reveals that at storage capacity costs κ of 1.5 million EUR/MWh (1,500 EUR/kWh) the annual savings are zero. I.e., the sum of capital and depreciation costs equals the benefits from arbitrage opportunities that could be realized due to sufficiently high spreads. Higher storage capacity costs will lead to negative savings - regardless of the amount of capacity installed. On the other extreme, if storage capacity costs are close to zero, an optimally sized system leads to approximately 14% annual savings.

Since capital costs are close to zero in this case, the result reveals the maximal arbitrage potential, which is determined through the load and the price curve distribution. For the reference case with storage capacity costs of 100,000 EUR/MWh, the analysis reveals maximal annual savings of 9% in the case of an optimally sized system. As shown in Figure 7.9, the optimal storage capacity is 3.7% of the average weekly system load.

Figure 7.10 presents an analysis of the optimal and the maximal total storage capacity of the system that can be operated economically. As already explained in the context of Figure 7.1, the difference between the optimal and the maximal volume for the installed capacity differ disproportionately high with decreasing storage capacity costs. While the maximal amount of capacity installed that can be operated economically for storage costs close to zero is around 150% of the average weekly load (about 8% for an optimally sized capacity installation), it is 0.5% if storage costs are at 1,000,000 EUR/MWh (0.2% for an optimally sized installation). This huge difference

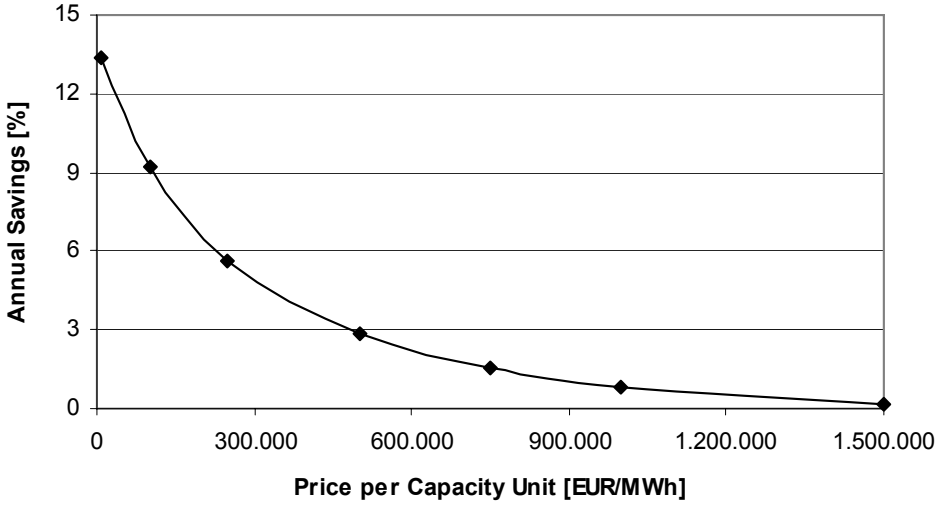

Figure 7.9: Results of the storage capacity cost analysis

in economically operable storage capacity reflects the different amounts of arbitrage opportunities that are directly linked to the storage depreciation costs per nominal discharge cycle.

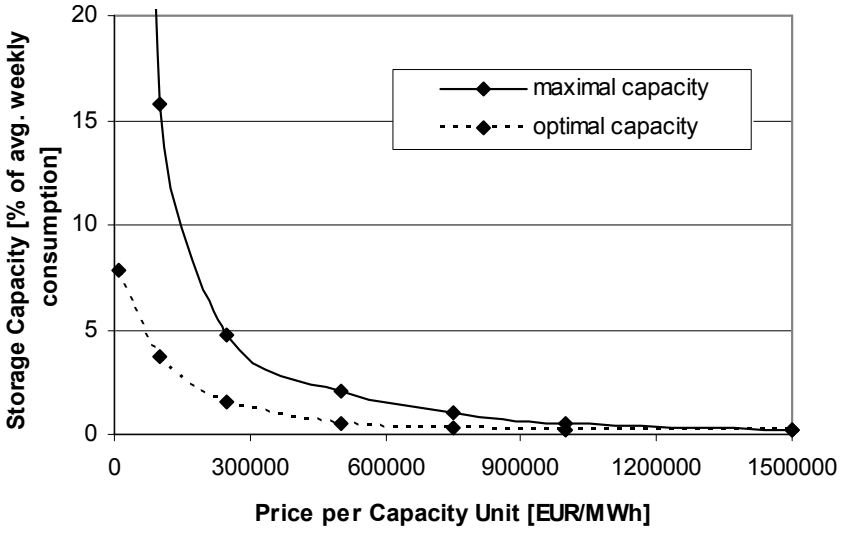

Figure 7.10: Optimal and maximal storage capacity sizes

7.4.4 Sensitivity Analysis

The sensitivity analysis separately varies each parameter value in four steps from its reference value (-10%, -1%, +1%, +10%). The results of the sensitivity analysis indicate the relative deviation from the results of the reference case for each parameter variation. Some values could not be varied in the previously explained manner, since the modified values would be out of a valid range. E.g., efficiency degrees must not be greater than 100%.

The results of the sensitivity analysis are valid for the reference case. For other cases, e.g., case with higher costs of storage capacity, sensitivity values will differ in absolute and relative terms. The non-linear plot and the slightly different shapes of the result curves in Figure 7.7 make this obvious. However the relative impact of a parameter in comparison with other parameters remains about the same for all analyzed cases.

Figure 7.11 shows the results of the sensitivity analysis of the reference case. The efficiency degrees η^{in}, η^{out}, and η^{store} have the highest sensitivity (up to 14.4% result deviation through a 10% parameter value variation). The second highest sensitivity values are observed for the costs per storage capacity unit κ, where a 10% variation of the reference parameter leads to a 4.1% deviation of the annual savings in opposite direction to the parameter variation, since lower costs lead to higher savings. A notable impact can fruther be assigned to the maximum DOD $\bar{\delta}$ (up to 2.2% deviation from the reference result in case of a 10% variation of the parameter value) and the interest rate i (up to 2.9% deviation).

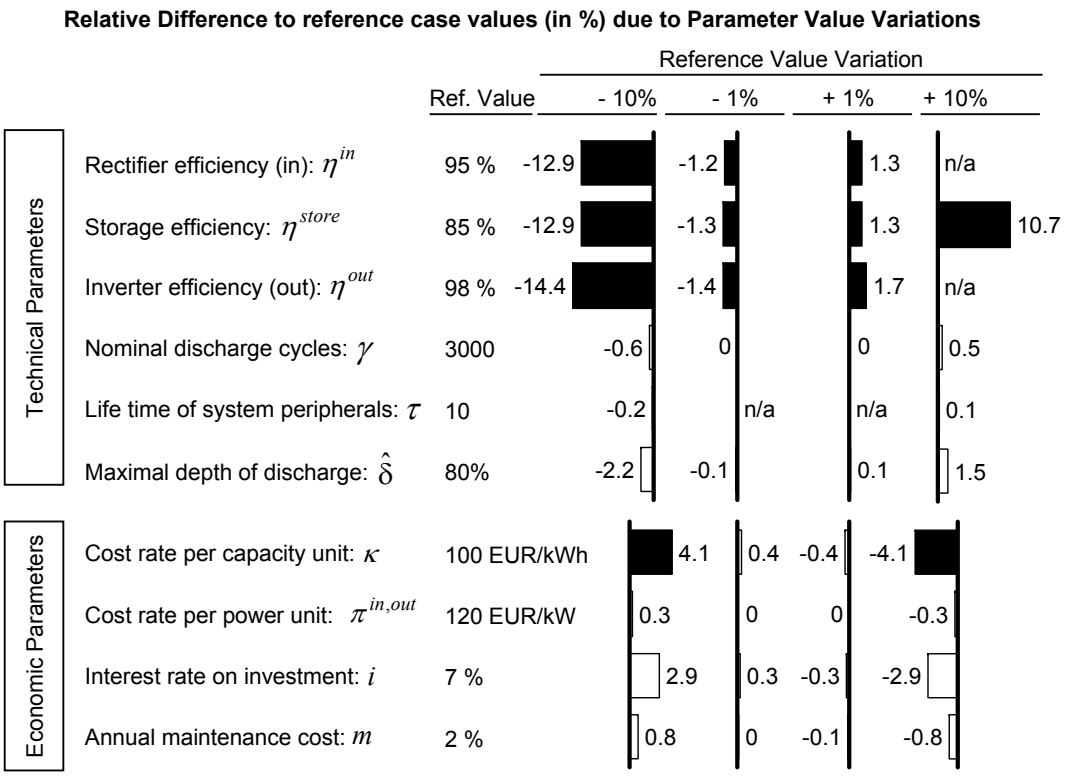

Figure 7.11: Results of the sensitivity analysis

The results of this sensitivity analysis of the technical and the economic parameters on the aggregated system level in the context of load-variable, daily prices are in line with the sensitivity results of the single consumer analysis (Section 3.2.4), where the storage system was modeled as a price taker, i.e., the electricity price was an exogenous, static variable. Overall, the sensitivities along with the annual savings (for the same storage parameters) were higher in the single household case. The main reasons for this difference are the different load curve distributions and the load-variable price curve.

The load curve distribution in the single household case is a standard household profile (average profile of a 2-person household in Germany), whereas the current analysis builds on the load profile for Germany in 2007 (ENTSOE, 2007), which includes all consumer groups. The slightly higher relative impact of the interest rate in case of the market-wide analysis (relative to the impact of other parameters) in comparison to the single household case indicates that capital costs have a higher influence on the market-wide result. I.e., the aggregated load curve for Germany offers a slightly lower load shifting potential than the standard household profile.

7.4.5 Spread Analysis

The average spread, i.e., the mean difference between low prices in charge timeslots and high prices in discharge timeslots, is a key factor of the price curve that determines the annual savings that can be realized through a storage system aiming at arbitrage accommodation. If the spreads of a price curve increase, this implies that also the price volatility increases. The spread analysis varies the reference price curve in four level. The new price curves are determined through equation (3.56) in Section 3.2.4. The values for α that scale the variation are 0.9, 0.99, 1.01, and 1.1. The regression analysis determines the daily price functions (see Section 7.1.2) for the modified price curves. I.e., the load-variable, daily prices reflect the new spread levels. Table 7.5 depicts the average volatility of each price curve. As previously stated, higher price spreads lead to higher volatility, which is reflected in a steeper price curve (Figure 7.3).

Figure 7.12 presents the results of the spread analysis. In Case 1 with a spread variation of $\alpha = 0.9$, the annual savings are 7.3%, which is 1.8% points (20%) lower than for the reference case. Case 2 with a slightly lower spread level than the reference case ($\alpha = 0.99$) reveals the same level of savings as the reference case. Case 3 with a slightly higher spread level than the reference case ($\alpha = 1.01$) reveals annual savings that are 0.4% points (4%) above the reference case. In Case 4, the annual savings are 1.3% points (14%) higher than for the reference case. The results show two important aspects: (1) The variation of the spreads has a substantial effect on the annual savings that can be achieved through load shifting. This result is in line with the results of the single household analysis in Section 3.2.4. (2) The spread variations do not have a linear effect on the annual savings, i.e., increasing or decreasing the spread factor α does not have a symmetric effect on the result. This is a major difference to the results in Section 3.2.4, which are perfectly symmetric. The explanation behind this difference is that the analysis in this section builds on load-variable prices. A price curve with higher spreads leads to a steeper slope of the load-variable daily price function.

Higher spreads certainly lead to higher annual savings, but not continuously over multiple load shifts. As Figure 7.3 shows, the same load variation leads to higher price variations in this case. In case of the lower spreads, this effect turns around. The daily price curves get flatter, while spreads by definition also get smaller. I.e., this implies a stronger reduction of the realizable arbitrage opportunities.

As explained in Section 3.2.4 and 6.2.4, the increase of Distributed Energy Resources (DER) and RES (intermittent and non-dispatchable resources) will lead to an increase in volatility of market prices, since the output of these resources is intermittent and the supply from these resources impacts the spot market price. Thus, arbitrage potentials for DSSs (and load shifting potentials in general) will increase, if the share of renewable and distributed generation units increases.

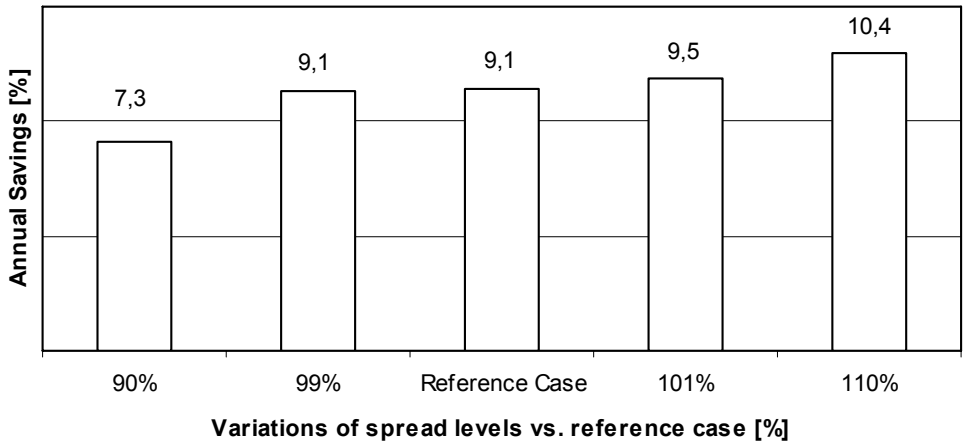

Figure 7.12: Results of the price spread analysis

7.5 Summary

This part of the thesis analyzed the economic impact of an increasingly large volume of installed capacity of DSSs at the end consumer level. The DSSs aim at arbitrage accommodation and charge at times of low prices and discharge during high-price periods. At the end consumer level, a DSS does not sell its energy back to the market, but it serves the end consumer's demand during peak-price periods. Prices are assumed flexible on an hourly basis. Additional load volumes due to charging DSSs cause a market price increase, and reduced load on the grid due to discharging the DSSs leads to decreasing market prices. The actual impact of load variations on the price is determined through daily price functions, which are derived as regression functions on historic data for the German market from 2007.

The analysis revealed that an optimally responsive load, i.e., a demand side that perfectly allocates its demand according to the derived daily price curves[4], would have achieved up to 24.8% savings on the annual electricity costs in the German electricity market in 2007. This value is a theoretical maximum, but it shows the enormous savings potential of demand responsiveness to compensate for fluctuations in the market. The literature review on DR programs showed that conventional DR programs can only achieve a fraction of these savings due to limited price elasticity degrees on the end consumer side. Therefore, this work investigates the net saving potential of DSSs on the end consumer level, which has the advantage of being a fully automated solution with minor technical constraints and, thus, high responsiveness. Disadvantageously, DSSs require significant investments and cause operational costs that need to be taken into account.

The economic analysis included the total costs of the DSSs. It revealed that such systems can realize about 36% of the maximal (theoretically possible) savings, i.e., about 9% savings on the annual electricity costs, if storage capacity costs are 100,000 EUR/MWh storage. In case of 500,000 EUR/MWh, about 5% savings on the annual electricity costs can be achieved. For each storage capacity cost level, the analyses calculated the optimal amount of storage capacity to install on the system. If the capacity installed is above or below this optimal value, the realizable savings decrease.

[4]Derived through a regression function on historic load and price data of the German electricity market in 2007; adjusted R^2 of the regression function is 0.8 (see Section 7.1.2).

If the capacity installed exceeds an upper bound, savings turn negative due to high capital costs that cannot be covered anymore. The optimal and the maximal value depend on the shape of the load and the price profiles of the market. In the analyzed case for Germany, the optimal value for the capacity to install is 4% of the weekly average load and the maximum capacity is 16%, if storage capacity costs are around 100,000 EUR/MWh. In case of 500,000 EUR/MWh, these values are 1% and 3%.

A sensitivity analysis of the reference case showed the strong impact of efficiency degree variations. E.g., a reduction of the storage efficiency by 10% would deteriorate the savings by 13%. Nevertheless, the overall most important parameter is the storage capacity costs (EUR/MWh), as it can be seen from the aforementioned figure.

As explained in the introduction of this part of the thesis, as well as in the related work discussion, increasing shares of RES will increase price volatility on the market, i.e., cause higher spreads. The spread variation analysis in this part of the work revealed similar results as in Section 3.2.4. A 10% increase of the average spread will increase the realizable savings by 1.3% points (14%) in comparison to the reference case. Similarly, a decrease of the spreads decreases the realizable savings. Thus, DSSs can mitigate the risk of supply fluctuations and price volatility effectively and therefore foster the integration of RES while reducing total costs for the end consumer.

7.5.1 Contribution to Scientific Literature

After reviewing the existing literature on market impacts through higher shares of RES and on the impact of DR programs on the electricity market, two main issues in the electricity sector became apparent. Firstly, increasing shares of RES will cause more volatility in electricity prices. Secondly, conventional DR programs are effective for peak load reductions, but they are not appropriate to let electricity demand follow supply from RES, since the reliably achieved elasticity is too low to compensate for fluctuations of RES. Furthermore, even RTP has little impact on the reduction of consumers' electricity costs in conventional DR programs that build on consumers reactions.

This work presents a model to estimate the value of an optimally responsive demand side, based on historic data for the German electricity market from 2007. In a second step, a model that builds its responsiveness on distributed electricity storage systems is presented. This model calculates the achievable savings for the consumer side that can be realized using optimally coordinated DSS. It takes the total costs of the storage systems into account and operates the storage devices as arbitrage-maximizing agents. It is shown that total costs of such a system will be lower than its benefits. Indeed, the analysis reveals significant savings for the consumer side, which are higher than savings achieved by conventional DR programs, even if unusually high price elasticity (below -0.5) is assumed. Additionally, the presented approach addresses both market issues identified in the literature review: Firstly, price-responsive DSSs decrease the market price volatility, since they operate as arbitrage agents. Increasing price volatility actually increases the profitability of DSSs. Secondly, the DSSs can make demand follow supply in a reliable manner through automated agents, if RTP reflects the current demand-supply-situation appropriately. I.e., in combination with the merit-order effect (Section 6.2.4), DSSs will effectively foster the integration of RES with low marginal costs.

This work complements the existing literature on DR programs by evaluating such programs when based on DSSs at the end consumer level. It continues the thought of implementing automated communication and control devices on the consumer side. Such devices help to let demand automatically follow supply to better integrate RES and to reduce critical peak loads without requiring the interaction and the behavioral change of the consumer. Consumers can systematically (automatically) adjust their load patterns according to real-time prices. Real-time prices mitigate a part of the risk (and the opportunity) of electricity supply to the consumer and DSSs help to manage the risk and to capture the opportunity.

7.5.2 Practical Relevance of the Findings

The model reveals that consumers would have had realized a substantial economic surplus from load shifting in Germany in 2007. Overall, up to 25% savings could have been achieved through load shifting under the given price curve assumptions (see beginning of Section 7.5). In the case of load shifting through storage systems, about 9% maximal savings could be realized due to capital and operational costs for the storage systems. Thus, the results of the model are relevant to regulators, consumers, utilities, and potentially investors.

Regulators can use the findings to create incentives for DSM programs that will lead to overall lower costs. The electricity systems could become more economic and more resource-efficient. Consumers can see the benefits and opportunities of flexible electricity prices in combination with DSM programs that help to reduce their electricity costs. Utilities can use the findings to create offers to their customers (tariffs, storage services, etc) and to evaluate alternatives to traditional asset investments. To not lose market shares in a long-term perspective, it might be a strategic advantage to shift from traditional control capacity (e.g., gas turbines) to DR programs that build on automated load control, which optionally include storage systems. For investors, the presented findings reveal first information on strategic investment opportunities into well-positioned utilities, new market entrants, and technology suppliers.

Chapter 8

Conclusions & Outlook

Distributed Storage Systems (DSSs) at the end consumer level have the potential to economically foster the integration of Renewable Energy Sources (RES) and Distributed Energy Resources (DER), if flexible electricity prices are provided to end consumers and storage costs further decrease. The DSSs provide demand-side flexibility by operating as arbitrage-maximizing agents. The analyses have shown that hourly flexible prices are most suitable[1] and that no less than 8 electricity prices per day should be provided. Storage costs must fall below 200-400 EUR/kWh to achieve profitable operations[2]. Both conditions have the potential to be satisfied in the future: As stated in §40 (3) EnWG, flexible tariffs must be available from 2011 onwards for end consumers in Germany (Federal Law Gazette, 2008). Storage costs are likely to further decrease during the next years due to increasing R&D efforts for and demand from Electric Vehicles (EVs). In a long-term perspective, used batteries from EVs could potentially serve stationary storage systems as low-cost storage components in the future. Overall, the economic analysis of DSSs at the end consumer level revealed a substantial cost reduction potential for the consumers under the given assumptions. The actually realizable savings for an end consumer depend on its individual load profile.

The trend of increasing shares of DER and especially RES, which can be observed in many countries, will lead to lower average market prices (merit-order effect) accompanied by higher market price volatility. Consumers will benefit from these market price fluctuations, if demand-side flexibility increases. The simulations and analyses within this research work have given first evidence that DSSs, which operate as autonomous Demand Response (DR) agents aiming at arbitrage accommodation, can economically capture a part of this potential. Indeed, increasing market price volatility will raise the profitability of such systems, which therefore economically support the integration of sources like wind and solar power.

The combination of results from different models presented in this thesis shows the economics of DSSs under price and load forecast uncertainty as well as under the condition of load-variable market prices. This research work presented three analytical models that investigate the influence of technical and economic parameters within and around DSSs.

[1] This would account in particular to Real-time pricing (RTP), but the only data available for the analyses were hourly flexible prices.

[2] The cost range reflects the dependence on other storage parameters, but the costs per storage capacity unit is a pivotal parameter. Further technical and economic storage parameters are provided in Part I and III of this work.

The first part of this thesis analyzed the economics of a single storage system on the grid. Such a system at the end consumer level does not impact the market price by its charge and discharge decisions and is therefore modeled as a price taker. The model addressed the research questions how a DSS influences the costs of a standard household (vs. a baseline case without a storage system) and which parameters have the greatest economic importance. For parameters of storage devices that are currently in a developmental stage, the linear optimization model resulted in a 17% reduction of total annual costs for a standard household in comparison to the baseline case without a storage system. The sensitivity analyses emphasize the outstanding impact of the costs per storage unit (EUR/kWh) and the highly sensitive impact of the efficiency degrees on the achievable benefits. Furthermore, the analyses show that an increase in market price volatility raises the profitability of the system and that hourly flexible prices are required to achieve a high level of profitability.

Part II presented a simulation model that analyzed the performance of DSSs under uncertainty. Instead of actual price and load data, the simulations used forecast data of different quality levels to derive the Charge-Discharge-Schedule (CDS) for a DSS. The obtained suboptimal schedules still delivered fairly robust economic results. The analyses addressed the research questions to what extent load and price forecast errors deteriorated the economics of DSSs and what level of cost reductions could be realized with available standard forecast methods. In conclusion, the system tolerates significant forecast errors while still operating close to the economic optimum. Even conservative assumptions regarding the forecast accuracy led to deviations of less than 15% from the optimum. The accuracies of available price and load forecast methods are sufficient to ensure economically beneficial operations of DSS. Overall, price forecast errors have a stronger negative impact on the economics of a DSS than load forecast errors. The key parameter of both price and load forecasts is the day-ahead Mean Absolute Percentage Error (MAPE) of the forecast.

The analysis of different scheduling algorithms showed that the choice of the best scheduling algorithms depends on the forecast characteristics. In case of a strong autocorrelation of price forecast errors, optimization algorithms deliver the best operation schedules for the DSS. In case of uncorrelated price forecast errors, the presented heuristic algorithm delivers better schedules. The linear optimization algorithm shows slightly better performance for forecasts with low MAPE, whereas the heuristic algorithms show a higher robustness in case of increasing forecast errors.

The model presented in the third part of this work took a market-wide perspective and modeled the impact that the aggregated charge and discharge volumes of multiple DSSs have on the electricity price. The underlying research questions were to estimate the cost reduction potential of a perfectly responsive demand side and to assess which share of this potential could be realized through DSSs. The analyses showed that the maximal cost reduction potential would have been 24.8% in Germany in 2007. The presented optimization model, which takes the total costs of a DSS into account, revealed that such systems can realize about 36% of the maximal cost reduction potential, i.e., about 9% savings on the annual electricity costs, if storage capacity costs are 100,000 EUR/MWh storage. Furthermore, the analysis results indicate for this case that the optimal volume for the capacity to install is 4% of the weekly average load and the maximum capacity is 16%.

8.1 Limitations of the Approach

All analysis and simulation models presented within this thesis simplify economic and technical interdependencies and constraints of the physical infrastructure and the energy markets in place. To a certain degree, the generality of the results is limited by several assumptions of the models.

All models exclude the investigation of transmission and distribution capacity constraints from their scope. Depending on the system's transmission constraints and the geographical distribution of the storage devices, real-world applications might have to take these constraints into account. Furthermore, all models build their analyses on load profiles of standard households. The standard household profiles represent the typical consumption of German households. Actual household profiles might vary from this profile and, thus, result in different level of realizable savings. Thirdly, all models use an hourly flexible electricity price curve. This price curve is an artificially derived price pattern that builds on the distribution of the wholesale market prices at the European Energy Exchange (EEX) in 2007 and has a weighted average electricity price of 0.20 EUR/kWh. I.e., also the price curve primarily reflects the situation on the German market, which makes the results of the study primarily applicable to markets that have a similar electricity load and price distribution as the German market.

Several critical reviews of the models challenged the presented results and provided further potential improvements and extensions for the models. Some of these aspects would further improve the economics of the basic linear optimization model in Part I, e.g., allowing the DSS to sell electricity back to the market or to provide services to the grid, others would decrease the resulting benefits, e.g., implementing price caps for the flexible consumer prices. A proposed enhancement to the forecast error simulation in Part II would be replacing the linear decrease of forecast accuracy over time with a more detailed function that is based on empirical values. In Part III, replacing the approximated daily price curves by actual merit-order curves from the EEX would strengthen the validity of the results. This enhancement would require the order book data of the EEX, which were not available for this study.

Overall, the presented combination of analyses reveals a first economically robust indication within the described assumptions that DSSs increase demand-side flexibility, decrease the consumers' costs for electricity supply, and foster the integration of RES and DER. Apart from the absolute cost reduction figures for the consumers, it is to emphasize that by no means the alternative, a rather traditional supply-side-oriented approach of installing more conventional control capacity, would integrate RES and DER at decreasing costs for the end consumers.

8.2 Further Research

The models in this thesis analyzed the saving potential through DSSs in three steps: (i) first on a household level without influencing the market price, (ii) then on the same household level but incorporating uncertainty of load and price forecasts when deriving the CDSs, (iii) and finally on a market-wide, aggregated level, where perfect coordination of distributed storage devices was assumed and therefore the aggregated storage capacity was treated as on large entity.

The coordination of distributed storage devices that operate autonomously is certainly a complex task. Thus, further research is needed regarding the market and

coordination mechanisms that incentivize or steer a DSS. Additionally interesting in this context is the question of the negative impact of insufficiently coordinated DSSs for both, the end consumer and the grid (operators). Another area of further research is the detailed integration of RES and DER through DSSs. E.g., the relation between installed capacity of renewable and distributed resources and the optimally installed storage capacity could be further investigated. A third area of further research are business models for the analyzed DSS. This field addresses the questions who owns and who operates the storage systems and who benefits to which degree from the realized savings. Since DSSs that aim at arbitrage accommodation require flexible prices, the design and analysis of new electricity tariffs from a consumer and a utility perspective will have high relevance. From the perspective of a storage system owner, which might be a consumer, a utility, or a third party, more detailed investment calculations will be of interest. E.g., conducting an investment appraisal for time periods of more than a year will further investigate the impact of capacity investments (e.g., sizing of individual storage system) on the absolute savings for a long-term perspective.

In the context of Smart Homes in combination with Smart Metering, load forecasting of households and other end consumer entities will become relevant. Smart Metering will provide the technical infrastructure for local, in-house data analysis of a consumer demand profile. In combination with sensor-equipped homes and learning algorithms, load forecasting of very small consumer units can be realized. Further research will have to investigate if the available methods are suitable or must be adapted for these situations and what forecast accuracies can be achieved with such methods.

Up to now, this research work has analyzed stationary storage systems. If grid-integrated EVs are included into an extension of the presented models, the temporal aspect of storage availability and other limiting factors become important. Overall, EVs have the potential to foster the development of DSSs substantially. First research results show that there could be huge storage capacity volumes available in parked EVs that could potentially be used for load shifting (arbitrage accommodation) or other services to the grid (Fluhr et al., 2010). Moreover, used batteries from EVs that must be replaced could be a source of economic storage capacity for stationary applications in future. EVs will typically have much higher performance requirements to a battery than a stationary battery that is used for arbitrage accommodation. When storage capacity becomes cheaper, more arbitrage accommodation could be realized and thus, RES and DER could be integrated more efficiently.

References

Aggarwal, S., Saini, L., and Kumar, A. (2009). Electricity price forecasting in deregulated markets: A review and evaluation. *International Journal of Electrical Power & Energy Systems*, 31(1):13–22.

Ahlert, K.-H. (2009a). Assessing the Economics of Distributed Storage Systems at the End Consumer Level. In *Proceedings of the 4th International Renewable Energy Storage Conference (IRES-4), 24.-25.11.*, Berlin.

Ahlert, K.-H. (2009b). Wirtschaftlichkeit dezentraler Stromspeicher-Systeme. *Solarzeitalter*, 21(4):31–37.

Ahlert, K.-H. and Block, C. (2010). Assessing the Impact of Price Forecast Errors on the Economics of Distributed Storage Systems. In *43rd Hawaii International Conference on System Science (HICSS-43), January 5-8*, Hawaii, USA.

Ahlert, K.-H. and Dinther, C. (2010). Robustness of Scheduling Algorithms for Distributed Storage Systems. In *Proceedings of the Multikonferenz Wirtschaftsinformatik (MKWI), 23.-25. Februar*, Göttingen, Germany (forthcoming).

Ahlert, K.-H. and van Dinther, C. (2008). Definition of an optimization model for scheduling electricity storage devices. In *Proceedings of Web 2008 - 7th Workshop on e-Business, December 13*, Paris, France.

Ahlert, K.-H. and van Dinther, C. (2009a). Estimating economic benefits of electricity storage at the end consumer level. In *Proceedings of 9. Internationale Tagung Wirtschaftsinformatik, 25.-27.2.*, pages 665–674, Wien, Austria.

Ahlert, K.-H. and van Dinther, C. (2009b). Sensitivity Analysis of the Economic Benefits from Electricity Storage at the End Consumer Level. In *Proceedings of the IEEE PowerTech Conference, 28.6.-2.7.*, Bucharest, Romania.

Albadi, M. H. and El Saadany, E. F. (2007). Demand response in electricity markets: an overview. In *IEEE Power Engineering Society General Meeting, 2007*, pages 1–5.

Alt, J. T., Anderson, M. D., and Jungst, R. G. (1997). Assessment of utility side cost savings from battery storage. *IEEE Transactions on Power Systems*, 12(3):1112–1120.

Amjady, N. (2006). Day-ahead price forecasting of electricity markets by a new fuzzy neural network. *IEEE Transactions on Power Systems*, 21(2):887–896.

Anderson, M. D. and Lo, C. H. (1999). Economic dispatch and optimal sizing of battery energy storage systems in utility load-leveling operations. *IEEE Transactions on Energy Conversion*, 14(3):824–829.

Ashok, S. and Banerjee, R. (2001). An optimization mode for industrial load management. *IEEE Transactions on Power Systems*, 16(4):879–884.

Aubin, C., Fougere, D., Husson, E., and Ivaldi, M. (1995). Real-Time Pricing of Electricity for Residential Customers: Econometric Analysis of an Experiment. *Journal of Applied Econometrics*, 10:S171–S191.

Barton, J. P. and Infield, D. G. (2004). Energy storage and its use with intermittent renewable energy. *IEEE Transactions on Energy Conversion*, 19(2):441–448.

Bashir, Z. A. and El-Hawary, M. E. (2009). Applying Wavelets to Short-Term Load Forecasting Using PSO-Based Neural Networks. *IEEE Transactions on Power Systems*, 24(1):20–27.

Bathurst, G. N. and Strbac, G. (2003). Value of combining energy storage and wind in short-term energy and balancing markets. *Electric Power Systems Research*, 67:1–8.

Baumann, P. D. (1992). Energy conservation and environmental benefits that may be realized from superconducting magnetic energy storage. *IEEE Transactions on Energy Conversion*, 7(2):253–259.

BDEW (2008). Energieverbrauch in Deutschland 2006. Technical report, Bundesverband der Energie- und Wasserwirtschaft e.V. (BDEW) (The German Energy and Water Association).

Benini, M., Marracci, M., Pelacchi, P., and Venturini, A. (2002). Day-ahead market price volatility analysis in deregulated electricity markets. In *IEEE Power Engineering Society Summer Meeting*, volume 3, pages 1354–1359.

Bodach, M. (2006). *Energiespeicher im Niederspannungsnetz zur Integration dezentraler, fluktuierender Energiequellen*. PhD thesis, Technische Universität Chemnitz.

Boisvert, R. N., Cappers, P., Goldman, C., Neenan, B., and Hopper, N. (2007). Customer Response to RTP in Competitive Markets: A Study of Niagara Mohawk's Standard Offer Tariff. *The Energy Journal*, 28(1):53–74.

Bompard, E., Ma, Y., Napoli, R., Abrate, G., and Ragazzi, E. (2007). The impacts of price responsiveness on strategic equilibrium in competitive electricity markets. *International Journal of Electrical Power & Energy Systems*, 29(5):397–407.

Borenstein, S. (2002). The trouble with electricity markets: understanding California's restructuring disaster. *Journal of economic perspectives*, 16(1):191–211.

Borenstein, S. (2005). The Long-Run Efficiency of Real-Time Electricity Pricing. *The Energy Journal*, 26(3):93–116.

Braithwait, S. (2000). Residential TOU Price Response in the Presence of Interactive Communication Equipment. In Faruqui, A. and Eakin, K., editors, *Priceing in Competitive Electricity Markets*, pages 359–373. Kluwer Academic Publishers.

Brooks, C. (2008). *Introductory Econometrics for Finance*. Cambridge University Press, second edition.

Bunn, D. (2000). Forecasting loads and prices in competitive power markets. *Proceedings of the IEEE*, 88(2):163–169.

Campbell, J. Y., Lo, A. W., and MacKinlay, A. C. (1997). *The Econometrics of Financial Markets*. Princeton University Press.

Caves, D. (1984). Consistency of residential customer response in time-of-use electricity pricing experiments. *Journal of Econometrics*, 26(1-2):179–203.

Chacra, F. A., Bastard, P., Fleury, G., and Clavreul, R. (2005). Impact of energy storage costs on economical performance in a distribution substation. *IEEE Transactions on Power Systems*, 20(2):684–691.

Chang, C. S. and Yi, M. (1998). Real-Time Pricing Related Short-Term Load Forecasting. In *International Conference on Energy Management and Power Delivery*, volume 2, pages 411–416.

Chen, H., Cong, T. N., Yang, W., Tan, C., Li, Y., and Ding, Y. (2009). Progress in electrical energy storage system: A critical review. *Progress in Natural Science*, 19(3):291–312.

Chowdhury, B. H. and Rahman, S. (1988). Analysis of interrelationships between photovoltaic power and battery storage for electric utility load management. *IEEE Transactions on Power Systems*, 3(3):900–907.

Chupka, M. (2003). Designing Effective Renewable Markets. *The Electricity Journal*, 16(4):46–57.

Clark, W. and Isherwood, W. (2004). Distributed generation: remote power systems with advanced storage technologies. *Energy Policy*, 32:1573–1589.

Coles, L. R., Chapel, S. W., and Iamucci, J. J. (1995). Valuation of modular generation, storage, and targeted demand-side management. *IEEE Transactions on Energy Conversion*, 10(1):182–187.

Comnes, A. G., Kahn, E., Pignone, C., and Warren, M. (1988). An integrated economic analysis of commercial thermal energy storage. *IEEE Transactions on Power Systems*, 3(4):1717–1722.

Conejo, A. J., Contreras, J., Espinola, R., and Plazas, M. A. (2005). Forecasting electricity prices for a day-ahead pool-based electric energy market. *International Journal of Forecasting*, 21(3):435–462.

Cook, G. M., Spindler, W. C., and Grefe, G. (1991). Overview of battery power regulation and storage. *IEEE Transactions on Energy Conversion*, 6(1):204–209.

Cuaresma, J. C., Hlouskova, J., Kossmeier, S., and Obersteiner, M. (2004). Forecasting electricity spot-prices using linear univariate time-series models. *Applied Energy*, 77(1):87–106.

Darby, S. (2006). The effectiveness of feedback on energy consumption. Technical report, Environmental Change Institute, University of Oxford.

Daryanian, B., Bohn, R. E., and Tabors, R. D. (1991). An experiment in real time pricing for control of electric thermal storage systems. *IEEE Transactions on Power Systems*, 6(4):1356–1365.

Delarue, E. and Dhaeseleer, W. (2008). Adaptive mixed-integer programming unit commitment strategy for determining the value of forecasting. *Applied Energy*, 85(4):171–181.

DENA (2005). Energiewirtschaftliche Planung für die Netzintegration von Windenergie in Deutschland an Land und Offshore bis zum Jahr 2020. Technical report, Deutsche Energie-Agentur GmbH (DENA).

DENA (2008). Kurzanalyse der Kraftwerks- und Netzplanung in Deutschland bis 2020 (mit Ausblick auf 2030). Technical report, Deutsche Energie-Agentur GmbH (DENA).

Divya, K. C. and Østergaard, J. (2009). Battery energy storage technology for power systems-an overview. *Electric Power Systems Research*, 79(4):511–520.

Durbin, J. and Watson, G. S. (1950). Testing for serial correlation in least squares regression. I. *Biometrika*, 37:409–428.

EEX (2007). Market data. European Energy Exchange, http://www.eex.com/en/Download/Market%20Data (last visit: 04/22/2009).

ENTSOE (2007). Hourly consumption profiles. European Network of Transmission System Operators for Electricity - ENTSOE (former Union for the Coordination of Transmission of Electricity - UCTE), http://www.entsoe.eu/resources/data/consumption/ (last visit: 07/11/2009).

Espinoza, M., Joye, C., Belmans, R., and Demoor, B. (2005). Short-term load forecasting, profile identification, and customer segmentation: A methodology based on periodic time series. *IEEE Transactions on Power Systems*, 20(3):1622–1630.

Eto, J. (1996). The Past, the Present, and Future of U.S. Utility Demand-Side Management Programs. Technical report, Ernest Orlando Lawrence Berkeley National Laboratory.

European Union (2008). Overview of activities in the energy sector. http://europa.eu/pol/ener/overview_en.htm (last visit: 04/22/2009).

Exarchakos, L., Leach, M., and Exarchakos, G. (2009). Modelling electricity storage systems management under the influence of demand-side management programmes. *International Journal of Energy Research*, 33(1):62–76.

Eyer, J. M., Iannucci, J. J., and Corey, G. P. (2004). Energy storage benefits and market analysis handbook: a study for the DOE Energy Storage Systems Program. *Prepared by Sandia National Laboratories*.

Faruqui, A. and George, S. (2002). The value of dynamic pricing in mass markets. *The Electricity Journal*, 15(6):45–55.

Faruqui, A. and Malko, J. R. (1983). The residential demand for electricity by time-of-use: a survey of twelve experiments with peak load pricing. *Energy (Oxford)*, 8(10):781–795.

Federal Law Gazette (2008). Law for liberalization of metering in electricity and gas grids. http://www.bgblportal.de/BGBL/bgbl1f/ bgbl108s1790.pdf (last visit: 04/22/2009).

FERC (2006). Assessment of Demand Response and Advanced Metering. Technical report, Federal Energy Regulatory Commission (FERC).

Ferreira, L. A. F. M. (1992). Short-term scheduling of a pumped storage plant. *IEE Proceedings-C*, 139:521–528.

Filippini, M. (1995). Swiss residential demand for electricity by time-of-use. *Resource and Energy Economics*, 17(3):281–290.

Fluhr, J., Ahlert, K.-H., and Weinhardt, C. (2010). A Stochastic Model for Simulating the Availability of Electric Vehicles to the Power Grid. In *43rd Hawaii International Conference on System Science (HICSS-43), January 5-8*, Hawaii, USA.

Galus, M. D. and Andersson, G. (2009). Integration of plug-in hyprid electric vehilces into energy networks. In *Proceedings of the IEEE PowerTech (28.6.-2.7.)*.

German government (2008). Energy for the future. http://www.bundesregierung.de/Webs/Breg/EN/Issues/Energyforthefuture/energy-for-the-future.html (last visit: 04/22/2009).

Graves, F., Jenkin, T., and Murphy, D. (1999). Opportunities for electricity storage in deregulating markets. *The Electricity Journal*, 12(8):46–56.

Hahn, G. J. and Shapiro, S. S. (1968). *Statistical models in engineering*. John Wiley & Sons.

Harty, F. R., Depenbrock, F., Ward, P. W., and Shectman, D. L. (1994). Options in energy storage technologies. *Electricity Journal*, 7(6):21–26.

Heffner, G. C. (2002). Configuring Load as a resource for competitive electricity markets–Review of demand response programs in the U.S. and around the world. In *Proceedings of the 14th Annual Conference of the Electric Power Supply Industry (CEPSI), Fukuoka*.

Hobbs, B. (1998). Artificial neural networks for short-term energy forecasting: Accuracy and economic value. *Neurocomputing*, 23(1-3):71–84.

Hobbs, B. F., Jitprapaikulsarn, S., Konda, S., Chankong, V., Loparo, K. A., and Maratukulam, D. J. (1999). Analysis of the value for unit commitment of improved load forecasts. *IEEE Transactions on Power Systems*, 14(4):1342–1348.

Holland, S. P. and Mansur, E. T. (2006). The short-run effects of time-varying prices in competitive electricity markets. *The Energy Journal*, 27(4):127–155.

Hu, Z., Yang, L., Wang, Z., Gan, D., Sun, W., and Wang, K. (2008). A game-theoretic model for electricity markets with tight capacity constraints. *International Journal of Electrical Power and Energy Systems*, 30(3):207–215.

Hwang, J. C. (2001). Assessment of air condition load management by load survey in Taipower. *Power Systems, IEEE Transactions on*, 16(4):910–915.

Hyndman, R. J. and Koehler, A. B. (2006). Another look at measures of forecast accuracy. *International Journal of Forecasting*, 22(4):679–688.

IEEE Committee Report (1980). Load Forecast Bibliography Phase I. *IEEE Transactions on Power Apparatus and Systems*, 99(1):53–58.

Ilic, M., Black, J. W., and Watz, J. L. (2002). Potential benefits of implementing load control. In *IEEE Power Engineering Society Winter Meeting*, volume 1, pages 177–182.

Jamasb, T. and Pollitt, M. (2005). Electricity market reform in the european union: Review of progress toward liberalization & integration. *The Energy Journal*, 26:11–41.

Jenkins, D., Fletcher, J., and Kane, D. (2008). Model for evaluating impact of battery storage on microgeneration systems in dwellings. *Energy Conversion and Management*, 49(8):2413–2424.

Jensen, S. G. and Skytte, K. (2003). Simultaneous attainment of energy goals by means of green certificates and emission permits. *Energy Policy*, 31(1):63–71.

Jewell, W., Gomatom, P., Bam, L., and Kharel, R. (2004). Evaluation of distributed electric energy storage and generation. Technical report, Power System Engineering Research Center.

Joskow, P. L. (2000). Deregulation and Regulatory Reform in the U.S. Electric Power Section. Technical report, Massachusetts Institute of Technology, Center for Energy and Environmental Policy Research, Working Paper 00-003.

Jung, K. H., Kim, H., and Rho, D. (1996). Determination of the installation site and optimal capacity of the battery energy storage system for load leveling. *IEEE Transactions on Energy Conversion*, 11(1):162–167.

Kandil, M. S., Farghal, S. A., and Hasanin, N. E. (1990). Economic assessment of energy storage options in generation expansion planning. *Generation, Transmission and Distribution, IEE Proceedings C*, 137(4):298–306.

Kempton, W. and Kubo, T. (2000). Electric-drive vehicles for peak power in Japan. *Energy Policy*, 28(1):9–18.

Kempton, W. and Letendre, S. E. (1997). Electric vehicles as a new power source for electric utilities. *Transportation Research Part D: Transport and Environment*, 2(3):157–175.

Kempton, W. and Tomic, J. (2005). Vehicle-to-grid power fundamentals: Calculating capacity and net revenue. *Journal of Power Sources*, 144(1):268–279.

Kempton, W., Tomic, J., Letendre, S., Brooks, A., and Lipman, T. (2001). Vehicle-to-grid power: battery, hybrid, and fuel cell vehicles as resources for distributed electric power in California. Technical report, University of Delaware.

Kim, C.-I., Yu, I.-K., and Song, Y. H. (2002). Prediction of system marginal price of electricity using wavelet transform analysis. *Energy Conversion and Management*, 43(14):1839–1851.

King, C. S. and Chatterjee, S. (2003). Predicting California Demand Response. *Public Utilities Fortnightly*, pages 27–32.

Kirkham, H. and Klein, J. (1983). Dispersed storage and generation impacts on energy management systems. *IEEE Transactions on Power Apparatus and Systems*, PAS-102(2):339–345.

Kirschen, D. S., Strbac, G., Cumperayot, P., and Mendes, D. P. (2000). Factoring the elasticity of demand in electricity prices. *IEEE Transactions on Power Systems*, 15(2):612–617.

Klobasa, M. and Ragwitz, M. (2006). Demand Response - A new Option for Wind Integration. In *Proceedings of the European Wind Energy Conference & Exhibition (EWEC) (27.2.-2.3.), Athens*, pages 85–89.

Kondoh, J., Ishii, I., Yamaguchi, H., Murata, A., Otani, K., Sakuta, K., Higuchi, N., Sekine, S., and Kamimoto, M. (2000). Electrical energy storage sytems for energy networks. *Energy Conversion & Management*, 41:1863–1874.

Konjic, T., Miranda, V., and Kapetanovic, I. (2005). Fuzzy inference systems applied to LV substation load estimation. *IEEE Transactions on Power Systems*, 20(2):742–749.

Korpaas, M. (2004). *Distributed Energy Systems with Wind Power and Energy Storage*. PhD thesis, Norwegian University of Science and Technology.

Korpaas, M., Holen Arne, T., and Hildrum, R. (2003). Operation and sizing of wind power plants in a market system. *Electrical Power and Energy Systems*, 25(8):599–606.

Kottick, D. and Blau, M. (1993). Operational and economic benefits of battery energy storage plants. *International Journal of Electrical Power & Energy Systems*, 15(6):345–349.

Kottick, D., Blau, M., and Edelstein, D. (1993). Battery energy storage for frequency regulation in an island power system. *IEEE Transactions on Energy Conversion*, 8(3):455–459.

Kowal, J. and Sauer, D. U. (2007). Detailed cost calculations for stationary battery storage systems. In *Second International Renewable Energy Storage Conference (IRES II), (November 19, Bonn, Germany)*.

Laffont, J. J. (1977). More on prices vs. quantities. *The Review of Economic Studies*, 44(1):177–182.

Lee, J.-K., Park, J.-B., Shin, J.-R., and Lee, K. Y. (2005). A system marginal price forecasting based on an artificial neural network adapted with rough set theory. In *IEEE Power Engineering Society General Meeting*, volume 1, pages 528–533.

Lee, K. Y., Cha, Y. T., and Park, J. H. (1992). Short-term load forecasting using an artificial neural network. *IEEE Transactions on Power Systems*, 7(1):124–132.

Lee, T.-Y. (1992). The effect of pumped storage and battery energy storage systems on hydrothermal generation coordination. *IEEE Transactions on Energy Conversion*, 7(4):631–637.

Lee, T.-Y. and Chen, N. (1993). Optimal capacity of the battery energy storage system in a power. *IEEE Transaction on Energy Conversion*, 8(4):667–673.

Lee, T. Y. and Chen, N. (1994). Effect of the battery energy storage system on the time-of-use rates industrial customers. *IEE Proceedings - Generation, Transmission, and Distribution*, 141(5):521–528.

Lee, T.-Y. and Chen, N. (1995). Determination of optimal contract capacities and optimal sizes of battery energy storage systems for time-of-use rates industrial customers. *IEEE Transactions on Energy Conversion*, 10(3):562–568.

Li, C. and Wang, S. (2006). Next-Day Power Market Clearing Price Forecasting Using Artificial Fish-Swarm Based Neural Network. *Lecture Notes in Computer Science*, 3972:1290–1295.

Liu, K., Subbarayan, S., Shoults, R. R., Manry, M. T., Kwan, C., Lewis, F. I., and Naccarino, J. (1996). Comparison of very short-term load forecasting techniques. *IEEE Transactions on Power Systems*, 11(2):877–882.

Lund, H. and Kempton, W. (2008). Integration of renewable energy into the transport and electricity sectors through V2G. *Energy Policy*, 36(9):3578–3587.

Mahmoud, A. A., Ortmeyer, T. H., and Reardon, R. E. (1981). Load Forecasting Bibliography Phase II. *IEEE Transactions on Power Apparatus and Systems*, 100(7):3217–3220.

Maly, D. K. and Kwan, K. S. (1995). Optimal battery energy storage system (BESS) charge scheduling with dynamic programming. *IEE Proceedings-Science, Measurement and Technology*, 142(6):453–458.

Martin, K. (2004). Thought Experiment - How PV Reduces Wholesale Power Prices in New England. *PHOTON International*, (December):38–41.

Metaxiotis, K. (2003). Artificial intelligence in short term electric load forecasting: a state-of-the-art survey for the researcher. *Energy Conversion and Management*, 44(9):1525–1534.

Misiorek, A., Trueck, S., and Weron, R. (2006). Point and interval forecasting of sport electricity prices. *The Berkeley Electronic Press*, 10(3).

Moghram, I. and Rahman, S. (1989). Analysis and evaluation of five short-term load forecasting techniques. *IEEE Transactions on Power Systems*, 4(4):1484–1491.

Nazarko, J. and Zalewski, W. (1999). The fuzzy regression approach to peak load estimation in power distribution systems. *IEEE Transactions on Power Systems*, 14(3):809–814.

Neubarth, J., Woll, O., Weber, C., and Gerecht, M. (2006). Beeinflussung der Spotmarktpreise durch Windstromerzeugung. *Energiewirtschaftliche Tagesfragen*, 56(7):42–45.

Ng'uni, A. and Tuan, L. A. (2006). Interruptible Load and Demand Response: Worldwide Picture and the Situation in Sweden. In *Power Symposium, 2006. NAPS 2006. 38th North American*, pages 121–127.

NIEIR (2007). The own-price elasticity of demand for electricity in NEM regions. Technical report, National Institute of Economic and Industry Research (NIEIR).

Nieuwenhout, F. D. J., Hommelberg, M. P. F., Schaeffer, G. J., Kester, J. C. P., and Visscher, K. (2006). Feasibility of distributed electricity storage. *International Journal of Distributed Energy Resources*, 2(4):307–323.

Nogales, F. J., Contreras, J., Conejo, A. J., and Espinola, R. (2002). Forecasting next-day electricity prices by time series models. *IEEE Power Engineering Review*, 22(3):58.

Ortega-Vazquez, M. A. and Kirschen, D. S. (2006). Economic impact assessment of load forecast errors considering the cost of interruptions. In *IEEE Power and Energy Society General Meeting*, pages 8 pp.+.

Pahasa, J. and Theera-Umpon, N. (2007). Short-term load forecasting using wavelet transform and support vector machines. In *International Power Engineering Conference (IPEC)*, pages 47–52.

Pahasa, J. and Theera-Umpon, N. (2008). Cross-substation short term load forecasting using support vector machine. In *5th International Conference on Electrical Engineering/Electronics, Computer, Telecommunications and Information Technology (ECTI-CON)*, volume 2, pages 953–956. IEEE.

Park, D. C., El-Sharkawi, M. A., Marks, R. J., Atlas, L. E., and Damborg, M. J. (1991). Electric load forecasting using an artificial neural network. *IEEE Transactions on Power Systems*, 6(2):442–449.

Patrick, R. H. and Wolak, F. A. (2001). Estimating the customer-level demand for electricity under real-time market prices. Technical report, Working Paper 8213, National Bureau of Economic Research.

Pecas Lopes, J. A., Soares, F. J., and Rocha Almeida, P. M. (2009). Identifying management procedures to dealwith connection of electric vehicles in the grid. In *Proceedings of the IEEE PowerTech (28.6.-2.7.)*.

Poonpun, P. and Jewell, W. T. (2008). Analysis of the cost per kilowatt hour to store electricity. *IEEE Transactions on Energy Conversion*, 23(2):529–534.

Ranaweera, D. K., Karady, G. G., and Farmer, R. G. (1997). Economic impact analysis of load forecasting. *IEEE Transactions on Power Systems*, 12(3):1388–1392.

Rau, N. S. and Short, W. D. (1996). Opportunities for the integration of intermittent renewable resources into networks using existing storage. *IEEE Transactions on Energy Conversion*, 11(1):181–187.

Rau, N. S. and Taylor, B. (1998). A central inventory of storage and other technologies to defer distribution upgrades - optimization and economics. *IEEE Transactions on Power Delivery*, 13(1):194–202.

Reckrodt, R. C., Anderson, M. D., and Kluczny, R. M. (1990). Economic models for battery energy strorage: Improvements for existing methods. *IEEE Transactions on Energy Conversion*, 5(4):659–665.

Rehtanz, C. (1999). Systemic use of multifunctional smes in electric power systems. *IEEE Transactions on Power Systems*, 14(4):1422–1427.

Ribeiro, P. F., Johnson, B. K., Crow, M. L., Arsoy, A., and Liu, Y. (2001). Energy storage systems for advanced power applications. *Proceedings of the IEEE*, 89(12):1744–1756.

Sáenz de Miera, G., del Río González, P., and Vizcaíno, I. (2008). Analysing the impact of renewable electricity support schemes on power prices: The case of wind electricity in spain. *Energy Policy*, 36(9):3345–3359.

Sargunaraj, S. and Gupta, S. (1997). Short-term load forecasting for demand side management. *IEE Proceedings. Generation, Transmission and Distribution*, 144(1):68–74.

Sauer, D. U. (2007). Optionen zur Speicherung elektrischer Energie in Energieversorgungssystemen mit regenerativer Stromerzeugung. *Kooperationsforum PV - Elektrische Energiespeicher im Niederspannungsnetz*.

Schoenung, S. M. and Burns, C. (1996). Utility energy storage applications studies. *IEEE Transactions on Energy Conversion*, 11(3):658–665.

Schoenung, S. M. and Eyer, J. (2005). Benefit and cost comparison of energy storage technologies for three emerging value propositions. In *EESAT*.

Schoenung, S. M. and Hassenzahl, W. V. (2003). Long-versus short-term energy storage technologies analysis a life-cycle cost study. *Prepared by Sandia National Laboratories*.

Sensfuss, F., Ragwitz, M., and Genoese, M. (2008). The merit-order effect: A detailed analysis of the price effect of renewable electricity generation on spot market prices in Germany. *Energy Policy*, 36(8):3086–3094.

Setiawan, E. A. (2007). *Concept and Controllability of Virtual Power Plant*. PhD thesis, University of Kassel, Germany.

Shahidehpour, M., Yamin, H., and Li, Z. (2002). *Market operations in electric power systems: forecasting, scheduling, and risk management*. Wiley-IEEE Press.

Sioshansi, R., Denholm, P., Jenkin, T., and Weiss, J. (2009). Estimating the value of electricity storage in PJM: Arbitrage and some welfare effects. *Energy Economics*, 31(2):269–277.

Sioshansi, R. and Short, W. (2009). Evaluating the impacts of real-time pricing on the usage of wind generation. *IEEE Transactions on Power Systems*, 24(2):516–524.

Sobieski, D. W. and Bhavaraju, M. P. (1985). An economic assessment of battery storage in electric utility systems. *IEEE Transactions on Power Apparatus and Systems*, 104(12):3453–3459.

Soliman, S. A., Helal, I., and Youssef, A. M. (2007). Electric load management using electricity tariff algorithm. *International Journal of Emerging Electric Power Systems*, 8(5).

Spees, K. and Lave, L. (2007a). Demand response and electricity market efficiency. *The Electricity Journal*, 20(3):69–85.

Spees, K. and Lave, L. (2007b). Impacts of Responsive Load in PJM: Load Shifting and Real Time Pricing. Technical report, Carnegie Mellon Electricity Industry Center, Working Paper CEIC-07-02, http://www.cmu.edu/electricity.

Spees, K. and Lave, L. (2008). Impacts of Responsive Load in PJM: Load Shifting and Real Time Pricing. *The Energy Journal*, 29(2):101–122.

Strbac, G., Farmer, E. D., and Cory, B. J. (1996). Framework for the incorporation of demand-side in a competitive electricity market. *Generation, Transmission and Distribution, IEE Proceedings-*, 143(3):232–237.

Su, W.-F. and Huang, S.-J. (2001). Economic analysis for demand-side hybrid photovoltaic and battery energy storage system. *IEEE Transactions on Industry Applications*, 37(1):171–176.

Sullivan, R. L. (1982). Simulating central battery storage using a levelized incremental cost method. *IEEE Transactions on Power Apparatus and Systems*, 101(9):3322–3327.

Tam, K.-S. and Kumar, P. (1990). Impact of superconductive magnetic energy storage on electric power transmission. *IEEE Transactions on Energy Conversion*, 5(3):501–511.

Teisberg, T. J., Weiher, R. F., and Khotanzad, A. (2005). The economic value of temperature forecasts in electricity generation. *Bulletin of the American Meteorological Society*, 86(12):1765–1771.

Ter-Gazarian, A. (1994). *Energy Storage for Power Systems*, volume 6 of *IEE energy series*. The Institution of Engineering and Technology, London.

USDE (2006). Benefits of Demand Response in Electricity Markets and Recommendations for Achieving Them. Technical report, United States Department of Energy (USDE).

VDEW (2006). Standard household load profiles. Technical report, Verband der deutschen Elektrizitätswirtschaft e.V. (VDEW) (Association of the German Electricity Industry).

Vosen, S. R. and Keller, J. O. (1999). Hybrid energy storage systems for stand-alone electric power systems: optimization of system performance and cost through control strategies. *International Journal of Hydrogen Energy*, 24:1139–1156.

Walawalkar, R., Apt, J., and Mancini, R. (2007). Economics of electric energy storage for energy arbitrage and regulation in New York. *Energy Policy*, 35(4):2558–2568.

Wang, J., Redondo, N. E., and Galiana, F. D. (2003). Demand-side reserve offers in joint energy/reserve electricity markets. *IEEE Transactions on Power Systems*, 18(4):1300–1306.

Weissbach, R. S., Karady, G. G., and Farmer, R. G. (1999). Dynamic voltage compensation on distribution feeders using flywheel energy storage. *IEEE Transactions on Power Delivery*, 14(2):465–471.

Weitzman, M. L. (1974). Prices vs. quantities. *The Review of Economic Studies*, 41(4):477–491.

Weron, R. and Misiorek, A. (2005). Forecasting spot electricity prices with time series models. In *Proceedings of the international conference on the European electricity market EEM, Lodz, Poland, 10-12 May*.

Worawit, T. and Wanchai, C. (2002). Substation short term load forecasting using neural network with genetic algorithm. In *TENCON '02. Proceedings. 2002 IEEE Region 10 Conference on Computers, Communications, Control and Power Engineering*, volume 3, pages 1787–1790. IEEE.

Wu, K., Kato, T., Yokomizu, Y., Okamoto, T., Goto, M., and Suzoki, Y. (2002). Economic Value of the Inverter in Residence-Use PV System Applied for Electricity Storage at Night. *IEEE Power Engineering Society Winter Meeting*.

Yau, T., Walker, L. N., Graham, H. L., Gupta, A., and Raithel, R. (1981). Effects of battery storage devices on power system dispatch. *IEEE Transactions on Power Apparatus and Systems*, PAS-100(1):375–383.

Yun, Z., Quan, Z., Caixin, S., Shaolan, L., Yuming, L., and Yang, S. (2008). RBF Neural Network and ANFIS-Based Short-Term Load Forecasting Approach in Real-Time Price Environment. *IEEE Transactions on Power Systems*, 23(3):853–858.

Zhai, D., Breipohl, A. M., Lee, F. N., and Adapa, R. (1994). The effect of load uncertainty on unit commitment risk. *IEEE Transactions on Power Systems*, 9(1):510–517.

Appendix A

Derivation of Storage Depreciation Costs

For each timeslot t, the sum of storage depreciations paid for the discharged volume until t accords to the investment cost divided by the expected number of nominal cycles in timeslot t. I.e., the average depreciation rate per discharged capacity unit should equal the depreciation rate for the in timeslot t expected number of charge cycles.

$$\frac{\sum^{t} paid\ depreciations}{\sum^{t} discharged\ capacity} \stackrel{!}{=} \frac{investment\ cost}{expected\ nominal\ cycles}$$

Using the mathematical notations defined in Section 3.2.2 instead of the verbal formulation above, one obtains the following equation:

$$\frac{\sum_{t'=1}^{t} K_{t'}^{storage\_depreciation}}{\hat{q}_t} = \frac{C \cdot \kappa}{\gamma_t}$$

$$\Leftrightarrow \qquad K_t^{storage\_depreciation} = \hat{q}_t \cdot \frac{C \cdot \kappa}{\gamma_t} - \sum_{t'=1}^{t-1} K_{t'}^{storage\_depreciation}$$

$$\text{Simplification:} \qquad K_t^{storage\_depreciation} = C \cdot \kappa \cdot \left(\frac{\hat{q}_t}{\gamma_t} - \frac{\hat{q}_{t-1}}{\gamma_{t-1}} \right)$$

By definition, the storage depreciation cost and the accumulated discharge volume in timeslot 0 equal 0:

$$K_0^{storage\_depreciation} := 0 \Rightarrow \sum_{t'=1}^{t} K_{t'}^{storage\_depreciation} = \sum_{t'=0}^{t} K_{t'}^{storage\_depreciation}$$

$$\hat{q}_0 := 0$$

The following equation will now be proved by induction.

$$\hat{q}_t \cdot \frac{C \cdot \kappa}{\gamma_t} - \sum_{t'=1}^{t} K_{t'}^{storage\_depreciation} = \left(\frac{\hat{q}_t}{\gamma_t} - \frac{\hat{q}_{t-1}}{\gamma_{t-1}} \right)$$

For $t = 1$:
$$C \cdot \kappa \cdot \left(\frac{\hat{q}_1}{\gamma_1} - \frac{\hat{q}_0}{\gamma_0} \right) = \hat{q}_1 \cdot \frac{C \cdot \kappa}{\gamma_1} - \sum_{t'=0}^{1-1} K_{t'}^{storage\_depreciation}$$

$\Leftrightarrow$
$$C \cdot \kappa \cdot \left(\frac{\hat{q}_1}{\gamma_1} - \frac{0}{\gamma_0} \right) = C \cdot \kappa \cdot \frac{\hat{q}_1}{\gamma_1} - 0$$

Thus, the identity of the original equation and the simplified equation has been proven for t. It remains to prove the identity for $t + 1$:

For $t + 1$:

$$C \cdot \kappa \cdot \left(\frac{\hat{q}_{t+1}}{\gamma_{t+1}} - \frac{\hat{q}_t}{\gamma_t} \right) = \hat{q}_{t+1} \cdot \frac{C \cdot \kappa}{\gamma_{t+1}} - \sum_{t'=0}^{t+1-1} K_{t'}^{storage\_deprecation}$$

$$\Leftrightarrow \quad C \cdot \kappa \left(\frac{\hat{q}_{t+1}}{\gamma_{t+1}} - \frac{\hat{q}_t}{\gamma_t} \right) = C \cdot \kappa \cdot \frac{\hat{q}_{t+1}}{\gamma_{t+1}} - K_t^{storage\_depreciation} - \sum_{t'=0}^{t-1} K_{t'}^{storage\_depreciation}$$

$$\Leftrightarrow \quad C \cdot \kappa \left(\frac{\hat{q}_{t+1}}{\gamma_{t+1}} - \frac{\hat{q}_t}{\gamma_t} \right) = C \cdot \kappa \cdot \frac{\hat{q}_{t+1}}{\gamma_{t+1}} - \left(C \cdot \kappa \cdot \frac{\hat{q}_t}{\gamma_t} - \sum_{t'=0}^{t-1} K_{t'}^{storage\_depreciation} \right) - \sum_{t'=0}^{t-1} K_{t'}^{storage\_depreciation}$$

$$\Leftrightarrow \quad C \cdot \kappa \left(\frac{\hat{q}_{t+1}}{\gamma_{t+1}} - \frac{\hat{q}_t}{\gamma_t} \right) = C \cdot \kappa \cdot \frac{\hat{q}_{t+1}}{\gamma_{t+1}} - C \cdot \kappa \cdot \frac{\hat{q}_t}{\gamma_t} + \sum_{t'=0}^{t-1} K_{t'}^{storage\_depreciation} - \sum_{t'=0}^{t-1} K_{t'}^{storage\_depreciation}$$

$$\Leftrightarrow \quad C \cdot \kappa \left(\frac{\hat{q}_{t+1}}{\gamma_{t+1}} - \frac{\hat{q}_t}{\gamma_t} \right) = C \cdot \kappa \cdot \frac{\hat{q}_{t+1}}{\gamma_{t+1}} - C \cdot \kappa \cdot \frac{\hat{q}_t}{\gamma_t}$$

q.e.d.

The number of expected nominal (full) charge cycles γ (#) of a storage device highly depends on the usage intensity, namely the average Depth of Discharge (DOD) δ (%) and the temperature of respectively around the storage system θ (°C). In the following, the temperature θ is assumed constant. A higher average DOD leads to a reduction of nominal charge cycles γ, which again has a direct influence on the depreciation of the storage device. One can formulate the costs for a full charge cycle ψ (EUR) as follows:

$$\psi = \frac{C \cdot \kappa}{\gamma}$$

The deeper the storage device is discharged, the higher the marginal cost per nominal charge cycle. Since a discharge cycle can last for several timeslots, the discharge action in timeslot t must also cover the increasing marginal costs for the previous discharge action. A discharge action is defined as a reduction of the system's storage level due to intended discharge or self-discharge of the storage device. Thus, the storage depreciation cost in timeslot t must cover the marginal depreciation cost for the discharge action in timeslot t and the difference between the marginal depreciation cost in t and $t - 1$ for the previous discharge:

$$K_t^{storage\_depreciation} = sg(1-\varphi_t)\cdot((\xi_t-\xi_{t-1})\cdot\varphi_t+\hat{q}_{t-1}\cdot(\psi_t-\psi_{t-1}))$$

The following transformation steps prove the identity of the two formulas derived above for the storage depreciation cost $K_t^{storage\_depreciation}$:

$$\begin{aligned}
& C\kappa\cdot\left(\frac{\hat{q}_t}{\gamma_t}-\frac{\hat{q}_{t-1}}{\gamma_{t-1}}\right) = sg(1-\varphi_t)\cdot((\xi_t-\xi_{t-1})\cdot\varphi_t+\hat{q}_{t-1}\cdot(\psi_t-\psi_{t-1})) \\
\Leftrightarrow\ & C\kappa\cdot\left(\frac{\hat{q}_t}{\gamma_t}-\frac{\hat{q}_{t-1}}{\gamma_{t-1}}\right) = sg(1-\varphi_t)\cdot\left((\xi_t-\xi_{t-1})\cdot\frac{C\kappa}{\gamma_t}+\hat{q}_{t-1}\cdot\left(\frac{C\kappa}{\gamma_t}-\frac{C\kappa}{\gamma_{t-1}}\right)\right) \\
\Leftrightarrow\ & C\kappa\cdot\left(\frac{\hat{q}_t}{\gamma_t}-\frac{\hat{q}_{t-1}}{\gamma_{t-1}}\right) = sg(1-\varphi_t)\cdot\left((\xi_t-\xi_{t-1})\cdot\frac{C\kappa}{\gamma_t}+\hat{q}_{t-1}\cdot\frac{C\kappa}{\gamma_t}-\hat{q}_{t-1}\cdot\frac{C\kappa}{\gamma_{t-1}}\right) \\
\Leftrightarrow\ & C\kappa\cdot\left(\frac{\hat{q}_t}{\gamma_t}-\frac{\hat{q}_{t-1}}{\gamma_{t-1}}\right) = sg(1-\varphi_t)\cdot C\kappa\cdot\left(\frac{\xi_t-\xi_{t-1}+\hat{q}_{t-1}}{\gamma_t}-\frac{\hat{q}_{t-1}}{\gamma_{t-1}}\right) \\
\Leftrightarrow\ & C\kappa\cdot\left(\frac{\hat{q}_t}{\gamma_t}-\frac{\hat{q}_{t-1}}{\gamma_{t-1}}\right) = sg(1-\varphi_t)\cdot C\kappa\cdot\left(\frac{\hat{q}_t}{\gamma_t}-\frac{\hat{q}_{t-1}}{\gamma_{t-1}}\right)
\end{aligned}$$

The equation above is obviously correct for $\varphi_t < 1$, since $sg(x) := 1$ for $x < 1$. Thus, identity remains to be proven for the case $\varphi_t = 1$ resulting in $sg(0) := 0$. $\varphi_t = 1$ implies that the storage device is charged during the entire timeslot t, i.e. it cannot be discharged or self-discharged. Therefore the accumulated discharge volume does not increase from $t-1$ to t ($\hat{q} = \hat{q}_{t-1}$) so that the average DOD does not change either ($\delta_t = \delta_{t-1}$). Since θ is assumed constant in this work, this implies $\gamma_t = \gamma_{t-1}$ by the definition of γ and finally proves the identity of the two formulas also for the case $\varphi_t = 1$:

$$\begin{aligned}
& C\cdot\kappa\cdot\left(\frac{\hat{q}_t}{\gamma_t}-\frac{\hat{q}_t}{\gamma_t}\right) = sg(1-1)\cdot C\cdot\kappa\cdot\left(\frac{\hat{q}_t}{\gamma_t}-\frac{\hat{q}_t}{\gamma_t}\right) \\
\Leftrightarrow\ & C\cdot\kappa\cdot(0) = 0\cdot C\cdot\kappa\cdot\left(\frac{\hat{q}_t}{\gamma_t}-\frac{\hat{q}_t}{\gamma_t}\right)
\end{aligned}$$

q.e.d.

Appendix B

Overview of Model Variables

Table B.1: Non-Technical Model Variables

Variable Description	Model	Symbol	Unit
Result Variables			
Total costs in analysis period	LO	K	(EUR)
Costs baseline in analysis period (without DSS)	LO	$K^{baseline}$	(EUR)
Total market-wide costs in analysis period	IM	$\hat{K}$	(EUR)
Market-wide costs baseline in analysis period (without DSS)	IM	$\hat{K}^{baseline}$	(EUR)
Total market-wide costs in analysis period after iteration j	IM	$\hat{K}^{j}$	
Maximal storage capacity that can be operated with marginally positive surplus at a storage cost level of κ	IM	$\hat{C}_{\kappa}^{max}$	(kWh)
Optimal storage capacity that must be operated for maximal surplus at a storage cost level of κ	IM	$\hat{C}_{\kappa}^{opt}$	(kWh)

LO=Implemented Linear Optimization Model (Section 3.2), IM=Iterative (linearized) Optimization Model (Section 7.3).

Table B.2: Non-Technical Model Variables

Variable Description	Model	Symbol	Unit	(Ref.) Value
Decision Variables				
Charge parameter for timeslot t	LO	φ_t	-	[0,1]
Discharge parameter for timeslot t	LO	λ_t	-	[0,1]
Charge parameter for timeslot t	IM	φ_t^j	-	[0,1]
Discharge parameter for timeslot t	IM	λ_t^j	-	[0,1]
Model Constants				
Timeslots per hour	all	T^h	(hour)	1
Incremental load variation	IM	ϵ	(kWh)	2000
Incremental charge volume including efficiency losses	IM	$\tilde{c}$	(kWh)	2477
Incremental discharge volume including efficiency losses	IM	$\tilde{d}$	(kWh)	1960
Consumer Variables				
Load in timeslot t	LO	l_t	(kWh)	VDEW load profile[a]
Aggregated (market-wide) load in timeslot t	IM	$\hat{l}_t$	(kWh)	ENTSOE load profile[b]
Altered aggregated load in timeslot t after iteration j	IM	$\hat{\ell}_t^j$	(kWh)	-
Market Variables				
Price per energy unit in timeslot t	all	p_t	(EUR/kWh)	Price data[c]
Load-dependent price function for timeslot t	IM	$f_t()$	(EUR/kWh)	-
Interest rate on investment	all	i	(%)	7

LO=Implemented Linear Optimization Model (Section 3.2), IM=Iterative (linearized) Optimization Model (Section 7.3).

[a] Standard household load profile in VDEW (2006).

[b] Total consumption profile of Germany, 2007, in ENTSOE (2007).

[c] Flexible end consumer price, weighted average 0.20 EUR/kWh, same distribution as spot market prices at the European Energy Exchange (EEX) in 2007.

Table B.3: Technical Model Variables

Variable Description	Model	Symbol	Unit	Ref. Value
State-independent Storage System Variables				
Annual maintenance cost as percentage of the initial investment	all	m	(%)	2
Estimated life time of system peripherals	all	τ	(years)	10
Maximal capacity of the storage device	LO	C	(kWh)	5.0
Cost per storage capacity unit	all	κ	(EUR/kWh)	100
Power (in) of the storage system (ac to dc)	LO	P^{in}	(kW)	1.0
Power (out) of the storage system (dc to ac)	LO	P^{out}	(kW)	0.5
Aggregated power (in) of the storage system	IM	$\hat{P}^{in}$	(GW)	9
Aggregated power (out) of the storage system	IM	$\hat{P}^{out}$	(GW)	11
Cost per power unit (in)	all	π^{in}	(EUR/kW)	120
Cost per power unit (out)	all	π^{out}	(EUR/kW)	120
Rectifier efficiency (in)	all	η^{in}	(%)	95
Storage efficiency	all	η^{store}	(%)	85
Inverter efficiency (out)	all	η^{out}	(%)	98
Self-discharge of the storage device per hour until T^{selfdch}	TM	η^{selfdch}	(%/hour)	0
Technology-dependent period with minimal self-discharge effect of the storage device	all	T^{selfdch}	(#)	168
Maximal charging speed of the storage device (required hours)	LO	v^{store}	(hours)	-
Maximal charging speed of storage system (required timeslots)	all	v	(#)	-
Temperature of the storage system	-	θ	($^{\circ}C$)	-

LO=Implemented Linear Optimization Model, TM=Theoretical Model (both Section 3.2), IM=Iterative (linearized) Optimization Model (Section 7.3).

Table B.4: Technical Model Variables

Variable Description	Model	Symbol	Unit	Ref. Value
State-dependent Storage System Variables				
Cost for a nominal (full) discharge cycle in timeslot t	all	ψ_t	(EUR)	-
Load state of storage device in timeslot t	TM	ξ_t	(kWh)	-
Average of storage states (storage levels) after completed discharge cycles until timeslot t	TM	$\tilde{\xi}_t$	(kWh)	-
Indicator for local minimum of load state in timeslot t	TM	ξ'_t	(kWh)	-
Average DOD until timeslot t	TM	δ_t	(%)	-
Maximal DOD allowed	all	$\bar{\delta}$	(%)	80
Expected nominal cycles of the storage device reflecting use profile until timeslot t	TM	γ_t	(#)	-
Expected nominal cycles of the storage device (constant average)	TM	γ	(#)	3000
Potential charge volume in timeslot t	all	q^{in}	(kWh)	-
Potential discharge volume in timeslot t	all	q_t^{out}	(kWh)	-
Accumulated discharge volume until timeslot t	TM	$\widehat{q}_t$	(kWh)	-

LO=Implemented Linear Optimization Model, TM=Theoretical Model (both Section 3.2), IM=Iterative (linearized) Optimization Model (Section 7.3).

Appendix C

Control Flows of the Heuristic Scheduling Algorithms

Chapter 5 (Section 5.2.2) presented 4 variants of a heuristic algorithm for determining the Charge-Discharge-Schedule (CDS) of a Distributed Storage System (DSS). Figure C.1 depicts this algorithm as a control flow diagram. The control flow contains 3 boxes that refer to further procedures:

- Determination of price limits (Figure C.2)
- Refinement of the charge condition (Figure C.3)
- Refinement of the discharge condition (Figure C.4)

The most complex variant *Heuristic 4* covers all steps of the control flow, whereas the other variants do not cover some of the steps, as marked in the control flow diagrams. The refinement of the discharge condition only applies to *Heuristic 3* and *Heuristic 4*. As indicated in Figure C.4, *Heuristic 3* does not cover an additional refinement condition in the middle of the algorithm. The refinement of the charge condition is part of the variants *Heuristic 2-4*, but *Heursitic 2* and *3* do not cover an additional refinement condition in the middle of the algorithm, as indicated in Figure C.3.

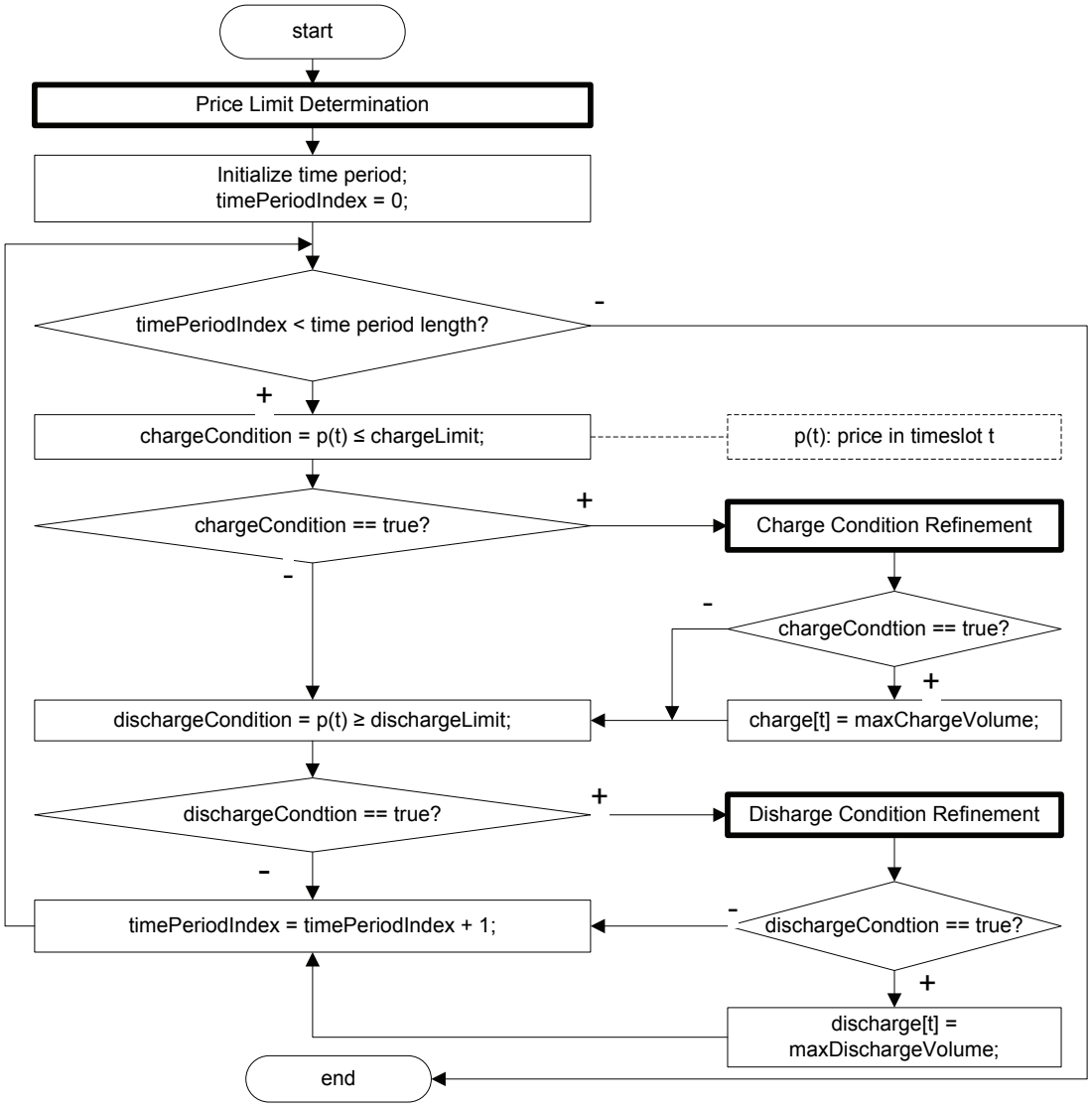

Figure C.1: Schedule generation algorithm

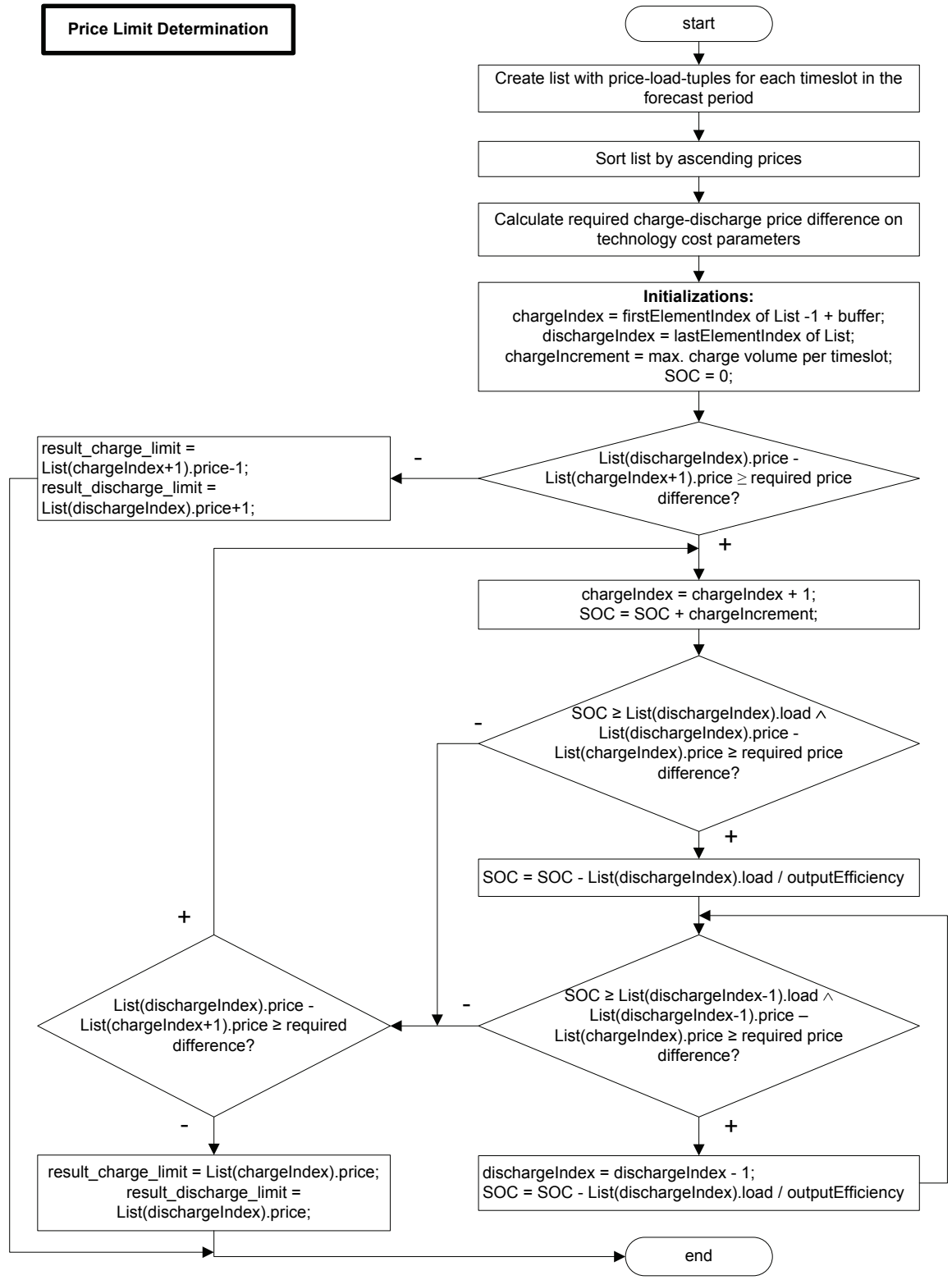

Figure C.2: Price limit determination algorithm

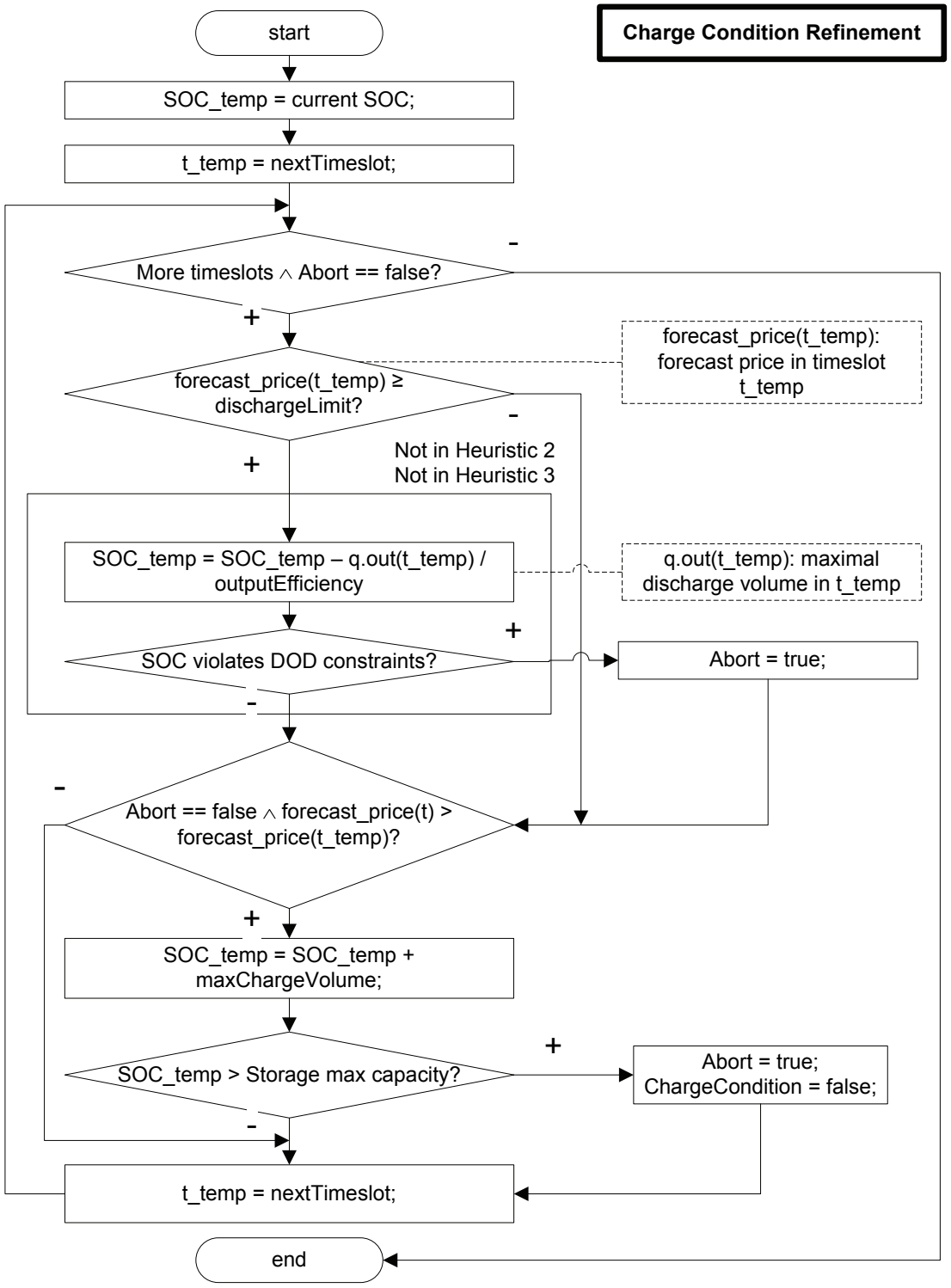

Figure C.3: Algorithm of the charge condition refinement procedure

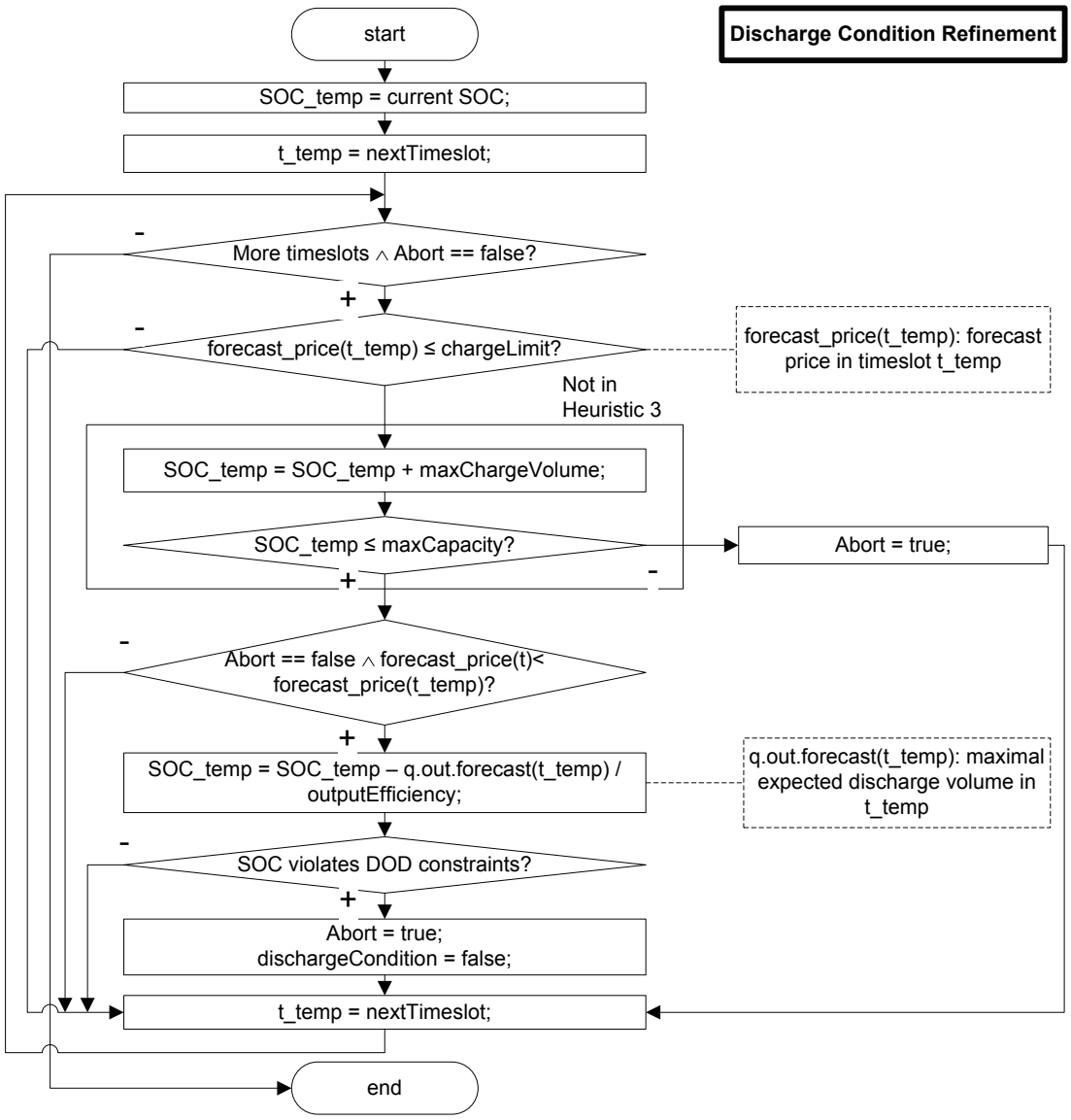

Figure C.4: Algorithm of the discharge condition refinement procedure

Increasing the shares of renewable energy resources is one of the most important levers in many countries to cope with the environmental, political, and economic challenges of future energy supply. Integrating intermittent resources like wind power into the power grid leads to a greater need for flexibility and higher market price volatility, which has raised the interest in electricity storage.

The underlying question of this research work is whether distributed storage systems at the end consumer level can economically foster the integration of such resources by providing demand-side flexibility. It investigates the technical and economic requirements for storage systems aiming at arbitrage realization, as well as the effects of an increasingly responsive demand side on the electricity market price.

ISBN 978-3-86644-561-1